Technische Universität München

Fakultät für Chemie

Synthesis and Reactivity of Low-Coordinate Germanium and Tin Compounds Stabilized by *N*-Heterocyclic Imines

Xuan-Xuan Zhao

Vollständiger Abdruck der von der Fakultät für Chemie der Technischen Universität München zur Erlangung des akademischen Grades eines

Doktors der Naturwissenschaften (Dr. rer. nat.)

genehmigten Dissertation.

Vorsitzender: Prof. Dr. Lukas Hintermann

Prüfende der Dissertation:

1. Prof. Dr. Shigeyoshi Inoue

2. Lecturer Dr. Catherine Weetman

Die Dissertation wurde am 23.08.2022 bei der Technischen Universität München eingereicht und durch die Fakultät für Chemie am 13.09.2022 angenommen

Acknowledgments

First and foremost, I would like to express my heartfelt and sincere gratitude to my supervisor Prof. Dr. Shigeyoshi Inoue, for providing me an opportunity to undertake interesting research in his group. He always gave me instructive advice and helpful suggestions during the whole study period. I thank him for his patient guidance and prompt response to my questions. I am so lucky to be a PhD student of him and I will benefit a lot from his profound knowledge and this experience.

I am grateful to Dr. Catherine Weetman for acting as the examiner for this thesis, and Prof. Dr. Lukas Hintermann for accepting the invitation to be the chairman of the examination committee.

I would like to thank Prof. Dr. Tibor Szilvási and Dr. Arseni Kostenko for their help with theoretical calculations.

I am very thankful to Dr. Daniel Franz, Dr. Franziska Hanusch, Dr. Shiori Fujimori, and Dr. Christian Jandl for measuring crystals and for their help in solving the crystal structures.

I would like to thank Dr. John A. Kelly for proof-reading and correcting this thesis. I thank Lisa Groll for translating the abstract.

I would like to thank Dr. Vitaly Nesterov, Dr. Amelie Porzelt, and Dr. Debotra Sarkar for the valuable scientific discussion.

I would like to thank all members of AK Inoue group for their support and help.

I would also like to thank all the staff of the analytic department of Catalysis Research Center, Technische Universität München for their excellent work and strong support. I would like to thank Florian S. Tschernuth for the VT-NMR measurements. I would like to thank Maximilian Muhr for the LIFDI-MS measurements. In addition, I would like to thank Ms. Ammari Ulrike for the elemental analysis measurements.

I would like to thank my family, and my friends for constantly supporting me during my PhD journey.

Finally, I would like to thank the China Scholarship Council (CSC) for the financial support with grant No. 201806360272. I would also like to thank the financial support from the Deutsche Forschungsgemeinschaft (In 234/7-1).

List of Abbreviations

Ad = adamantly; $C_{10}H_{15}$

BAr^F_4 = $B\{3,5\text{-}(CF_3)_2\text{-}C_6H_3\}_4$

Bbt = (2,6-[$CH(SiMe_3)_2]_2$-4-[$C(SiMe_3)_3]C_6H_2$)

BCF = Tris(pentafluorophenyl)borane; $B(C_6F_5)_3$

Bisap = 2,6-bis(1-naphtyl)phenyl

Cat. = Catalyst

Cp = Cyclopentadiene; C_5H_5

Cp* = 1,2,3,4,5-pentamethyl-cyclopentadiene; C_5Me_5

CAAC = Cyclic alkyl-amino carbene

CH_3CN = Acetonitrile

DFT = Density Functional Theory

DMAP = 4-(dimethylamino)-pyridine

dme = dimethoxyethane

Eind = 1,1,3,3,5,5,7,7-octaethyl-*s*-hydrindacen-4-yl

etc. = Latin (et cetera): “and other similar things”

Et_2O = Diethylether

FLP = Frustrated Lewis Pair

e.g. = Latin (exempli gratia): “for example”

et al. = Latin (et alii): “and others”

Et = Ethyl

Hal. = Halogen

HOMO = Highest Occupied Molecular Orbital

HBpin = Pinacolborane

IDipp = 1,3-bis(2,6-diisopropyl-phenyl)-imidazol-2-ylidene

IMe_4 = 1,3,4,5-tetramethyl-imidazol-2-ylidene

$^{i}Pr_2Me_2$ = 1,3-diisopropyl-4,5-dimethyl-imidazol-2-ylidene

LA = Lewis acids

LB = Lewis bases

LUMO = Lowest Occupied Molecular Orbital

Mes = 2,4,6-trimethylphenyl; mesityl

m-Ter = ^{Mes}Ter = 2,6-bis(2,4,6-trimethyl-phenyl)phenyl

Naph = Naphthalene; $C_{10}H_8$

NBO = Natural Bond Orbital

^{n}Bu = *n*-butyl

NHBO = *N*-heterocyclic boryloxy

NHC = *N*-heterocyclic carbene

NHI = *N*-heterocyclic imine

NMR = Nuclear Magnetic Resonance

NHSi = *N*-heterocyclic silylene

OTf = Triflate

ppm = parts per million

PCy_3 = Tricyclohexyl phosphine

PPh_3 = Triphenyl phosphine

R = substituent / functional group

rt. = room temperature

SC-XRD = Single crystal X-ray diffraction

SIDipp = saturated IDipp; 1,3-bis(2,6-diisopropyl-phenyl)-imidazolidin-2-ylidene

^{t}Bu = Tertiarybutyl

Tbt = 2,4,6-tris[bis(trimethylsilyl)methyl]phenyl

THF = Tetrahydrofuran

Tipp = 2,4,6-triisopropylphenyl

TMS = Trimethylsilyl

Triph = 2,4,6-triphenylphenyl

Tsi = Tris(trimethylsilyl)methyl; $C(SiMe_3)_3$

WCA = Weakly Coordinating Anion

δ = chemical shift

Publication List

1. An Isolable Three-Coordinate Germanone and Its Reactivity

<u>Xuan-Xuan Zhao</u>, Tibor Szilvási, Franziska Hanusch, Shigeyoshi Inoue*

Chem. Eur. J., **2021**, *27*, 15914-15917.

2. Isolation and Reactivity of Tetrylene-Tetrylone-Iron Complexes Supported by Bis(*N*-Heterocyclic Imine) Ligands

<u>Xuan-Xuan Zhao</u>, Tibor Szilvási, Franziska Hanusch, John A. Kelly, Shiori Fujimori, Shigeyoshi Inoue*

Angew. Chem. Int. Ed. **2022**, e202208930.

3. *N*-Heterocyclic Imine-Stabilized Binuclear Tin(II) Cations: Synthesis, Reactivity, and Catalytic Application

<u>Xuan-Xuan Zhao</u>, John A. Kelly, Arseni Kostenko, Shiori Fujimori, Shigeyoshi Inoue*

Z. Anorg. Allg. Chem. **2022**, e202200220.

4. Isolation and Reactivity of Stannylenoids Stabilized by Amido/Imino Ligands

<u>Xuan-Xuan Zhao</u>, Shiori Fujimori, John A. Kelly, Shigeyoshi Inoue*

Draft (Reserch Article)

Conference Contributions

Utilization of *N*-Heterocyclic Imine (NHI) Ligands for the Isolation of Low-valent Germanium Compounds

<u>Xuan-Xuan Zhao</u>, Shigeyoshi Inoue*

44th International Conference on Coordination Chemistry, Rimini, Italy, 28th August to 2nd September **2022**.

Abstract

This thesis comprises of the synthesis and characterization of the bis(*N*-heterocyclic imine)-stabilized chlorotetrylenes and their reactivity towards various reagents. This led to the synthesis of tetrylene-tetrylone-iron complexes, Li/Sn/Fe trimetallic complex, and bis(imino)tetrylenes. Moreover, the synthesis and reactivity of a novel three-coordinate bis(imino)germanone was described. Initial application of the bis(*N*-heterocyclic imine)-stabilized binuclear tin(II) cations in the catalytic hydroboration of carbonyls demonstrates their potential as alternatives to expensive transition-metals. In addition, a novel stannylenoid was isolated by using a bulky amido ligand.

Kurzusammenfassung

Diese Dissertation umfasst die Synthese und Charakterisierung der Bis(*N*-heterocyclischen Imin)-stabilisierten Chlorotetrylenen und ihre Reaktivität mit verschiedenen Reagenzien. Dies führte zur Synthese von Tetrylen-Tetrylon-Eisen-Komplexen, Li/Sn/Fe-Trimetallkomplexen und Bis(imino)tetrylenen. Darüber hinaus wurde die Synthese und Reaktivität eines neuen dreifach koordinierten Bis(imino)germanons beschrieben. Erste Anwendung der Bis(*N*-heterocyclischen Imin)-stabilisierten zweikernigen Zinn(II)-kationen in der katalytischen Hydroborierung von Carbonylen demonstriert ihr Potenzial als Alternative zu teuren Übergangsmetallen. Außerdem wurde ein neuartiges Stannylenoid unter Verwendung eines sterisch anspruchsvollen Amidoliganden isoliert.

Table of Contents

1. Introduction

One of the fundamental interests in chemistry is to understand the similarities and differences of the elements/compounds, particularly comparing those in the same periodic group. Carbon (C), silicon (Si), germanium (Ge), tin (Sn), and lead (Pb) belong to Group 14 in the periodic table. Carbon dioxide (CO_2) possesses two C=O double bonds and is a monomeric gaseous material. In contrast, silicon dioxide (SiO_2) is a solid material, and consists of polymeric Si–O single bond frameworks. Furthermore, upon comparison of methane (CH_4) and silane (SiH_4): silane decomposes explosively upon contact with air whilst methane is stable. This indicates that the properties of carbon and its heavier homologue silicon diverge drastically: the electronegativity (Pauling electronegativity scale) decreases from 2.55 to 1.90, silicon is more polarizable, and its atomic radius is significantly increased (C: 0.70 Å, Si: 1.10 Å).[1]

Low-coordinate compounds of carbon play an integral role in chemistry and have been the subject of intense study for nearly 200 years. However, the first low-coordinate compound of silicon (disilene) was reported on in 1981. Since the isolation of Lappert's stannylene ($Sn[N(SiMe_3)_2]_2$),[2] and West's disilene ($Mes_2Si{=}SiMes_2$, Mes = 2,4,6-$Me_3C_6H_2$),[3] followed by the isolation of P=P and Si=C containing complexes by Yoshifuji[4] and Brook[5], respectively. These reports disproved the so-called "double-bond rule"[6], which relates to the supposed inability of elements (principal quantum number ≥3) to form multiple bonds.[7] Using kinetic and/or thermodynamic stabilization has provided access to various low-coordinate species (Figure 1). Heavier element analogues of low-coordinate organic compounds have fascinated chemists both in the field of organic and inorganic chemistry because they often have unique chemical features.[8,9]

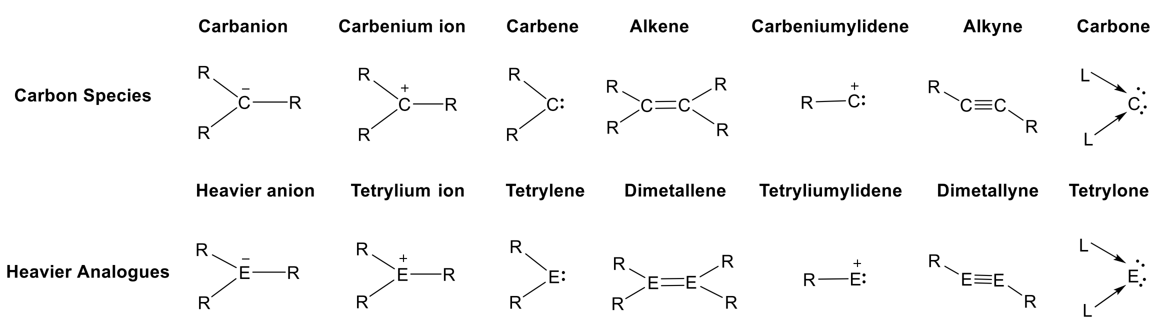

Figure 1. Overview of low-coordinate carbon and its heavier analogues (E = Si, Ge, Sn, Pb; R or L = supporting ligand).

Low-valent main group compounds have shown their ability to mimic transition-metals in the activation of small molecules and cleavage of strong σ-bonds under mild conditions.[10] In 2005, Power and coworkers reported that the "digermyne" $Ar^{Tipp}Ge{\equiv}GeAr^{Tipp}$ (Ar^{Tipp} = 2,6-$Tipp_2$-C_6H_3, Tipp = 2,4,6-tri-*iso*-$propyl_3$-C_6H_2) reacts directly with H_2 in hexane at room temperature at atmospheric pressure to yield the mixture of a "digermene ($Ar^{Tipp}(H)Ge{=}Ge(H)Ar^{Tipp}$)", a digermane ($Ar^{Tipp}(H)_2Ge{-}Ge(H)_2Ar^{Tipp}$), and a primary germane ($Ar^{Tipp}GeH_3$).[11] Computational studies revealed that this was possible through synergistic interaction of its frontier orbitals with H_2, which is analogous reactivity to that observed for transition-metals.[12] Electron donation from the *s*-orbital of H_2 into the LUMO of the Ge species as well as a synergic electron donation from the π-HOMO orbital of $Ar^{Tipp}Ge{\equiv}GeAr^{Tipp}$ into the σ*-orbital of H_2 weakens the H−H bond, reminiscent of interactions between H_2 and a transition-metal complex (Figure 2). Small molecule activation with singlet tetrylenes, in which the main group element possesses a lone pair of electrons and a vacant *p*-orbital, also show similar reactivity to transition-metals and multiply bonded main group species.[13, 14]

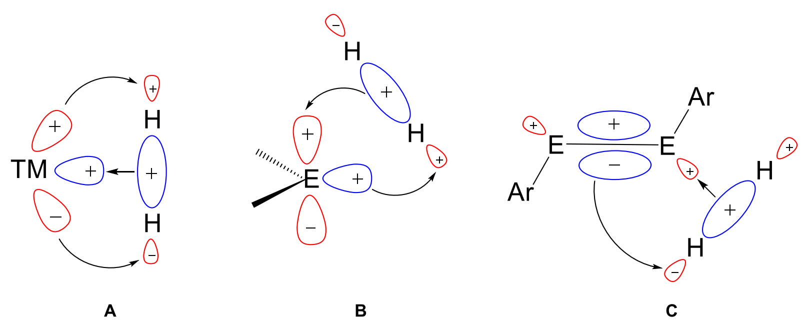

Figure 2. Frontier orbital interactions of H_2 with transition-metals (TMs) (**A**), carbenes and its heavier congeners (tetrylenes) (**B**), as well as multiply bonded main group compounds (**C**).

In catalysis, main group compounds also exhibit transition-metals-like behavior.[15] Different with transition-metals, low-valent main group species tend to form relatively stable addition products (Figure 3).[9] In 2009, Power and coworkers showed the reversible reactions of ethylene with distannynes ($Ar^{iPr}Sn{\equiv}SnAr^{iPr}$, Ar^{iPr} = C_6H_3-2,6-(C_6H_3-2,6-${}^{i}Pr_2$)$_2$ or C_6H-2,6-(C_6H_2-2,4,6-${}^{i}Pr_3$)$_2$-3,5-${}^{i}Pr_2$) under ambient conditions.[16] Moreover, in 2019, Fritz-Langhals revealed the Si(II) cation ($Cp^*Si{:}^+[BAr^F_4]^-$) to be an active catalyst in the hydrosilylation of terminal olefins with a variety of silanes or siloxanes yielding the anti-Markovnikov products as well as internal olefins and terminal alkynes.[17] The suggested mechanism is outlined in Figure 3.

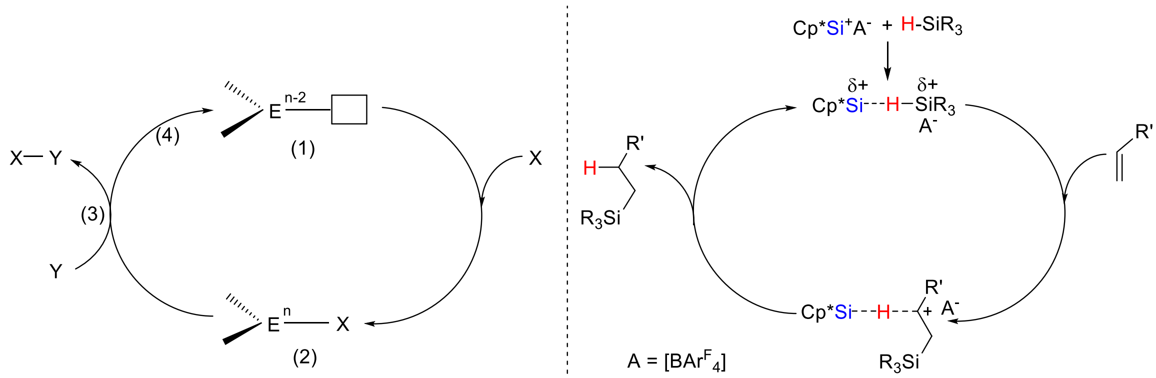

Figure 3. Catalytic cycle for the functionalization of small molecules (left). E = main group elements; n = oxidation state; X = small molecules; Y = reagents; Proposed mechanism for the hydrosilylation catalyzed by $Cp^{*}Si^{+}[BAr^{F}_{4}]^{-}$ (right).

2. Low-Coordinate Group 14 Compounds

2.1 *N*-Heterocyclic Carbenes (NHCs)

Carbenes are neutral compounds featuring a divalent carbon atom with only six electrons in its valence shell.[18] Methylene, which is referred to as the simplest parent carbene with the chemical formula H_2C:, possesses a triplet ground state with singlet-triplet energy separation ($E_{S\text{-}T}$ = $E_{triplet}-E_{singlet}$) of -14.0 kcal mol^{-1}. As for triplet carbenes, two nonbonding electrons are in the two different orbitals with parallel spins, which are regarded as diradicals (Figure 4, left).

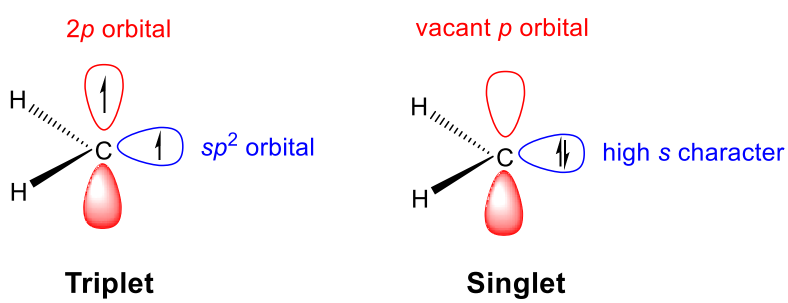

Figure 4. Electronic structures of the triplet carbene and the singlet carbene.

On the other hand, singlet carbenes have the paired electrons located in the sp^2 orbital due to the lower energy level of sp^2-orbital than p_π-orbital (Figure 4, right). Generally, electron-withdrawing groups increase the *s*-character of the carbon lone pair *via* inductive effects. In combination with π-donor properties, e.g. as being the case for nitrogen-, phosphorous- or sulphur-based ligands, the empty *p*-orbital at the carbon center becomes partially occupied, thereby reducing the Lewis acidity of the respective carbenes (Figure 5, left). On the other hand, kinetic stabilization can be achieved by introducing sterically demanding ligands (Figure 5, right).

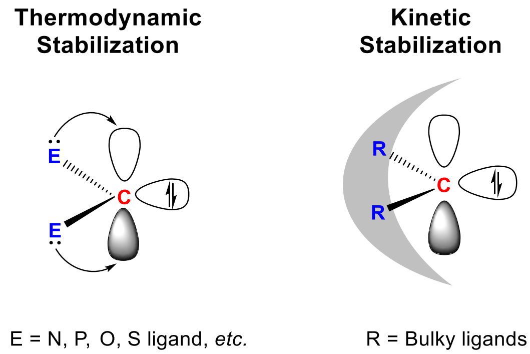

Figure 5. Orbital interactions for stabilization *via* intramolecular electron donation and steric protection of the empty *p*-orbital.

Although carbenes were elusive species for decades, they were efficiently generated *in situ* and used in multiple organic transformations and transition-metal mediated reactions (such as Fischer and Schrock carbenes).[19] Among them, *N*-heterocyclic carbenes (NHCs) represent the most important and investigated class of compound, widely used as ligands in transition-metal chemistry and catalysis, in *f*-block element chemistry, as organo-catalysts, and beyond.[20] In 1968, Öfele reported the application of the *N*-heterocyclic carbene as a ligand for chromium complex **L1** (Figure 6).[21] Within the same year, Wanzlick and Schönherr described the direct synthesis of a mercury salt-carbene complex **L2**.[22] Eventually, Bertrand and coworkers reported the isolation of phosphinocarbene **L3** in 1988,[23] and Arduengo et al. published the first stable crystalline *N*-heterocyclic carbene **L4** in 1991.[24] Initially regarded as laboratory curiosities, stable carbenes, constitute a booming field of research in organic,[25] main group element chemistry,[26] transition-metal homogeneous catalysis,[27] and medicinal applications of NHC-metal complexes.[28] There are many types of stable carbenes isolated in the solid state. In all cases, stabilization is provided with a heteroatom directly attached to the ylidene center or communicating with it through the cyclic aromatic system in combination with steric shielding.

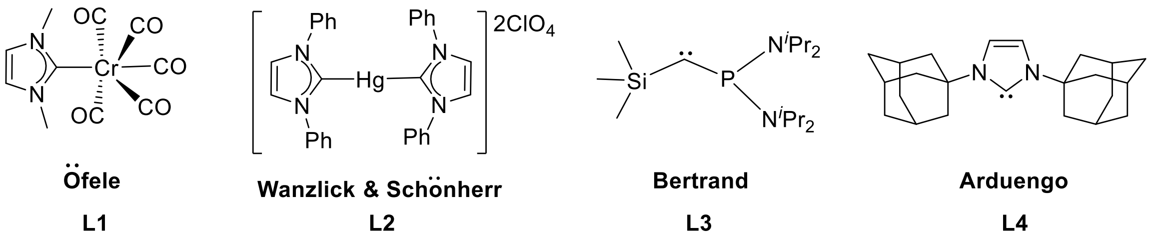

Figure 6. Selected early carbene transition-metal complexes and isolable carbenes.

In main group element and transition-metal chemistry, NHCs proved to be an effective tool for the stabilization of low-coordinate elements in different oxidation states, which are difficult to access using alternative approaches. This provided wide opportunities to not only characterize and gain insights into the bonding of these reactive species, but also to explore their unique reactivity and their potential in synthesis and catalysis.

Electronic structures of NHCs have been discussed in depth. The σ-electron-withdrawing and π-electron-donating effects of N atoms within the ring of NHCs (Figure 7, left) decrease the HOMO and increase the LUMO energies, thus increasing the energy gap between the singlet and triplet ground states. This suggests that the properties of NHCs are very different from other classes of carbenes. However, in cyclic (alkyl)(amino)carbenes (CAACs), one N atom adjacent to the carbene atom is replaced by a σ-donor carbon, decreasing the HOMO−LUMO as well as the singlet-triplet gap (Figure 7, right).[29]

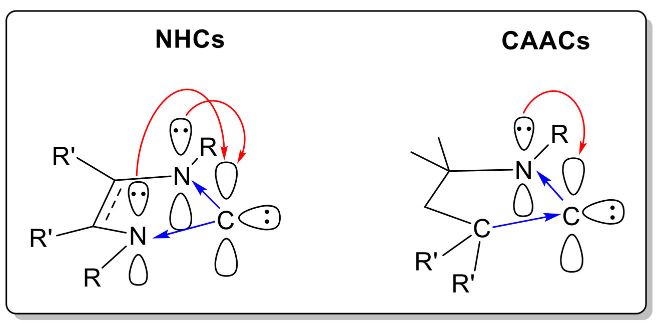

Figure 7. Representation of electronic effects in NHCs and CAACs.

The best-known example of NHC applications is the development of the ruthenium-based Grubb's olefin metathesis catalysts: Grubb's 1st generation catalyst **L5**[30] offers simpler handling and higher compatibility with functional groups of substrates compared than previous transition-metal catalysts (Figure 8). However, this phosphine complex suffers low thermal stability which arises from its weak P−C bond. Herrmann and coworkers substituted the phosphine with two NHC ligands, and a similar catalytic reactivity was observed but with improved stability and more potential for modification (Figure 8, middle).[31]

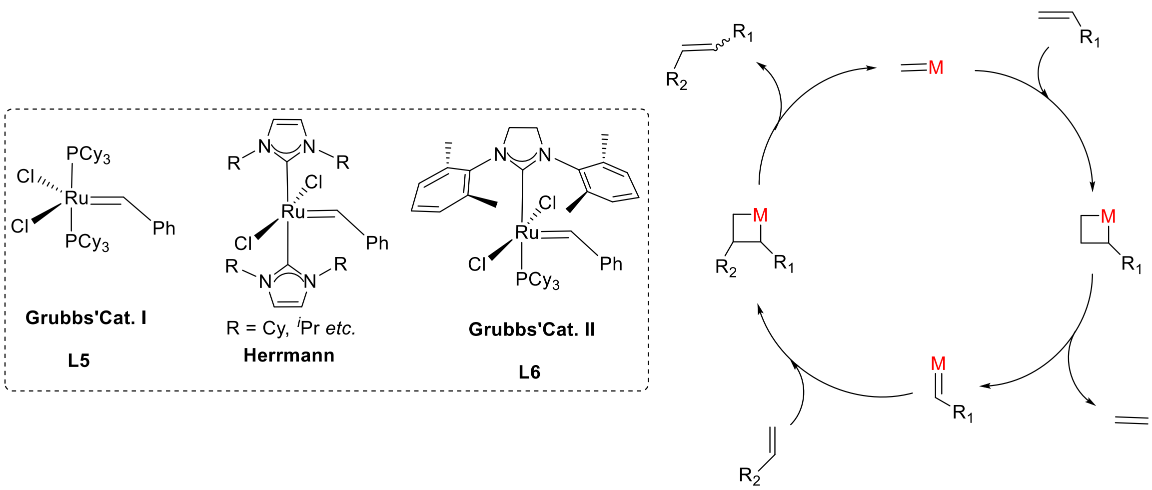

Figure 8. Structures of First-generation Grubb's catalyst **L5** and Second-generation Grubb's catalyst **L6**, as well as proposed mechanism of transition-metal alkene metathesis.

Extensive studies revealed that the activation of First-generation Grubb's catalyst in olefin metathesis relies on the phosphine dissociation progress from the ruthenium. Later in 1999, inspired by earlier insightful studies conducted by Herrmann et al., the Second-generation Grubb's catalyst **L6**[32] substituted one phosphine with one NHC ligand. The stronger σ-donating and weaker π-accepting properties of the NHC ligand render their binding stronger to the metal center and results in a significant improvement in air and moisture stability. Furthermore, the increased σ-donor character of the NHC ligand enhances the affinity of olefin substrates to the ruthenium center, as well as it may aid in the dissociation of the phosphine ligand, leading to improved catalytic ability.

2.2 *N*-Heterocyclic Imines (NHIs)

A different type of ligand used in low-valent main group chemistry is the variant of the well-established NHC ligands, such as *N*-heterocyclic imines (NHIs)[33] and *N*-heterocyclic olefins (NHOs).[34] The NHI ligands with a lone pair of electrons at the exocyclic nitrogen atom are strong electron donors ($2\sigma+4\pi$) (Figure 9). They are the ideal candidates to stabilize the electron-deficient low-valent element centers. The steric demand is adjustable *via* modification of the wingtips in the imidazoline moiety with the ability to delocalize a positive charge within this ring being an additional advantage of NHIs over amine ligands.

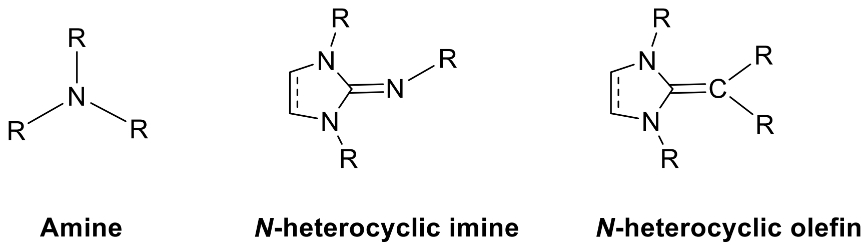

Figure 9. Selected N-donor ligands and the related *N*-heterocyclic olefins (R = organyl or H).

Due to the presence of the nominally vacant p_π-orbital, NHCs still possess some π-accepting ability, which may vary significantly depending on the carbene structure. Thus, dependent on the element E and its coordination number, NHC adducts with main group elements possess either single dative covalent C_{NHC}–E bonds (π-back-donation from E is negligible or absent) or double bonds. The π-back-donation ability of E and the π-accepting property of the used NHC determine the relative contributions of the possible resonance Lewis structures. The classical C=E double bonds are often formed by lighter elements such as C, N and O. The varying nature of these bonds can generally be presented by the ylene structure with a C_{NHC}–E double bond (**A**, E = N, Figure 10), and by the ylide resonance structure with two formal anionic charges at the E atom and positive charge delocalized over the heterocycle (**B**, E = N, Figure 10). For heavier elements, a decreased tendency towards hybridization leads to increased contribution of the ylide resonance structure when descending the group in the periodic table. NHI-metal complexes (**I**) may exhibit significant metalla-2-aza-allene (**II**) or metalimide (**III**) character (Figure 10).

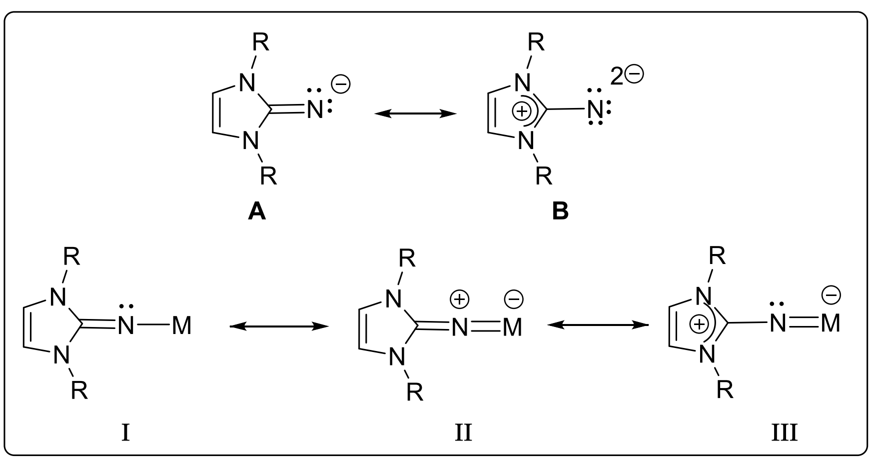

Figure 10. Selected resonance structures for NHI ligands, as well as a model complex with M^+ (R = substituted group).

The NHI ligands were introduced to the chemical community by the Kuhn group in 1995.[35] Today the NHI ligand is an efficient tool for the thermodynamic stabilization of electron-poor species in the modern main group chemistry. For example, in 2012, Bertrand and Dielmann et al. reported on the synthesis of a bis(NHI)phosphinonitrene **L9**,[36] which is stable at room temperature in solution and can also be isolated in the solid state (Figure 11). The bonding between phosphorus and nitrogen is analogous to that observed for metallonitrenes. **L9** reacts with isopropyl isocyanide (^{i}PrNC), affording carbodiimide **L10**. Addition of isopropyltriflate (^{i}PrOTf) completes the nitrogen atom transfer synthetic cycle, giving back the starting phosphenium salt **L7** and a mixture of cyanamide **L11** and carbodiimide **L12**.

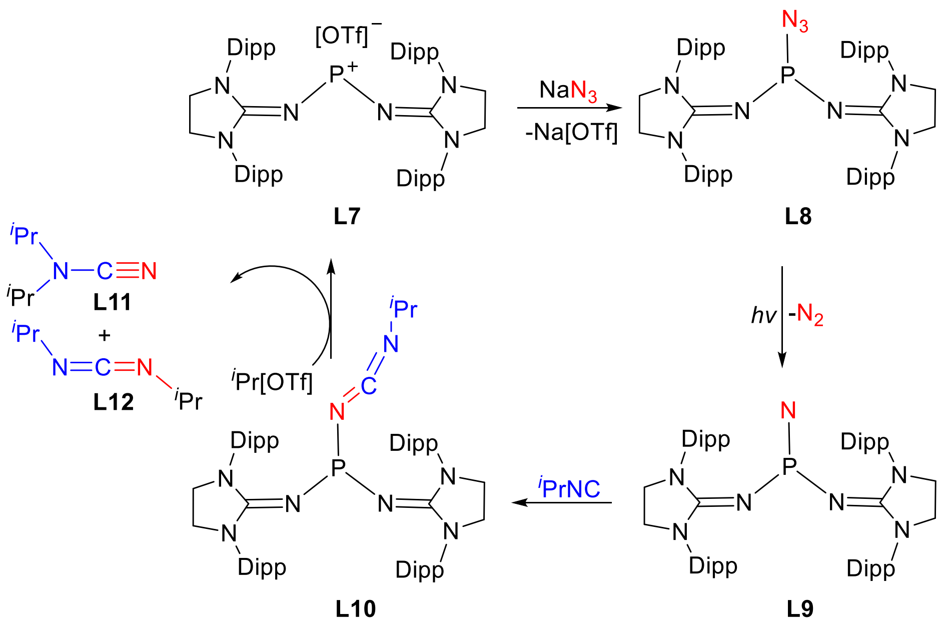

Figure 11. Synthesis of the phosphinonitrene **L9**, and its reaction with isopropyl isocyanide (^{i}PrNC) to afford cyanamide **L11** and carbodiimide **L12**.

More recently, Aldridge and coworkers described the isolation and structural characterization of a rare singly protonated carbonyl mono-cation **L16** and the first example of a doubly protonated carbonyl dication (superelectrophile) **L17** by successive protonation of an NHI-derived carbonyl species **L15** (Figure 12).[37] The isolation of these compounds has been attributed to the strongly donating and sterically demanding nature of the NHI ligands.

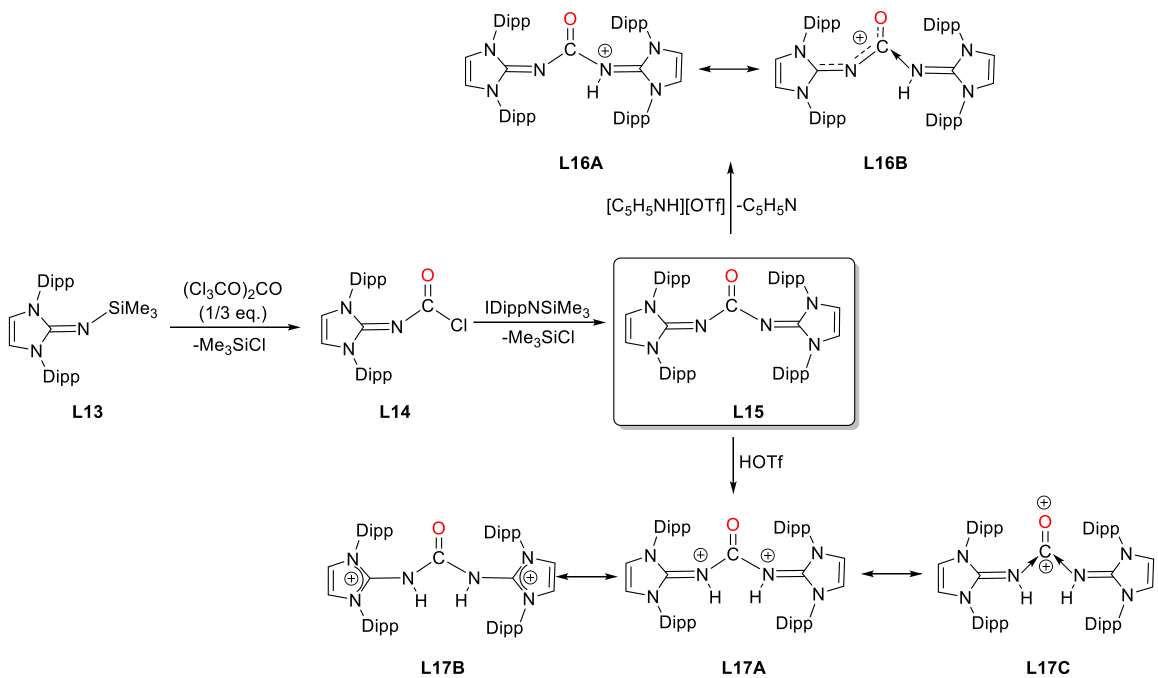

Figure 12. Synthesis of the NHI-substituted carbonyl species **L15** and its protonation.

2.3 Tetrylenes

In contrast to the triplet parent carbene H_2C: (methylene), a parent heavier Group 14 element congener of carbene, H_2E: (E = Si, Ge, Sn, Pb), possesses a singlet ground state.[38] The $E_{S\text{-}T}$ values of H_2Si:, H_2Ge:, H_2Sn:, and H_2Pb: are found to be 16.7, 21.8, 24.8, and 34.8 kcal mol^{-1} (Table 1), respectively, which are sharp contrast to methylene H_2C: ($E_{S\text{-}T}$ = -14.0 kcal mol^{-1}).[39] In addition, the H–E–H bond angle steadily decreases with increasing atomic number of the tetrel atoms (H_2Si: 92.7°, H_2Ge: 91.5°, H_2Sn: 91.1°, and H_2Pb: 90.5°) demonstrating the trend of the increased *s*-orbital character of the lone pair in singlet H_2E: as the Group 14 element becomes heavier. The tetrylenes, R_2E: have the central atom of the oxidation state +II and their stability increases as the principal quantum number (*n*) increases due to the inert pair effect. Because tetrylenes have both a vacant orbital and a lone pair of electrons, they can act as Lewis acids and Lewis bases (ambiphilic character).

Table 1. Electronic features of tetrylenes (ground state).

H_2E:	H_2C:	H_2Si:	H_2Ge:	H_2Sn:	H_2Pb:
$\Delta E_{S\text{-}T}$ (kcal mol^{-1})	-14.0	16.7	21.8	24.8	34.8
∡**H–E–H** (º)	134.0	92.7	91.5	91.1	90.5

Tetrylenes have been widely investigated since the seminal reports on $[(TMS)_2N]_2E$ (E = Ge, Sn, Pb): **L19-21**,[2] $[(TMS)_2CH]_2E$ (E = Ge, Sn, Pb): **L22-24**[40] and Cp*$_2$E (E = Si, Ge, Sn, Pb): **L25-28**,[41] prepared by Lappert and Jutzi et al., respectively (Figure 13). In terms of silicon, West et al. found that $[(TMS)_2N]_2Si$: **L18**,[42] although stable at low temperatures in solution, undergoes rapid decomposition above ~0 °C. It is noteworthy to add that $[(TMS)_2CH]_2Sn$: **L23**[40b] exists as a dimer $[(TMS)_2CH]_2Sn{=}Sn[CH(TMS)_2]_2$ [Sn–Sn bond length: 2.764(2) Å] in the solid state. A milestone in the chemistry of carbocyclic tetrylenes was reached by Kira and coworkers with the isolation of the dialkyl-substituted tetrylenes **L29-31**.[43] In 1982, Veith and Grosser synthesized a series of cyclic tetrylenes **L32-34**.[44] The group of Lappert reported the silylene **L35**,[45] the first *N*-heterocyclic silylene (NHSi) containing a phenyl ring in the backbone (conjugated *π*-framework). In 2019, Khan and Pati et al. reported the *N*-heterocyclic germylene **L36** and stannylene **L37** catalyzed cyanosilylation and hydroboration of aldehydes.[46]

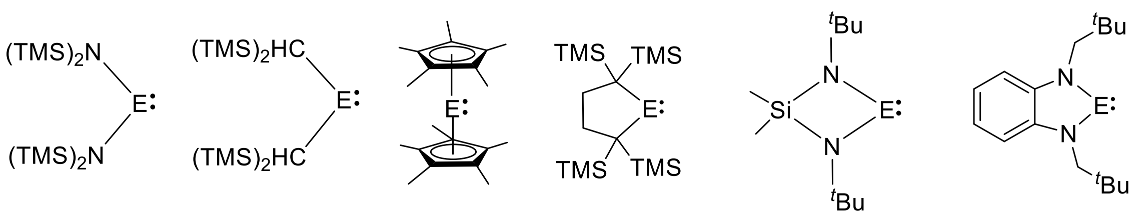

L18, E = Si
L19, E = Ge
L20, E = Sn
L21, E = Pb

L22, E = Ge
L23, E = Sn
L24, E = Pb

L25, E = Si
L26, E = Ge
L27, E = Sn
L28, E = Pb

L29, E = Si
L30, E = Ge
L31, E = Sn

L32, E = Ge
L33, E = Sn
L34, E = Pb

L35, E = Si
L36, E = Ge
L37, E = Sn

Figure 13. Literature known examples of tetrylenes.

The mechanistic pathway of the hydroboration proceeds *via* the formation of a donor-acceptor complex between HBpin and the catalyst followed by the attack of aldehydes (Figure 14). The catalytic activity of both the germanium and tin derivatives (**L36’** and **L37’**) can be attributed to the higher Lewis acidity of Group 14 heavier congeners.

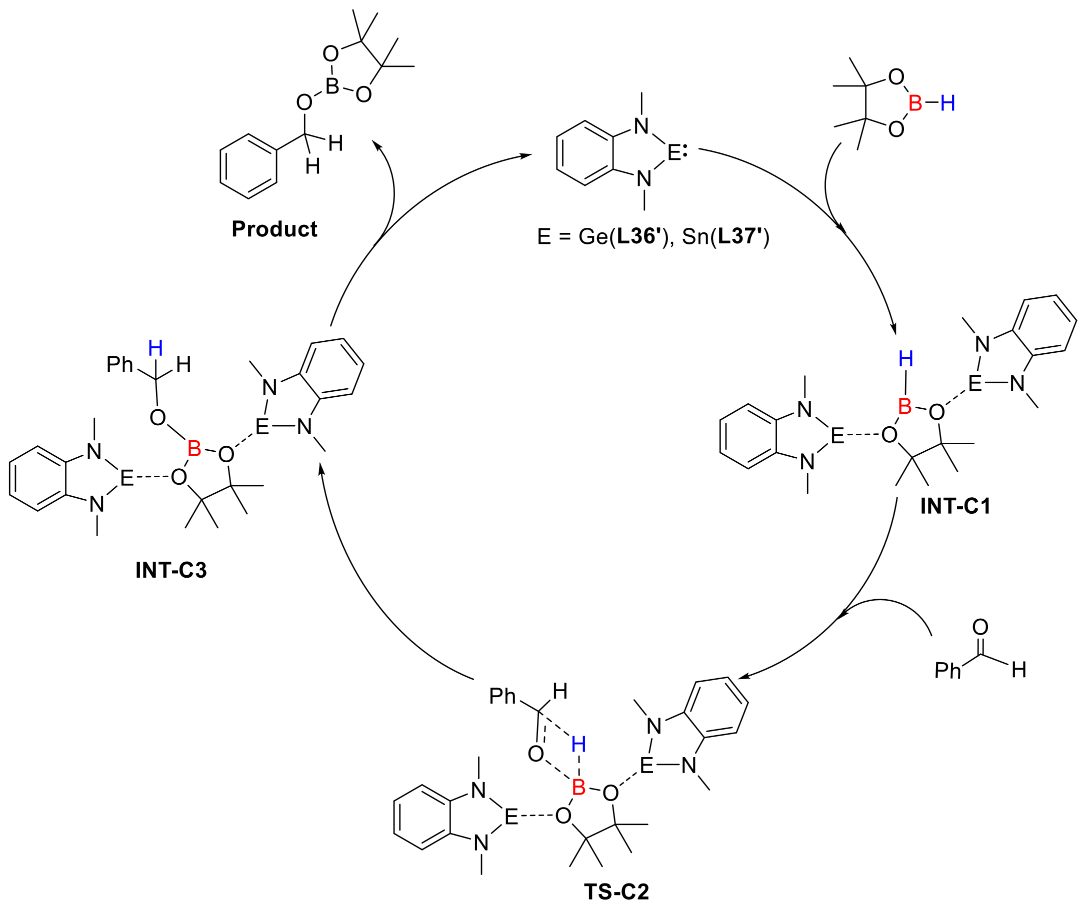

Figure 14. Catalytic cycle and proposed mechanism for the hydroboration of benzaldehyde using model catalyst **L36’** or **L37’**.

Several stable acyclic tetrylenes have been reported by taking advantage of bulky ligands. The isolation of thiolate-, boryl-, silyl-, and amido-substituted acyclic tetrylenes was successfully achieved by steric protection and/or electronic stabilization (Figure 15). Thanks to the smaller HOMO−LUMO gap relative to cyclic systems, the acyclic tetrylenes can activate small molecules (H_2, CO_2, NH_3, P_4, *etc.*).[47] The groups of Power and Tuononen found that silylene **L38** reacts with ethylene or alkynes to afford the [1+2]-cycloaddition products.[48] The groups of Aldridge, Jones, Kaltsoyannis, and Mountford reported two thermally stable acyclic silylenes **L39**[49] and **L40**.[50] These silylenes undergo facile oxidative addition reactions with dihydrogen or with alkyl C−H bonds of the ligands, demonstrating fundamental modes of reactivity more characteristic of transition-metal systems. In 2016, the same groups isolated an acyclic di(amino)silylene **L41** by using an extremely bulky boryl-amide ligand, thereby isolating di(amino)stannylene **L42** and di(amino)plumbylene **L43**.[51] As for germanium, only the amidogermylene chloride was isolated from the reaction with approximately half of the starting materials remaining unreacted. Aldridge and coworkers also reported on the development of a new class of strongly donating *N*-heterocyclic boryloxy (NHBO) ligands, isoelectronic with the well-known NHI ligands. Employment of this ligand enables the successful stabilization of the first two-coordinate acyclic dioxysilylene **L44** together with its heavier congeners **L45-47**.[52]

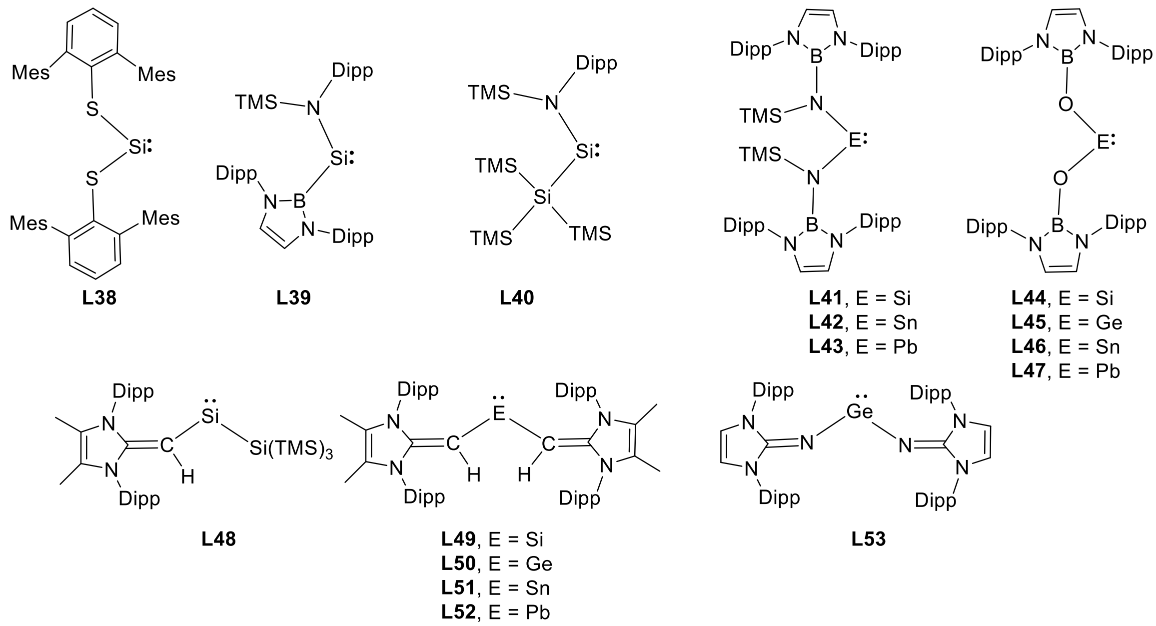

Figure 15. Selected examples of two-coordinate acyclic tetrylenes.

In 2019, Rivard et al. reported on the synthesis of a thermally stable, two-coordinate acyclic silylene **L48**,[53] supported by an NHO ligand and the strongly *s*-donating hypersilyl group. This compound exhibits high reactivity towards small molecules (e.g. MeOTf, HBpin, $HSiCl_3$, P_4, and ^{t}BuCN). Subsequently, they synthesized a complete di(vinyl)tetrylene series **L49-52**.[54] Similarly, in 2015, they reported on the synthesis of a two-coordinate acyclic germylene **L53** supported by two bulky and electron donating NHI ligands.[55] However, their attempts to isolate the corresponding silylene $[IPrN]_2Si$: **INT-L54A** led to the complex **L55** *via* an unexpected ligand activation/rearrangement process involving N−C(aryl) bond cleavage within the NHI ligand (Figure 16). This transformation was also studied by computational methods.

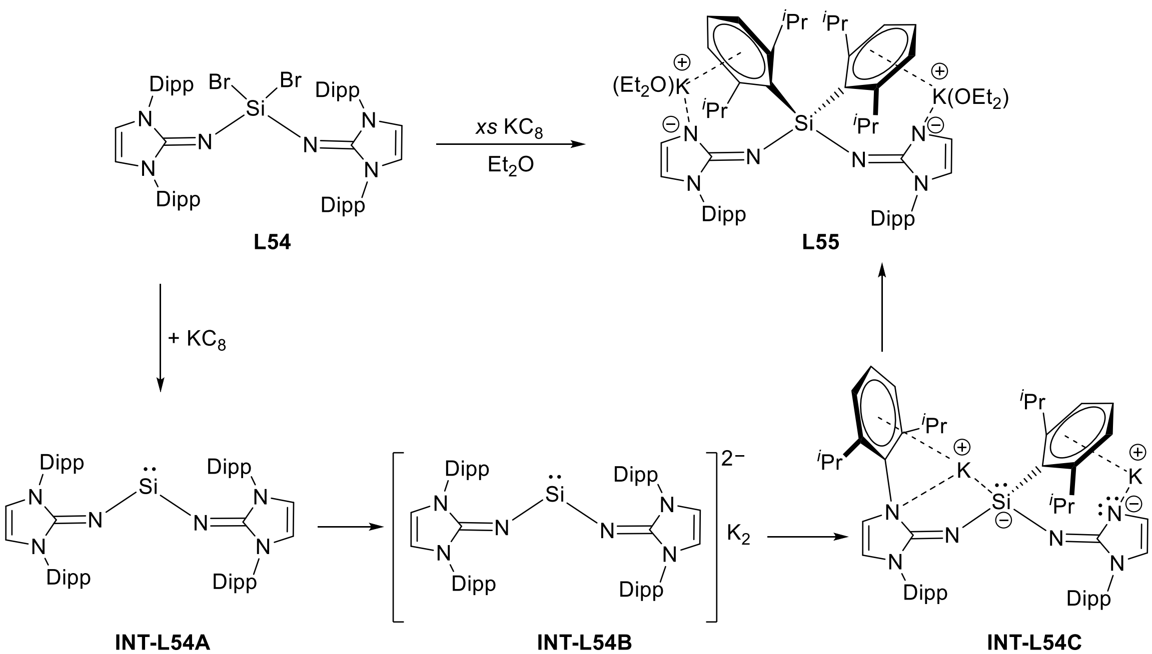

Figure 16. Possible pathway for the formation of **L55**.

Rivard and coworkers also reported that the reduction of a dimeric [NHOGeCl]$_2$ species (NHO = [(^{Me}CNDipp)$_2$C=CH]$^-$) did not give the expected acyclic RGeGeR analogue of an alkyne **INT-L56B**, but rather ligand migration/disproportionation transpired to yield the known bis(imino)germylene R$_2$Ge: **L57** and Ge metal (Figure 17).[56] This process was examined computationally. They started with the assumption that the reduction of **L56** would initially yield the cyclic Ge(I) dimer cyclic-Ge(μ-R)$_2$Ge **INT-L56A**. A plausible isomer of **INT-L56A** would be the open digermylene form, acyclic-RGeGeR **INT-L56B**, which was computed to be only +3.8 kcal mol^{-1} higher in energy. The digermavinylidene R$_2$Ge=Ge: **INT-L56D** is formed *via* 1,2-ligand migration. Decomposition of R$_2$Ge=Ge: into R$_2$Ge: **L57** and Ge(s) was predicted to be an exothermic process [ΔH = -33.9 kcal mol^{-1}].

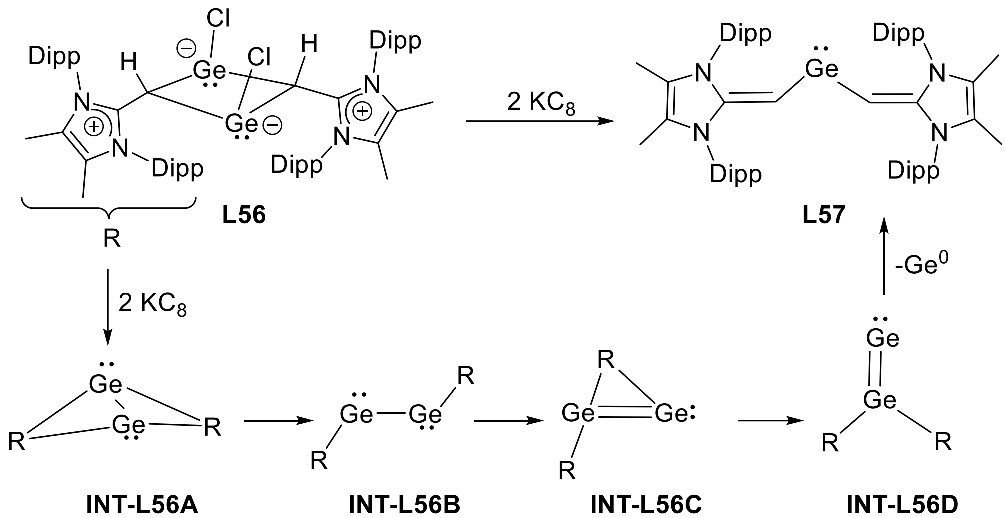

Figure 17. Computed pathway for the formation of **L57** from **INT-L56A**.

Our group commenced work on main group element complexes of the imidazolin-2-iminato ligand a few years ago and described its complex with a Si(II) center in 2012 (**L58**, Figure 18).[57] We also reported the highly reactive acyclic silylene **L59** stabilized by an NHI ligand.[58] It readily undergoes an intramolecular C=C insertion into its aromatic ligand framework, affording the room temperature stable silacycloheptatriene (silepin) **L60**. Moreover, variable temperature UV-*vis* measurements and DFT calculations were conducted and suggested thermally accessible interconversion between **L59** and **L60** at higher temperatures (e.g. 100 °C). This equilibrium was also evidenced by the isolation of a silylene-borane adduct upon addition of $B(C_6F_5)_3$. Therefore, silepin **L60** acts as a "masked" silylene and takes part in the H_2 bond activation process. In addition, treatment of the analogue of **L59** (with a supersilyl group) towards N_2O led to the formation of imino-siloxy-silylene **L61** *via* rearrangement of the proposed silanone intermediate.[59]

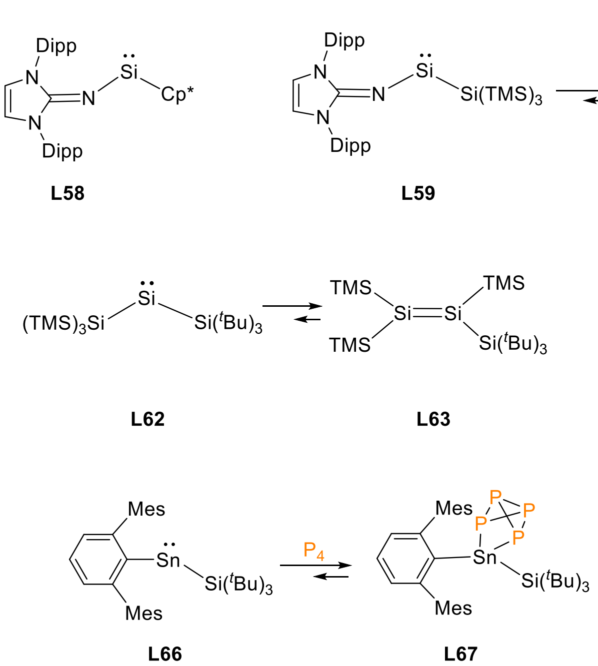

Figure 18. Examples of tetrylenes reported by our group.

Reductive debromination of [$(TMS)_3Si$]($^tBu_3Si$)$SiBr_2$ with two molar equivalents of potassium graphite (KC_8) at low temperatures results in the formation of tetrasilyldisilene **L63**, the isomer of (hypersilyl)(supersilyl)silylene **L62**.[60] An equilibrium between **L62** and **L63** in solution is suggested, and the disilene/silylene equilibrium mixture is capable of H_2 activation at low temperatures. We also described the synthesis and electronic structures of germylene- and stannylene-phosphinidenes **L64** and **L65** stabilized by NHC at the phosphorus atom.[61] These compounds contain reactive P–E bonds (E = Ge, Sn), and allow access to zwitterionic heavier imine analogues, as demonstrated for the tin derivative. Notably, the latter (**L65**) showed higher catalytic activity in the hydroboration of aromatic aldehydes and ketones, drastically different to that of the germanium congener. Use of a silyl-supported stannylene **L66** enables activation of white phosphorus (P_4) under mild conditions, which is reversible under UV light.[62]

2.4 Tetrylenoids

Metal@MX complexes (M = alkali metal, X = leaving group) are common organometallic reagents.[63] For example, Luo and coworkers reported the rare-earth metal complexes **L68**,[64] **L69**,[65] and **L70**[66] bearing the bulky amido ancillary ligands (Figure 19). These complexes are thermally stable at ambient temperature. In contrast, Group 14-element@MX complexes are relatively unstable and elusive.

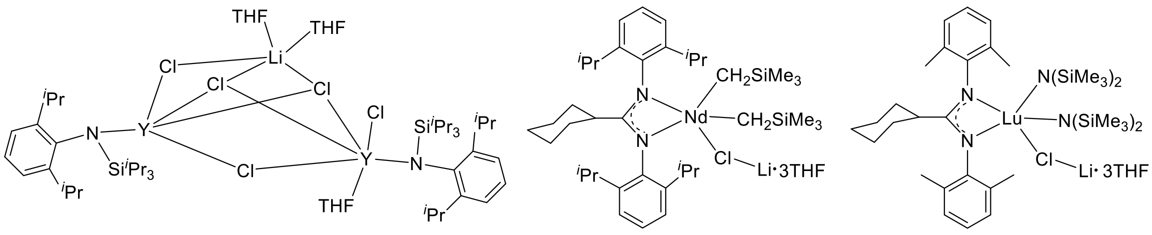

L68 **L69** **L70**

Figure 19. Selected examples of rare-earth-metal@LiCl complexes.

As for main group elements, carbenoids with the formula R_2CMX (M = alkali metal, X = leaving group) have attracted much attention owing to their unique reactivity.[67] In recent years, there have been important developments in the search for stable Li–Cl carbenoid species.

In 1993, Boche and coworkers reported on the isolation of a lithium/halogen alkylidenecarbenoid **L71**,[68] which was stable up to -60 ºC (Figure 20). Later, Niecke and coworkers synthesized more stable phosphanylcarbenoid **L72** stabilized by delocalization of the anionic charge over the π system.[69] Afterwards, they reported on the preparation of the phosphavinylidene carbenoid **L73** containing a P(III) atom,[70] which decomposed on warming to room temperature. In 2007, Le Floch and coworkers isolated the first example of room temperature stable carbenoid **L74** by chlorination of the corresponding dianion by mild oxidation of stable geminal dianions.[71]

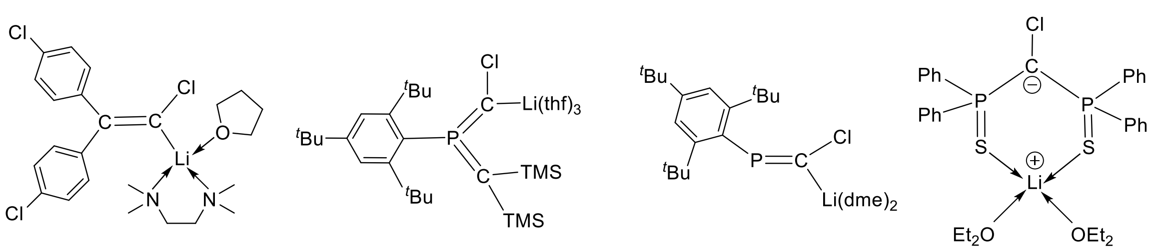

L71 **L72** **L73** **L74**

Figure 20. Examples of reported carbenoids.

In sharp contrast, heavier analogues of carbenoids, that are tetrylenoids with the general formula R_2EMX (E = Si, Ge, Sn, Pb; M = alkali metal, X = leaving group), have been studied only marginally. Dependent on the property of the leaving group, the high ambiphilic character ascribed to tetrylenoids is exhibited when X is a good leaving group, such as halide, alkoxide, *etc.*; the compound acts as a typical metallyl anion when X is a poor leaving group, e.g. organyl, amide.

Like carbenoids, the isolation of tetrylenoids is hampered by their inherent instability leading to α-elimination of MX or self-condensation (Figure 21).

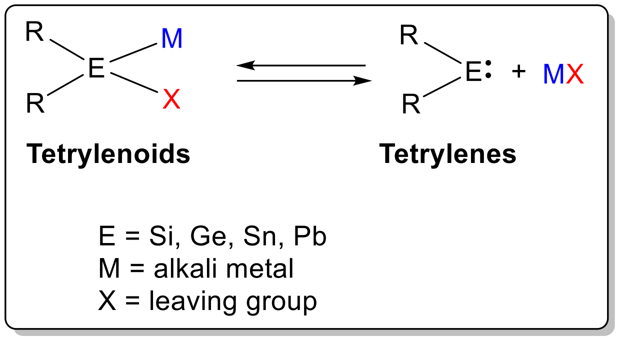

Figure 21. Interconversion between tetrylenoids and tetrylenes.

The pioneering work of silylenoids was performed by Tamao and coworkers.[72] In 1997, they investigated the alkoxyl-substituted silylenoid (^{t}BuO)Ph_2SiLi **L75** (Figure 22),[73] which underwent bimolecular self-condensation at 0 ºC. In 1999, they also studied the intramolecular amine-stabilized silylenoild **L76**.[72] Within the same year, lithium/halogen silylenoid Tbt(Dipp)Si@LiBr **L77** was generated by the reduction of the dibromosilane with lithium naphthalide reported by Tokitoh and coworkers.[74] In 2004, Lee and coworkers have been widely investigated the reactivity of metal/halogen silylenoids (M = Li, K; Hal. = Cl, Br) **L78**.[75]

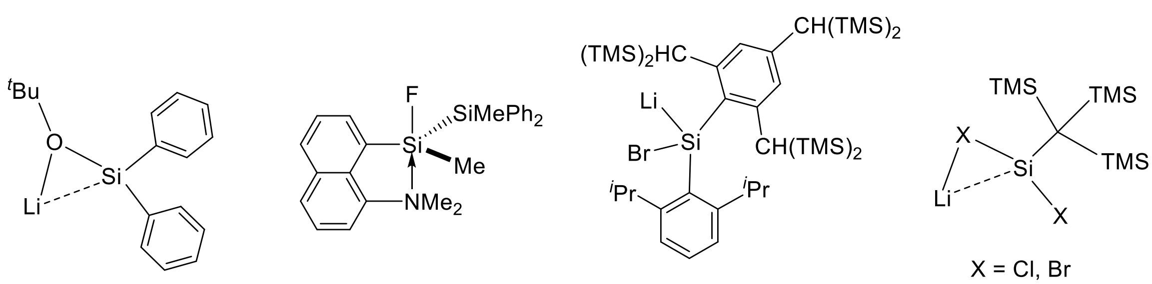

L75 **L76** **L77** **L78**

Figure 22. Selected examples of reported silylenoids.

The field of the heavier Group 14 element congeners (e.g. Ge, Sn) remains largely unexplored mainly due to the increased stability of the divalent Ge(II) and Sn(II) atom in comparison to the lighter congeners. As a consequence, the elimination of metal halide from the high-coordinate germanium or tin center is strongly favored. In 1996, Ando and Ohtaki described the synthesis of a trisyl-substituted chlorogermylenoid **L79**,[76] however, the molecular structure of this compound in the solid state was not reported (Figure 23). In 2016, Sasamori and coworkers successfully synthesized the chlorogermylenoid **L80** that was studied by X-ray crystallography.[77]

$TsiGeCl \cdot LiCl \cdot 3THF$

L79

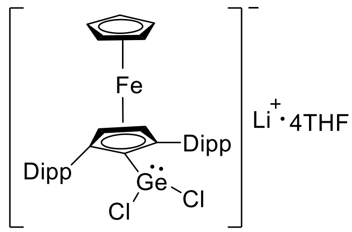

L80

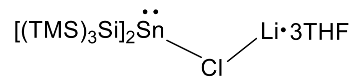

L81

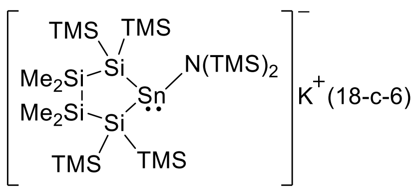

L82

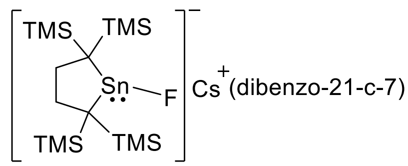

L83

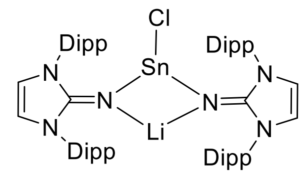

L84

Figure 23. Examples of reported germylenoids and stannylenoids.

As for the stannylenoids, in 1987, Cowley and coworkers reported the silyl-substituted stannylenoid **L81**.[78] With the help of crown ethers, stannylenoids **L82**[79] and **L83**[80] were isolated and characterized by X-ray crystallography. In 2016, we reported a rare example of a lithium stannylenoid **L84** prepared by using an imidazolin-2-iminato ligand and verified the high stannylenoid character of this compound by demonstrating its ambiphilic reactivity.[81]

2.5 Tetryliumylidenes

Tetryliumylidene ions are E(II) cations of the type $[R{-}E:]^+$ (E = Si, Ge, Sn, Pb), and can be considered to be related to both tetrylenes, R_2E:, and tetrylium ions, $[R_3E]^+$ (Figure 24).[82] They possess only four valence electrons, two as a localized lone pair, and two degenerate vacant *p*-orbitals on the E center (Figure 24). No mono-coordinate tetryliumylidene ions have been isolated in the condensed phase, although the parent $[H{-}E:]^+$ ion has been observed experimentally as a short-lived intermediate in the gas phase and has been observed spectroscopically in astrochemical processes.

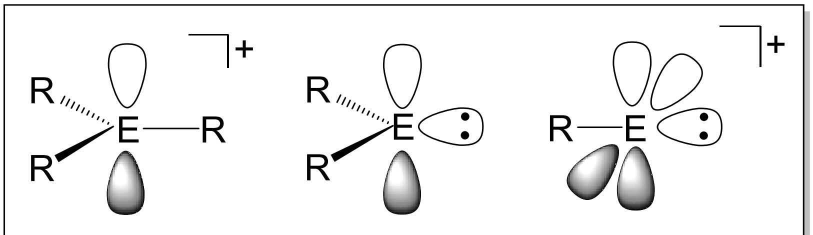

Figure 24. Electronic structures of tetryliun ions, tetrylenes, and tetryliumylidenes (E = Si, Ge, Sn, Pb; R = supporting ligand).

To date, donor stabilization has been required for the isolation of tetryliumylidene ions in the laboratory. In 1979, the first reported stannyliumylidene ion [Cp*Sn][BF_4] **L85** came from Jutzi and coworkers (Figure 25).[83] The penta-coordinate compound **L85** relies on the delocalized electronic structure of the SnC_5 skeleton for stabilization and required a very weakly coordinating anion (WCA) for successful isolation. In 1990, the Sn(II) complex, [2.2.2]-paracyclophane **L86** was reported by Schmidbaur and coworkers.[84] Notably, the compound was embedded with threefold internal η^6-coordination. Later, several groups have stabilized low-valent Sn(II) centered cations by employing various mono-anionic bulky N-donor ligands, such as aminotroponiminato **L87**[85] and β-diketiminato **L88**.[86] In 2012, Jones and Krossing et al. synthesized the quasimono coordinate Sn(II) cation **L89** by using a bulky amido ligand, which are intramolecularly stabilized by weak η^2-arene interactions.[87] Within the same year, the groups of Baines and Macdonald published the crown ethers and cryptand complexes of Sn[OTf]$^+$, (**L90**)[88] and SnX^+ (X = Cl, Br, I; **L91**).[89] In 2013, Fischer and Flock et al. isolated the Sn(II) cation **L92** stabilized by a 2,6-diaminopyridine ligand.[90] Jambor and coworkers prepared the cationic complex **L93** using a neutral chelating ligand.[91] Moreover, the synthesis of a $[L\rightarrow SnCl]^+$ structure **L94** has been isolated as a dimer by employing hexaphenylcarbodiphosphorane as a neutral monodentate ligand, able to donate two electron pairs.[92] More recently, the pseudo-one-coordinated Sn(II) cation **L95** stabilized by a bulky carbazolyl ligand was reported by Hinz.[93]

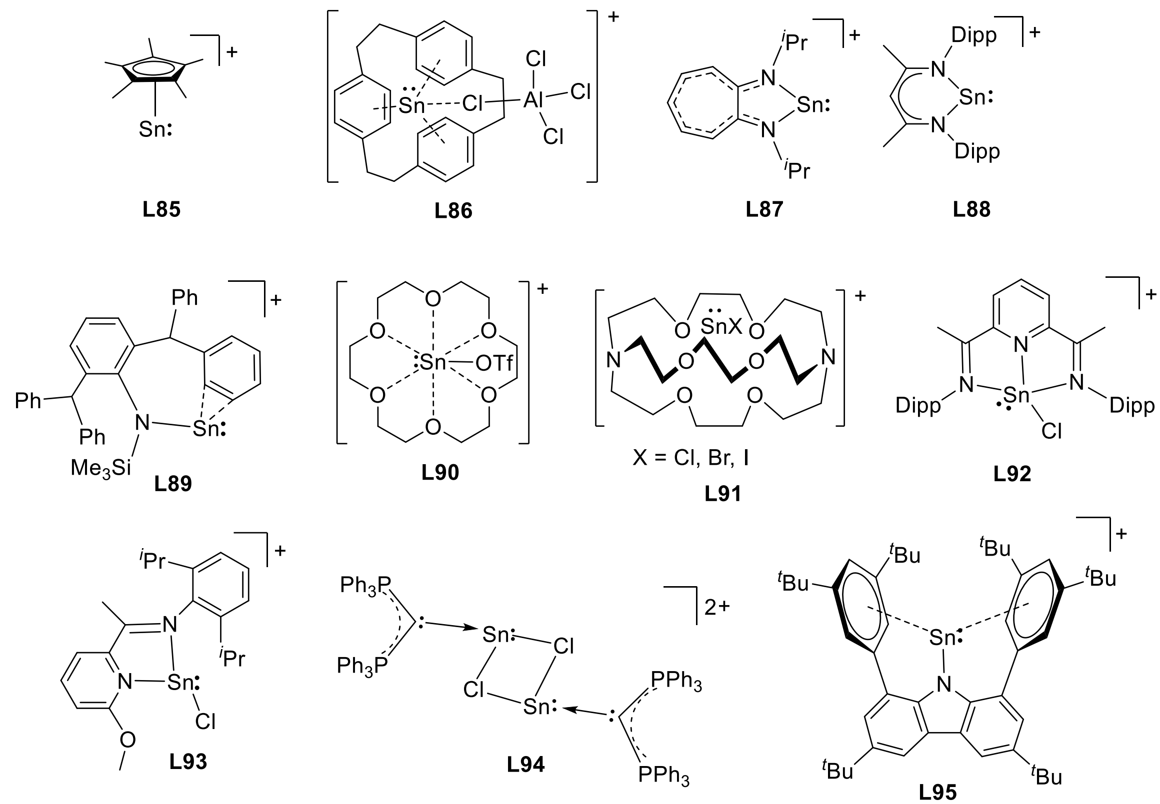

Figure 25. Selected examples of reported tin(II) cations.

Recently, our group has described a variety of NHC- or NHI-stabilized tetryliumylidenes $[R{-}E{:}]^+$ (E = Si,[94] Ge,[95] Sn[96]). We have shown the synthesis of a cyclic Ge(II) cation **L96**,[97] and tin(II) cation **L97**[98] from the corresponding amino(imino)tetrylenes (Figure 26). Moreover, the imino ligand can also be implemented in the isolation of the triflate-bridged germanium complex **L98**,[99] which has significant bis(germyliumylidene) dication character. Bis(NHC)-stabilized bulky aryl-substituted tetryliumylidenes **L99**[100] and **L100**,[101] of general formula $[Ar{-}E(NHC)_2]^+X^-$ (Ar = aryl group; E = Si, Ge; X = Cl^-, $[BAr^F{}_4]^-$), represent the most suitable candidates for fulfilling the desired electronic features to enable versatile small molecule activation (such as CO_2,[102] N_2O,[101] H_2O,[103] *etc.*). In addition, by using the ethylene-bridged bidentate bis(NHI) ligand towards the complexation of $ECl_2{\cdot}$(donor) (E = Si, Ge, Sn; donor = NHC or dioxane, *etc.*), the synthesis of the bis(NHI)-stabilized chlorotetryliumylidenes **L101-103** were achieved recently.[96a, 104]

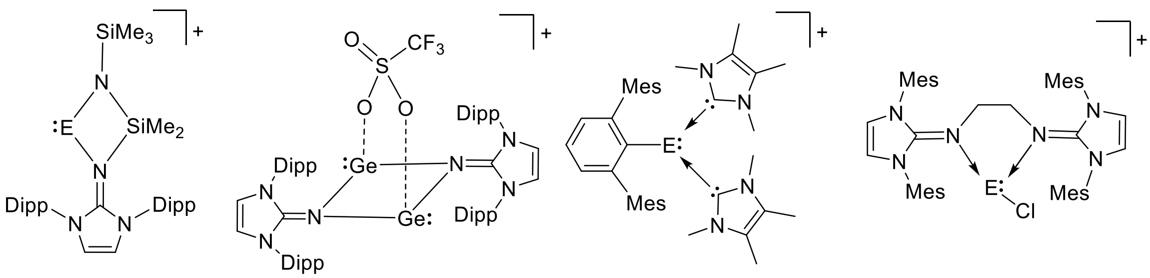

Figure 26. Examples of tetryliumylidene ions reported by our group.

2.6 Tetrylones

It has been shown that there is a class of organic compounds with the general formula EL_2 (E = Si, Ge, Sn, Pb), in which the tetrel atom retains its four valence electrons as two lone pairs of electrons, and in which the tetrel atom is bonded to the ligands L through donor-acceptor interactions (L→E←L).[105] The term "tetrylone" has been suggested for these compounds because they possess a different bonding situation than tetrylenes R_2E:, which have only one lone pair of electrons and two electron-sharing bonds E–R.[106]

2.6.1 Multinuclear zero-valent Group 14 element complexes

Over the past two decades, the isolation and reactivity of tetrylones has garnered much attention.[107] The synthesis of the tristannaallene **L104** by Wiberg et al. in 1999 could be described as the first example of a heavier tetrylone (Figure 27).[108] In 2005, Kira and coworkers reported on the synthesis of the thermally stable, crystalline trisilaallene **L105**,[109] and trigermaallene **L106**.[110] In 2008, utilizing a bulky NHC as strong σ-donor, Robinson and coworkers successfully isolated the first NHC-stabilized diatomic zero-valent silicon compound **L107** with a lone pair of electrons on each silicon atom, representing a landmark and paving the way for zero-valent silicon chemistry.[111] One year later, the germanium and tin analogues of this compound (**L108**[112] and **L109**[113]) were reported by the groups of Jones, Stasch, and Frenking. In 2013, the first sila-, and germa-dicarbene complexes **L110**[114] and **L111**[115] were reported by Roesky, Stalke, and Frenking et al. In 2014, Roesky et al. also reported the CAAC-supported dinuclear Si species **L112**,[116] comprising a Si=Si bond. In the same year, by taking a similar synthetic strategy, the first NHSi-stabilized dinuclear Ge(0) complex **L113** was isolated by the So group.[117] In 2016, a triatomic Si(0) cluster **L114** stabilized by a CAAC ligand was synthesized by Mondal, Dittrich, Frenking, and Roesky et al.[118]

Within the same year, a simple monomeric digermavinylidene compound, (boryl)$_2$Ge=Ge: (**L115**, boryl = (HCDippN)$_2$B), was synthesized by Aldridge and coworkers.[119]

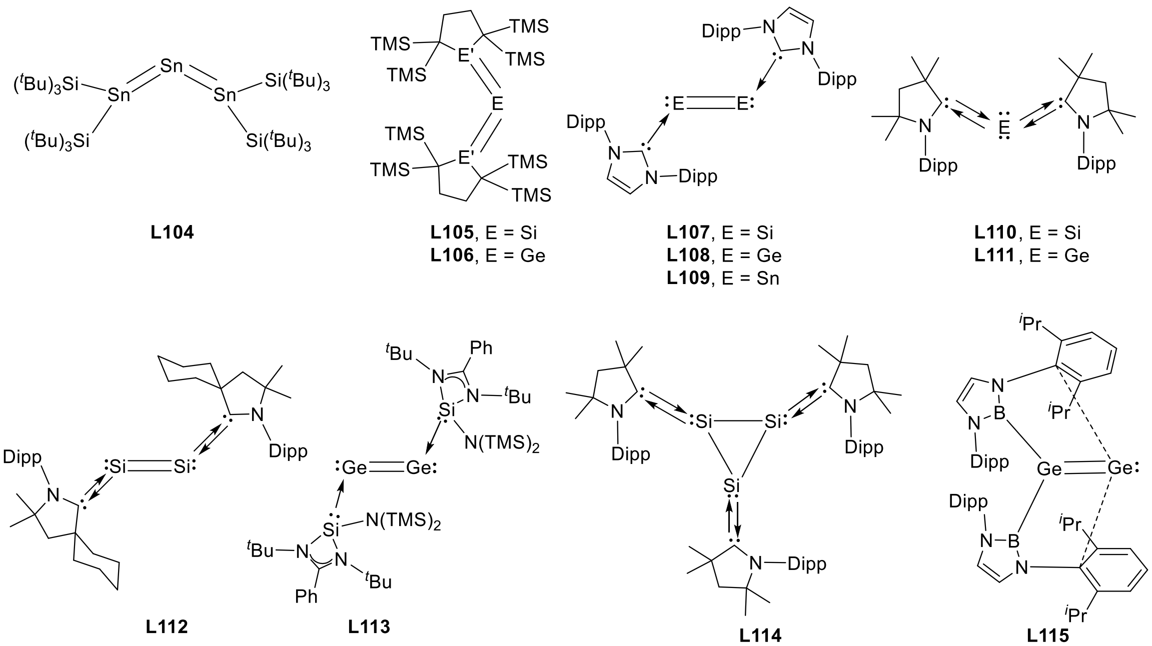

Figure 27. Selected examples of reported multinuclear zero-valent Group 14 compounds.

2.6.2 Mononuclear zero-valent Group 14 element complexes

In 2013, Driess and coworkers synthesized the first examples of cyclic silylone **L116**[120] and germylone **L117**[121] employing a chelating bis(NHC) ligand (Figure 28). Later, a coordination compound of Ge(0) **L118** stabilized by a di(imino)pyridine ligand was reported by Nikonov and coworkers.[122] Employing a similar ligand, Flock and co-workers achieved the complex **L119** containing a tin atom in the oxidation state of zero.[90] In 2016, Kinjo and coworkers reported on the synthesis of a Ge(0) species **L120** supported by a bidentate imino-*N*-heterocyclic carbene.[123] Within the same year, Saito and coworkers reported on the (η^4-butadiene)Sn(0) complexes **L121** and **L122** that uses butadiene as a 4π-electron donor to stabilize zero-valent tin center.[124] In 2017, a 1,3-digerma-2-silaallene **L123** incorporated into a five-membered ring system, was synthesized by Sasamori and Tokitoh.[125] In 2019, a novel Si(0) species **L124** with a bis(NHC)-stabilized four-membered Si ring was synthesized by Lips and coworkers.[126] In 2020, a Ge(0) compound **L125** stabilized by a di(imino)-carbene ligand was successfully prepared by the Nikonov group.[127]

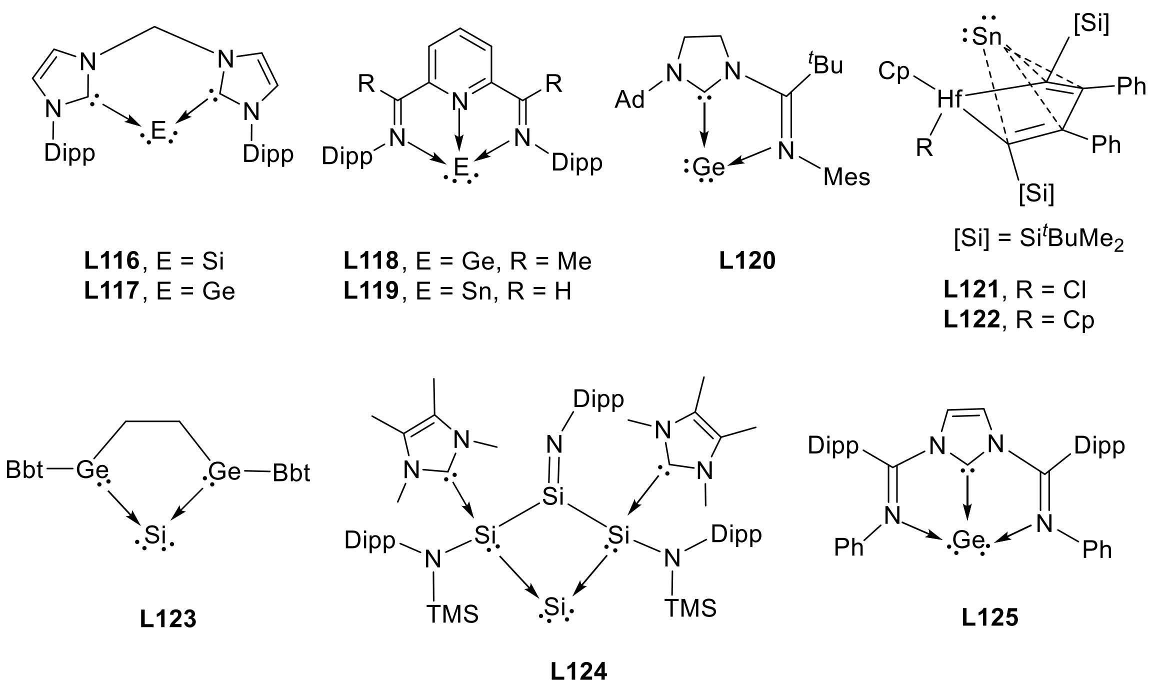

Figure 28. Selected examples of monoatomic zero-valent Group 14 compounds.

NHSis with strongly *σ*-donating nature have been widely utilized as powerful tools to stabilize zero-valent Group 14 elements.[128] In 2016, Driess and coworkers reported the bis(silylenyl)pyridine-stabilized germylone iron carbonyl complex **L126** (Figure 29).[129] Utilizing the strongly donating bis(NHSi) ligands, they developed the bis(NHSi)-stabilized zero-valent silicon **L127**,[130] germanium **L128**,[131] and tin **L129**.[132] Very recently, utilizing the *C*,*C*'-dicarborandiyl-substituted bis(NHSi) ligand, they also achieved the synthesis of the bis(NHSi)-supported silylone **L130**[133] and germylone **L131**.[134]

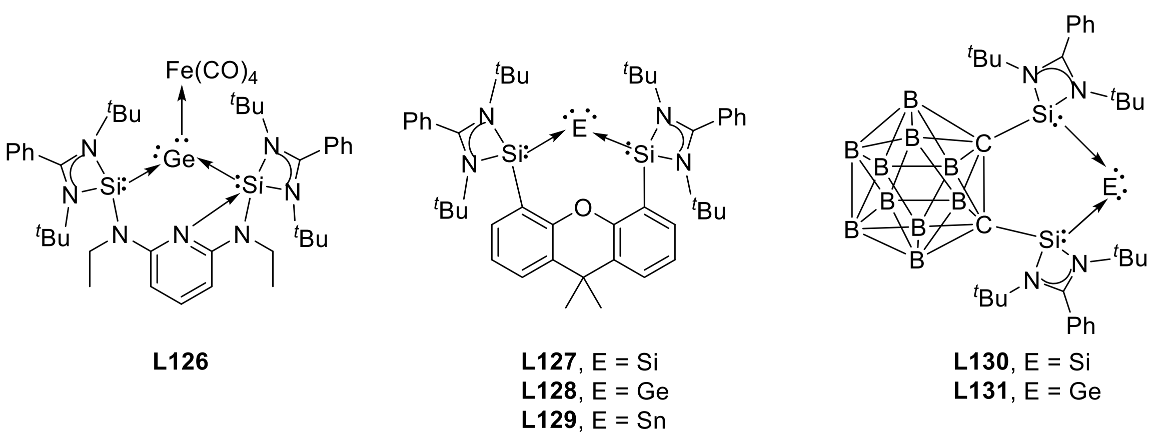

Figure 29. Examples of tetrylones reported by the Driess group.

2.7 Heavier Ketones

Carbonyl compounds are one of the most important building blocks in organic synthetic chemistry, and its chemistry has been well-established. In contrast, the analogous compounds $R_2E{=}O$ (E = Si, Ge, Sn, Pb) have been much less explored. This is mainly because of the weaker and more polar E=O double bonds based on less effective *sp*-hybridization in the heavier E elements and the greater difference in the electronegativity between O and E atoms (Figure 30).[135] For example, silanones possess a highly reactive Si=O double bond, which tends to undergo rapid head-to-tail polymerization to form stable Si–O σ-bonds with no activation barrier.[136] Based on the thermodynamic and kinetic stabilization concept, some of stable heavier ketones ($R_2E{=}X$) with a terminal heavier Group 16 element (X = S, Se, Te) have already been synthesized successfully and structurally characterized. Meanwhile, much effort has also been devoted to achieving heavier ketone homologues ($R_2E{=}O$; E = Si, Ge, Sn, Pb) with a terminal oxygen atom.[137]

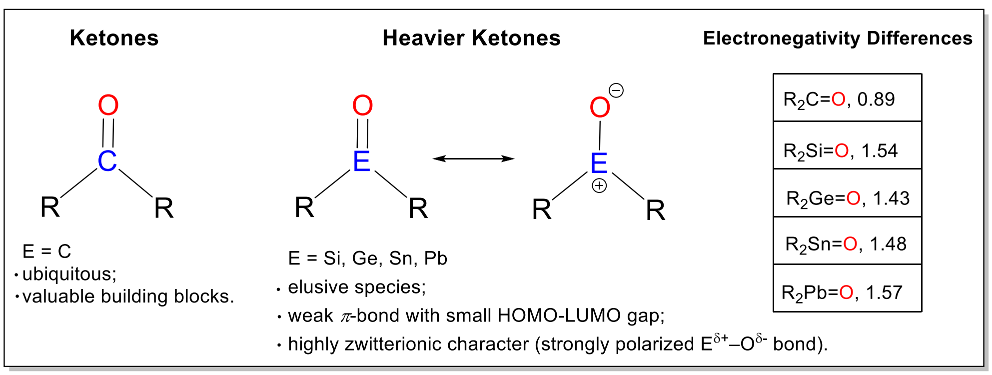

Figure 30. Comparison of ketones and heavier ketones.

At the beginning of the 20th century, organosilicon pioneer Frederic S. Kipping thought he had synthesized the first silanone, $Ph_2Si{=}O$ (Ph = phenyl),[138] but it turned out to be the polysiloxanes $(R_2SiO)_n$, one of the most important organic-inorganic hybrid polymers. Since then, the isolation of a truly monomeric silanone that is stable at room temperature has inspired generations of silicon chemists. However, the last three decades have witnessed several attempts to tame the polarized Si=O double bond by additional coordination to Lewis acids or bases, giving a variety of isolable donor-acceptor-[139] or donor-stabilized[140] complexes. The unique donor-acceptor stabilized silaformamide **L132** was accessible by treating the six-membered NHSi with an equimolar amount of the water-borane adduct H_2O@BCF (Figure 31).[141] Subsequent oxygenation with N_2O or CO_2 selectively provided the four-coordinate silanoic ester derivative **L133** *via* concomitant liberation of gaseous N_2 or CO.[142] Driess and coworkers also reported the NHC-stabilized silanone **L134**.[140] In addition, related cationic silanones and germanones, such as the NHC-stabilized sila-acylium ion **L135**[102] and germa-acylium ion **L136**[101] were synthesized by our group.

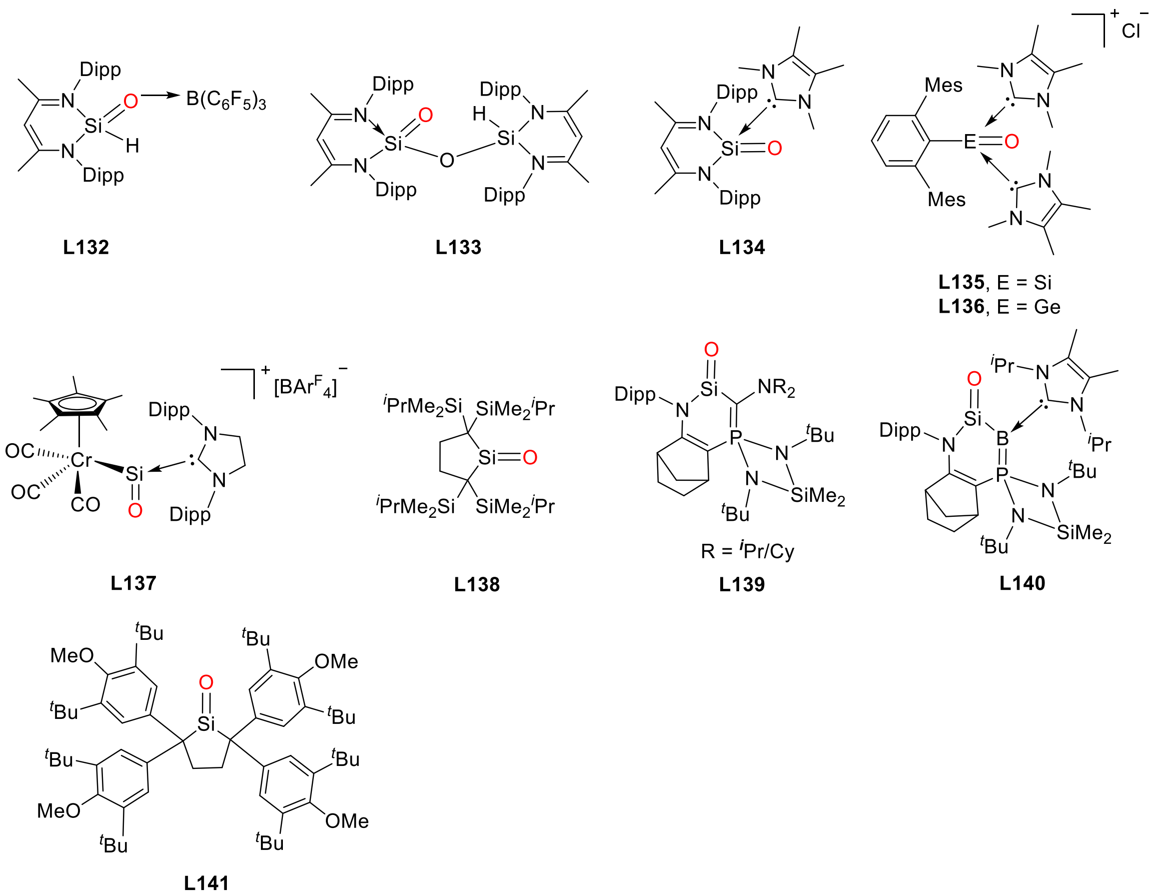

Figure 31. Examples of reported compounds containing a Si=O bond, as well as the NHC-stabilized germa-acylium ion **L136**.

Some recent approaches to form a three coordinate silylone rely on the basic idea of kinetic and thermodynamic stabilization of the Si=O moiety by only two adjacent ligands. The isolation of the NHC-stabilized cationic chromiosilanone **L137** bearing a three-coordinate silicon center was presented by Filippou and coworkers in 2014.[143] Iwamoto and Kira et al. investigated the synthesis of the cyclic donor-free dialkylsilanone **L138** stable at -80 °C.[144] However, due to the insufficient kinetic and thermodynamic stabilization of the generated silanone, only the corresponding 1,3-dioxadisiletane was observed. Moreover, Baceiredo, Kato and coworkers isolated the first cyclic three-coordinate silanones **L139**[145] and **L140**[146], which are stable at room temperature in the solid state. In 2019, Iwamoto et al. also synthesized the first room temperature stable, three-coordinate dialkylsilanone **L141** by the oxygenation of the corresponding silylene with N_2O in quantitative yield.[147]

For a long time, germanones and stannanones have often been postulated as reactive intermediates.[148] In fact, the first evidence for germanones was reported by Satgé and coworkers in 1971.[149] Since then, considerable efforts have been devoted to the isolation of germanones by the introduction of bulky protecting groups on the Ge atom.[150] For example, in 1995, Tokitoh et al. employed a sterically congested diarylgermylene **L142** to prepare the diarylgermanone **L143** (Tbt)(Tipp)Ge=O (Tbt = 2,4,6-tris[bis(trimethylsilyl)methyl]phenyl, Tipp = 2,4,6-triisopropylphenyl), which is only moderately stable in solution at room temperature and undergoes intramolecular cyclization to form benzogermacyclobutenes **L144** and **L145** (Figure 32).[151]

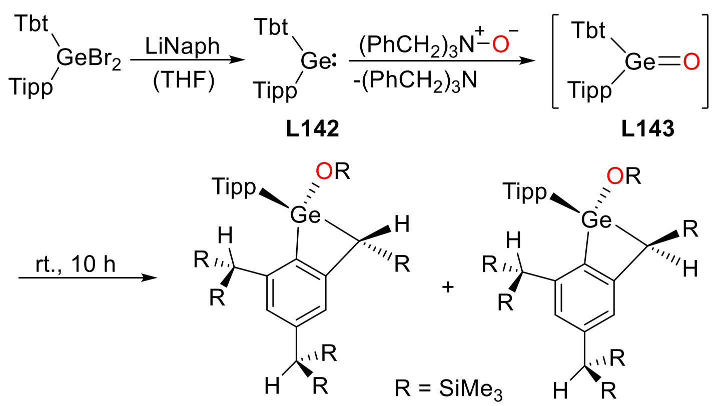

Figure 32. Formation of **L144** and **L145** *via* intramolecular cyclization of the possible intermediate **L143**.

Furthermore, in 2001, Schmidbaur and coworkers described the mass spectrometric evidence for two diarylgermanones $(Bisap)_2Ge=O$ (Bisap = 2,6-bis(1-naphtyl)phenyl) and $(Triph)_2Ge=O$ (Triph = 2,4,6-triphenylphenyl), resulted from oxygenation of the corresponding diarylgermylenes with N_2O.[152] Although the two compounds have been obtained as solids, their molecular structures have not been confirmed by X-ray diffraction analysis yet.

As for the stannanones, in 1996, Schleyer et al. investigated the relative stability of $R_2Sn=O$ (R = H, CH_3) by DFT pseudopotential calculations, which revealed that the formation of dimethylstannanone is unfavorable, and unsaturated species with double bonds between oxygen and tin are not likely to exist, whatever the substituents or conditions might be.[153] Despite the significant advances made in the field, the synthesis of stable germanones and stannanones is notoriously difficult and challenging.[154]

During the last decade, several germylenes have been synthesized and probed for their applicability in the synthesis of germanones. A breakthrough towards four-coordinate germanones was achieved by Driess and coworkers, stabilizing the Ge=O moiety using a Lewis base that coordinated to the electron-deficient Ge center to form a distorted geometry. For example, in 2009, they reported the facile synthesis and structural characterization of the first NHC-stabilized germanones **L148** and **L149**, starting from the corresponding NHC-germylene precursors **L146** and **L147** through oxygenation with N_2O (Figure 33).[155]

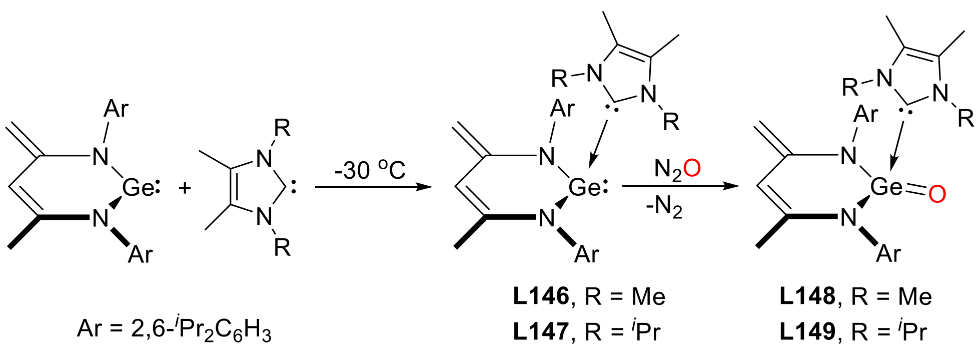

Figure 33. Synthesis of the NHC-stabilized germanones **L148** and **L149**.

Two years later, they also reported on the synthesis of the first germanone-pyridine complex **L151**, which resulted from oxygenation of the DMAP-germylene precursor **L150**.[156] Furthermore, they also described the unexpected reactivity of **L151** towards trimethylaluminum ($AlMe_3$), which solely gives the adduct product **L152** (Figure 34).

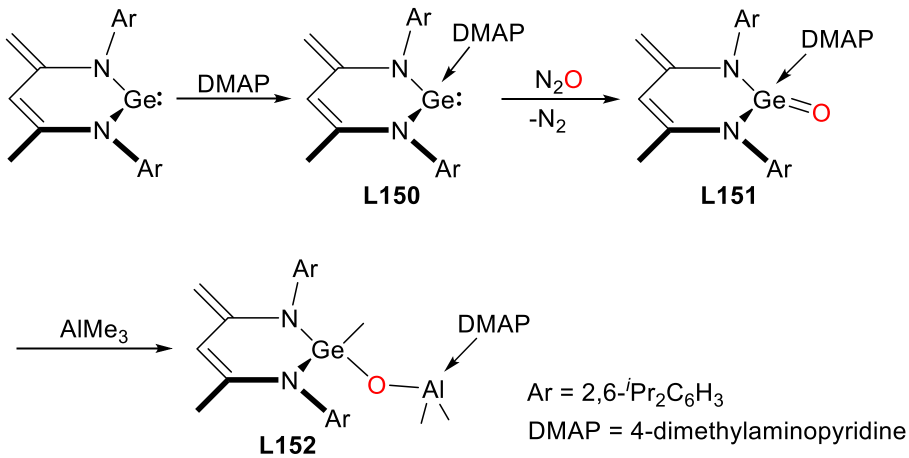

Figure 34. Synthesis of the DMAP-stabilized germanone **L151**, and its addition reaction with $AlMe_3$.

In 2012, Tamao et al. reported the first isolation of a "genuine" germanone **L154** with the planar three-coordinate Ge atom and a terminal oxygen atom, which was stabilized by two rigid and bulky 1,1,3,3,5,5,7,7-octaethyl-*s*-hydrindacen-4-yl (Eind) groups (Figure 35).[157] As expected, the resulted germanone **L154** can be reduced by $LiAlH_4$ and undergo addition reactions with diverse substrates (such as H_2O, Me_2CO, $PhSiH_3$, CO_2) to furnish the corresponding addition products **L157-160**.

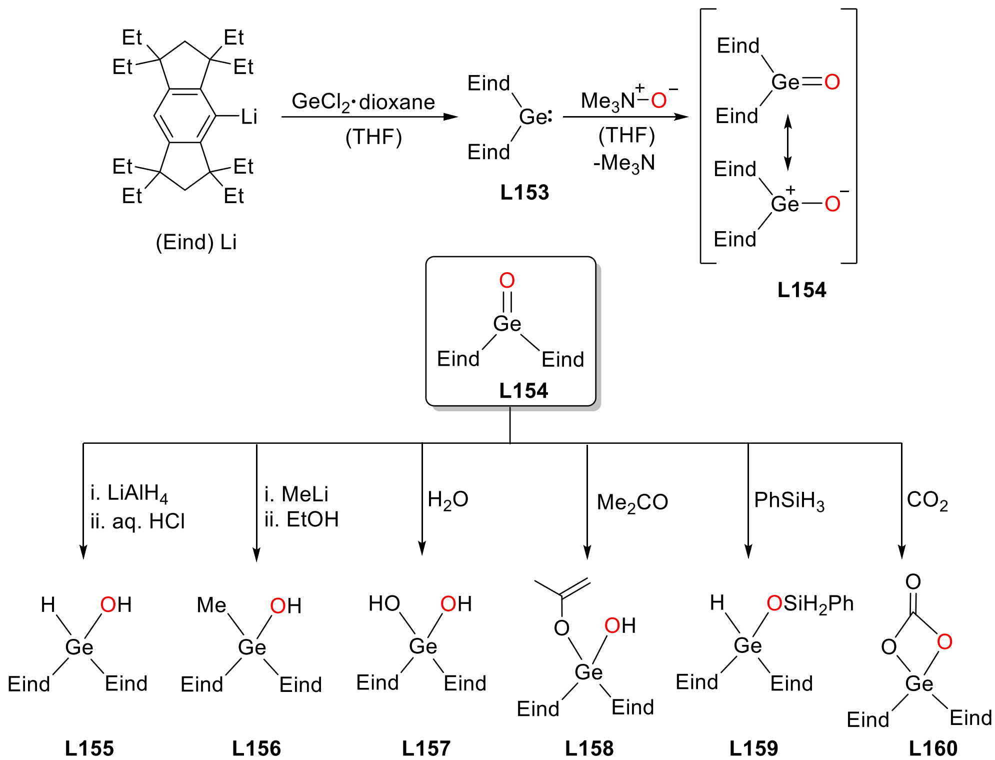

Figure 35. Synthesis and reacrivity of the first three-coordinate germanone **L154**.

In 2019, Aldridge et al. reported on the synthesis of *N*-heterocyclic germylene **L161** featuring two diazaborolyl groups, $\{(HCDippN)_2B\}$, as the N-bound substituents (Figure 36).[158] The reactivity of **L161** towards oxygen atom transfer agents was examined, with 2:1 reaction stoichiometries being observed for both Me_3NO and pyridine *N*-oxide (pyO), leading to the formation of products **L162** and **L163** thought to be derived from the activation of the C–H bonds by a transient germanone.

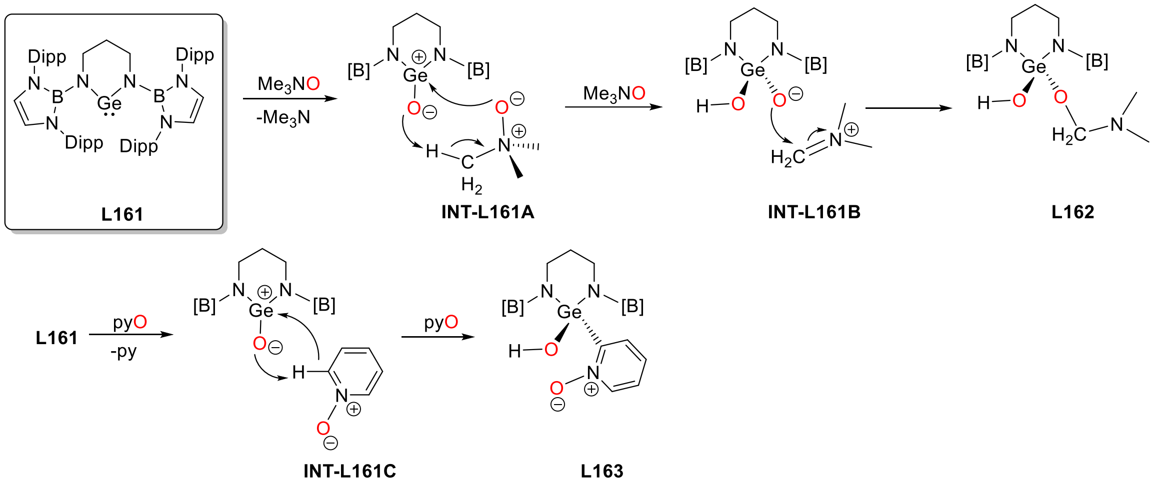

Figure 36. Proposed mechanism for the reaction of **L161** with Me_3NO or pyridine *N*-oxide.

In 2020, our group reported the first acceptor-free heavier germanium analogue of an acylium ion **L165** (Figure 37).[101] The polarized terminal GeO bond in the germa-acylium ion **L165** was utilized to activate CO_2 and silane, with the former found to be an example of reversible activation of CO_2, thus mimicking the behavior of transition-metal oxides. Furthermore, its transition-metal like nature is demonstrated as it was found to be an active catalyst in both CO_2 hydrosilylation and reductive *N*-functionalization of amines using CO_2 as the C1 source. Mechanistic studies were undertaken both experimentally and computationally, which revealed that the reaction proceeds *via* an NHC-siloxygermylene [(NHC)ArGe(OSiHPh$_2$)] **L166**.

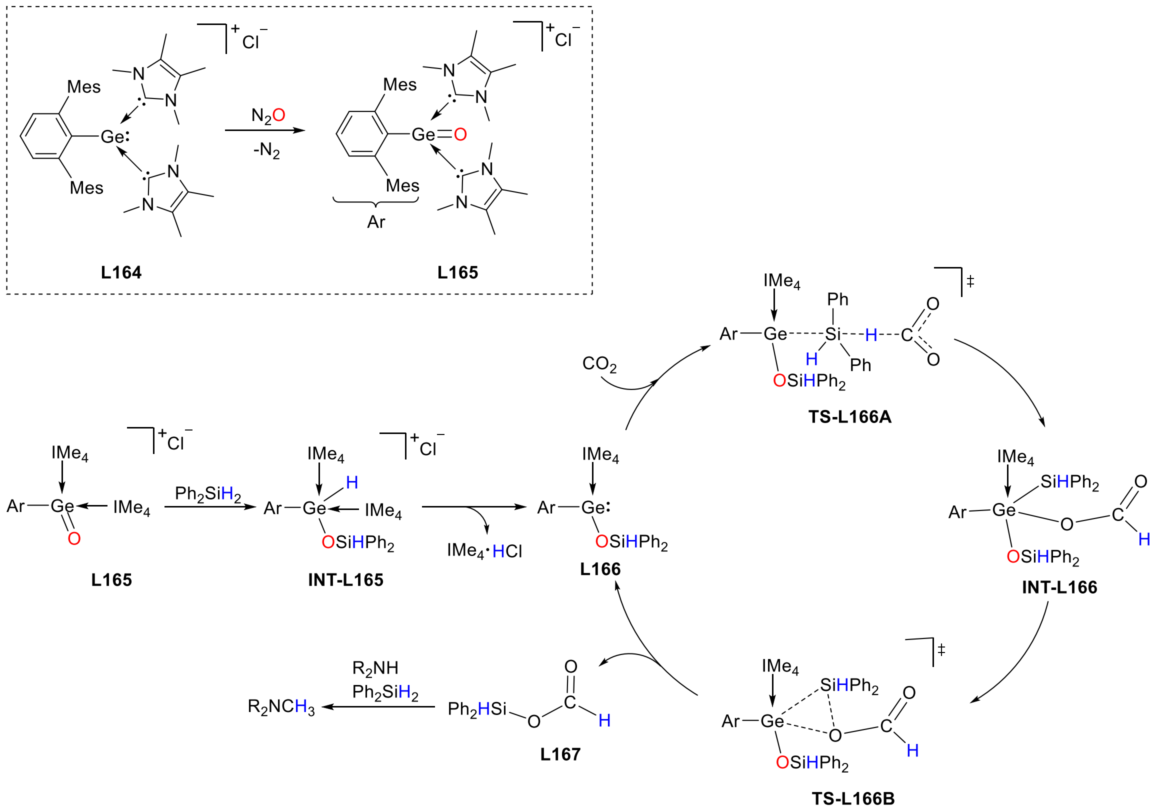

Figure 37. Synthesis of NHC-stabilized germa-acylium ion **L165**, as well as proposed mechanism for the germanium-catalyzed *N*-functionalization of amine with CO_2.

Compared with silanones and germanones, investigations on stable stannanones have been scarcely reported to date. The only experimental evidence for the existence of Sn=O double bond was obtained by Hahn and coworkers through the intramolecular trapping reaction in 2008.[159] They prepared a lutidine-linked bisstannylene ligand **L168** with pincer topology, which is capable of binding and stabilizing Sn=O moiety to form isolable molecular complex **L169** (Figure 38). Like the donor- and acceptor-stabilized silanones and germanones mentioned above, the divalent species **L169** features a formal Sn=O subunit with the tin atom and the oxygen atom stabilized by Lewis bases and acids, respectively.

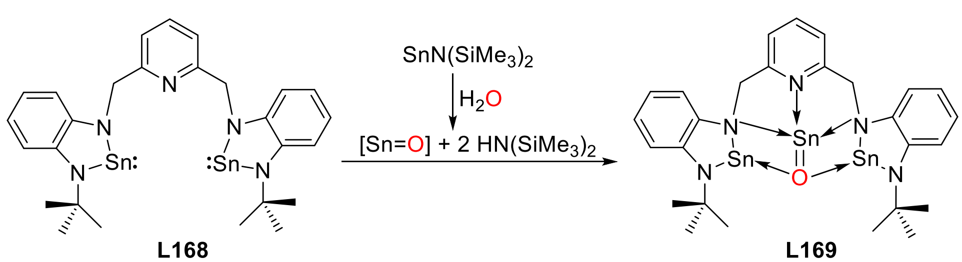

Figure 38. Synthesis of the species **L169** with a formal Sn=O subunit.

3. Scope of This Work

Main group chemistry has been well developed in recent times, which has even garnered much attention from industry. As highlighted in the prior chapters, low-valent germanium and tin compounds can mimic transition-metals. Thus, this thesis aims to synthesize low-valent germanium and tin compounds, namely tetrylenes, tetrylenoids, tetrylones, and tetryliumylidenes. The study here is to understand the effect of different ligands on the stability and reactivity of the resulting complexes. A particular emphasis is laid on the activation of small molecules (H_2, CO, CO_2, N_2O, NH_3, *etc.*), as this is a fundamental elementary step in catalytic cycles. The obtained knowledge of how these low-valent species activate bonds can then be further applied towards catalysis (Figure 39).

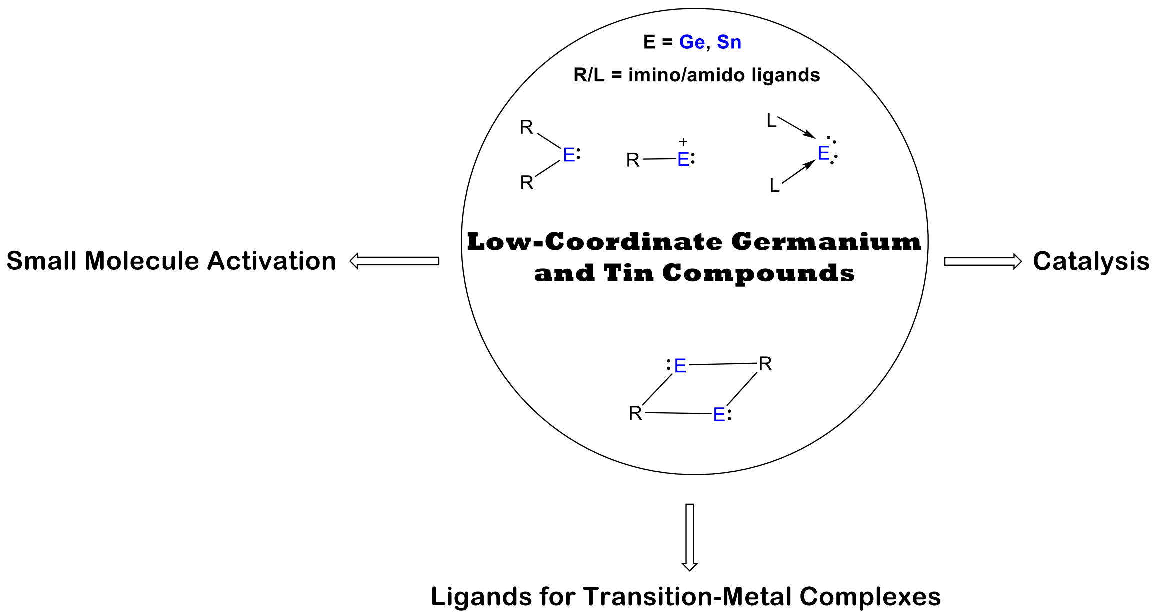

Figure 39. Scope of this thesis on N-donor substituted low-valent germanium and tin compounds.

Another major goal of this work is the isolation of a room temperature stable, three-coordinate germanone and stannanone by using NHI ligands. In contrast to the ubiquitous lighter homologous carbonyls, a donor and/or acceptor-free germanone or stannanone is still less explored. Particularly because of their high reactivity (decomposition or favorable polymerization), the synthesis of germanone and stannanone remains a challenge for main group chemists. A potential approach to gain access to these elusive species will be the oxygenation of the corresponding tetrylenes with various oxidizing agents, such as CO_2, N_2O, and Me_3NO et al. (Figure 40, right). Isolation could be feasible with a suitable ligand framework that ensures adequate stabilization. Following the successful synthesis, a detailed reactivity study of the unique heavy ketones will be performed.

Similar with the sila-wittig reaction, it is possible to study the reactivity of germanones and stannanones in terms of germa- and stanna-wittig type reactions (Figure 40, left). At the beginning of the investigations, it will focus on the oxygen transfer reactions of the prepared germanones and stannanones. Based on this stage, it will attempt the catalytic oxygenation of organic substrates in the presence of oxidants. For example, the oxygen atom of E=O compounds can be transferred to alkene, alkyne, or other unsaturated compounds, resulting the either epoxides or heterocycle containing oxygen (Figure 40, right). In addition, it is also possible to oxidize other general organic molecules to produce the corresponding oxidation products in the presence of this catalytic system.

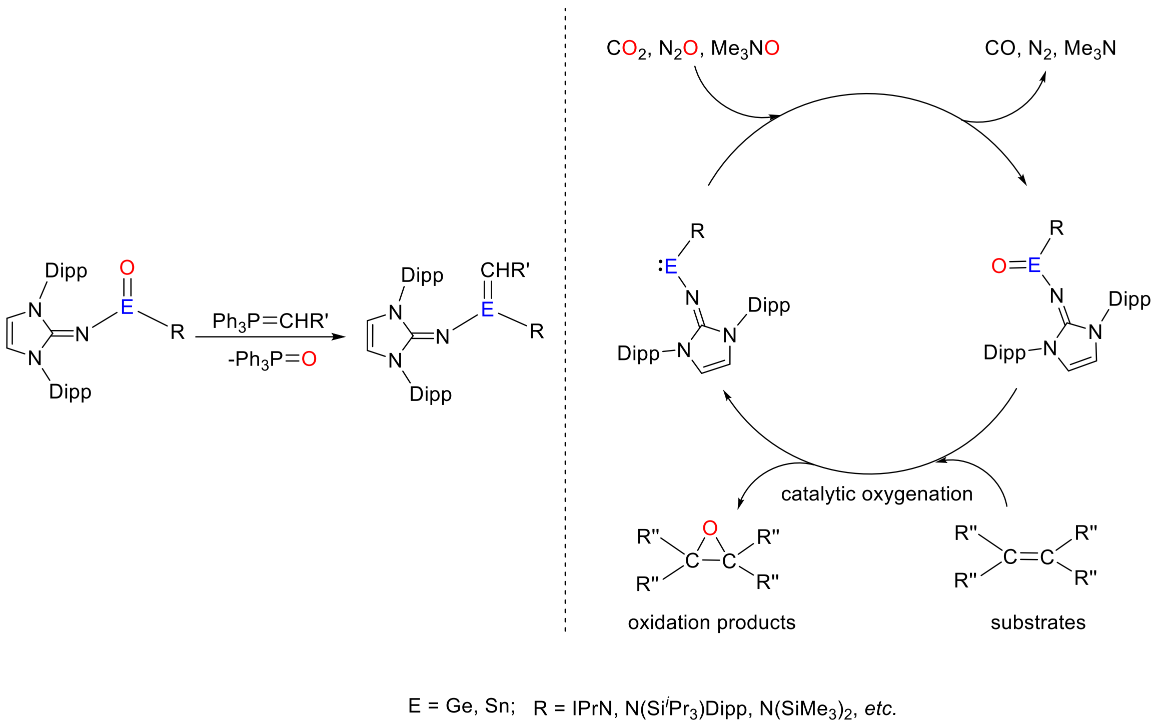

Figure 40. Targeted synthetic approach for unprecedented acyclic, two-coordinate germanone or stannanone *via* oxygenation of the corresponding tetrylenes, and planned reactivity including a potential catalytic cycle.

Overall, this work is intended to gain a deeper understanding of the chemistry of low-coordinate germanium and tin compounds. The fundamental differences and/or similarities between germanium/tin and its lighter congener carbon/silicon should be revealed, which could eventually facilitate the synthesis of novel compounds and applications in homocatalysis. Moreover, the potential of these low-coordinate germanium and tin compounds as mimics of transition-metal complexes will be further investigated. The knowledge obtained in this project could open new avenues, which ideally make the development of novel catalytic processes with these low-coordinate germanium and tin compounds.

4. An Isolable Three-Coordinate Germanone and Its Reactivity

Title: An Isolable Three-Coordinate Germanone and Its Reactivity

Status: Communication, published online September 16, 2021

Journal: Chemistry - A European Journal, 2021, 27, 15914-15917.

Publisher: John Wiley & Sons, Inc.

DOI: 10.1002/chem.202102972

Authors: Xuan-Xuan Zhao, Tibor Szilvási, Franziska Hanusch, Shigeyoshi Inoue*

Content:

A rare three-coordinate germanone $[IPrN]_2Ge{=}O$ (IPrN = bis(2,6-diisopropylphenyl)imidazolin-2-imino) was successfully isolated. The germanone has a rather high thermal stability in arene solvent, and no detectable change was observed at 80 °C for at least one week. However, high thermal stability of $[IPrN]_2Ge{=}O$ does not prevent its reactivity toward small molecules. Structural analysis and initial reactivity studies revealed the highly polarized nature of the terminal Ge=O bond. Besides, the addition of phenylacetylene, as well as O-atom transfer with 2,6-dimethylphenyl isocyanide make it a mimic of nucleophilic transition-metal oxides. Mechanism for O-atom transfer reaction was investigated *via* DFT calculations, which revealed that the reaction proceeds *via* a [2+2]-cycloaddition intermediate.

* X.-X. Zhao planned and executed all experiments including analysis and wrote the manuscript. F. Hanusch conducted all SC-XRD measurements and managed the processing of the respective data. T. Szilvási designed and performed the theoretical analysis and contributed to the manuscript. All work was performed under the supervision of S. Inoue.

Chemistry–A European Journal | Communication
doi.org/10.1002/chem.202102972

Chemistry Europe
European Chemical Societies Publishing

An Isolable Three-Coordinate Germanone and Its Reactivity

Xuan-Xuan Zhao,[a] Tibor Szilvási,[b] Franziska Hanusch,[a] and Shigeyoshi Inoue*[a]

Abstract: A rare three-coordinate germanone $[IPrN]_2Ge{=}O$ (IPrN = bis(2,6-diisopropylphenyl)imidazolin-2-imino) was successfully isolated. The germanone has a rather high thermal stability in arene solvent, and no detectable change was observed at 80 °C for at least one week. However, high thermal stability of $[IPrN]_2Ge{=}O$ does not prevent its reactivity toward small molecules. Structural analysis and initial reactivity studies revealed the highly polarized nature of the terminal Ge=O bond. Besides, the addition of phenylacetylene, as well as O-atom transfer with 2,6-dimethylphenyl isocyanide make it a mimic of nucleophilic transition-metal oxides. Mechanism for O-atom transfer reaction was investigated via DFT calculations, which revealed that the reaction proceeds via a [2+2] cycloaddition intermediate.

Whereas carbonyl compounds are irreplaceable and highly versatile building blocks in today's organic synthesis, their heavier analogues ($R_2E{=}O$, E = group 14 element), are still rare and have been much less explored. Specifically germanones ($R_2Ge{=}O$), were long thought to be elusive and unstable intermediates,[1] until the first evidence of organogermanium oxides was reported by Satgé in 1971.[2] The high reactivity stems from the unfavorable $p\pi$-$p\pi$ overlap between oxygen and electropositive germanium atoms, that results in weak and polarized Ge–O bonds.[3] Thermodynamic and kinetic stabilization was utilized to prevent their oligomerization/polymerization,[3g] thus affording several milestones in germanone chemistry. Besides the stable heavier ketones $R_2Ge{=}X$ with a terminal heavier group 16 element (X=S, Se, or Te),[4] the isolation of several donor-acceptor- or solely donor-stabilized Ge=O complexes has been achieved by employing additional Lewis acids or bases.[5] Following this strategy, the seminal breakthrough towards tetra-coordinate germanones **I** was described by Driess in 2009 (Scheme 1). Coordination of NHC or 4-*N*,*N*-dimethylaminopyridine (DMAP) results in a distorted tetrahedral geometry around the electron-deficient germanium center.[5a,b]

More recently, we have shown the successful isolation of the NHC-stabilized germa-acylium ion **II**, which was utilized in catalytic CO_2 functionalizations (Scheme 1).[6] In 2012, Tamao, Matsuo and coworkers reported the first isolation of the "genuine" germanone **III** with a three-coordinate germanium atom multiply bonded to oxygen, which is stabilized by the rigid and bulky Eind groups (Eind = 1,1,3,3,5,5,7,7-octaethyl-*s*-hydrindacen-4-yl; Scheme 1).[7a] The landmark discovery opened the door for the chemistry of heavier group 14 carbonyls.[8] Whilst significant advances have been made, the isolation of acid-base free germanones still remains challenging.

In 2017, we successfully isolated the first stable neutral acyclic three-coordinate silanones by combining π-donating *N*-heterocyclic imino (NHI) and σ-donating silyl groups.[8e] Moreover, in 2018, the group of Dielmann reported two NHI supported Lewis base free oxophosphonium monocations, which represent the first example of a phosphacarbonyl species.[9] Motivated by these results, we set out to stabilize the polarized Ge=O moiety by using two NHI ligands.[10] Accordingly, we found that the bis(imino)germylene,[11] reported by the group of Rivard, could be an ideal precursor for our targeted three-coordinate germanones. Herein we disclose the isolation, structural characterization, and initial reactivity study of a three-coordinate germanone with two NHI ligands.

The bis(imino)germylene **1** was synthesized in a modified literature-known procedure.[11] Reaction of $GeCl_2$•dioxane with two equivalents of IPrNLi (IPrN = bis(2,6-diisopropylphenyl) imidazolin-2-imino) in dry THF gave **1** in high yield (88%). Indeed, treatment of a toluene solution of **1** with gaseous N_2O (1.0 bar) at room temperature led to the desired product **2** as

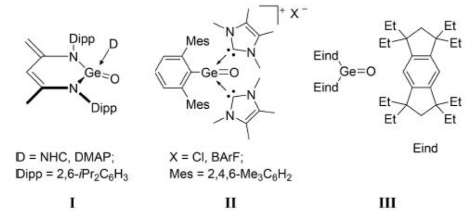

Scheme 1. Selected examples of germanones, as well as the NHC-stabilized germa-acylium Ion II.

[a] X.-X. Zhao, F. Hanusch, Prof. Dr. S. Inoue
Department of Chemistry
WACKER-Institute of Silicon Chemistry and Catalysis Research Center
Technische Universität München
Lichtenbergstraße 4, 85748 Garching bei München (Germany)
E-mail: s.inoue@tum.de

[b] Prof. Dr. T. Szilvási
Department of Chemical and Biological Engineering
University of Alabama
Tuscaloosa, AL 35487 (USA)

Supporting information for this article is available on the WWW under https://doi.org/10.1002/chem.202102972 an orange solid (89%; Scheme 2). The bis(imino)germanone **2** has a rather high thermal stability in arene solvent; no detectable change was observed in the ^{1}H NMR spectrum of **2** in C_6D_6 at 80 °C for at least one week. The characteristic Ge=O stretching vibration was found at 912 cm^{-1} in the IR spectrum (calc. 907 cm^{-1}), which is comparable to the reported Ge=O stretching in $Eind_2Ge$=O (**III**; 916 cm^{-1}).

Pale-yellow crystals of **2** were obtained from a saturated solution in Et_2O at −30 °C. Single crystal X-ray diffraction (SC-XRD) analysis unambiguously confirmed the monomeric structure of **2** in the solid state (Figure 1a).[12] In addition, the Ge=O moiety in **2** lies within a protecting pocket formed by the flanking shielding ligands (Figure 1b). The molecular structure revealed a trigonal planar geometry at the germanium center (sum of bonding angles: 360°) and the Ge1–O1 bond length of **2** (1.6494(10) Å), which is almost identical to that in $Eind_2Ge$=O (**III**; 1.6468(5) Å), and generally shorter than that in base-stabilized tetra-coordinate germanones (1.664–1.718 Å).[5] The Ge–N bonds (Ge1–N1 1.7819(12) Å / Ge1–N4 1.7825(12) Å) are shortened and neighboring N–C bonds (N1–C1 1.2872(18) Å / N4–C28 1.2914(18) Å) are elongated, compared to that in precursor **1** (Ge–N: 1.8194(15) Å; N–C: 1.273(2) Å), thus suggesting admixture of a partial metalimide character in the neutral complex **2**.[10]

Density Functional Theory (DFT) calculations were performed to understand the electronic structure of **2**. We found that the Wiberg Bond Index (WBI; Table S3) indicates partial double bond character for Ge=O (1.30). Natural Population Analysis showed a positive Ge center (+1.89; Table S3) and a negatively charged O center (−1.02), whereas Natural Bond Orbital analysis shows only one Ge–O bond (Table S2). Analyzing the molecular orbitals (Figure S35) shows that the HOMO is mainly located on the π-system of the IPrN groups, while the LUMO is associated with the π-system of the phenyl rings of **2**. HOMO−3 and LUMO+9 are the orbitals that are directly associated with the Ge=O π-bonding (Figure S35), which depict an O-dominated π-orbital and a Ge-dominated π*-orbital, respectively. Interestingly, HOMO−3 and LUMO+9 indicate very little coupling to the N atoms of the IPrN groups, which also suggests that Ge=O can be described as a double bond although the zwitterionic resonance structure **2'** (Scheme 2) should not be neglected based on the other computational metrics.

The polarized Ge=O bond of **2** is reflected by the following reactivity study (Scheme 3 and 4). The products in all cases were identified by multinuclear and 2D NMR spectroscopy, and elemental analysis (EA; see Supporting Information for details). Germanone **2** shows reactivity toward pinacolborane (HBpin), bromotrimethylsilane (TMSBr) and phenylsilane ($PhSiH_3$), with polarized B–H, Si–Br or Si–H single bonds, to immediately afford the corresponding 1,2-adducts **3**, **4** and **5** at room temperature. The ^{1}H NMR signal of the Ge–H bond in **3** appears at 5.04 ppm, which is similar to that in **5** (4.78 ppm).

Compared to the analog $PhSiH_3$ reaction product of **III** ($Eind_2Ge(H)OSiH_2Ph$; Ge–H: 7.94 ppm), the Ge–H signal in **5** is significantly upfield shifted, which could be attributed to the strongly π-electron donating NHI ligands. In consequence, full conversion of **2** to **5** was observed after 30 min, whereas **III** was

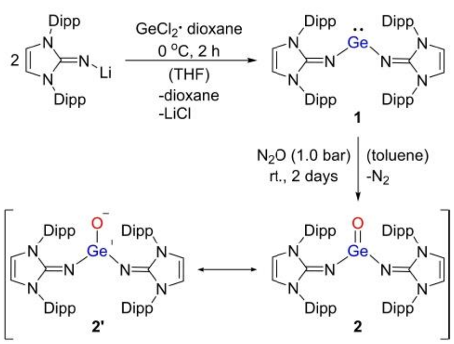

Scheme 2. Synthesis of bis(imino)germanone **2** from bis(imino)germylene **1**.

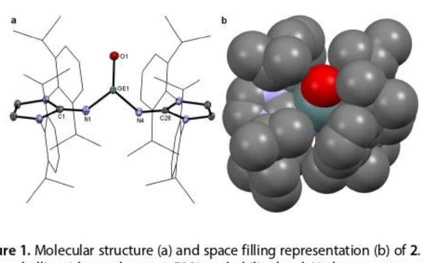

Figure 1. Molecular structure (a) and space filling representation (b) of **2**. Thermal ellipsoids are shown at 50% probability level. Hydrogen atoms are omitted for clarity. Selected bond lengths [Å] and angles [°]: Ge1–O1 1.6494(10), Ge1–N1 1.7819(12), Ge1–N4 1.7825(12), N1–C1 1.2872(18), N4–C28 1.2914(18), O1–Ge1–N1 125.94(6), O1–Ge1–N4 125.41(6), N1–Ge1–N4 108.65(6), Ge1–N1–C1 127.81(10), Ge1–N4–C28 125.02(10).

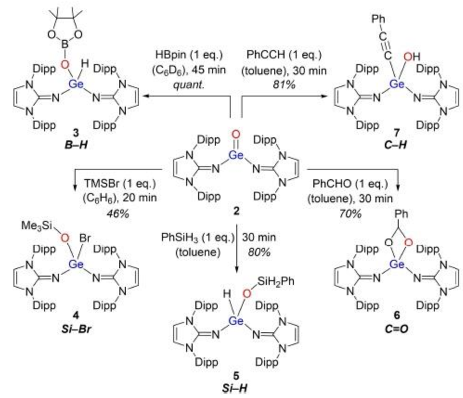

Scheme 3. Reactivity of bis(imino)germanone **2**.

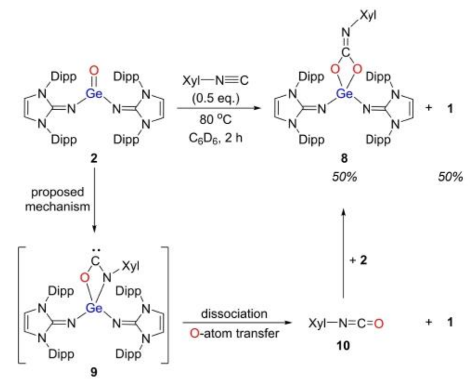

Scheme 4. Reaction of bis(imino)germanone **2** with 2,6-dimethylphenyl isocyanide (CNXyl).

reacted for one day with $PhSiH_3$ until completion of the reaction could be confirmed.[7a]

Moreover, **2** reacted with the C=O bond of benzaldehyde (PhCHO), to smoothly furnish the cyclic product **6**. The formation of the four-membered heterocycle in **6** was confirmed by $^1H/^{13}C$ HSQC and HMBC NMR spectroscopy, revealing a singlet at 99.7 ppm for the ring carbon atom, and a singlet at 5.10 ppm for the ring proton.

Since the formation of products **3** to **6** can be attributed to the highly polarized $Ge^{\delta+}$–$O^{\delta-}$ bond, it has been the scope to test the reactivity of **2** towards other small molecules. Treatment of **2** with H_2 and NH_3 showed no conversion and reaction with CO_2 formed an unidentified product mixture. Upon exposure towards MeOH, germanone **2** was directly converted into the imine IPrNH as a result of high proton affinity of the imidazolin-2-iminato ligand. However, the reaction of **2** with a terminal alkyne (phenylacetylene, PhCCH) at room temperature resulted in direct conversion to the hydroxoacetylide complex **7** in good yield (81%; Scheme 3). The acetylide complex **7**, identified by 2D NMR spectroscopy, shows a sharp OH signal in the ^1H NMR spectrum at -0.77 ppm (C_6D_6). This reactivity is reminiscent of pyridine-stabilized Ti(IV) oxo complex Cp^*_2(pyridine)Ti=O ($Cp^* = \eta^5$-C_5Me_5) reported by Bergman and coworkers.[13]

More interestingly, reaction of **2** with 0.5 equivalent of 2,6-dimethylphenyl isocyanide (CNXyl) led to a mixture of the [2+2] cycloaddition product **8** (50% NMR yield) and the O-atom transfer product **1** (50% NMR yield; Scheme 4). Several attempts to separate product **8** from the reaction mixture remained unsuccessful. To clarify the mechanism, we performed the reaction of **2** with commercially available **10** (1 equiv.) at room temperature, which immediately resulted in the desired compound **8** in nearly quantitative yield.

Computational analysis using DFT was carried out to understand the reactivity of **2** with CNXyl (Figure S34). We found that the [2+2] cycloaddition product **9** is an energetically favored intermediate (−15.4 kcal/mol), while the dissociation and formal O-atom transfer leads to **10** (−28.0 kcal/mol), which can react with another molecule of **2** to provide the thermodynamically stable product **8** (−52.3 kcal/mol). We note that the calculated high barriers (20.5 kcal/mol and 22.5 kcal/mol) are in general agreement with the observed very slow reaction at room temperature and reaction mechanism can explain the observed mixture of products (**1**+**8**). We also studied other possible pathways but all attempts to locate the direct coordination of CNXyl to Ge and a GeOC three membered ring intermediate with an exocyclic=NXyl unit were not successful. Additionally, we found a direct O-atom transfer mechanism, but it was less favorable than the cycloaddition pathway (26.0 kcal/mol; Figure S34).

For comparison, the reactivity of a rhenium(III) terminal oxo complex, (η^2-DHF)(BDI)Re=O, (DHF=dihydrofulvalene; BDI=*N,N'*-bis(2,6-diisopropylphenyl)-2,4-dimethyl-β-diketiminate) with isocyanides, R–NC (R=^{t}Bu, 2,6-xylyl) was described in 2018.[14] This is suggested to be initiated by the nucleophilic character of the rhenium oxo moiety. Moreover, similar reactions of (Tbt)(Tip)Ge=X (X=S, Se; Tbt=2,4,6-tris[bis(trimethylsilyl)methyl]phenyl; Tip=2,4,6-triisopropylphenyl) and PhN=C=S have been reported by Tokitoh.[3d] Therefore, in this reaction, germanone **2** acted not only as a heavy ketone, but also as a mimic of nucleophilic transition metal oxides (TMO). In fact, the O-atom transfer reaction with isocyanides is prototypical for TMO.

To clarify the reaction mechanism of O-atom transfer by aiming at the isolation of isocyanide complexes similar to known silicon derivatives,[15] we conducted the reaction of **1** with CNXyl. Surprisingly, **1** does not react with CNXyl (1 equiv.) even at elevated temperatures.

In summary, we have achieved the synthesis and isolation of bis(imino)germanone **2** with a trigonal planar geometry. Thanks to the efficient stabilization by two bulky and strongly π-donating NHI substituents, germanone **2** is remarkable stable in arene solvent for at least one week. High stability makes it easier to handle and allows us to investigate its reactivity towards various molecules. The addition reactions of **2** with pinacolborane (HBpin), bromotrimethylsilane (TMSBr), phenylsilane ($PhSiH_3$), and benzaldehyde (PhCHO) demonstrated polarized $Ge^{\delta+}$–$O^{\delta-}$ reactivity. In addition, the conversion of phenylacetylene (PhCCH), as well as the O-atom transfer reaction with 2,6-dimethylphenyl isocyanide (CNXyl) displayed its transition metal oxide-like behavior. This similarity may provide new opportunities for main group metal mediated catalytic applications in the future.

Acknowledgements

We gratefully acknowledge financial support from the Deutsche Forschungsgemeinschaft (In 234/7-1) and the European Research Council (SILION 637394). X.Z. gratefully acknowledges financial support from the China Scholarship Council. T.S. would like to thank the University of Alabama and the Office of Information Technology for providing high performance computing resources and support that have contributed to these research results. This work was made possible in part by a grant of high-performance computing resources and technical support from the Alabama Supercomputer Authority. We thank Maximilian Muhr for the LIFDI-MS measurements. Open Access funding enabled and organized by Projekt DEAL.

Conflict of Interest

The authors declare no conflict of interest.

Keywords: carbonyls · germanone · *N*-heterocyclic imines · O-atom transfer · small molecule activation

[1] a) D. Ellis, P. B. Hitchcock, M. F. Lappert, *J. Chem. Soc. Dalton Trans.* **1992**, 3397–3398; b) N. Tokitoh, T. Matsumoto, R. Okazaki, *Chem. Lett.* **1995**, *24*, 1087–1088; c) P. Jutzi, H. Schmidt, B. Neumann, H.-G. Stammler, *Organometallics* **1996**, *15*, 741–746; d) L. Pu, N. J. Hardman, P. P. Power, *Organometallics* **2001**, *20*, 5105–5109; e) G. L. Wegner, R. J. F. Berger, A. Schier, H. Schmidbaur, *Organometallics* **2001**, *20*, 418–423.

[2] J. Barrau, M. Massol, D. Mesnard, J. Satgé, *J. Organomet. Chem.* **1971**, *30*, C67–C69.

[3] a) J. Barrau, J. Escudie, J. Satge, *Chem. Rev.* **1990**, *90*, 283–319; b) J. Barrau, G. Rima, *Coord. Chem. Rev.* **1998**, *178*, 593–622; c) P. P. Power, *Chem. Rev.* **1999**, *99*, 3463–3503; d) R. Okazaki, N. Tokitoh, *Acc. Chem. Res.* **2000**, *33*, 625–630; e) N. Tokitoh, R. Okazaki, *Adv. Organomet. Chem.* **2001**, *47*, 121–166; f) R. C. Fischer, P. P. Power, *Chem. Rev.* **2010**, *110*, 3877–3923; g) Y. Xiong, S. Yao, M. Driess, *Angew. Chem. Int. Ed.* **2013**, *52*, 4302–4311; *Angew. Chem.* **2013**, *125*, 4398–4407; h) Y. K. Loh, S. Aldridge, *Angew. Chem. Int. Ed.* **2021**, *60*, 8626–8648; *Angew. Chem.* **2021**, *133*, 8708–8730; i) M. Driess, H. Grutzmacher, *Angew. Chem. Int. Ed.* **1996**, *35*, 828–856; *Angew. Chem.* **1996**, *108*, 900–929.

[4] a) N. Tokitoh, T. Matsumoto, K. Manmaru, R. Okazaki, *J. Am. Chem. Soc.* **1993**, *115*, 8855–8856; b) T. Matsumoto, N. Tokitoh, R. Okazaki, *Angew. Chem. Int. Ed.* **1994**, *33*, 2316–2317; *Angew. Chem.* **1994**, *106*, 2418–2420; c) N. Tokitoh, T. Matsumoto, R. Okazaki, *J. Am. Chem. Soc.* **1997**, *119*, 2337–2338; d) N. Fujita, L. Li, N. Lentz, S. Konaka, A. Kuroda, R. Ohno, N. Hayakawa, K. Tamao, D. Madec, T. Kato, A. Rosas-Sánchez, D. Hashizume, T. Matsuo, *Chem. Lett.* **2020**, *49*, 141–144; e) Y. Xiong, S. Yao, M. Karni, A. Kostenko, A. Burchert, Y. Apeloig, M. Driess, *Chem. Sci.* **2016**, *7*, 5462–5469.

[5] a) S. Yao, Y. Xiong, M. Driess, *Chem. Commun.* **2009**, 6466–6468; b) S. Yao, Y. Xiong, W. Wang, M. Driess, *Chem. Eur. J.* **2011**, *17*, 4890–4895; c) S. Sinhababu, D. Yadav, S. Karwasara, M. K. Sharma, G. Mukherjee, G. Rajaraman, S. Nagendran, *Angew. Chem. Int. Ed.* **2016**, *55*, 7742–7746; *Angew. Chem.* **2016**, *128*, 7873–7877; d) M. K. Sharma, S. Sinhababu, P. Mahawar, G. Mukherjee, B. Pandey, G. Rajaraman, S. Nagendran, *Chem. Sci.* **2019**, *10*, 4402–4411.

[6] D. Sarkar, C. Weetman, S. Dutta, E. Schubert, C. Jandl, D. Koley, S. Inoue, *J. Am. Chem. Soc.* **2020**, *142*, 15403–15411.

[7] a) L. Li, T. Fukawa, T. Matsuo, D. Hashizume, H. Fueno, K. Tanaka, K. Tamao, *Nat. Chem.* **2012**, *4*, 361–365; b) P. P. Power, *Nat. Chem.* **2012**, *4*, 343–344; c) K. K. Pandey, *Comput. Theor. Chem.* **2015**, *1073*, 20–26.

[8] a) A. C. Filippou, B. Baars, O. Chernov, Y. N. Lebedev, G. Schnakenburg, *Angew. Chem. Int. Ed.* **2014**, *53*, 565–570; *Angew. Chem.* **2014**, *126*, 576–581; b) S. S. Sen, *Angew. Chem. Int. Ed.* **2014**, *53*, 8820–8822; *Angew. Chem.* **2014**, *126*, 8964–8966; c) I. Alvarado-Beltran, A. Rosas-Sanchez, A. Baceiredo, N. Saffon-Merceron, V. Branchadell, T. Kato, *Angew. Chem. Int. Ed.* **2017**, *56*, 10481–10485; *Angew. Chem.* **2017**, *129*, 10617–10621; d) A. Rosas-Sanchez, I. Alvarado-Beltran, A. Baceiredo, N. Saffon-Merceron, S. Massou, D. Hashizume, V. Branchadell, T. Kato, *Angew. Chem. Int. Ed.* **2017**, *56*, 15916–15920; *Angew. Chem.* **2017**, *129*, 16132–16136; e) D. Wendel, D. Reiter, A. Porzelt, P. J. Altmann, S. Inoue, B. Rieger, *J. Am. Chem. Soc.* **2017**, *139*, 17193–17198; f) R. Kobayashi, S. Ishida, T. Iwamoto, *Angew. Chem. Int. Ed.* **2019**, *58*, 9425–9428; *Angew. Chem.* **2019**, *131*, 9525–9528; g) S. Takahashi, K. Nakaya, M. Frutos, A. Baceiredo, N. Saffon-Merceron, S. Massou, N. Nakata, D. Hashizume, V. Branchadell, T. Kato, *Angew. Chem. Int. Ed.* **2020**, *59*, 15937–15941; *Angew. Chem.* **2020**, *132*, 16071–16075; h) D. Reiter, P. Frisch, T. Szilvási, S. Inoue, *J. Am. Chem. Soc.* **2019**, *141*, 16991–16996.

[9] a) M. A. Wunsche, T. Witteler, F. Dielmann, *Angew. Chem. Int. Ed.* **2018**, *57*, 7234–7239; *Angew. Chem.* **2018**, *130*, 7354–7359; b) P. Lowe, M. Feldt, M. A. Wunsche, L. F. B. Wilm, F. Dielmann, *J. Am. Chem. Soc.* **2020**, *142*, 9818–9826.

[10] a) T. Ochiai, D. Franz, S. Inoue, *Chem. Soc. Rev.* **2016**, *45*, 6327–6344; b) X. Wu, M. Tamm, *Coord. Chem. Rev.* **2014**, *260*, 116–138.

[11] M. W. Lui, C. Merten, M. J. Ferguson, R. McDonald, Y. Xu, E. Rivard, *Inorg. Chem.* **2015**, *54*, 2040–2049.

[12] Deposition Number 2053427 (for **2**) contains the supplementary crystallographic data for this paper. These data are provided free of charge by the joint Cambridge Crystallographic Data Centre and Fachinformationszentrum Karlsruhe Access Structures service.

[13] J. L. Polse, R. A. Andersen, R. G. Bergman, *J. Am. Chem. Soc.* **1995**, *117*, 5393–5394.

[14] T. D. Lohrey, R. G. Bergman, J. Arnold, *Organometallics* **2018**, *37*, 3552–3557.

[15] a) C. Ganesamoorthy, J. Schoening, C. Wolper, L. Song, P. R. Schreiner, S. Schulz, *Nat. Chem.* **2020**, *12*, 608–614; b) D. Reiter, R. Holzner, A. Porzelt, P. Frisch, S. Inoue, *Nat. Chem.* **2020**, *12*, 1131–1135; c) S. Fujimori, S. Inoue, *Commun. Chem.* **2020**, *3*; d) N. Takeda, T. Kajiwara, H. Suzuki, R. Okazaki, N. Tokitoh, *Chem. Eur. J.* **2003**, *9*, 3530–3543.

Manuscript received: August 14, 2021
Accepted manuscript online: September 16, 2021
Version of record online: October 5, 2021

5. Isolation and Reactivity of Tetrylene-Tetrylone-Iron Complexes Supported by Bis(*N*-Heterocyclic Imine) Ligands

Title: Isolation and Reactivity of Tetrylene-Tetrylone-Iron Complexes Supported by Bis(*N*-Heterocyclic Imine) Ligands

Status: Research Article, published online August 04, 2022

Journal: Angewandte Chemie International Edition, 2022, e202208930.

Publisher: John Wiley & Sons, Inc.

DOI: 10.1002/anie.202208930 and 10.1002/ange.202208930

Authors: Xuan-Xuan Zhao, Tibor Szilvási, Franziska Hanusch, John A. Kelly, Shiori Fujimori, Shigeyoshi Inoue*

Content:

The germanium iron carbonyl complex **3** was prepared by the reaction of dimeric chloro(imino)germylene $[IPrNGeCl]_2$ (IPrN = bis(2,6-diisopropylphenyl)imidazolin-2-iminato) with one equivalent of Collman's reagent ($Na_2Fe(CO)_4$) at room temperature. Similarly, reaction of the chloro(imino)stannylene $[IPrNSnCl]_2$ with $Na_2Fe(CO)_4$ (1 eq.) resulted in the $Fe(CO)_4$-bridged bis(stannylene) complex **4** . We observed reversible manifestation of bis(tetrylene) and tetrylene-tetrylone character in complexes **3** *vs.* **5** and **4** *vs.* **6**, which was supported by DFT calculations. Moreover, the Li/Sn/Fe trimetallic complex **12** has been isolated from the reaction of $[IPrNSnCl]_2$ with cyclopentadienyl iron dicarbonyl anion. The computational analysis further rationalizes the reduction pathway from these chlorotetrylenes to the corresponding complexes.

* X.-X. Zhao planned and executed all experiments including analysis and wrote the manuscript. F. Hanusch, J. A. Kelly, and S. Fujimori conducted all SC-XRD measurements and managed the processing of the respective data. T. Szilvási designed and performed the theoretical analysis and contributed to the manuscript. All work was performed under the supervision of S. Inoue.

A Journal of the Gesellschaft Deutscher Chemiker
Angewandte Chemie
International Edition
www.angewandte.org

Accepted Article

Title: Isolation and Reactivity of Tetrylene-Tetrylone-Iron Complexes Supported by Bis(N-Heterocyclic Imine) Ligands

Authors: Xuan-Xuan Zhao, Tibor Szilvási, Franziska Hanusch, John Kelly, Shiori Fujimori, and Shigeyoshi Inoue

To be cited as: *Angew. Chem. Int. Ed.* **2022**, e202208930

Link to VoR: https://doi.org/10.1002/anie.202208930

WILEY-VCH

WILEY-VCH

RESEARCH ARTICLE

Isolation and Reactivity of Tetrylene-Tetrylone-Iron Complexes Supported by Bis(*N*-Heterocyclic Imine) Ligands

Xuan-Xuan Zhao,[a] Tibor Szilvási,[b] Franziska Hanusch,[a] John A. Kelly,[a] Shiori Fujimori,[a] and Shigeyoshi Inoue*[a]

Dedicated to Professor Norihiro Tokitoh on the occasion of his 65th birthday

[a] X.-X. Zhao, Dr. F. Hanusch, Dr. J. A. Kelly, Dr. S. Fujimori, Prof. Dr. S. Inoue
School of Natural Sciences, Department of Chemistry,
WACKER-Institute of Silicon Chemistry and Catalysis Research Center, Technische Universität München
Lichtenbergstraße 4, 85748 Garching bei München (Germany)
E-mail: s.inoue@tum.de
[b] Prof. Dr. T. Szilvási
Department of Chemical and Biological Engineering,
University of Alabama
Tuscaloosa, AL 35487 (USA)

Supporting information for this article is given *via* a link at the end of the document.

Abstract: The germanium iron carbonyl complex **3** was prepared by the reaction of dimeric chloro(imino)germylene $[IPrNGeCl]_2$ (IPrN = bis(2,6-diisopropylphenyl)imidazolin-2-iminato) with one equivalent of Collman's reagent ($Na_2Fe(CO)_4$) at room temperature. Similarly, the reaction of chloro(imino)stannylene $[IPrNSnCl]_2$ with $Na_2Fe(CO)_4$ (1 eq.) resulted in the $Fe(CO)_4$-bridged bis(stannylene) complex **4**. We observed reversible formation of bis(tetrylene) and tetrylene-tetrylone character in complexes **3** *vs.* **5** and **4** *vs.* **6**, which was supported by DFT calculations. Moreover, the Li/Sn/Fe trimetallic complex **12** has been isolated from the reaction of $[IPrNSnCl]_2$ with cyclopentadienyl iron dicarbonyl anion. The computational analysis further rationalizes the reduction pathway from these chlorotetrylenes to the corresponding complexes.

Introduction

Low-valent heavy Group 14 compounds are of great interest in contemporary research, due to their intriguing bonding, structures, and transition metal-like reactivity.[1] Monomeric divalent compounds of the heavier Group 14 elements (also known as tetrylenes), possess a lone pair of electrons and a vacant *p*-orbital (Figure 1a, left), and as a consequence have seen use in applications including small molecule activation, catalysis, and coordination chemistry.[2] Zerovalent compounds of Group 14 (tetrylones), in which the central tetrel atom is stabilized by two ligands *via* a donor-acceptor interaction, possess four valence electrons in the form of two lone pairs of electrons (Figure 1a, right).[3] Over the past two decades, the isolation and reactivity of tetrylones has garnered much attention.

Figure 1 outlines recently reported low-valent germanium and tin compounds supported by various donor ligands.[4,5] For instance, in 2016, Driess and coworkers reported the bis(silylenyl)pyridine-stabilized germylone iron carbonyl complex **A** and its tin derivative (Figure 1b).[6] In addition, two acceptor free E^0 compounds (E = Ge (**B**), Sn (**C**)) stabilized by a bis(imino)pyridine pincer ligand were isolated by Nikonov, Fischer and Flock *et al.*, respectively.[4e,j] More recently, Rivard and coworkers reported on the synthesis of the dimeric Ge(II) species **E** (Figure 1b), in which the two Ge centers are linked by anionic *N*-heterocyclic olefin (NHO) ligands.[4n]

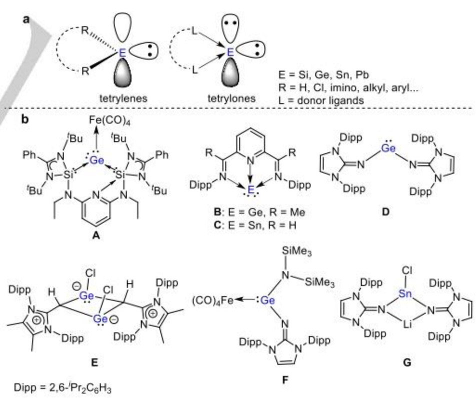

Figure 1. (a) Electronic structures of tetrylenes (left) and tetrylones (right). (b) Selected examples of low-valent germanium and tin compounds.

Ligand design plays an integral role in modern main group chemistry, with the use of functional ligands providing access to various reactive low-coordinate compounds. *N*-heterocyclic imine (NHI) ligands may act as a 2*σ*- and either 2*π*- or 4*π* electron donors.[7] Therefore, the imino group is an excellent choice for thermodynamic stabilization of electron-deficient species. For example, in 2015, the Rivard group described the synthesis of a two-coordinate acyclic germylene **D** supported by two NHI ligands.[8] Recently, we have developed a number of synthetic methods to stabilize low-coordinate Group 14 element compounds using NHIs as supporting ligands.[9b,10] For example, we reported the germylene iron carbonyl complex **F** with a trigonal planar-coordinate germanium atom,[10b] and also a rare example of the lithium bis(imino)stannylenoid **G** as a heavier carbenoid congener.[9] To expand this chemistry, we were interested in exploring the synthetic potential of dimeric chloro(imino)tetrylenes as a precursor for novel low-valent species for applications in bond activation and catalysis.

We have previously reported the isolation of dimeric chloro(imino)stannylene **2** (Scheme 1), but its reactivity has not yet been explored.[9b,10g] Continuing this study, herein we show a simplified route to the chlorotetrylenes **1** and **2**, and report on tetrylene-tetrylone complexes prepared by the reaction of chlorotetrylenes with anionic iron carbonyls ($Na_2Fe(CO)_4$ and $M[Fe(CO)_2(\eta^5\text{-}C_5H_5)]$, M = Li, K).

Results and Discussion

The reaction of ECl_2•dioxane (E = Ge, Sn) with one equivalent of IPrNLi (IPrN = bis(2,6-diisopropylphenyl)imidazolin-2-iminato) in THF at room temperature led to the corresponding chlorotetrylenes $[IPrNECl]_2$ **1** (E = Ge) and **2** (E = Sn) in high yields (**1**: 97% and **2**: 67%; Scheme 1). Compounds **1** and **2** are soluble in polar solvents such as chloroform and acetonitrile, but dissolve poorly in nonpolar hydrocarbons. The structure of **1** and **2** were both characterized by multinuclear NMR spectroscopy and elemental analysis (EA).

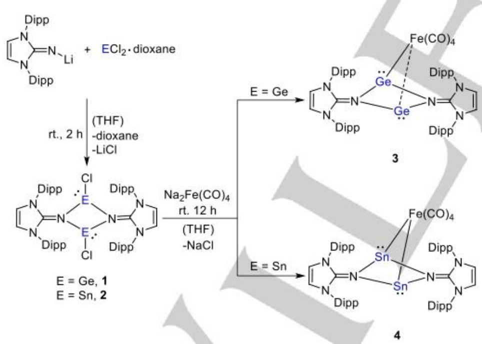

Scheme 1. Synthesis of $Fe(CO)_4$-bridged germanium and tin complexes **3** and **4** from chloro(imino)tetrylenes **1** and **2**, respectively.

Single crystal X-ray diffraction (SC-XRD) analysis of **1** revealed that the molecular structure in the solid state comprises of a centrosymmetric dimer, with a planar and rhombic N_2Ge_2 ring (sum of internal tetragonal angles: 360°, Figure 2). The Ge–Cl bonds adopt a *trans* configuration with respect to the Ge_2N_2 ring. In comparison, Rivard's NHO-Ge(II) dimer **E** contains a puckered Ge_2N_2 ring, which is capped by *syn*-arranged Ge–Cl bonds. The Ge–N bond lengths of 1.956(7) Å and 2.003(7) Å are significantly longer than that in $[IPrN]_2Ge$ (**D**) [1.8194(15) Å] and **F** [1.755(2) Å]. They are comparable to that in imino-stabilized Ge(II) monocation[10b] [1.9694(14) Å] and **B** [Ge–N_{imino} 2.047(7) Å], indicating a partial dative bond character for the germanium-nitrogen interactions in **1**. The structural features are very similar to that seen in **2**.[9b] However, further structure discussion is restricted, due to enlarged thermal ellipsoids and disorder resulting from data collection at 200K.

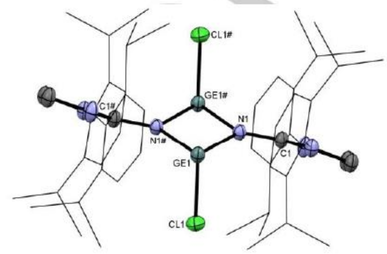

Figure 2. Molecular structure of **1**.[13] Thermal ellipsoids are shown at 30% probability level. Hydrogen atoms are omitted for clarity. Selected bond lengths [Å] and angles [°]: Ge1–Cl1 2.385(7), Ge1–N1 1.956(7), N1–C1 1.305(13), Ge1–N1# 2.003(7), Cl1–Ge1–N1 94.0(3), Cl1–Ge1–N1# 89.5(3), N1–Ge1–N1# 79.5(3), Ge1–N1–C1 131.2(6), Ge1–N1#–C1# 127.6(6), Ge1–N1–Ge1# 100.5(4).

Treating chlorogermylene **1** with $Na_2Fe(CO)_4$ (1 eq.) results in the formation of germanium iron carbonyl complex **3**, isolated in good yield (82%) as a red crystalline solid (Scheme 1). The CO-signal of the $Fe(CO)_4$ moiety in the $^{13}C\{^1H\}$ NMR spectrum (C_6D_6) appears at 217.7 ppm and the solid state IR spectrum shows the characteristic CO stretching vibration of **3** at 1975, 1909, 1877, and 1862 cm^{-1}, which are comparable to those in complex **A** [1969, 1886, 1865, and 1830 cm^{-1}], but are red-shifted compared to those in **F** [2039, 1965, and 1930 cm^{-1}],[10b] suggesting that the carbonyl groups experience a strong electron back-donation.

The molecular structure and Density Functional Theory (DFT) calculations revealed that complex **3** contains two Ge(II) atoms, bridged by a $Fe(CO)_4$ moiety (Figure 3). The Ge1 center adopts a trigonal-pyramidal geometry (sum of the angles around the Ge1 atom: 260.33°), which is similar to that in bis(*N*-heterocyclic carbene) supported germylone-$GaCl_3$ adduct (266.33°)[4g] and complex **A** (322.59°), but different from the trigonal planar Ge moiety in **F**. The Ge1–Fe1 bond length of 2.6968(6) Å is longer than that in **A** [2.4987(5) Å] and **F** [2.3026(5) Å]. Moreover, the X-ray structure of **3** revealed a Ge2⋯Fe1 distance of 2.9670(5) Å, and a wider angle of C55–Fe1–C57 (144.23°) than the expected 120°, thus indicating a weak interaction between Fe1 and Ge2. The Ge1–N1 and Ge1–N4 bond lengths [2.0601(12) Å and 2.0219(12) Å] are almost identical to that in Nikonov's germylone **B** [Ge–N_{imino} 2.047(7) Å]. Accordingly, the Ge2–N_{imino} distances are increased with respect to Rivard's bis(imino)germylene **D** [1.9585(12) Å and 1.9888(13) Å *vs.* 1.8194(15) Å]. The Ge1⋯Ge2 separation in **3** [2.7678 Å] is consistent with an absence of Ge1–Ge2 bonding (sum of two Ge covalent radii = 2.44 Å).[11] In

10.1002/anie.202208930

addition, the N1−Ge2−N4 angle of 79.26(5)° is considerably more acute than that in **D** [99.48(10)°].

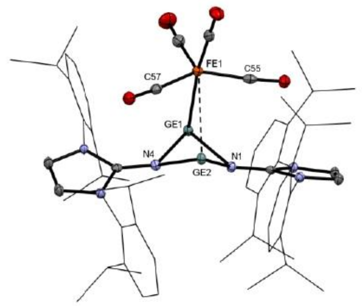

Figure 3. Molecular structure of **3**.[13] Thermal ellipsoids are shown at 50% probability level. Hydrogen atoms and solvent molecules are omitted for clarity. Selected bond lengths [Å] and angles [°]: Ge1–Fe1 2.6968(6), Ge2···Fe1 2.9670(5), Ge1–N1 2.0601(12), Ge1–N4 2.0219(12), Ge2–N1 1.9585(12), Ge2–N4 1.9888(13), C1–N1 1.3066(18), C4–N4 1.3042(18), Fe1–Ge1–N1 92.37(4), Fe1–Ge1–N4 91.80(4), N1–Ge1–N4 76.16(5), N1–Ge2–N4 79.26(5), Ge1–N1–Ge2 87.03(5), Ge1–N4–Ge2 87.27(5), Ge1–N1–C1 132.59(9), Ge1–N4–C4 134.85(10), Ge2–N1–C1 126.98(9), Ge2–N4–C4 125.76(9), C55–Fe1–C57 144.23.

To gain further insight into the electronic structure and bonding of **3**, DFT calculations were carried out at the ωB97X-D/def2-TZVPP//B97-D/def2-SVP level of theory. Natural Bond Orbital (NBO) analysis of **3** shows N centered lone pairs and empty Ge orbitals (Table S8) indicating donation from the nitrogen to the germanium center. Analysis of the frontier orbitals (Figure 4) shows that HOMO and HOMO-5 depict lone pairs of electrons on the Ge centers while HOMO-1 and HOMO-5 feature out-of-plane (π) and in-plane (σ) type contribution from the N atoms.

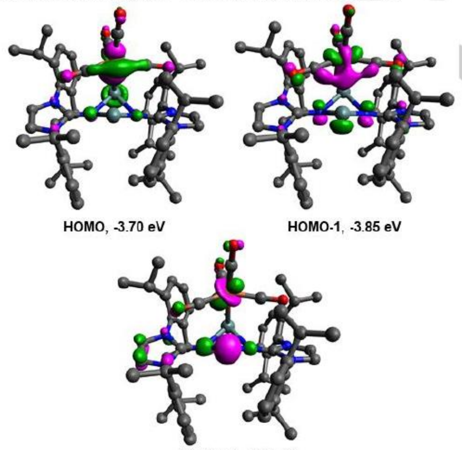

Figure 4. Molecular orbitals of **3**. Hydrogens are omitted for clarity.

Similarly, the chlorostannylene **2** was treated with $Na_2Fe(CO)_4$ (1 eq.) to give the $Fe(CO)_4$-bridged bis(stannylene) complex **4** in 74% yield (Scheme 1). The $^{13}C\{^1H\}$ NMR spectrum (C_6D_6) of **4** displays one carbonyl signal at 216.9 ppm. The characteristic iron-carbonyl vibrations were found at 1976, 1899, and 1870 cm^{-1} in the solid-state IR spectrum. Analysis of the frontier orbitals (Figure 5) shows that the HOMO and HOMO-5 depict lone pairs of electrons on the Sn centers.

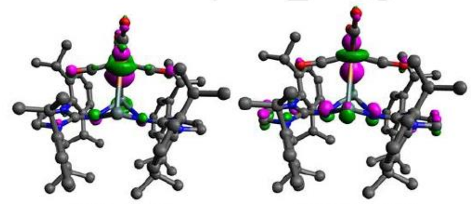

HOMO, -3.76 eV HOMO-5, -4.98 eV

Figure 5. Molecular orbitals of **4**. Hydrogens are omitted for clarity.

SC-XRD analysis of **4** revealed that the $Fe(CO)_4$ fragment bridges the two tin(II) centers with bond lengths 2.8511(10) Å (Sn1–Fe1) and 2.9432(10) Å (Sn2–Fe1) (Figure 6). Notably, the imino groups link the two Sn atoms almost symmetrically in the N_2Sn_2 ring [bond lengths for Sn–N: 2.204(3) Å, 2.240(3) Å, 2.237(3) Å and 2.180(3) Å]. One signal (357.3 ppm, C_6D_6) was observed in the $^{119}Sn\{^1H\}$ NMR spectrum, which is confirmed by Gauge-Independent Atomic Orbital (GIAO) calculations ($\delta_{calcd.}$ = 360 ppm). This indicates the Sn–Fe bond lengths equilibrate in solution.

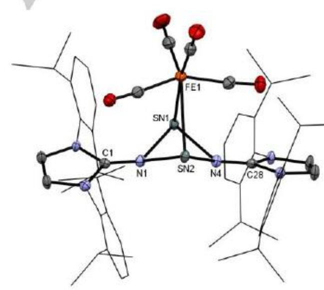

Figure 6. Molecular structure of **4**.[13] Thermal ellipsoids are shown at 50% probability level. Hydrogen atoms are omitted for clarity. Selected bond lengths [Å] and angles [°]: Sn1–Fe1 2.8511(10), Sn2–Fe1 2.9432(10), Sn1–N1 2.204(3), Sn1–N4 2.240(3), Sn2–N1 2.237(3), Sn2–N4 2.180(3), N1–C1 1.291(5), N4–C28 1.300(5), Sn1–Fe1–Sn2 64.65(2), Fe1–Sn1–N1 86.97(8), Fe1–Sn1–N4 87.21(8), Fe1–Sn2–N1 84.13(8), Fe1–Sn2–N4 86.03(9), Sn1–N1–Sn2 88.51(11), Sn1–N4–Sn2 89.05(10), N1–Sn1–N4 75.80(10), N1–Sn2–N4 76.35(11), Sn1–N1–C1 130.2(2), Sn1–N4–C28 129.6(3), Sn2–N1–C1 129.5(2), Sn2–N4–C28 129.7(3).

In addition, NBO analysis shows only one Ge−Fe bond in **3**, whereas each Sn center has one bond with Fe in **4** (Table S8 and Table S9). Wiberg Bond Index (WBI) indicates weak E−Fe (E = Ge or Sn) single bonds (~0.40-0.58, Table S10) which are consistent with the large polarization of the E−Fe bonds (Fe1 in **3**: 65.50%; Fe1 in **4**: 88.02% and 66.29%). Second order perturbation analysis of the Ge2 vacant orbital and Fe1 lone pair of electrons shows large donor-acceptor stabilization energy of

10.1002/anie.202208930
WILEY-VCH

57.10 kcal mol^{-1}. DFT analysis indicates an equilibrium between **3** and **4** with their respective monocoordinated structures **5** and **6** (Scheme 2), whereby the $Fe(CO)_4$ fragment sits almost perpendicular to the N_2E_2 ring bound to only one tetrel atom (see Supporting Information for calculated structures of **5** and **6**, Figure S55 and Figure S56, respectively). The variable temperature (VT) ^{119}Sn NMR analysis of **4** shows the signal is high field shifted and broadens at lower temperatures, possibly showing the monocoordinated **6** being "frozen out" at lower temperatures in solution (Figure S22). GIAO NMR calculations indicate that the values for the different Sn centers in both the mono-coordinate and bridged species are almost equivalent.

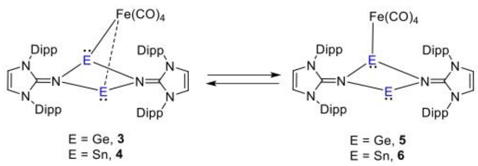

Scheme 2. Temperature-dependent exchange of the E−Fe bonding (E = Ge, Sn).

To investigate the reactivity of these complexes, **3** was treated with two equivalents of $GaCl_3$ in C_6D_6 which led to the formation of complex [(IPrNGe)$_2$(μ-Cl)][$GaCl_4$] **7** (Scheme 3). The yellow-orange solid was identified by multinuclear NMR spectroscopy and single-crystal X-ray diffraction (see Supporting Information for details). Compound **7** is comparable to that of Rivard's complex, [{(^{Me}IPrCH)Ge}$_2$(μ-Cl)][BAr$^F_4$] [Ar^F = 3,5-(CF_3)$_2$-C_6H_3].[4n] Similarly, treatment of **4** with $GaCl_3$ (2 eq.) resulted in complex **8** as an orange-red solid (Scheme 3). The ^{119}Sn{^{1}H} NMR spectrum of **8** in THF-d_8 shows a signal at σ = 139.6 ppm that is shifted to higher field compared to that of **4** (357.3 ppm, C_6D_6).

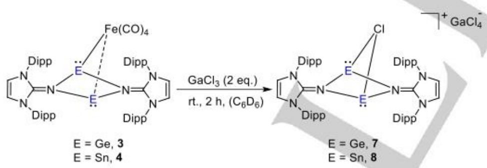

Scheme 3. Reaction of **3** and **4** with $GaCl_3$ to **7** and **8**.

Motivated by the above results, we investigated the reactivity of **1** and **2** towards K[Fe(CO)$_2$(η^5-C_5H_5)] (FpK). Reaction of **1** with three equivalents of FpK resulted in a complex product mixture which contains **D**, large amount of free ligand IPrNH, and other undefined species. Similarly, treatment of **2** with FpK (3 eq.) in THF led to the formation of a complicated mixture of products. However, the one-pot reaction of IPrN-Li and $GeCl_2$•dioxane with three equivalents of FpK in THF, forms already reported bis(imino)germylene **D** in reasonable yields (62%) confirmed by ^{1}H NMR spectroscopy.[8] In comparison, the reaction of **2** with FpK (3 eq.) in THF resulted in the Li/Sn/Fe trimetallic complex **12** in 60% yield (Scheme 4). In addition, the isolated yields of **D** and **12** did not significantly deviate if isolated **1** and **2** reacted directly with Li[Fe(CO)$_2$(η^5-C_5H_5)] (FpLi, 3 eq.) instead of the *in-situ* protocol.

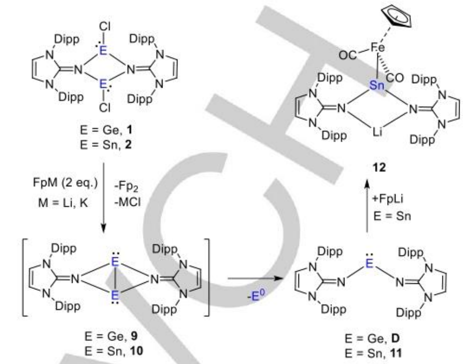

Scheme 4. Reaction of chloro(imino)tetrylenes **1** and **2** with M[Fe(CO)$_2$(η^5-C_5H_5)] (M = Li, K), as well as proposed mechanism.

The formation of bis(imino)germylene **D** can be rationalized by the release of Ge metal *via* the intermediate **9**. Notably, the reduction of **E** led to similar disproportionation products (Ge metal and R_2Ge:, R = NHO).[4n] It appears that the plausible intermediate **10** readily decomposes to yield Sn metal and the bis(imino)stannylene **11**, which can react with FpLi to yield complex **12** (Scheme 4). To clarify the mechanism, we performed the reaction of isolated **11** with FpLi (1 eq.) at room temperature, which formed the desired product **12** in nearly quantitative yield. No reaction was observed between **D** and FpLi even at elevated temperatures. All attempts to isolate **9** and **10** by reducing the corresponding chlorotetrylenes **1** and **2** with common reducing agents (such as K, KC_8) have so far been unsuccessful.

Computational analysis using DFT was carried out to understand the reduction pathway from chloro(imino)tetrylenes [IPrNECl]$_2$ (E = Ge, **1**; Sn, **2**) to bis(imino)tetrylenes [IPrN]$_2$E (E = Ge, **D**; Sn, **11**) and bulk E metal (Figure S48). We found that the reduction of **1** and **2** to **9** and **10** is strongly favored in internal energy similar to the Ge/Sn metal deposition (-58.4/-42.2 kcal mol^{-1}) that drives the reaction toward **D** and **11** (Figure S48). In addition, we have also studied possible intermediates with different geometry and canonical forms during the reduction reaction (Scheme 5). Interestingly, our calculations indicate that both type **II** and **III** structures converge to **I**, which is equivalent to **9** and **10** and has a more butterfly structure compared to **II** and **III**, without having a local minimum for type **II** and **III** structures. We have also considered Fp as a substituent for **9** and **10** (Figure S48). Computations showed the dissociation of the Fe-substituted dimer (**IV**) presumably due to steric reasons, however the formation of its monomer is thermodynamically favored, although it is less favorable than the experimentally observed metal deposition. The acyclic E(I) dimers (**V**) are less stable by more than 15 kcal mol^{-1} than **I**.

10.1002/anie.202208930

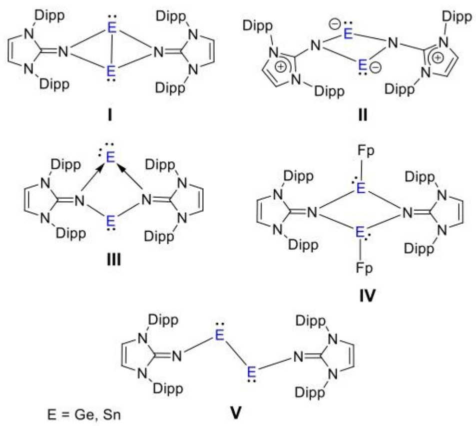

Scheme 5. Potential intermediates in the reaction of **1** and **2** with FpM (M = Li, K).

Interestingly, the lithium stannylenoid (**G**) is energetically favored relative to the corresponding lithium germylenoid (-1.6 kcal mol^{-1} *vs.* +8.5 kcal mol^{-1}, Figure S48). In addition, we found that the potassium derivative of **12** is less stable than the lithium analogue (-50.4 kcal mol^{-1} *vs.* -63.4 kcal mol^{-1}). The product derived from insertion of the Sn center in compound **11** into the Fe−Li bond of FpLi is higher by +41.8 kcal mol^{-1} in energy than its isomer **12** (Figure S48).

Complex **12** has a relatively high thermal stability in C_6D_6, with no elimination of FpLi observed even after heating to 80 °C for 16 hours. However, treatment of **12** with N_2O immediately resulted in the formation of **11**, which then further reacts with N_2O leading to decomposition products. The ^{119}Sn{^{1}H} NMR spectrum of **12** in C_6D_6 displays a singlet at 314.0 ppm, which is significantly shifted to lower field as compared to **G** [-52.1 ppm, C_6D_6], but higher field shifted compared to Power's ferrio-stannylene ArSnFe(CO)$_2$(η^5-C_5H_5) (Ar = 2,6-(2,6-^{i}Pr$_2$C$_6$H$_3$)$_2$C$_6$H$_3$) [2951 ppm, C_6D_6].[12c] The iron-carbonyl (CO) signal in the ^{13}C{^{1}H} NMR spectrum (C_6D_6) appears at 222.6 ppm. The CO stretching vibration was found at 2006 and 1925 cm^{-1} in the solid state IR spectrum, which is comparable to that in ferrio-stannylene [1970 and 1921 cm^{-1}] and Driess's iron-stannylene complex LSnFe(CO)$_2$(η^5-C_5H_5) (L = β-diketiminate) [1961 and 1907 cm^{-1}].[12b]

SC-XRD study revealed that **12** contains a four-membered LiN$_2$Sn ring, in which the sum of the internal bond angles amounts to 354.83° (Figure 7). The Sn−N bond lengths [2.1763(11) Å and 2.1717(11) Å] in **12** are comparable to that in **G** [2.143(5) Å and 2.179(4) Å]. The Sn1−Fe1 bond length [2.7671(6) Å] is significantly elongated in comparison to that in the ferrio-stannylene [2.5634(5) Å], but shorter than those in **4** [2.8511(10) Å and 2.9432(10) Å].

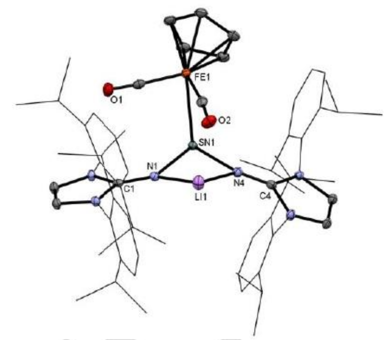

Figure 7. Molecular structure of **12**.[13] Thermal ellipsoids are shown at 50% probability level. Hydrogen atoms and solvent molecules are omitted for clarity. Selected bond lengths [Å] and angles [°]: Sn1–Fe1 2.7671(6), Sn1–N1 2.1763(11), Sn1–N4 2.1717(11), Li1–N1 1.950(3), Li1–N4 1.945(3), C1–N1 1.2713(18), C4–N4 1.2650(18), Fe1–Sn1–N1 96.24(3), Fe1–Sn1–N4 100.66(3), Sn1–N1–C1 129.16(9), Sn1–N4–C4 132.68(9), Li1–N1–C1 141.33(12), Li1–N4–C4 134.92(12), Sn1–N1–Li1 89.40(9), Sn1–N4–Li1 89.66(9), N1–Sn1–N4 81.83(4), N1–Li1–N4 93.94(11).

Treatment of **12** with the nucleophilic reagent LiI (1 eq.) afforded the iodo-substituted tin complex **13** (Scheme 6). The formation of **13** demonstrates the electrophilicity of the tin(II) center in **12**. In the ^{119}Sn{^{1}H} NMR spectrum, one signal appears at σ = 61.6 ppm (C_6D_6), which is shifted upfield in comparison to **12** [314.0 ppm, C_6D_6], presumably because the electron-donating capacity of the iodide is higher than that of the Fp group.

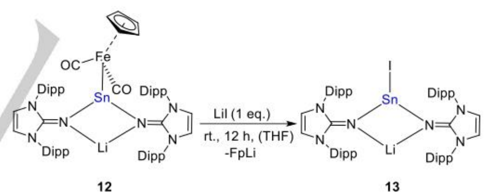

Scheme 6. Reaction of **12** with LiI to **13**.

The molecular structure of **13** was also determined by single crystal X-ray diffraction analysis (Figure 8). The structural features are very similar to that seen in **G** and **12**. The Sn–I bond in **13** is oriented nearly perpendicular to both Sn–N bonds, with I1–Sn1–N1 and I1–Sn1–N4 bond angles of 98.13(5) and 88.86(5), respectively.

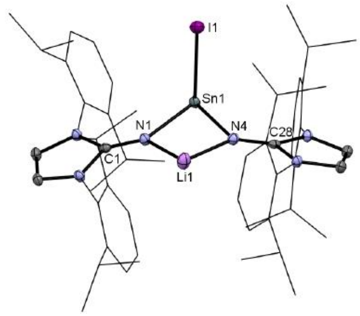

Figure 8. Molecular structure of **13**.[13] Thermal ellipsoids are shown at 50% probability level. Hydrogen atoms and solvent molecules are omitted for clarity. Selected bond lengths [Å] and angles [°]: Sn1–I1 3.0218(6), Sn1–N1 2.136(2), Sn1–N4 2.136(2), Li1–N1 1.944(4), Li1–N4 1.923(4), C1–N1 1.273(3), C28–N4 1.278(2), I1–Sn1–N1 98.13(5), I1–Sn1–N4 88.86(5), Sn1–N1–C1 135.8(1), Sn1–N4–C28 130.7(1), Li1–N1–C1 131.0(2), Li1–N4–C28 135.7(2), Sn1–N1–Li1 93.0(1), Sn1–N4–Li1 93.6(1), N1–Sn1–N4 80.48(6), N1–Li1–N4 91.1(2).

Conclusion

In summary, we have reported on the synthesis of the centrosymmetric chloro(imino)tetrylenes [IPrNECl]$_2$ (E = Ge (**1**), Sn (**2**)), with a planar and rhombic N_2E_2 ring. The reaction of [IPrNECl]$_2$ with one equivalent of $Na_2Fe(CO)_4$ led to the corresponding germanium and tin iron carbonyl complexes. Notably, the $Fe(CO)_4$ fragment shows different bonding situations in solution and solid state of these complexes (E−Fe bonding: mono-coordinate *vs.* bridged, E = Ge, Sn). Moreover, we isolated the Li/Sn/Fe trimetallic complex **12** by the reaction of chloro(imino)stannylene **2** with K[Fe(CO)$_2$(η^5-C_5H_5)]. Further coordination chemistry, bond activation and catalytic applications of these low-valent compounds are currently under investigation.

Acknowledgements

We gratefully acknowledge financial support from the Deutsche Forschungsgemeinschaft (In 234/7-1). X.Z. gratefully acknowledges financial support from the China Scholarship Council. We thank Dr. Christian Jandl for the SC-XRD measurements of compound **3** and **12**. We thank Florian Tschernuth for the VT-NMR measurements, as well as Maximilian Muhr for the LIFDI-MS measurements.

Conflict of interest

The authors declare no conflict of interest.

Keywords: germanium • iron carbonyl complexes • low-valent compounds • trimetallic complexes • tin

[1] a) P. P. Power, *Nature* **2010**, *463*, 171-177; b) D. Martin, M. Soleilhavoup, G. Bertrand, *Chem. Sci.* **2011**, *2*, 389-399; c) C. Weetman, S. Inoue, *ChemCatChem* **2018**, *10*, 4213-4228; d) T. J. Hadlington, M. Driess, C. Jones, *Chem. Soc. Rev.* **2018**, *47*, 4176-4197; e) R. L. Melen, *Science* **2019**, *363*, 479-484; f) F. Hanusch, L. Groll, S. Inoue, *Chem. Sci.* **2021**, *12*, 2001-2015; g) M. M. D. Roy, A. A. Omana, A. S. S. Wilson, M. S. Hill, S. Aldridge, E. Rivard, *Chem. Rev.* **2021**, *121*, 12784-12965.

[2] a) M. Veith, *Angew. Chem. Int. Ed.* **1987**, *26*, 1-14; *Angew. Chem.* **1987**, *99*, 1-14; b) W. P. Neumann, *Chem. Rev.* **1991**, *91*, 311-334; c) H. V. R. Dias, Z. Y. Wang, W. C. Jin, *Coord. Chem. Rev.* **1998**, *176*, 67-86; d) M. Weidenbruch, *Eur. J. Inorg. Chem.* **1999**, *1999*, 373-381; e) N. Tokitoh, R. Okazaki, *Coord. Chem. Rev.* **2000**, *210*, 251-277; f) O. Kuhl, *Coord. Chem. Rev.* **2004**, *248*, 411-427; g) I. Saur, S. G. Alonso, J. Barrau, *Appl. Organomet. Chem.* **2005**, *19*, 414-428; h) W. P. Leung, K. W. Kan, K. H. Chong, *Coord. Chem. Rev.* **2007**, *251*, 2253-2265; i) S. Nagendran, H. W. Roesky, *Organometallics* **2008**, *27*, 457-492; j) A. V. Zabula, F. E. Hahn, *Eur. J. Inorg. Chem.* **2008**, *2008*, 5165-5179; k) Y. Mizuhata, T. Sasamori, N. Tokitoh, *Chem. Rev.* **2009**, *109*, 3479-3511; l) M. Asay, C. Jones, M. Driess, *Chem. Rev.* **2011**, *111*, 354-396; m) S. Khan, *Adv. Organometal. Chem.* **2020**, *74*, 105-152.

[3] a) N. Takagi, T. Shimizu, G. Frenking, *Chem. Eur. J.* **2009**, *15*, 8593-8604; b) D. J. Wilson, J. L. Dutton, *Chem. Eur. J.* **2013**, *19*, 13626-13637; c) G. Frenking, M. Hermann, D. M. Andrada, N. Holzmann, *Chem. Soc. Rev.* **2016**, *45*, 1129-1144; d) S. Yao, Y. Xiong, M. Driess, *Acc. Chem. Res.* **2017**, *50*, 2026-2037; e) L. Zhao, M. Hermann, N. Holzmann, G. Frenking, *Coord. Chem. Rev.* **2017**, *344*, 163-204; f) P. K. Majhi, T. Sasamori, *Chem. Eur. J.* **2018**, *24*, 9441-9455; g) S. Yao, Y. Xiong, A. Saddington, M. Driess, *Chem. Commun.* **2021**, *57*, 10139-10153.

[4] a) T. Iwamoto, H. Masuda, C. Kabuto, M. Kira, *Organometallics* **2005**, *24*, 197-199; b) T. Iwamoto, T. Abe, C. Kabuto, M. Kira, *Chem. Commun.* **2005**, 5190-5192; c) Y. Xiong, S. Yao, G. Tan, S. Inoue, M. Driess, *J. Am. Chem. Soc.* **2013**, *135*, 5004-5007; d) Y. Li, K. C. Mondal, H. W. Roesky, H. Zhu, P. Stollberg, R. Herbst-Irmer, D. Stalke, D. M. Andrada, *J. Am. Chem. Soc.* **2013**, *135*, 12422-12428; e) T. Chu, L. Belding, A. van der Est, T. Dudding, I. Korobkov, G. I. Nikonov, *Angew. Chem. Int. Ed.* **2014**, *53*, 2711-2715; *Angew. Chem.* **2014**, *126*, 2749-2753; f) B. Su, R. Ganguly, Y. Li, R. Kinjo, *Angew. Chem. Int. Ed.* **2014**, *53*, 13106-13109; *Angew. Chem.* **2014**, *126*, 13322-13325; g) Y. Xiong, S. Yao, M. Karni, A. Kostenko, A. Burchert, Y. Apeloig, M. Driess, *Chem. Sci.* **2016**, *7*, 5462-5469; h) Y. Wang, M. Karni, S. Yao, Y. Apeloig, M. Driess, *J. Am. Chem. Soc.* **2019**, *141*, 1655-1664; i) M. T. Nguyen, D. Gusev, A. Dmitrienko, B. M. Gabidullin, D. Spasyuk, M. Pilkington, G. I. Nikonov, *J. Am. Chem. Soc.* **2020**, *142*, 5852-5861; j) J. Flock, A. Suljanovic, A. Torvisco, W. Schoefberger, B. Gerke, R. Pottgen, R. C. Fischer, M. Flock, *Chem. Eur. J.* **2013**, *19*, 15504-15517; k) T. Kuwabara, M. Nakada, J. Hamada, J. D. Guo, S. Nagase, M. Saito, *J. Am. Chem. Soc.* **2016**, *138*, 11378-11382; l) Z. Dong, K. Bedbur, M. Schmidtmann, T. Muller, *J. Am. Chem. Soc.* **2018**, *140*, 3052-3060; m) V. Nesterov, R. Baierl, F. Hanusch, A. E. Ferao, S. Inoue, *J. Am. Chem. Soc.* **2019**, *141*, 14576-14580; n) E. Hupf, F. Kaiser, P. A. Lummis, M. M. D. Roy, R. McDonald, M. J. Ferguson, F. E. Kuhn, E. Rivard, *Inorg. Chem.* **2020**, *59*, 1592-1601; o) D. Sarkar, C. Weetman, D. Munz, S. Inoue, *Angew. Chem. Int. Ed.* **2021**, *60*, 3519-3523; *Angew. Chem.* **2021**, *133*, 3561-3565; p) S. Yao, A. Kostenko, Y. Xiong, C. Lorent, A. Ruzicka, M. Driess, *Angew. Chem. Int. Ed.* **2021**, *60*, 14864-14868; *Angew. Chem.* **2021**, *133*, 14990-14994; q) A. Caise, L. Griffin, A. Heilmann, C. McManus, J. Campos, S. Aldridge, *Angew. Chem. Int. Ed.* **2021**, *60*, 15606-15612; *Angew. Chem.* **2021**, *133*, 15734-15740.

[5] For selected examples of E_2N_2 and $E_4(NR)_4$ species in Group 14 elements, and coordination of low-valent germanium to iron, see: a) M. Veith, S. Becker, V. Huch, *Angew. Chem. Int. Ed.* **1990**, *29*, 216-218; *Angew. Chem.* **1990**, *102*, 186-188; b) M. Veith, A. Rammo, *Z. Anorg. Allg. Chem.* **2001**, *627*, 662-668; c) E. H. Brooks, M. Elder, W. A. G. Graham, D. Hall, *J. Am. Chem. Soc.* **2002**, *90*, 3587-3588; d) C. Cui, M. Brynda, M. M. Olmstead, P. P. Power, *J. Am. Chem. Soc.* **2004**, *126*, 6510-

10.1002/anie.202208930

6511; e) C. Cui, M. M. Olmstead, J. C. Fettinger, G. H. Spikes, P. P. Power, *J. Am. Chem. Soc.* **2005**, *127*, 17530-17541; f) J. F. Eichler, O. Just, W. S. Rees, Jr., *Inorg. Chem.* **2006**, *45*, 6706-6712; g) N. Wiberg, P. Karampatses, C. K. Kim, *Chem. Ber.* **2006**, *120*, 1203-1212; h) N. Wiberg, G. Preiner, P. Karampatses, C. K. Kim, K. Schurz, *Chem. Ber.* **2006**, *120*, 1357-1368; i) X. Wang, C. Ni, Z. Zhu, J. C. Fettinger, P. P. Power, *Inorg. Chem.* **2009**, *48*, 2464-2470; j) A. Jana, V. Huch, H. S. Rzepa, D. Scheschkewitz, *Organometallics* **2014**, *34*, 2130-2133; k) A. Jana, M. Majumdar, V. Huch, M. Zimmer, D. Scheschkewitz, *Dalton Trans.* **2014**, *43*, 5175-5181.

[6] a) Y. P. Zhou, M. Karni, S. Yao, Y. Apeloig, M. Driess, *Angew. Chem. Int. Ed.* **2016**, *55*, 15096-15099; *Angew. Chem.* **2016**, *128*, 15320-15323; b) J. Xu, C. Dai, S. Yao, J. Zhu, M. Driess, *Angew. Chem. Int. Ed.* **2022**, *61*, e202114073; *Angew. Chem.* **2022**,*134*, e202114073.

[7] a) T. Ochiai, D. Franz, S. Inoue, *Chem. Soc. Rev.* **2016**, *45*, 6327-6344; b) X. Wu, M. Tamm, *Coord. Chem. Rev.* **2014**, *260*, 116-138.

[8] a) M. W. Lui, C. Merten, M. J. Ferguson, R. McDonald, Y. Xu, E. Rivard, *Inorg. Chem.* **2015**, *54*, 2040-2049; b) X. Zhao, T. Szilvási, F. Hanusch, S. Inoue, *Chem. Eur. J.* **2021**, *27*, 15914-15917.

[9] For selected examples of stannylenoid, see: a) H. Arp, J. Baumgartner, C. Marschner, T. Muller, *J. Am. Chem. Soc.* **2011**, *133*, 5632-5635; b) T. Ochiai, D. Franz, X. N. Wu, E. Irran, S. Inoue, *Angew. Chem. Int. Ed.* **2016**, *55*, 6983-6987; *Angew. Chem.* **2016**, *128*, 7097-7101.

[10] a) S. Inoue, K. Leszczynska, *Angew. Chem. Int. Ed.* **2012**, *51*, 8589-8593; *Angew. Chem.* **2012**, *124*, 8717-8721; b) T. Ochiai, D. Franz, X. N. Wu, S. Inoue, *Dalton Trans.* **2015**, *44*, 10952-10956; c) T. Ochiai, D. Franz, E. Irran, S. Inoue, *Chem. Eur. J.* **2015**, *21*, 6704-6707; d) T. Ochiai, S. Inoue, *Phosphorus Sulfur Silicon Relat. Elem.* **2016**, *191*, 624-627; e) T. Ochiai, T. Szilvasi, D. Franz, E. Irran, S. Inoue, *Angew. Chem. Int. Ed.* **2016**, *55*, 11619-11624; *Angew. Chem.* **2016**, *128*, 11791-11796; f) T. Ochiai, T. Szilvasi, S. Inoue, *Molecules* **2016**, *21*, 1155-1167; g) T. Ochiai, S. Inoue, *RSC Adv.* **2017**, *7*, 801-804; h) D. Wendel, A. Porzelt, F. A. D. Herz, D. Sarkar, C. Jandl, S. Inoue, B. Rieger, *J. Am. Chem. Soc.* **2017**, *139*, 8134-8137; i) D. Wendel, T. Szilvasi, C. Jandl, S. Inoue, B. Rieger, *J. Am. Chem. Soc.* **2017**, *139*, 9156-9159; j) D. Wendel, T. Szilvasi, D. Henschel, P. J. Altmann, C. Jandl, S. Inoue, B. Rieger, *Angew. Chem. Int. Ed.* **2018**, *57*, 14575-14579; *Angew. Chem.* **2018**, *130*, 14783-14787; k) D. Wendel, D. Reiter, A. Porzelt, P. J. Altmann, S. Inoue, B. Rieger, *J. Am. Chem. Soc.* **2017**, *139*, 17193-17198; l) D. Reiter, P. Frisch, T. Szilvasi, S. Inoue, *J. Am. Chem. Soc.* **2019**, *141*, 16991-16996; m) D. Reiter, P. Frisch, D. Wendel, F. M. Hormann, S. Inoue, *Dalton Trans.* **2020**, *49*, 7060-7068; n) F. S. Tschernuth, F. Hanusch, T. Szilvási, S. Inoue, *Organometallics* **2020**, *39*, 4265-4272.

[11] J. Li, C. Schenk, C. Goedecke, G. Frenking, C. Jones, *J. Am. Chem. Soc.* **2011**, *133*, 18622-18625.

[12] a) P. Jutzi, C. Leue, *Organometallics* **1994**, *13*, 2898-2899; b) S. Inoue, M. Driess, *Organometallics* **2009**, *28*, 5032-5035; c) H. Lei, J. D. Guo, J. C. Fettinger, S. Nagase, P. P. Power, *Organometallics* **2011**, *30*, 6316-6322.

[13] Deposition Numbers 2086600 (**1**), 2053426 (**3**), 2053428 (**4**), 2053429 (**12**) and 2178695 (**13**) contain the supplementary crystallographic data for this paper. These data are provided free of charge by the joint Cambridge Crystallographic Data Centre and Fachinformationszentrum Karlsruhe Access Structures service www.ccdc.cam.ac.uk/structures.

10.1002/anie.202208930

Entry for the Table of Contents

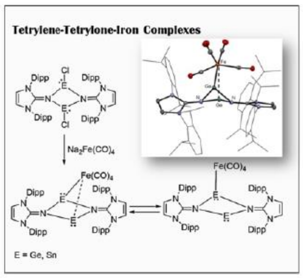

The germanium and tin iron carbonyl complexes were prepared by the reaction of dimeric chloro(imino)tetrylenes $[IPrNECl]_2$ (E = Ge, Sn; IPrN = bis(2,6-diisopropylphenyl)imidazolin-2-iminato) with one equivalent of $Na_2Fe(CO)_4$ at room temperature. Besides, a Li/Sn/Fe trimetallic complex was isolated by the reaction of chloro(imino)stannylene with cyclopentadienyl iron dicarbonyl anion.

Institute and/or researcher Twitter usernames: @InoueGroupTUM

6. *N*-Heterocyclic Imine-Stabilized Binuclear Tin(II) Cations: Synthesis, Reactivity, and Catalytic Application

Title: *N*-Heterocyclic Imine-Stabilized Binuclear Tin(II) Cations: Synthesis, Reactivity, and Catalytic Application

Status: Research Article, published online August 04, 2022

Journal: Zeitschrift für Anorganische und Allgemeine Chemie, 2022, e202200220.

Publisher: John Wiley & Sons, Inc.

DOI: 10.1002/zaac.202200220

Authors: Xuan-Xuan Zhao, John A. Kelly, Arseni Kostenko, Shiori Fujimori, Shigeyoshi Inoue*

Content:

The reaction of Cp*Sn[OTf] (Cp* = C_5Me_5; OTf = O_3SCF_3) with one equivalent of IPrNLi (IPrN = bis(2,6-diisopropylphenyl)imidazolin-2-iminato) resulted in the binuclear [OTf]-bridged tin complex **1**. Similarly, the [BF_4]-bridged bimetallic complex **2** was synthesized by the reaction of Cp*Sn[BF_4] with IPrNLi (1 eq.). It was also possible to prepare **1** from **2** *via* an anion exchange reaction. The high-yield conversion of **2** into the binuclear iodostannylene $[IPrNSnI]_2$ **3** was accomplished by treatment with LiI. The catalytic potential of **1** and **2** was demonstrated in the hydroboration of carbonyls.

* X.-X. Zhao planned and executed all experiments including analysis and wrote the manuscript. S. Fujimori conducted all SC-XRD measurements and managed the processing of the respective data. J. A. Kelly and A. Kostenko contributed to the manuscript. All work was performed under the supervision of S. Inoue.

Journal of Inorganic and General Chemistry

ZAAC

Zeitschrift für anorganische und allgemeine Chemie

Accepted Article

Title: N-Heterocyclic Imine-Stabilized Binuclear Tin(II) Cations: Synthesis, Reactivity, and Catalytic Application

Authors: Xuan-xuan Zhao, John A. Kelly, Arseni Kostenko, Shiori Fujimori, and Shigeyoshi Inoue

To be cited as: *Z. anorg. allg. Chem.* **2022**, e202200220

Link to VoR: https://doi.org/10.1002/zaac.202200220

WILEY-VCH

www.zaac.wiley-vch.de

WILEY-VCH

ARTICLE

N-Heterocyclic Imine-Stabilized Binuclear Tin(II) Cations: Synthesis, Reactivity, and Catalytic Application

Xuan-Xuan Zhao,[a] John A. Kelly,[a] Arseni Kostenko,[a] Shiori Fujimori,[a] and Shigeyoshi Inoue*[a]

Dedicated to Professor Cameron Jones on the occasion of his 60th birthday

[a] X.-X. Zhao, Dr. J. A. Kelly, Dr. A. Kostenko, Dr. S. Fujimori, Prof. Dr. S. Inoue
School of Natural Sciences, Department of Chemistry,
WACKER-Institute of Silicon Chemistry and Catalysis Research Center, Technische Universität München
Lichtenbergstraße 4, 85748 Garching bei München (Germany)
E-mail: s.inoue@tum.de

Supporting information for this article is given *via* a link at the end of the document.

Abstract: The reaction of Cp*Sn[OTf] (Cp* = C_5Me_5; OTf = O_3SCF_3) with one equivalent of IPrNLi (IPrN = bis(2,6-diisopropylphenyl)imidazolin-2-iminato) resulted in the binuclear [OTf]-bridged tin complex **1**. Similarly, the [BF_4]-bridged bimetallic complex **2** was synthesized by the reaction of Cp*Sn[BF_4] with IPrNLi (1 eq.). It was also possible to prepare **1** from **2** *via* an anion exchange reaction. The high-yield conversion of **2** into the binuclear iodostannylene $[IPrNSnI]_2$ **3** was accomplished by treatment with LiI. The catalytic potential of **1** and **2** was demonstrated in the hydroboration of carbonyls.

Introduction

Low-valent tin cations have attracted wide interest in inorganic and organometallic chemistry due to their intriguing electronic structure and their capability to activate small molecules akin to transition metals.[1] Monovalent tin(II) cations, featuring a lone pair of electrons and two vacant *p*-orbitals at the tin center (stannyliumylidenes [R−Sn:]$^+$), combine the properties of stannylenes and stannylium ions, thereby exhibiting both electrophilic and nucleophilic character (Figure 1, top).[1a] Owing to their high reactivity, stannyliumylidenes have been utilized in the activation of small molecules,[1g] and have shown potential as Lewis acidic catalysts in the hydrosilylation of alkenes and alkynes.[1h]

Since the seminal reports of Jutzi and coworkers on half-sandwich stannocene cations (**A**, Figure 1),[2] only a handful of examples of monomeric tin cations stabilized by suitable donor ligands have been reported. For it to be possible to isolate stable Sn(II) cations several groups have utilized various mono-anionic bulky N-donor ligands, such as aminotroponiminato (**B**),[3] *β*-diketiminato (**C**),[4] diaminopyridine (**D**),[5] and monoaminopyridine (**E**).[6] In 2012, the groups of Jones and Krossing reported the extremely bulky amido-tin(II) cation (**F**), which is intramolecularly stabilized by weak η^2-arene interactions.[7] More recently, the pseudo-one-coordinated Sn(II) cation (**G**) stabilized by a bulky carbazolyl moiety was reported by Hinz.[8] The dimeric tin cation $[LSnCl]_2^+$ (**H**, L = hexaphenylcarbodiphosphorane) was isolated by Alcarazo and coworkers.[9] Compounds **F** and **H** readily react with 4-(dimethylamino)pyridine (DMAP) to afford the corresponding adducts, demonstrating their electrophilicity.

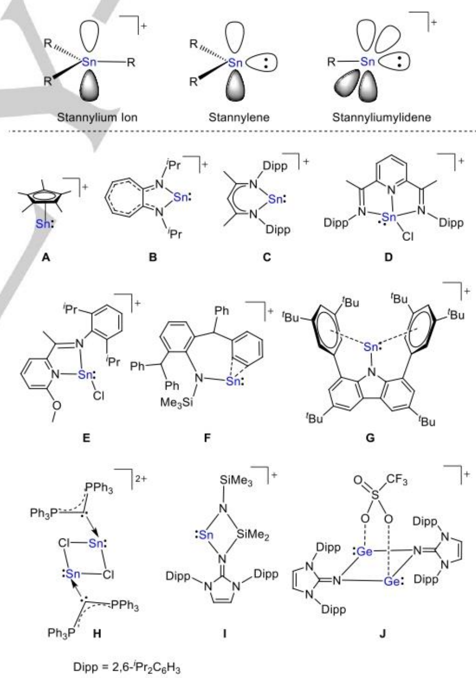

Figure 1. Electronic structures of low-valent tin compounds (top), and selected examples of low-valent tin cations, as well as the triflate-bridged germanium complex **J** (bottom).

Recently, our group has described a variety of *N*-heterocyclic carbene (NHC) or *N*-heterocyclic imine (NHI) stabilized

10.1002/zaac.202200220

tetryliumylidenes [R−E:]$^+$ (E = Si, Ge, Sn).[10] These low-valent cations exhibit reactivity towards various small molecules (*e.g.* CO_2, H_2O, chalcogens, and coinage metals *etc.*). Moreover, they can be used as versatile catalysts in the cyanosilylation and hydroboration of carbonyls, as well as the reductive *N*-functionalization of amines with CO_2 and silane. We have shown the synthesis of a cyclic tin(II) cation (**I**) from an amino(imino)stannylene (Figure 1).[11] In addition, the imino ligand can also be implemented in the isolation of triflate-bridged germanium complex (**J**),[12] which has significant bis(germyliumylidene) dication character. The non-coordinated counterion (OTf) can be replaced by anion exchange with Na[BAr$^F_4$] [Ar^F = 3,5-$(CF_3)_2$-C_6H_3] or Ag[Al(OR^F)$_4$] [R^F = C$(CF_3)_3$]. To expand this chemistry, we were interested in preparing the tin analogues of complex **J** and explore their potential applications in bond activation and catalysis.

Results and Discussion

The reaction of Cp*Sn[OTf] (Cp* = C_5Me_5; OTf = O_3SCF_3) with one equivalent of IPrNLi (IPrN = bis(2,6-diisopropylphenyl)imidazolin-2-iminato) in dry THF at -78 °C followed by warming to room temperature gave the binuclear tin complex [IPrNSnOTf]$_2$ **1** in moderate yield (61%; Scheme 1 , path **a**). Compound **1** is soluble in CD_3CN, but the solubility decreases significantly in THF. Compound **1** was characterized by multinuclear NMR, LIFDI-MS measurements, and elemental analysis (see the Supporting Information for more details). The ^{119}Sn{^{1}H} NMR spectrum of **1** displays a signal at 146.0 ppm in CD_3CN, which is downfield shifted in comparison to **I** (33.5 ppm, CD_3CN), indicating a more electron-poor Sn(II) center. The NHI backbone signal in the ^{1}H NMR spectrum of **1** (6.88 ppm, CD_3CN) is more high-field shifted compared to that of **I** (7.02 ppm, CD_3CN). The signals of the Dipp groups are also shifted to higher field than those of **I**.

Single crystal X-ray diffraction (SC-XRD) analysis revealed that **1** contains a planar and rhombic N_2Sn_2 ring. The triflate group bridges the two tin centers with the formation of two coordinative interactions between the tin centers and two oxygen atoms (see Figure S31). The structural features are very similar to that seen in **J**. However, further structure discussion regarding bond lengths and angles is restricted, due to the poor quality of the obtained data.

In a similar fashion to **1**, the reaction of Cp*Sn[BF_4] with IPrNLi (1 eq.) resulted in the [BF_4]-bridged binuclear tin complex **2** in 53% yield (Scheme 1, path **b**), which was characterized by multinuclear NMR and elemental analysis (see the Supporting Information for more details). Compound **2** is soluble in polar solvents such as THF and acetonitrile, but dissolves poorly in nonpolar hydrocarbons. The ^{119}Sn{^{1}H} NMR spectrum shows a doublet at 81.9 ppm with a J(^{119}Sn,^{19}F) value of 610 Hz, which is shifted upfield in comparison to **1** [146.0 ppm, CD_3CN], presumably because the electron-donating capacity of the two [BF_4] moieties is higher than that of the triflate anion. The low number of signals for the Dipp groups in the ^{1}H NMR spectrum of **2** reflects a more symmetric structure compared to that of **1** in solution (CD_3CN). The J(Sn,F) value is significantly smaller than those for neutral covalently bonded fluorostannanes (2286−2893 Hz),[13] indicating the absence of Sn−F covalent bonding in **2**.

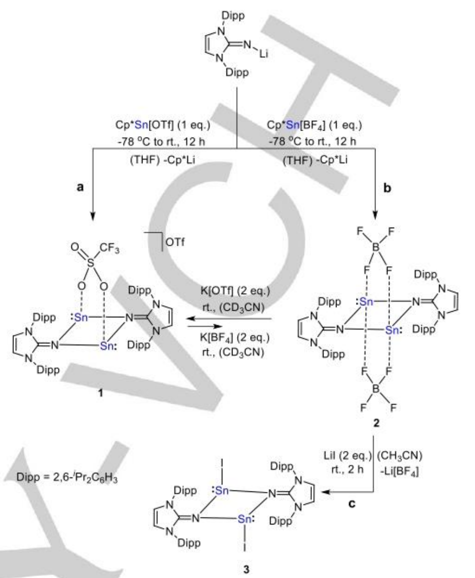

Scheme 1. Synthesis of [OTf]-bridged tin complex **1** and [BF_4]-bridged tin complex **2**, as well as anion exchange reactions.

Colorless crystals of **2** were obtained by slow diffusion of Et_2O into a saturated THF solution at -30 °C for several days. It crystallizes in the space group $P2_1/n$. SC-XRD analysis of **2** revealed that the molecular structure in the solid state comprises a centrosymmetric dimer, with a planar and rhombic N_2Sn_2 ring (sum of internal tetragonal angles: 360°, Figure 2). A related structure was observed in the cyclic bis(triflate)dibismadiazane [ArNBiOTf]$_2$ [Ar = 2,6-bis(2,4,6-trimethylphenyl)phenyl], with a planar N_2Bi_2 ring and two bridging triflate anions.[14] The Sn–N bond lengths (Sn1–N1 2.155(3) Å; Sn1–N1# 2.166(3) Å) are comparable to that in complex **I** (Sn–N$_{imino}$ 2.197(2) Å),[11] in which a high dative bond character between the tin(II) center and the imino-nitrogen atom was reported. The Sn···F distance (Sn1···F1 2.461(2) Å; Sn1···F2# 2.501(2) Å) is significantly longer than those in monomeric fluorostannanes such as Mes_3SnF (1.961 Å; Mes = 2,4,6-trimethylphenyl),[13b] $TpsiSnMe_2F$ (1.965(2) Å; Tpsi = $(PhMe_2Si)_3C$),[13a] and polymeric Me_2SnF_2 (2.12(1) Å).[13d]

10.1002/zaac.202200220

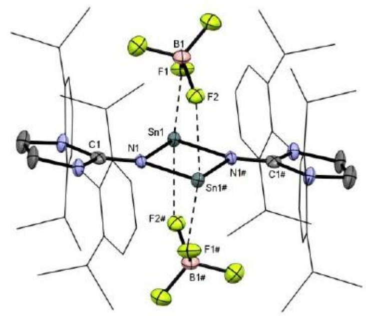

Figure 2. Molecular structure of **2**.[17] Thermal ellipsoids are shown at 50% probability level. Hydrogen atoms are omitted for clarity. Selected bond lengths [Å] and angles [°]: Sn1–N1 2.155(3), Sn1–N1# 2.166(3), Sn1···F1 2.461(2), Sn1···F2# 2.501(2), N1–C1 1.296(4), Sn1–N1–C1 129.1(2), Sn1–N1#–C1# 128.1(2), Sn1–N1–Sn1# 102.1(1), N1–Sn1–N1# 77.9(1).

It was also possible to form **1** by the reaction of **2** with K[OTf] (2 eq.) in CD_3CN at room temperature, albeit in a product ratio of 73:27 (**1**:**2**), as confirmed by ^{1}H NMR spectroscopy (Scheme 1). In addition, the yields of **1** and **2** did not significantly change when **1** was reacted with two equivalents of K[BF_4]. Interestingly, we did not observe the expected BF_4/OTf-mixed intermediate in the ^{1}H NMR spectrum.

With compound **2** in hand, we investigated its reactivity towards the nucleophiles Cp*Li, $Na_2Fe(CO)_4$, and LiI. No reaction was observed between **2** and Cp*Li (2 eq.) or $Na_2Fe(CO)_4$ (1 eq. or 2 eq.) in CD_3CN, even at elevated temperatures. The reaction of **2** towards LiI (2 eq.) in CD_3CN at room temperature was also performed and the selective formation of the dimeric imino(iodo)stannylene **3** was obtained (Scheme 1, path **c**). Due to its poor solubility in common organic solvents, it was not possible to observe any signals in the ^{119}Sn{^{1}H} NMR spectrum. The NHI backbone signal in the ^{1}H NMR spectrum of **3** (6.34 ppm, $CDCl_3$) is high-field shifted compared to that of **1** (6.88 ppm, CD_3CN) and **2** (6.83, CD_3CN). It should be noted that the reaction of **1** and LiI (2 eq.) in CD_3CN at room temperature led to an undefined product mixture.

Colorless crystals of **3** were obtained from a saturated dichloromethane solution stored at -30 °C. Compound **3** crystallizes in the $P2_1/n$ space group. SC-XRD analysis revealed that **3** consists of a centrosymmetric dimer, with a planar and rhombic N_2Sn_2 ring with two additional terminal iodine atoms (sum of internal tetragonal angles: 360°, Figure 3). The two iodine atoms adopt a *trans* configuration with respect to the N_2Sn_2 ring. The structural features are very similar to those of iminostannylenes [IPrNSnX] (X = Cl, Br, N_3),[11, 15] but differ from the dimeric cyclopentadienyl(imino)stannylene [IPrNSn(η^1-Cp)]$_2$ in which the two η^1-Cp ligands have a *cis* orientation with respect to the N_2Sn_2 ring.[15b] The Sn–N distances of 2.168(1) Å and 2.182(1) Å are in the range of Sn–N bond lengths reported for halo(imino)stannylenes [IPrNSnX] (X = Cl, Br) [2.161(3)–2.216(4)]. The Sn–I bond in **3** is oriented perpendicularly to both Sn–N bonds, with I1–Sn1–N3 and I1–Sn1–N3# bond angles of 85.90(4)° and 87.87(4)°, respectively.

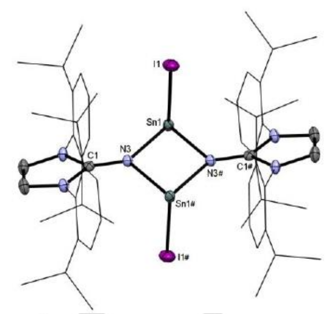

Figure 3. Molecular structure of **3**.[17] Thermal ellipsoids are shown at 50% probability level. Hydrogen atoms are omitted for clarity. Selected bond lengths [Å] and angles [°]: Sn1–I1 2.9176(4), Sn1–N3 2.168(1), Sn1–N3# 2.182(1), N3–C1 1.295(2), I1–Sn1–N3 85.90(4), I1–Sn1–N3# 87.87(4), N3–Sn1–N3# 77.72(5), Sn1–N3–C1 126.4(1), Sn1–N3#–C1# 130.3(1), Sn1–N3–Sn1# 102.28(5).

Next, we examined the reactivity of **2** towards small molecules. Exposure of a CD_3CN solution of **2** to an atmosphere of H_2 or N_2O showed no conversion, even at elevated temperatures. Treatment of **2** with CO_2 (1 bar) at room temperature formed an unidentified product mixture. The reaction of **2** with Na[BAr$^F{}_4$] (1 eq.) in CD_3CN at ambient temperature resulted in decomposition containing a large amount of free ligand IPrNH, and other undefined species.

The application of heavy Group 14 compounds in catalytic transformations have garnered much attention in the last decades, with many examples of tetrylenes and tetryliumylidenes being effective as catalysts.[10d, 16] Our preliminary study on the catalytic application of complexes **1** and **2** revealed that both complexes catalyze the hydroboration of aldehydes and ketones with pinacolborane (HBpin) (Table 1), with complex **2** having a higher activity. Because of its poor solubility in common organic solvents the catalytic activity of **3** was not examined.

Various aldehydes and ketones were screened for the hydroboration reaction catalyzed by **1** or **2** (Table 1). The reduction of benzaldehyde in the presence of 0.5 mol% of **1** was completed within 5 hours, whereas a shorter reaction time of only 0.5 h was observed when using the same loading of **2**. The reaction proceeds with a lower catalyst loading than those previously reported for neutral bis-amido tin catalysts in which 2 mol% catalyst loading in toluene at room temperature gave a conversion of 80~87% within 4–6 h.[16f] However, the catalytic activity is less efficient than other tin examples.[16a] It should be noted that both **1** and **2** are much more effective in the hydroboration of benzaldehyde compared to Na[BF_4] and K[OTf] (Table 1, entries 8 and 9). When isobutyraldehyde was used as the substrate, full conversion was observed after 2 h when using **2** (Table 1, entry 3). Substituted aromatic aldehydes with electron-donating groups (Table 1, entries 4 and 5) resulted in high yields, however longer reaction times were needed. The hydroboration of aromatic ketones was also possible utilizing **2** (Table 1, entries 6 and 7). In these cases, higher catalyst concentration was necessary to obtain satisfactory yields, compared to the reduction of aldehydes. The reduction of acetophenone in the presence of

10.1002/zaac.202200220

WILEY-VCH

5 mol% of **2** was completed within 19 h whereas for benzophenone, a longer reaction time was needed (Table 1, entry 7).

Table 1. Hydroboration of aldehydes and ketones with pinacolborane (HBpin), catalyzed by **1** or **2**.[a]

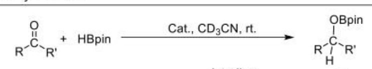

Entry	Substrate	Cat.	Loading, mol %	Conv.,[b] %	Time, h
1	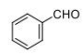	**1**	0.5	99	5
2	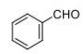	**2**	0.5	95	0.5
3	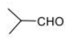	**2**	0.5	99	2
4	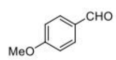	**2**	0.5	84	120
5	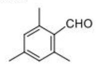	**2**	0.5	99	36
6	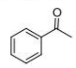	**2**	5	83	19
7	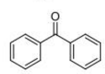	**2**	5	99	156
8	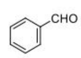	Na[BF$_4$]	0.5	63	24
9	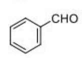	K[OTf]	0.5	36	24

[a] All reactions were carried out with 1.0 mmol of carbonyl compounds, 1.0 mmol of HBpin, in CD$_3$CN (0.4 mL) at room temperature. [b] NMR yield.

Conclusions

In summary, we have reported on the synthesis of the [OTf]- and [BF$_4$]-bridged binuclear tin complexes **1** and **2**, with a planar and rhombic N$_2$Sn$_2$ ring. Complex **2** reacts with LiI to afford the dimeric iodostannylene [IPrNSnI]$_2$ **3**. Notably, complex **2** showed higher catalytic activity in the hydroboration of aldehydes and ketones than that for **1**. The further reactivity and catalytic applications of these low-valent tin cations are currently under investigation.

Experimental Section

General Considerations

All experiments and manipulations were carried out under a dry oxygen-free argon atmosphere using standard Schlenk techniques or in a glovebox. All glass junctions were coated with PTFE-based grease, Merkel Triboflon III. All the solvents were dried and freshly distilled under Ar atmosphere prior to use by standard techniques. The ^{1}H, ^{19}F, ^{13}C{^{1}H}, ^{11}B{^{1}H} and ^{119}Sn{^{1}H} NMR spectra were recorded on Bruker 400 MHz spectrometer. Chemical shifts are referenced to (residual) solvent signals (CD$_3$CN: δ(^{1}H) = 1.94 ppm and δ(^{13}C) = 1.32 ppm; CDCl$_3$: δ(^{1}H) = 7.26 ppm and δ(^{13}C) = 77.16 ppm). Abbreviations: s = singlet, d = doublet, t = triplet, m = multiplet. Elemental analysis (EA) was conducted with a EURO EA (HEKA tech) instrument equipped with a CHNS combustion analyzer. Liquid Injection Field Desorption Ionization Mass Spectrometry (LIFDI-MS) was measured directly from an inert atmosphere glovebox with a Thermo Fisher Scientific Exactive Plus Orbitrap equipped with an ion source from Linden CMS. Unless otherwise stated, all commercially available chemicals were purchased from *abcr GmbH*, *Sigma-Aldrich Chemie GmbH* or *Tokyo Chemical Industry Co., Ltd.*, and used without further purification. The starting materials IPrNLi (IPrN = bis(2,6-diisopropylphenyl)imidazolin-2-imino),[18] Cp*Sn[BF$_4$],[2b] and Cp*Sn[OTf],[2c] were prepared according to the literature procedures, respectively.

Synthesis of [IPrNSnOTf]$_2$, (1)

IPrNLi (203 mg, 496 μmol) dissolved in THF (6 mL) was added dropwise to a solution of Cp*Sn[OTf] (200 mg, 496 μmol, 1.0 eq.) in THF (4 mL) at -78 °C. The reaction mixture was stirred for 12 h followed by warming to room temperature. The solvent was removed *in vacuo* and the solid residue was washed with toluene (5 mL × 3) and dried *in vacuo* to give pure **1** (180 mg, 61%) as a white powder. Colorless crystals of **1** suitable for single crystal X-ray analysis were obtained from a saturated solution in CD$_3$CN at -30 °C for several days.

^{1}H NMR (400 MHz, CD$_3$CN) δ = 7.42 (t, *J* = 7.7 Hz, 4H, Ar*H*), 7.29 (d, *J* = 7.7 Hz, 8H, Ar*H*), 6.88 (s, 4H, NC*H*), 2.67 – 2.56 (m, 8H, C*H*(CH$_3$)$_2$), 1.21 (d, *J* = 6.8 Hz, 24H, CH(C*H*$_3$)$_2$), 1.09 (d, *J* = 6.8 Hz, 24H, CH(C*H*$_3$)$_2$).

^{13}C{^{1}H} NMR (101 MHz, CD$_3$CN) δ = 153.3 (N*C*N), 148.5 (N*C*Ar), 133.4 (Ar*C*), 132.9 (Ar*C*), 129.9 (Ar*C*), 129.2 (Ar*C*), 127.5 (Ar*C*), 126.3 (Ar*C*), 118.3 (N*C*H), 68.3 (SO$_3$*C*F$_3$), 29.4 (*C*H(CH$_3$)$_2$), 26.2 (CH(*C*H$_3$)$_2$), 25.7 (CH(*C*H$_3$)$_2$), 23.1 (CH(*C*H$_3$)$_2$), 21.5 (CH(*C*H$_3$)$_2$).

^{119}Sn{^{1}H} NMR (149 MHz, CD$_3$CN) δ = 146.0.

^{19}F NMR (376 MHz, CD$_3$CN) δ = -79.4.

Anal. Calcd. [%] for $C_{56}H_{72}F_6N_6O_6S_2Sn_2$: C, 50.17; H, 5.41; N, 6.27. Found [%]: C, 50.10; H, 5.48; N, 6.35.

LIFDI-MS (positive ion mode): calculated for [M-OTf]$^+$: 1193.33826. Found: 1193.32344.

Synthesis of [IPrNSnBF$_4$]$_2$, (2)

IPrNLi (223 mg, 543 μmol) dissolved in THF (6 mL) was added dropwise to a solution of Cp*Sn[BF$_4$] (185 mg, 543 μmol, 1.0 eq.) in THF (4 mL) at -78 °C. The reaction mixture was stirred for 12 h followed by warming to room temperature. The solvent was removed *in vacuo* and the solid residue was washed with toluene (5 mL × 3) and dried *in vacuo* to give pure **2** (174 mg, 53%) as a white powder. Colorless crystals of **2** suitable for single crystal X-ray analysis were obtained by slow diffusion of Et$_2$O into a saturated THF solution at -30 °C for several days.

^{1}H NMR (400 MHz, CD$_3$CN) δ = 7.43 (t, *J* = 7.7 Hz, 4H, Ar*H*), 7.26 (d, *J* = 7.7 Hz, 8H, Ar*H*), 6.83 (s, 4H, NC*H*), 2.60 (septet, *J* = 6.8 Hz, 8H, C*H*(CH$_3$)$_2$), 1.12 (d, *J* = 6.8 Hz, 48H, CH(C*H*$_3$)$_2$).

$^{13}C\{^1H\}$ NMR (101 MHz, CD_3CN) δ = 152.4 (N<u>C</u>N), 148.3 (N<u>C</u>Ar), 133.0 (Ar<u>C</u>), 132.4 (Ar<u>C</u>), 130.0 (Ar<u>C</u>), 129.3 (Ar<u>C</u>), 127.0 (Ar<u>C</u>), 126.3 (Ar<u>C</u>), 125.5 (Ar<u>C</u>), 117.4 (N<u>C</u>H), 29.8 (<u>C</u>H($CH_3)_2$), 25.0 (CH(<u>C</u>$H_3)_2$), 23.4 (CH(<u>C</u>$H_3)_2$).
$^{119}Sn\{^1H\}$ NMR (149 MHz, CD_3CN) δ = 81.9 (d, J = 609.9 Hz).
$^{11}B\{^1H\}$ NMR (128 MHz, CD_3CN) δ = -1.2.
^{19}F NMR (376 MHz, CD_3CN) δ = -41.2 (Sn<u>F</u>), -152.5.
Anal. Calcd. [%] for $C_{54}H_{72}B_2F_8N_6Sn_2$: C, 53.33; H, 5.97; N, 6.91. Found [%]: C, 53.26; H, 6.05; N, 7.00.

Synthesis of [IPrNSnI]₂, (3)

LiI (11 mg, 82 µmol, 2.0 eq.) dissolved in CH_3CN (2 mL) was added dropwise to a solution of **2** (50 mg, 41 µmol, 1.0 eq.) in CH_3CN (4 mL) at room temperature. The reaction mixture was stirred for 2 h. The volatiles were removed *in vacuo* and the solid residue was dissolved in dichloromethane (DCM) and the solution was concentrated by slow evaporation of the solvent until formation of the crystalline product commenced. The crystals were separated from the liquid phase to afford colorless **3** after drying *in vacuo* (41 mg, 76%).
^1H NMR (400 MHz, $CDCl_3$) δ = 7.27 (t, J = 7.7 Hz, 4H, Ar<u>H</u>), 7.12 (d, J = 7.7 Hz, 8H, Ar<u>H</u>), 6.34 (s, 4H, NC<u>H</u>), 3.22 – 3.17 (m, 8H, C<u>H</u>($CH_3)_2$), 1.39 (d, J = 6.8 Hz, 24H, CH(C<u>H</u>$_3)_2$), 1.04 (d, J = 6.8 Hz, 24H, CH(C<u>H</u>$_3)_2$).
$^{13}C\{^1H\}$ NMR (101 MHz, $CDCl_3$) δ = 148.3 (N<u>C</u>N), 133.1 (Ar<u>C</u>), 130.6 (Ar<u>C</u>), 124.9 (Ar<u>C</u>), 116.6 (N<u>C</u>H), 28.3 (<u>C</u>H($CH_3)_2$), 26.1 (CH(<u>C</u>$H_3)_2$), 24.3 (CH(<u>C</u>$H_3)_2$).
Anal. Calcd. [%] for $C_{54}H_{72}I_2N_6Sn_2$: C, 50.03; H, 5.60; N, 6.48. Found [%]: C, 49.96; H, 5.68; N, 6.56.

Electronic Supporting Information available: NMR spectra, crystallographic details including ORTEP representations, and catalysis studies details.

Acknowledgements

We gratefully acknowledge financial support from the Deutsche Forschungsgemeinschaft (In 234/7-1). X.Z. gratefully acknowledges financial support from the China Scholarship Council. We thank Maximilian Muhr for the LIFDI-MS measurements.

Keywords: anion exchange • catalysis • hydroboration • stannylene • stannyliumylidene

[1] a) V. S. Swamy, S. Pal, S. Khan, S. S. Sen, *Dalton Trans.* **2015**, *44*, 12903-12923; b) I. Objartel, H. Ott, D. Stalke, *Z. Anorg. Allg. Chem.* **2008**, *634*, 2373-2379; c) R. Bandyopadhyay, B. F. T. Cooper, A. J. Rossini, R. W. Schurko, C. L. B. Macdonald, *J. Organomet. Chem.* **2010**, *695*, 1012-1018; d) H. Arii, M. Matsuo, F. Nakadate, K. Mochida, T. Kawashima, *Dalton Trans.* **2012**, *41*, 11195-11200; e) M. Bouška, L. Dostál, A. Růžička, R. Jambor, *Organometallics* **2013**, *32*, 1995-1999; f) A. P. Singh, H. W. Roesky, E. Carl, D. Stalke, J. P. Demers, A. Lange, *J. Am. Chem. Soc.* **2012**, *134*, 4998-5003; g) M. Wagner, T. Zoller, W. Hiller, M. H. Prosenc, K. Jurkschat, *Chem. Eur. J.* **2013**, *19*, 9463-9467; h) P. M. Keil, T. J. Hadlington, *Angew. Chem. Int. Ed.* **2022**, *61*, e202114143; i) P. M. Keil, T. J. Hadlington, *Chem. Commun.* **2022**, *58*, 3011-3014; j) M. K. Sharma, T. Glodde, B. Neumann, H. G. Stammler, R. S. Ghadwal, *Chem. Eur. J.* **2020**, *26*, 11113-11118; k) M. K. Sharma, D. Rottschafer, T. Glodde, B. Neumann, H. G. Stammler, R. S. Ghadwal, *Angew. Chem. Int. Ed.* **2021**, *60*, 6414-6418.
[2] a) P. Jutzi, F. Kohl, C. Krüger, *Angew. Chem. Int. Ed.* **1979**, *18*, 59-60; b) P. Jutzi, F. Kohl, P. Hofmann, C. Krüger, Y.-H. Tsay, *Chem. Ber.* **1980**, *113*, 757-769; c) F. X. Kohl, P. Jutzi, *Chem. Ber.* **1981**, *114*, 488-494.
[3] H. V. R. Dias, W. Jin, *J. Am. Chem. Soc.* **1996**, *118*, 9123-9126.
[4] M. J. Taylor, A. J. Saunders, M. P. Coles, J. R. Fulton, *Organometallics* **2011**, *30*, 1334-1339.
[5] J. Flock, A. Suljanovic, A. Torvisco, W. Schoefberger, B. Gerke, R. Pottgen, R. C. Fischer, M. Flock, *Chem. Eur. J.* **2013**, *19*, 15504-15517.
[6] M. Bouška, L. Dostál, A. Růžička, R. Jambor, *Organometallics* **2013**, *32*, 1995-1999.
[7] J. Li, C. Schenk, F. Winter, H. Scherer, N. Trapp, A. Higelin, S. Keller, R. Pottgen, I. Krossing, C. Jones, *Angew. Chem. Int. Ed.* **2012**, *51*, 9557-9561.
[8] A. Hinz, *Chem. Eur. J.* **2019**, *25*, 3267-3271.
[9] S. Khan, G. Gopakumar, W. Thiel, M. Alcarazo, *Angew. Chem. Int. Ed.* **2013**, *52*, 5644-5647.
[10] a) S. L. Powley, S. Inoue, *Chem. Rec.* **2019**, *19*, 2179-2188; b) P. Frisch, S. Inoue, *Dalton Trans.* **2020**, *49*, 6176-6182; c) D. Sarkar, C. Weetman, S. Dutta, E. Schubert, C. Jandl, D. Koley, S. Inoue, *J. Am. Chem. Soc.* **2020**, *142*, 15403-15411; d) D. Sarkar, S. Dutta, C. Weetman, E. Schubert, D. Koley, S. Inoue, *Chem. Eur. J.* **2021**, *27*, 13072-13078; e) F. S. Tschernuth, F. Hanusch, T. Szilvasi, S. Inoue, *Organometallics* **2020**, *39*, 4265-4272; f) R. Baierl, A. Kostenko, F. Hanusch, S. Inoue, *Dalton Trans.* **2021**, *50*, 14842-14848; g) S. V. Hirmer, F. S. Tschernuth, F. Hanusch, R. Baierl, M. Muhr, S. Inoue, *Mendeleev Commun.* **2022**, *32*, 16-18.
[11] T. Ochiai, D. Franz, E. Irran, S. Inoue, *Chem. Eur. J.* **2015**, *21*, 6704-6707.
[12] T. Ochiai, T. Szilvasi, D. Franz, E. Irran, S. Inoue, *Angew. Chem. Int. Ed.* **2016**, *55*, 11619-11624.
[13] a) S. S. Al-Juaid, S. M. Dhaher, C. Eaborn, P. B. Hitchcock, J. D. Smith, *J. Organomet. Chem.* **1987**, *325*, 117-127; b) I. Wharf, A.-M. Lebuis, G. A. Roper, *Inorg. Chim. Acta* **1999**, *294*, 224-231; c) G. Anselme, H. Ranaivonjatovo, J. Escudie, C. Couret, J. Satge, *Organometallics* **2002**, *11*, 2748-2750; d) E. O. Schlemper, W. C. Hamilton, *Inorg. Chem.* **2002**, *5*, 995-998.
[14] M. Lehmann, A. Schulz, A. Villinger, *Angew. Chem. Int. Ed.* **2012**, *51*, 8087-8091.
[15] a) T. Ochiai, D. Franz, X. N. Wu, E. Irran, S. Inoue, *Angew. Chem. Int. Ed.* **2016**, *55*, 6983-6987; b) T. Ochiai, S. Inoue, *RSC Adv.* **2017**, *7*, 801-804.
[16] a) T. J. Hadlington, M. Hermann, G. Frenking, C. Jones, *J. Am. Chem. Soc.* **2014**, *136*, 3028-3031; b) Y. Wu, C. Shan, Y. Sun, P. Chen, J. Ying, J. Zhu, L. L. Liu, Y. Zhao, *Chem. Commun.* **2016**, *52*, 13799-13802; c) T. J. Hadlington, C. E. Kefalidis, L. Maron, C. Jones, *ACS Catal.* **2017**, *7*, 1853-1859; d) J. Schneider, C. P. Sindlinger, S. M. Freitag, H. Schubert, L. Wesemann, *Angew. Chem. Int. Ed.* **2017**, *56*, 333-337; e) M. M. D. Roy, S. Fujimori, M. J. Ferguson, R. McDonald, N. Tokitoh, E. Rivard, *Chem. Eur. J.* **2018**, *24*, 14392-14399; f) R. Dasgupta, S. Das, S. Hiwase, S. K. Pati, S. Khan, *Organometallics* **2019**, *38*, 1429-1435; g) S. Sinhababu, D. Singh, M. K. Sharma, R. K. Siwatch, P. Mahawar, S. Nagendran, *Dalton Trans.* **2019**, *48*, 4094-4100; h) V. Nesterov, R. Baierl, F. Hanusch, A. E. Ferao, S. Inoue, *J. Am. Chem. Soc.* **2019**, *141*, 14576-14580; i) E. Fritz-Langhals, *Org. Process Res. Dev.* **2019**, *23*, 2369-2377; j) B. X. Leong, J. Lee, Y. Li, M. C. Yang, C. K. Siu, M. D. Su, C. W. So, *J. Am. Chem. Soc.* **2019**, *141*, 17629-

17636; k) J. Lee, J. Fan, A. P. Koh, W. J. Joslyn Cheang, M. C. Yang, M. D. Su, C. W. So, *Eur. J. Inorg. Chem.* **2022**, e202200129; l) A. P. Khuntia, N. Sarkar, A. G. Patro, R. K. Sahoo, S. Nembenna, *Eur. J. Inorg. Chem.* **2022**, e202200209.

[17] Deposition Number 2174491 (**2**) and 2174492 (**3**) contain the supplementary crystallographic data for this paper. These data are provided free of charge by the joint Cambridge Crystallographic Data Centre and Fachinformationszentrum Karlsruhe Access Structures service.

[18] D. Franz, E. Irran, S. Inoue, *Dalton Trans.* **2014**, *43*, 4451-4461.

10.1002/zaac.202200220

Entry for the Table of Contents

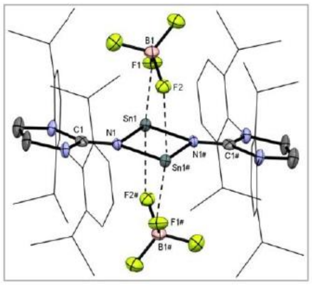

The $[BF_4]$- and [OTf]-bridged binuclear tin complexes were prepared by the reaction of $Cp^*Sn^+A^-$ ($Cp^* = C_5Me_5$; A = BF_4 or OTf) with one equivalent of IPrNLi (IPrN = bis(2,6-diisopropylphenyl)imidazolin-2-iminato). The high-yield conversion of the $[BF_4]$-bridged tin complex into the dimeric iodostannylene $[IPrNSnI]_2$ was accomplished by treatment with LiI. We also show the potential of these complexes in catalytic hydroboration of carbonyls.

Institute and/or researcher Twitter usernames: @InoueGroupTUM

7. Isolation and Reactivity of Stannylenoids Stabilized by Amido/Imino Ligands

Title: Isolation and Reactivity of Stannylenoids Stabilized by Amido/Imino Ligands

Status: Draft (Research Article)

Authors: Xuan-Xuan Zhao, Shiori Fujimori, John A. Kelly, Shigeyoshi Inoue*

Content:

The reaction of the lithium aryl(silyl)amide Dipp(^{i}Pr$_3$Si)NLi (Dipp = 2,6-^{i}Pr$_2$C$_6$H$_3$) with one equivalent of $SnCl_2$ in THF gave a novel stannylenoid **1**. Heating up the solution of **1** in toluene at 80 °C resulted in the dimeric amido(chloro)stannylene **2**, which can be converted to the bis(amido)stannylene **3** and amido(imino)stannylene **4**. Treatment of bis(imino)stannylenoid **J** with N_2O resulted in the dimeric complex [IPrNSn(Cl)OLi]$_2$ **5** (IPrN = bis(2,6-diisopropylphenyl)imidazolin-2-imino). All compounds were characterized by NMR, elementary analysis, and X-ray structural determination.

* X.-X. Zhao planned and executed all experiments including analysis and wrote the manuscript. S. Fujimori conducted all SC-XRD measurements and managed the processing of the respective data. J. A. Kelly contributed to the manuscript. All work was performed under the supervision of S. Inoue.

Isolation and Reactivity of Stannylenoids Stabilized by Amido/Imino Ligands

Xuan-Xuan Zhao,[a] Shiori Fujimori,[a] John A. Kelly,[a] and Shigeyoshi Inoue*[a]

[a] X.-X. Zhao, Dr. S. Fujimori, Dr. J. A. Kelly, Prof. Dr. S. Inoue
Department of Chemistry,
WACKER-Institute of Silicon Chemistry and Catalysis Research Center, Technische Universität München
Lichtenbergstraße 4, 85748 Garching bei München (Germany)
E-mail: s.inoue@tum.de

Supporting information for this article is given *via* a link at the end of the document.

Abstract: The reaction of the lithium aryl(silyl)amide Dipp(^{i}Pr$_3$Si)NLi (Dipp = 2,6-^{i}Pr$_2$C$_6$H$_3$) with one equivalent of $SnCl_2$ in THF gave a novel stannylenoid **1**. Heating up the solution of **1** in toluene at 80 °C resulted in the dimeric amido(chloro)stannylene **2**, which can be converted to the bis(amido)stannylene **3** and amido(imino)stannylene **4**. Treatment of bis(imino)stannylenoid **J** with N_2O resulted in the dimeric complex [IPrNSn(Cl)OLi]$_2$ **5** (IPrN = bis(2,6-diisopropylphenyl)imidazolin-2-imino). All compounds were characterized by NMR, elemental analysis, and X-ray structural determination.

Introduction

Metal@MX complexes (M = alkali metal, X = leaving group) are commonly observed in organometallic chemistry.[1] For example, Xi and coworkers reported the metallacycle of indium (**I**) bearing a Cl−Li(THF)$_3$ moiety (Figure 1, top).[2] Subsequently, they synthesized the nonplanar metalla-aromatics complexes (**II**) with two iron centers coordinated by four bromides.[3] They also reported the lutetacyclopentadiene@LiCl complex (**III**).[4] Moreover, the Luo group also described some rare-earth-metal @LiCl complexes, which are thermally stable at ambient temperature.[5] In contrast, Group 14-element@MX complexes are relatively unstable and less explored.

Carbenoids with the formula R$_2$CMX (M = alkali metal, X = leaving group) have attracted much attention owing to their unusual reactivity. In recent years, there have been important developments in the search for stable LiCl carbenoid species. In 1993, Boche and coworkers reported on the isolation of a LiCl alkylidenecarbenoid (**IV**),[6] which was stable up to -60 °C (Figure 1, bottom). Two years later, Niecke and coworkers synthesized the phosphavinylidene carbenoid (**V**) containing a P(III) atom,[7] which was decomposed on warming to room temperature. In 2007, Le Floch and coworkers isolated the first example of room temperature stable carbenoid (**VI**) by the chlorination of the corresponding dianion by mild oxidation of stable geminal dianions.[8]

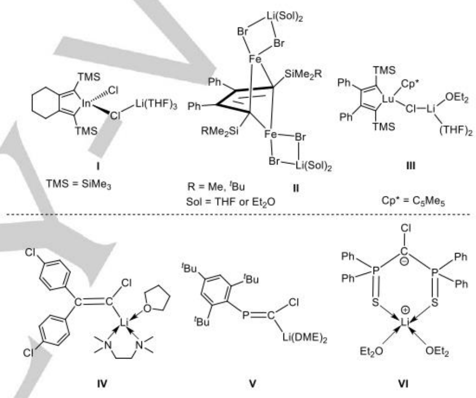

Figure 1. Metal@MX (M = alkali metal, X = leaving group) complexes (top) and selected examples of carbenoids (bottom).

Like carbenoids, the isolation of heavier congeners (R$_2$EMX; E = Si, Ge, Sn, Pb; M = alkali metal, X = leaving group), is also largely hampered. For example, in 1997, Tamao and coworkers investigated the alkoxyl-substituted silylenoid (^{t}BuO)Ph$_2$SiLi (**A**) (Figure 2),[9] which underwent bimolecular self-condensation at 0 °C. Within the same year, the silylenoid Tbt(Dipp)Si@LiBr (**B**) (Tbt = 2,4,6-[CH(SiMe$_3$)$_2$]$_3$C$_6$H$_2$; Dipp = 2,6-^{i}Pr$_2$C$_6$H$_3$) was synthesized by the reduction of dibromosilane with lithium naphthalide.[10] Moreover, Lee and coworkers have been widely investigated the reactivity of metal/halogen silylenoids **C**.[11] It should be noted that the first structurally characterized silylenoid **D** was reported in 2006.[12]

Up to now, the germanium and tin congeners remain largely unexplored mainly due to the increased stability of the divalent Ge(II) and Sn(II) atom in comparison to the lighter congeners. As a consequence, the elimination of metal halide (MX, M = alkali metal, X = leaving group) from the high-coordinate germanium or tin center is strongly favored. In 1996, Ando and Ohtaki described the synthesis of a trisyl-substituted chlorogermylenoid **E**,[13] however, the molecular structure of this compound in the solid state was not reported (Figure 2). In 2016, Sasamori and coworkers successfully synthesized the chlorogermylenoid **F** that was studied by X-ray crystallography.[14]

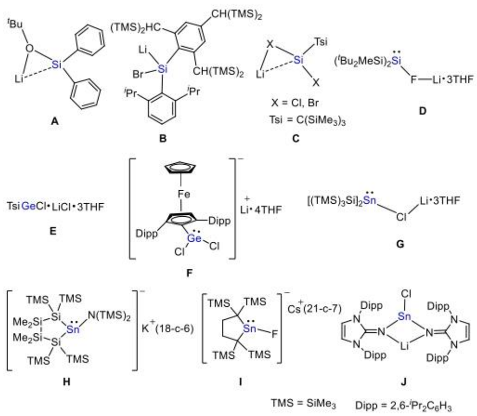

Figure 2. Literature known examples of heavy tetrylenoids.

As for the stannylenoids, in 1987, Cowley and coworkers reported the silyl-substituted stannylenoid **G**.[15] Notably, some efforts to remove the solvated LiCl from **G** were unsuccessful, which sublimation or prolonged refluxing in toluene resulted in decomposition. With the help of crown ethers, the stannylenoids **H** [16] and **I** [17] were isolated and characterized by X-ray crystallography. In 2016, we reported a rare example of a lithium stannylenoid **J** prepared by using the *N*-heterocyclic imine (NHI) ligand and verified the high stannylenoid character of this compound by demonstrating its ambiphilic reactivity.[18]

Motivated by the above results, herein we report on a room temperature stable stannylenoid by using a bulky amido ligand. We also show its facile transformations into the corresponding amidostannylenes. Moreover, we investigate the further reactivity of bis(imino)stannylenoid **J** towards N_2O.

Results and Discussion

The reaction of Dipp(^{i}Pr$_3$Si)NLi with one equivalent of $SnCl_2$ in THF at room temperature led to the formation of the amidostannylenoid **1** in high yield (97%; Scheme 1). No elimination of LiCl was observed in C_6D_6 at room temperature for at least one week. **1** was characterized by multinuclear NMR and elemental analysis (see the Supporting Information for more details). The ^{29}Si{^{1}H} NMR spectrum of **1** displays a signal at 7.8 ppm in C_6D_6, which is downfield shifted in comparison to Dipp(^{i}Pr$_3$Si)NLi (-5.6 ppm, C_6D_6). The signals of the Dipp group in the ^{1}H NMR spectrum of **1** are also shifted to lower field than those of Dipp(^{i}Pr$_3$Si)NLi, indicating a strong electron-donating from the amido ligand to the tin center. The ^{119}Sn{^{1}H} NMR spectrum shows a signal at 197.7 ppm, which is downfield shifted in comparison to **J** [-52.1 ppm, C_6D_6], indicating a more electron-poor Sn(II) center.

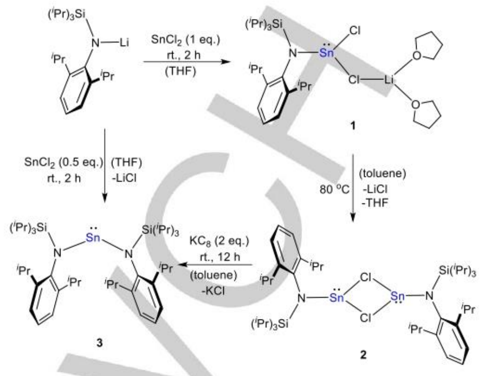

Scheme 1. Synthesis of amido-substituted stannylenoid **1** and its facile transformation into the dimeric amido(chloro)stannylene **2**, as well as the synthesis of bis(amido)stannylene **3**.

Colorless crystals of complex **1** suitable for X-ray diffraction (XRD) were grown from *n*-pentane at -30 °C. It crystallizes in the space group $P2_1/c$. The molecular structure is shown in Figure 3. **1** contains one equivalent of Cl−Li(THF)$_2$ moiety. In **1**, the tin center is three-coordinated by one chlorine atom, one amido ligand, and one Cl−Li(THF)$_2$ moiety to form a triangular pyramid geometry (sum of angles at Sn is 285.86°). The distance of Sn1−N1 is 2.115(1) Å, which is longer than those in Lappert's stannylene Sn[N(SiMe$_3$)$_2$]$_2$ [2.09(1) Å].[19] The bond length of Sn1−Cl1 [2.5679(6) Å] is longer than that of Sn1−Cl2 [2.5077(5) Å], indicating a stronger interaction between Sn1 and Cl2. The amido(chloro) tin moiety is linked with Li$^+$(THF)$_2$ moiety by a chlorine atom. The wide bond angle of Sn1−Cl2−Li3 [107.82(7)°] may reduce the steric repulsion between the amido(chloro) tin moiety and Li$^+$(THF)$_2$ moiety.

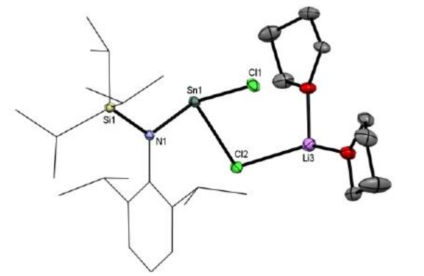

Figure 3. Molecular structure of **1**.[25] Thermal ellipsoids are shown at 50% probability level. Hydrogen atoms are omitted for clarity. Selected bond lengths [Å] and angles [°]: Sn1–Cl1 2.5679(6), Sn1–Cl2 2.5077(5), Sn1–N1 2.115(1), Si1–N1 1.752(1), Cl2–Li3 2.410(3), Cl1–Sn1–Cl2 88.96(2), Cl1–Sn1–N1 100.81(4), Cl2–Sn1–N1 96.09(4), Sn1–N1–Si1 121.20(7), Sn1–Cl2–Li3 107.82(7).

Due to the efficient stabilization by two bulky and strongly π-donating NHI substituents, the lithium stannylenoid **J** has a rather high thermal stability in C_6D_6 at 80 °C, with no elimination of LiCl observed in ^{1}H NMR. The reactivity of **J** was well investigated, revealing that it undergoes oxidative addition of I_2 and CH_3I, with the elimination of LiCl from the tin center.

By contrast, heating up a C_6D_6 solution of **1** at 80 °C for 2 h readily yields the dimeric amido(chloro)stannylene **2** in nearly quantitative yield. **2** was characterized by multinuclear NMR and XRD (see the Supporting Information for more details). The ^{119}Sn{^{1}H} NMR spectrum shows a signal at 187.2 ppm (C_6D_6), which is comparable to **1** (197.7 ppm, C_6D_6), but shifted to high field in comparison to Power's chlorostannylene $[ArSnCl]_2$ (Ar = 2,6-bis(2,4,6-trimethylphenyl)phenyl) [562 ppm, C_6D_6],[20] indicating a more electron-rich Sn(II) center. In addition, the high number of signals of the Dipp groups in the ^{1}H NMR spectrum of **2** reflects its less symmetric structure than **1** in solution (C_6D_6). It should be noted that **2** has been described by Hadlington *et al.* recently.[21]

Given that two reactive Sn(II)-halide environments are held in close proximity within **2**, we attempted to promote Sn–Sn bond formation *via* reduction. Treatment of **2** with two equivalents of potassium graphite (KC_8) in toluene at room temperature, resulted in the bis(amido)stannylene **3** (Scheme 1). The orange-red solid was characterized by multinuclear NMR, LIFDI-MS measurements, and elemental analysis (see the Supporting Information for more details). The ^{119}Sn{^{1}H} NMR spectrum of **3** in C_6D_6 shows a signal at σ = 517.5 ppm that is shifted to higher field as compared to that of Power's stannylene Ar_2Sn (Ar = 2,6-bis(2,4,6-trimethylphenyl)phenyl) [635 ppm, C_6D_6],[20] and Rivard's stannylene $(^{Me}IPr{=}CH)_2Sn$ (^{Me}IPr = $[(MeCNDipp)_2C:)$ [1162 ppm, toluene-d_8].[22] It was also possible to form **3** by the reaction of Dipp($^i Pr_3Si$)NLi with $SnCl_2$ (0.5 eq.) in THF at room temperature (Scheme 1).

Red crystals of **3** were obtained in a saturated Et_2O solution at -30 °C for several days. **3** crystallizes in the *P* -1 space group. In the solid state, compound **3** exists as a V-shaped, discrete monomer with the closest Sn–Sn distance [11.649 Å] (Figure 4). The Sn–N bond lengths are 2.091(7), and 2.124(8) Å, with any further metal-ligand interaction being longer than 3.0 Å. The bond angle of N1–Sn1–N2 [118.3(3)°] in **3** is larger than that in $Sn[N(SiMe_3)_2]_2$ [104.7(2)°].[19]

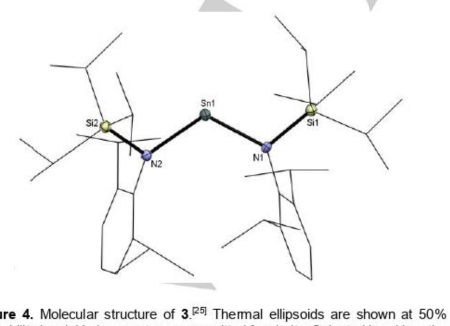

Figure 4. Molecular structure of **3**.[25] Thermal ellipsoids are shown at 50% probability level. Hydrogen atoms are omitted for clarity. Selected bond lengths [Å] and angles [°]: Sn1–N1 2.091(7), Sn1–N2 2.124(8), N1–Si1 1.784(9), N2–Si2 1.780(8), N1–Sn1–N2 118.3(3), Sn1–N1–Si1 114.0(4), Sn1–N2–Si2 111.3(4).

Reaction of **2** with two equivalents of IPrNLi (IPrN = bis(2,6-diisopropylphenyl)imidazolin-2-iminato) resulted in the amido(imino)stannylene **4** in 70% yield (Scheme 2, path **a**). **4** was also characterized by multinuclear NMR, LIFDI-MS measurements, and elemental analysis (see the Supporting Information for more details). In addition, the isolated yield of **4** did not significantly change when compound **1** reacted directly with IPrNLi (1 eq.) in THF at room temperature (Scheme 2, path **b**). Compound **4** is soluble in THF, but the solubility decreases significantly in C_6D_6. Notably, it was not possible to observe any signals in the ^{119}Sn{^{1}H} NMR spectrum. The NHI signals in the ^{1}H NMR spectrum of **4** are more high-field shifted compared to those of the amido(imino)syannylene $IPrNSnN(TMS)_2$ reported by our group in 2015.[23]

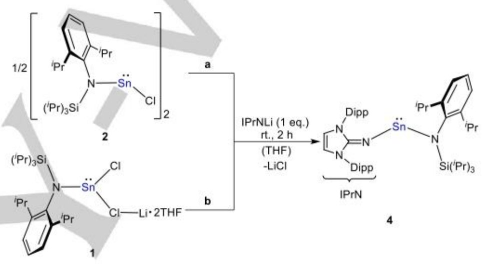

Scheme 2. Synthesis of amido(imino)stannylene **4** from **2** or **1** with IPrNLi.

Red crystals of **4** were obtained in a saturated Et_2O solution at -30 °C for several days. **4** crystallizes in the *P* -1 space group. X-ray diffraction analysis of **4** revealed a monomeric structure (Figure 5). The Sn1−N1 distance of 2.023(2) Å is shorter than the Sn1−N4 distance of 2.112(2) Å, which suggests that the tin center interacts more strongly with the nitrogen atom of the imino ligand than it does with the nitrogen atom of the amido group. Due to the two bulky substituents the Sn1−N4 distance [2.112(2) Å] in **4** is increased in comparison to that in Lappert's stannylene $Sn[N(SiMe_3)_2]_2$ [2.09(1) Å].[19] The bond angle of N1–Sn1–N4 [100.42(7)°] in **4** is more acute than that in **3** [118.3(3)°].

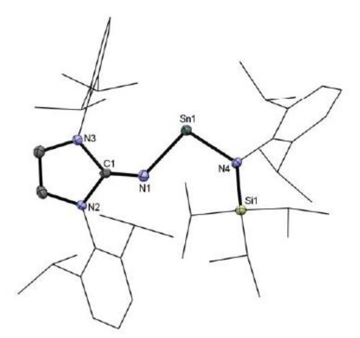

Figure 5. Molecular structure of **4**.[25] Thermal ellipsoids are shown at 50% probability level. Hydrogen atoms are omitted for clarity. Selected bond lengths [Å] and angles [°]: Sn1–N1 2.023(2), Sn1–N4 2.112(2), N1–C1 1.281(3), N4–Si1 1.758(2), N1–Sn1–N4 100.42(7), Sn1–N4–Si1 133.5(1), Sn1–N1–C1 128.1(2).

With **3** and **4** in hand, we carried out the targeted oxygenation reactions. Unfortunately, both **3** and **4** showed no reactivity towards N_2O (1 bar) in C_6D_6, even at elevated temperatures. Then, we turned to the previously reported bis(imino)stannylenoid **J**. Interestingly, exposure of a toluene solution of **J** with gaseous N_2O (1 bar) at room temperature led to a tin analogue of lithium alkoxides $[IPrNSn(Cl)OLi]_2$ **5** in 89% yield (Scheme 3). The NHI backbone signal in the ^1H NMR spectrum of **5** (5.86 ppm, C_6D_6) is high field shifted compared to that of **J** (5.94 ppm, C_6D_6). Moreover, the high number of signals of the Dipp groups in the ^1H NMR spectrum of **5** reflects its less symmetric structure than **J** in solution (C_6D_6). **5** has a high thermal stability in C_6D_6, and no detectable change was observed in the ^1H NMR spectrum of **5** in C_6D_6 at 80 °C for 24 h. The $^{119}Sn\{^1H\}$ NMR spectrum of **5** in C_6D_6 displays a signal for the central tin atom at -273.2 ppm, which is shifted to higher field compared to that of **J** (-52.1 ppm, C_6D_6). Notably, treating a toluene solution of **1** with N_2O (1 bar) at room temperature resulted in decomposition.

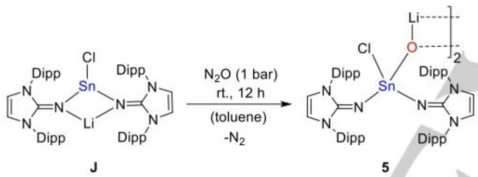

J **5**

Scheme 3. Reaction of bis(imino)stannylenoid **J** and N_2O to **5**.

Colorless crystals of **5** were obtained in a saturated THF solution at -30 °C for several months. **5** crystallizes in the *C*2/*c* space group. SC-XRD study revealed that **5** contains a four-membered Li_2O_2 ring (Figure 6). A related structure was observed in the cyclic lithium alkoxide $[^tBu_3COLi]_2$ reported by Lappert and coworkers.[24] The Sn−N bond lengths [Sn1−N1 1.991(6) Å and Sn1−N2 2.010(5) Å] in **5** are shorter than those in **J** [2.143(5) Å and 2.179(4) Å]. The Sn1−Cl1 bond length [2.384(2) Å] is significantly shorten in comparison to that in **J** [2.532(2) Å].

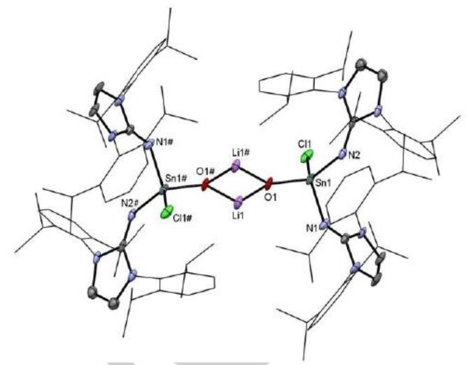

Figure 6. Molecular structure of **5**.[25] Thermal ellipsoids are shown at 50% probability level. Hydrogen atoms and solvent molecules are omitted for clarity. Selected bond lengths [Å] and angles [°]: Sn1–N1 1.991(6), Sn1–N2 2.010(5), Sn1–O1 1.886(4), Sn1–Cl1 2.384(2), O1–Li1 1.71(1), O1–Li1# 1.96(1), N1–Sn1–N2 110.4(2), N1–Sn1–Cl1 109.5(2), N1–Sn1–O1 101.6(2), N2–Sn1–O1 119.7(2), N2–Sn1–Cl1 106.4(2), Cl1–Sn1–O1 109.1(1), Sn1–O1–Li1 124.3(5), Sn1–O1–Li1# 152.2(4).

Conclusion

In summary, we have synthesized a novel stannylenoid **1** bearing a bulky amido ligand, which was obtained from the salt metathesis reaction of $Dipp(^iPr_3Si)NLi$ with one equivalent of $SnCl_2$ in THF at room temperature. Compound **1** can be converted to the dimeric chlorostannylene **2** at 80 °C, with the elimination of LiCl. Reduction of **2** by two equivalents of KC_8 in toluene resulted in the bis(amido)stannylene **3**. Moreover, treatment of **2** with IPrNLi (1 eq.) in THF at room temperature led to the formation of the amido(imino)stannylene **4**. In addition, treating a toluene solution of bis(imino)stannylenoid **J** with N_2O resulted in the dimeric complex $[IPrNSn(Cl)OLi]_2$ in high yield. Further small molecule activation, coordination chemistry, and catalytic applications are currently under investigation.

Experimental Section

Experimental details including synthesis, NMR spectra, and crystallographic data are reported in the Supporting Information.

Acknowledgements

We gratefully acknowledge financial support from the Deutsche Forschungsgemeinschaft (In 234/7-1). X.Z. gratefully acknowledges financial support from the China Scholarship Council. We thank Maximilian Muhr for the LIFDI-MS measurements.

Conflict of interest

The authors declare no conflict of interest.

Keywords: low-coordinate compounds • *N*-donor ligands • oxidation • stannylene • stannylenoid

[1] a) F. T. Edelmann, D. M. Freckmann, H. Schumann, *Chem. Rev.* **2002**, *102*, 1851-1896; b) G.-X. Wang, J. Yin, J. Li, Z.-B. Yin, W.-X. Zhang, Z. Xi, *Inorg. Chem. Front.*, **2019**, *6*, 428-433; c) C. Yu, W. Ma, W.-X. Zhang, Z. Xi, *Organometallics* **2020**, *39*, 793-796; d) C. Yu, B. Wu, Z. Yang, H. Chen, W.-X. Zhang, Z. Xi, *Bull. Chem. Soc. Jpn.* **2020**, *93*, 1314-1318; e) Y. Zheng, C. S. Cao, W. Ma, T. Chen, B. Wu, C. Yu, Z. Huang, J. Yin, H. S. Hu, J. Li, W. X. Zhang, Z. Xi, *J. Am. Chem. Soc.* **2020**, *142*, 10705-10714.

[2] Y. Zhang, Z. Yang, W. X. Zhang, Z. Xi, *Chem. Eur. J.* **2019**, *25*, 4218-4224.

[3] C. Yu, M. Zhong, Y. Zhang, J. Wei, W. Ma, W. X. Zhang, S. Ye, Z. Xi, *Angew. Chem. Int. Ed.* **2020**, *59*, 19048-19053.

[4] L. Xu, Y. C. Wang, J. Wei, Y. Wang, Z. Wang, W. X. Zhang, Z. Xi, *Chem. Eur. J.* **2015**, *21*, 6686-6689.

[5] a) B. Shen, L. Ying, J. Chen, Y. J. Luo, *Inorg. Chim. Acta* **2008**, *361*, 1255-1260; b) Y. Luo, X. Wang, J. Chen, C. Luo, Y. Zhang, Y. Yao, *J. Organomet. Chem.* **2009**, *694*, 1289-1296; c) Y. Luo, S. Fan, J. Yang, J. Fang, P. Xu, *Dalton Trans.* **2011**, *40*, 3053-3059.

[6] a) G. Boche, M. Marsch, A. Müller, K. Harms, *Angew. Chem. Int. Ed.* **1993**, *32*, 1032-1033; b) G. Boche, J. C. Lohrenz, *Chem. Rev.* **2001**, *101*, 697-756..

[7] a) E. Niecke, P. Becker, M. Nieger, D. Stalke, W. W. Schoeller, *Angew. Chem. Int. Ed.* **1995**, *34*, 1849-1852; b) E. Niecke, M. Nieger, O. Schmidt, D. Gudat, W. W. Schoeller, *J. Am. Chem. Soc.* **1999**, *121*, 519-522.

[8] T. Cantat, X. Jacques, L. Ricard, X. F. Le Goff, N. Mezailles, P. Le Floch, *Angew. Chem. Int. Ed.* **2007**, *46*, 5947-5950.

[9] a) A. Kawachi, K. Tamao, *Bull. Chem. Soc. Jpn.* **1997**, *70*, 945-955; b) Y. Tanaka, M. Hada, A. Kawachi, K. Tamao, H. Nakatsuji, *Organometallics* **1998**, *17*, 4573-4577; c) K. Tamao, A. Kawachi, M. Asahara, A. Toshimitsu, *Pure Appl. Chem.* **1999**, *71*, 393-400; d) D. Feng, J. Xie, S. Feng, *Chem. Phys. Lett.* **2004**, *396*, 245-251.

[10] a) N. Tokitoh, K. Hatano, T. Sadahiro, R. Okazaki, *Chem. Lett.* **1999**, *28*, 931-932; b) K. Hatano, N. Tokitoh, N. Takagi, S. Nagase, *J. Am. Chem. Soc.* **2000**, *122*, 4829-4830.

[11] a) M. E. Lee, H. M. Cho, Y. M. Lim, J. K. Choi, C. H. Park, S. E. Jeong, U. Lee, *Chem. Eur. J.* **2004**, *10*, 377-381; b) Y. M. Lim, H. M. Cho, M. E. Lee, K. K. Baeck, *Organometallics* **2006**, *25*, 4960-4964; c) H. M. Cho, Y. M. Lim, M. E. Lee, *Dalton Trans.* **2010**, *39*, 9232-9234; d) H. M. Cho, Y. M. Lim, B. W. Lee, S. J. Park, M. E. Lee, *J. Organomet. Chem.* **2011**, *696*, 2665-2668.

[12] G. Molev, D. Bravo-Zhivotovskii, M. Karni, B. Tumanskii, M. Botoshansky, Y. Apeloig, *J. Am. Chem. Soc.* **2006**, *128*, 2784-2785.

[13] T. Ohtaki, W. Ando, *Organometallics* **1996**, *15*, 3103-3105.

[14] Y. Suzuki, T. Sasamori, J. D. Guo, S. Nagase, N. Tokitoh, *Chem. Eur. J.* **2016**, *22*, 13784-13788.

[15] A. M. Arif, A. H. Cowley, T. M. Elkins, *J. Organomet. Chem.* **1987**, *325*, C11-C13.

[16] a) H. Arp, J. Baumgartner, C. Marschner, T. Muller, *J. Am. Chem. Soc.* **2011**, *133*, 5632-5635; b) H. Zhao, J. Li, X. Q. Xiao, M. Kira, Z. Li, T. Muller, *Chem. Eur. J.* **2018**, *24*, 5967-5973.

[17] C. Yan, Z. Li, X. Q. Xiao, N. Wei, Q. Lu, M. Kira, *Angew. Chem. Int. Ed.* **2016**, *55*, 14784-14787.

[18] T. Ochiai, D. Franz, X. N. Wu, E. Irran, S. Inoue, *Angew. Chem. Int. Ed.* **2016**, *55*, 6983-6987.

[19] T. Fjeldberg, H. Hope, M. F. Lappert, P. P. Power, A. J. Thorne, *J. Chem. Soc. Chem. Commun.* **1983**, 639-641.

[20] R. S. Simons, L. Pu, M. M. Olmstead, P. P. Power, *Organometallics* **1997**, *16*, 1920-1925.

[21] P. M. Keil, T. J. Hadlington, *Chem. Commun.* **2022**, *58*, 3011-3014.

[22] M. M. D. Roy, S. R. Baird, E. Dornsiepen, L. A. Paul, L. Miao, M. J. Ferguson, Y. Zhou, I. Siewert, E. Rivard, *Chem. Eur. J.* **2021**, *27*, 8572-8579.

[23] T. Ochiai, D. Franz, E. Irran, S. Inoue, *Chem. Eur. J.* **2015**, *21*, 6704-6707.

[24] G. Beck, P. B. Hitchcock, M. F. Lappert, I. A. MacKinnon, *J. Chem. Soc. Chem. Commun.* **1989**, 1312-1314.

[25] Deposition Number 2191800 (**1**), 2191801 (**2**), 2191802 (**3**), 2191803 (**4**), and 2191804 (**5**) contain the supplementary crystallographic data for this paper. These data are provided free of charge by the joint Cambridge Crystallographic Data Centre and Fachinformationszentrum Karlsruhe Access Structures service.

Entry for the Table of Contents

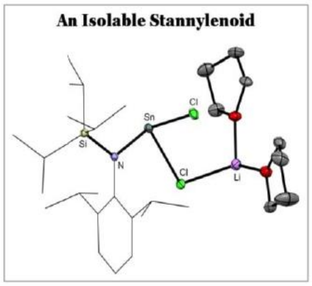

A novel stannylenoid was isolated by using a bulky amido ligand. It can be converted to the dimeric chlorostannylene at 80 °C with the elimination of LiCl. Treatment of the amidostannylenoid with IPrNLi (IPrN = bis(2,6-diisopropylphenyl)imidazolin-2-iminato) led to the formation of the amido(imino)stannylene. In addition, the reaction of bis(imino)stannylenoid with N_2O resulted in a dimeric Sn/O/Li complex.

Institute and/or researcher Twitter usernames: @InoueGroupTUM

8. Summary and Outlook

N-heterocyclic imine (NHI) ligands may act as a 2σ- and either 2π- or 4π electron donors. Therefore, the imino group is an excellent choice for thermodynamic stabilization of electron-deficient species. Low-valent and low-oxidation state germanium and tin complexes have attracted much attention due to their unique electronic properties and reactivity. Recently, we have developed facile synthetic methods to stabilize low-coordinate Group 14 compounds using NHIs as supporting ligands. To expand this chemistry, this thesis presents low-coordinate germanium and tin compounds and its reactivity towards bond activation and catalysis.

The germanium iron carbonyl complex **3** was prepared by the reaction of dimeric chloro(imino)germylene $[IPrNGeCl]_2$ (IPrN = bis(2,6-diisopropylphenyl)imidazolin-2-iminato) with one equivalent of Collman's reagent ($Na_2Fe(CO)_4$) at room temperature (Scheme 1). Similarly, the reaction of the chloro(imino)stannylene $[IPrNSnCl]_2$ with $Na_2Fe(CO)_4$ (1 eq.) resulted in the $Fe(CO)_4$-bridged bis(stannylene) complex **4**. We observed reversible manifestation of bis(tetrylene) and tetrylene-tetrylone character in these complexes, by variable temperature (VT) NMR analysis. Moreover, the Li/Sn/Fe trimetallic complex **9** has been isolated from the reaction of $[IPrNSnCl]_2$ with cyclopentadienyl iron dicarbonyl anion. The computational analysis further rationalizes the reduction pathway from these chlorotetrylenes to the corresponding complexes. The mixed tetrylene-tetrylone complexes represent a new and interesting structure type in main group element chemistry. These metal complexes may provide new opportunities for main group metal mediated cooperative catalytic applications in the future.

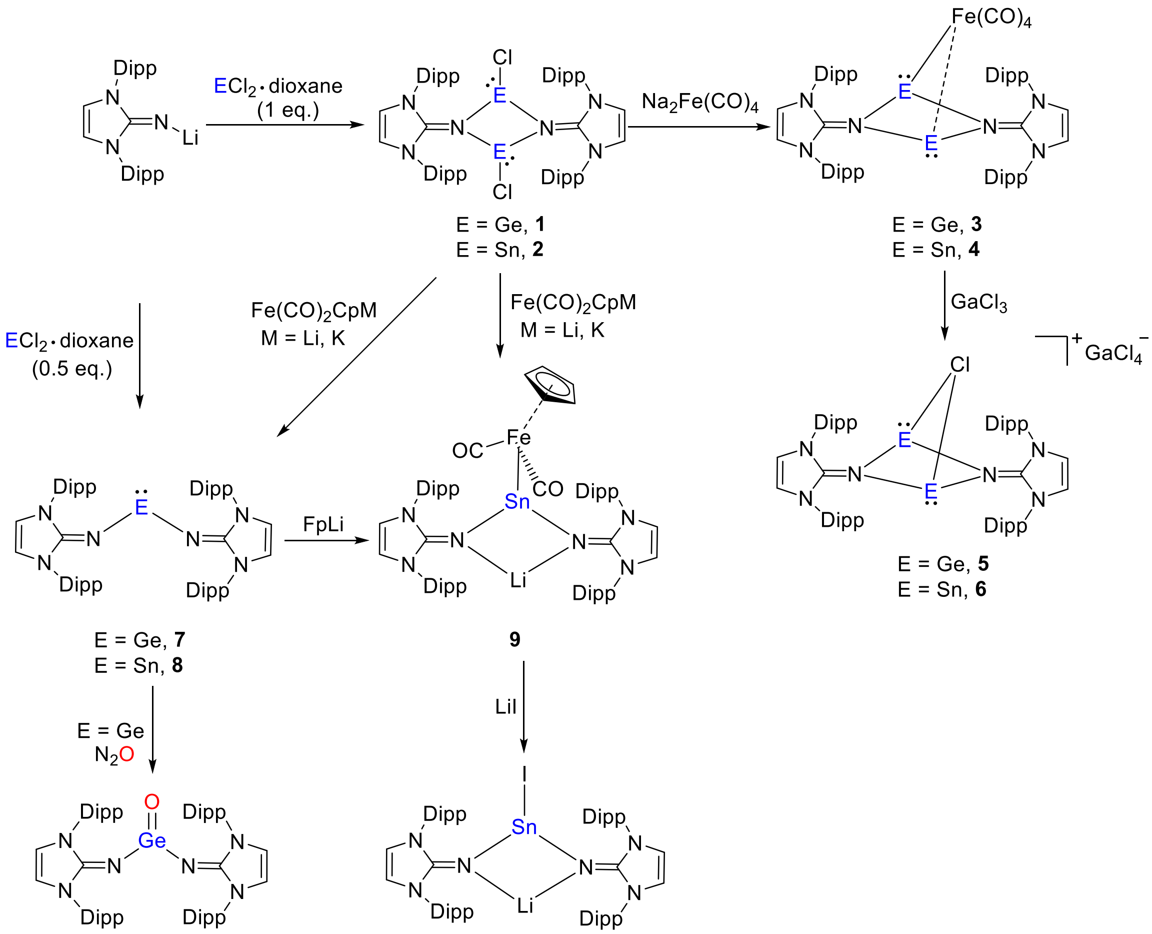

Scheme 1. Synthesis and reactivity of tetrylene-tetrylone-iron complexes **3** and **4**, as well as the synthesis of bis(imino)germanone **10**.

A rare three-coordinate germanone $[IPrN]_2Ge{=}O$ **10** was successfully isolated (Scheme 1). The germanone has a high thermal stability in arene solvent, with no detectable change observed at 80 ºC for at least one week. Structural analysis and initial reactivity studies revealed the highly polarized nature of the terminal Ge=O bond (Scheme 2). The addition of phenylacetylene, as well as O-atom transfer with 2,6-dimethylphenyl isocyanide mimics that of nucleophilic transition-metal oxides. The mechanism for O-atom transfer reaction was investigated *via* DFT calculations, which revealed that the reaction proceeds *via* a [2+2]-cycloaddition intermediate **17**.

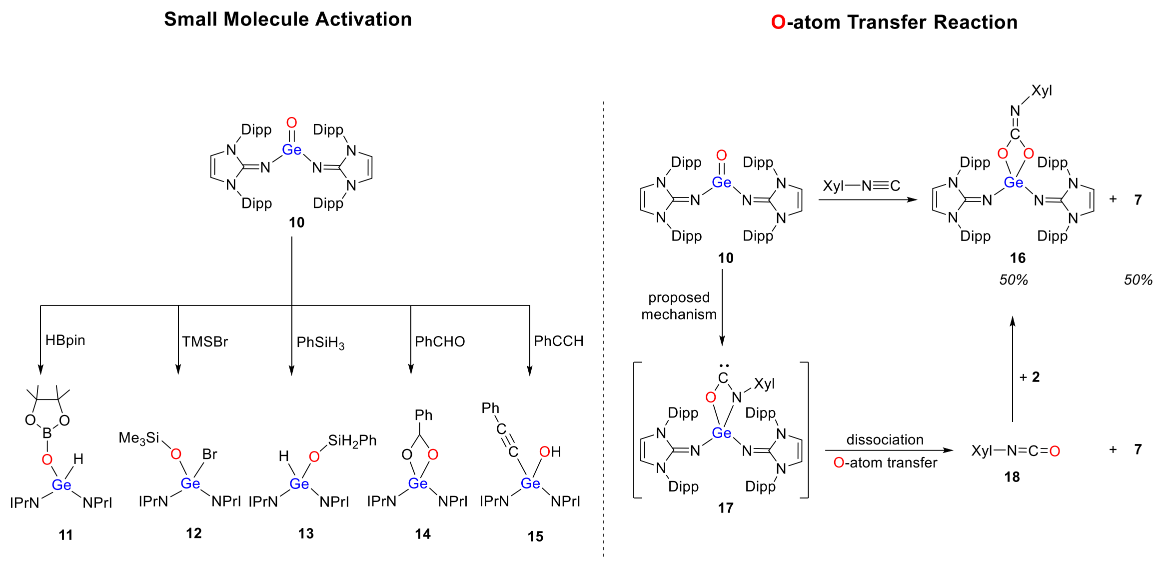

Scheme 2. Reactivity of bis(imino)germanone **10**.

The reaction of Cp*Sn[OTf] (Cp* = C_5Me_5; OTf = O_3SCF_3) with one equivalent of IPrNLi resulted in the binuclear [OTf]-bridged tin complex **19** (Scheme 3). Similarly, the $[BF_4]$-bridged bimetallic complex **20** was synthesized by the reaction of Cp*Sn$[BF_4]$ with IPrNLi (1 eq.). It was also possible to prepare **19** from **20** *via* an anion exchange reaction. The high-yield conversion of **20** into the binuclear iodostannylene $[IPrNSnI]_2$ **21** was accomplished by treatment with LiI. The catalytic potential of **19** and **20** was demonstrated with the hydroboration of carbonyls.

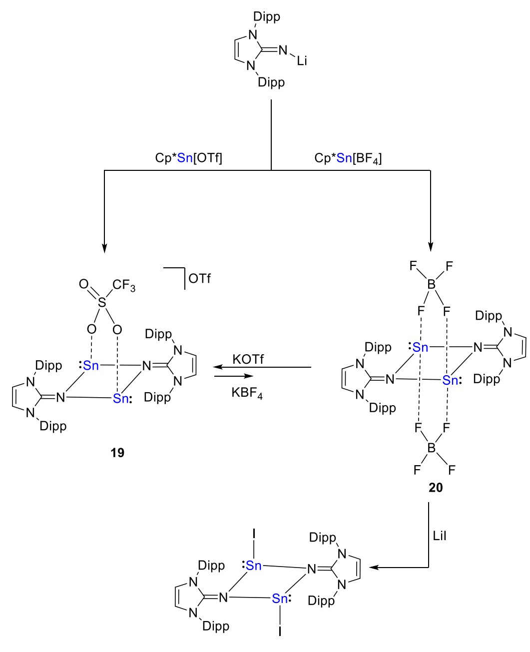

Scheme 3. Synthesis and reactivity of binuclear tin(II) cations **19** and **20**.

The reaction of the lithium silyl(aryl)amide Dipp($^{i}Pr_3Si$)NLi (Dipp = 2,6-$^{i}Pr_2C_6H_3$) with one equivalent of $SnCl_2$ in THF gave a novel stannylenoid **22** (Scheme 4). Heating up the solution of **22** in toluene at 80 ºC resulted in the dimeric amido(chloro)stannylene **23**, which can be converted into the bis(amido)stannylene **24** and amido(imino)stannylene **25**. All compounds were characterized by NMR, elementary analysis, and X-ray structural determination.

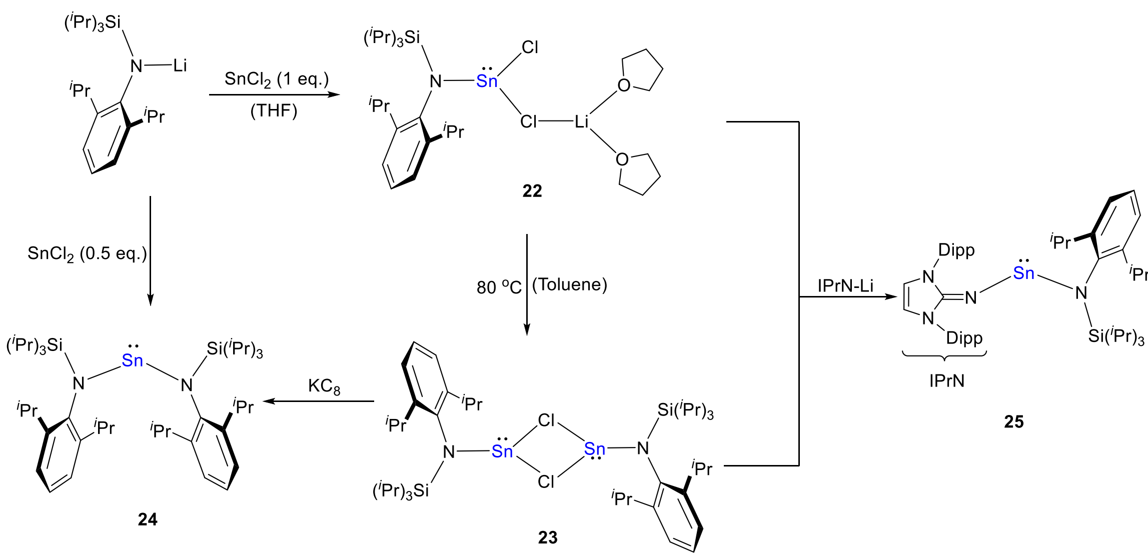

Scheme 4. Synthesis and reactivity of amidostannylenoid **22**.

9. Appendix

9.1 Supporting Information for Chapter 4

Chemistry–A European Journal

Supporting Information

An Isolable Three-Coordinate Germanone and Its Reactivity

Xuan-Xuan Zhao, Tibor Szilvási, Franziska Hanusch, and Shigeyoshi Inoue*

Table of Contents

1. Experimental Section

General Considerations

All experiments and manipulations were carried out under dry oxygen-free argon atmosphere using standard Schlenk techniques or in a glovebox. All glass junctions were coated with PTFE-based grease Merkel Triboflon III. All the solvents were dried and freshly distilled under Ar atmosphere prior to use by standard techniques. The ^{1}H, $^{13}C\{^{1}H\}$, $^{11}B\{^{1}H\}$ NMR spectra were recorded on Bruker 400 MHz spectrometer. Chemical shifts are referenced to (residual) solvent signals. Abbreviations: s = singlet, br = broadened, d = doublet, t = triplet, m = multiplet. ATRFT-IR spectra were recorded on a Bruker Alpha FT-IR spectrometer (diamond ATR, located inside an argon-filled glovebox) in a range of 400 – 4000 cm^{-1}. Elemental analysis (EA) were conducted with a EURO EA (HEKA tech) instrument equipped with a CHNS combustion analyzer. Unless otherwise stated, all commercially available chemicals were purchased from *abcr GmbH*, *Sigma-Aldrich Chemie GmbH* or *Tokyo Chemical Industry Co., Ltd.*, and used without further purification. Dinitrogen monoxide (N_2O) 5.0 (≥99.999%) was purchased from *Westfalen AG* and used as received. The starting materials IPrNLi (IPrN = bis(2,6-diisopropylphenyl)imidazolin-2-imino)[S1] and $GeCl_2$•dioxane[S2] were prepared according to the literature procedures, respectively.

Synthetic Procedures

Synthesis of bis(imino)germylene 1

$GeCl_2$•dioxane (566 mg, 2.44 mmol, 1.0 eq.) dissolved in THF (40 mL) was added dropwise to a solution of IPrNLi (2.0 g, 4.88 mmol, 2.0 eq.) in THF (60 mL) at 0 ºC. The reaction mixture was stirred for 2 h at 0 ºC. The volatiles were removed *in vacuo* and the solid residue was extracted with toluene (10 mL × 3). After filtration the solvent was removed from the filtrate *in vacuo* to obtain a yellow solid (1.89 g, 88%).

^{1}H NMR (400 MHz, C_6D_6) δ = 7.25 (t, J = 7.7 Hz, 4H, Ar$\underline{H}$), 7.10 (d, J = 7.7 Hz, 8H, Ar$\underline{H}$), 5.93 (s, 4H, NC$\underline{H}$), 3.07 (septet, J = 6.8 Hz, 8H, C$\underline{H}$(CH_3)$_2$), 1.18 (d, J = 6.8 Hz, 24H, CH(C$\underline{H}_3$)$_2$), 1.15 (d, J = 6.8 Hz, 24H, CH(C$\underline{H}_3$)$_2$).

^{13}C NMR (101 MHz, C_6D_6) δ = 148.6 (N$\underline{C}$N), 148.6 (N$\underline{C}$Ar), 134.6 (Ar$\underline{C}$), 129.1 (Ar$\underline{C}$), 123.8 (Ar$\underline{C}$), 113.9 (N$\underline{C}$H), 28.9 ($\underline{C}$H(CH_3)$_2$), 24.5 (CH($\underline{C}H_3$)$_2$), 23.7 (CH($\underline{C}H_3$)$_2$).

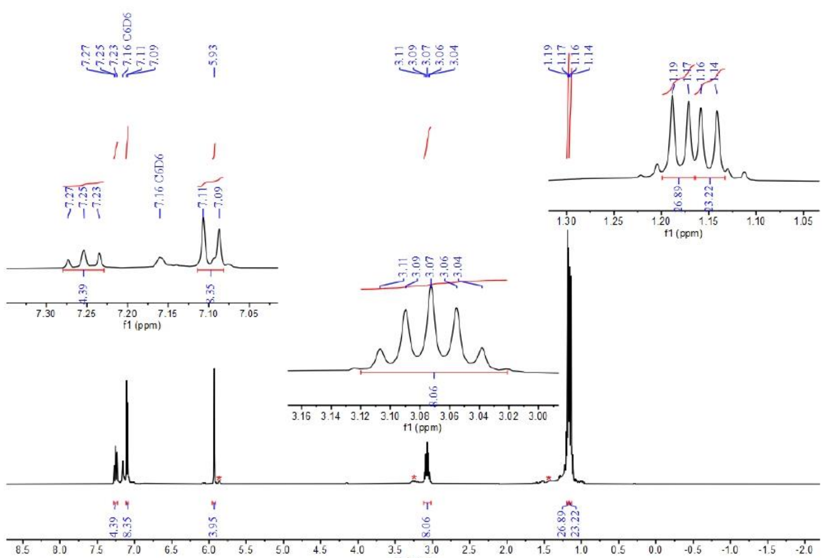

Figure S1. ^{1}H NMR spectrum of bis(imino)germylene **1**. The resonances of IPrNH, resulting from minor complex decomposition in solution, are marked with asterisks *.

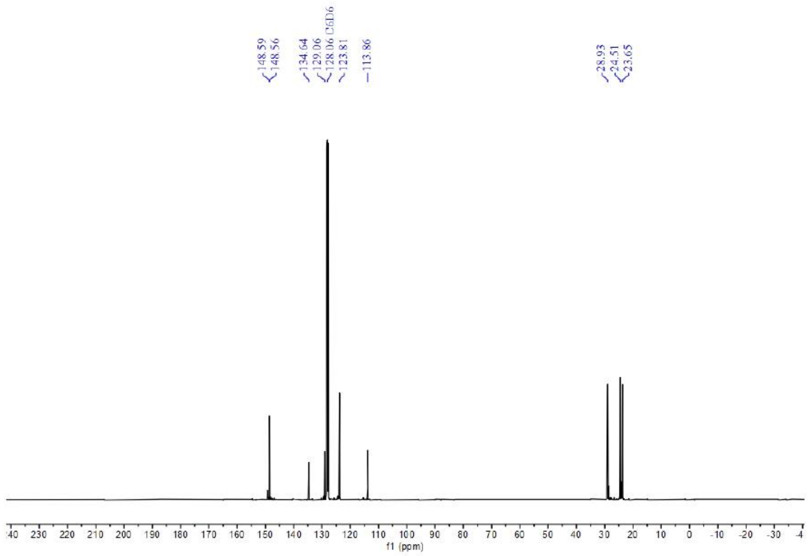

Figure S2. ^{13}C NMR spectrum of bis(imino)germylene **1**.

Synthesis of bis(imino)germanone 2

The solution of **1** (1.14 g, 1.30 mmol) in toluene (20 mL) in a Schlenk tube equipped with a PTFE-coated magnetic stirring bar was cooled to be solidified. The upper argon atmosphere was replaced with N_2O gas (1.0 bar). The reaction mixture was allowed to warm to room temperature, and then was stirred for 2 days. Removal of the solvent gave an orange crude solid, and **2** was recrystallized from a saturated solution in Et_2O at –30 °C as pale-yellow crystals (1.03 g, 89%).

^{1}H NMR (400 MHz, C_6D_6) δ = 7.27 (t, J = 7.7 Hz, 4H, Ar*H*), 7.12 (d, J = 7.7 Hz, 8H, Ar*H*), 5.92 (s, 4H, NC*H*), 2.93 (septet, J = 6.8 Hz, 8H, C*H*(CH_3)$_2$), 1.24 (d, J = 6.9 Hz, 24H, CH(C*H*$_3$)$_2$), 1.12 (d, J = 6.9 Hz, 24H, CH(C*H*$_3$)$_2$).

^{13}C NMR (101 MHz, C_6D_6) δ = 149.5 (N*C*N), 148.2 (N*C*Ar), 133.1 (Ar*C*), 129.8 (Ar*C*), 124.4 (Ar*C*), 114.4 (N*C*H), 29.1 (*C*H(CH_3)$_2$), 24.8 (CH(*C*H$_3$)$_2$), 23.6 (CH(*C*H$_3$)$_2$).

Anal. Calcd. [%] for $C_{54}H_{72}GeN_6O$: C, 72.56; H, 8.12; N, 9.40. Found [%]: C, 72.46; H, 8.23; N, 9.52.

IR: $\nu_{Ge=O}$ = 912 cm^{-1}.

S4

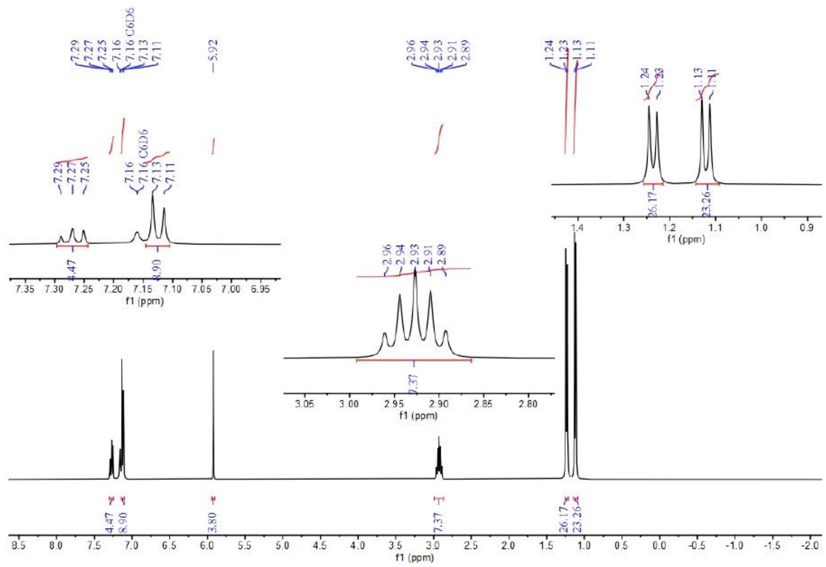

Figure S3. ^{1}H NMR spectrum of bis(imino)germanone **2**.

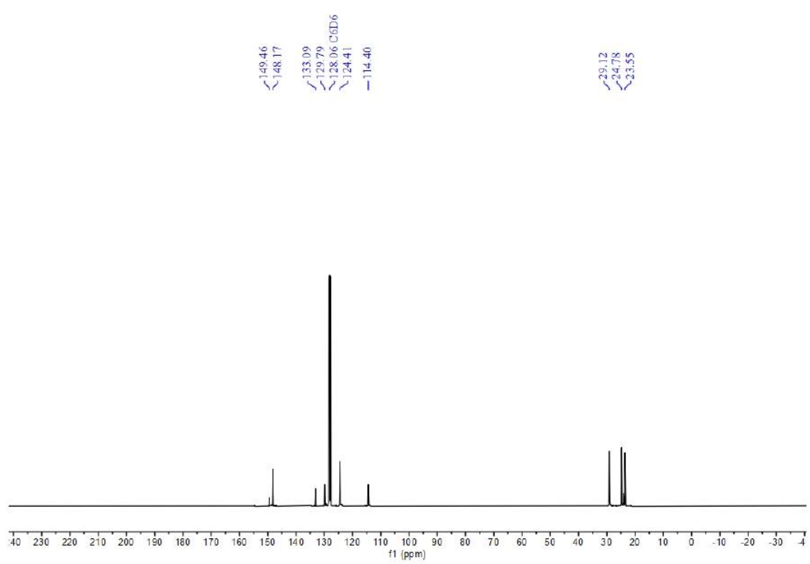

Figure S4. ^{13}C NMR spectrum of bis(imino)germanone **2**.

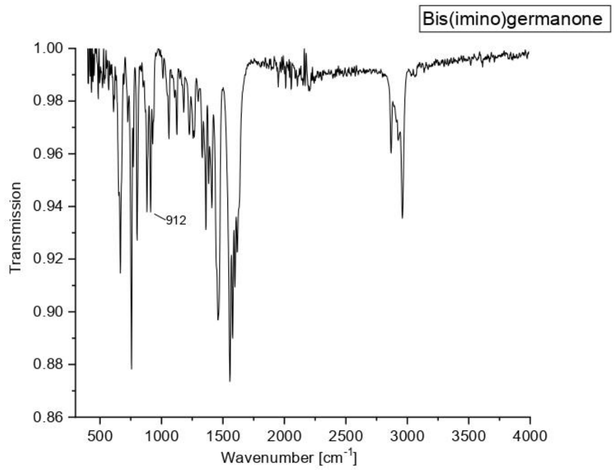

Figure S5. IR spectrum of bis(imino)germanone **2**.

Assignment of the Ge=O peak

There are two relevant peaks around 900 cm^{-1} that can be assigned to the Ge=O bond. DFT calculations indicated that Ge=O stretching is at 907 cm^{-1} while there is another notable peak at 861 cm^{-1} that mainly belongs to the C=N moiety of the IPrN groups. We emphasize that the N-Ge π-interactions weakens the degree of Ge=O π-bonding in **2**. However, the phenyl rings in $(Eind)_2Ge=O$ are not perpendicular to the Ge=O bond and as such also have a weakening effect on the Ge=O bond. Therefore, the Ge=O π-bonding in **2** may not be significantly different than that in $(Eind)_2Ge=O$, which can explain the similar IR frequency. This is backed up by the fact that the measured Ge=O bond length is almost identical in **2** (1.6494(10) Å) and in $(Eind)_2Ge=O$ (1.6468(5) Å). Additionally, the detailed orbital analysis shows clear Ge=O π and π* orbitals in **2,** which are barely coupled with the N of the twisted IPrN groups.

Synthesis of compound 3

To the solution of **2** (40 mg, 45 µmol) in C_6D_6 (0.4 mL) in a J. Young PTFE tube, pinacolborane (HBpin) (7 µL, 45 µmol, 1.0 eq.) was added at room temperature. After 45 min, the completion of the reaction was confirmed by ^{1}H NMR. The solvent was removed *in vacuo* to afford **3** as an orange solid (45 mg, 98%).

^{1}H NMR (400 MHz, C_6D_6) δ = 7.26 (t, J = 7.7 Hz, 4H, Ar*H*), 7.14 – 7.10 (m, 8H, Ar*H*), 5.86 (s, 4H, NC*H*), 5.04 (s, 1H, Ge*H*), 3.19 – 3.06 (m, 8H, C*H*(CH_3)$_2$), 1.24 (d, J = 6.9 Hz, 24H, CH(C*H*$_3$)$_2$), 1.19 (d, J = 6.8 Hz, 12H, CH(C*H*$_3$)$_2$), 1.17 (d, J = 6.8 Hz, 12H, CH(C*H*$_3$)$_2$), 1.18 (s, 6H, BOC(C*H*$_3$)$_2$), 1.11 (s, 6H, BOC(C*H*$_3$)$_2$).

^{13}C NMR (101 MHz, C_6D_6) δ = 154.6 (N*C*N), 148.0 (N*C*Ar), 147.9 (N*C*Ar), 146.5 (N*C*Ar), 135.4 (Ar*C*), 129.1 (Ar*C*), 124.1 (Ar*C*), 114.4 (N*C*H), 80.2 (BO*C*(CH_3)$_2$), 28.8 (*C*H(CH_3)$_2$), 25.5 (*C*H$_3$), 24.9 (*C*H$_3$), 24.6 (*C*H$_3$), 24.0 (*C*H$_3$), 23.9 (*C*H$_3$).

^{11}B NMR (128 MHz, C_6D_6) δ = 28.5.

Anal. Calcd. [%] for $C_{60}H_{85}BGeN_6O_3$: C, 70.53; H, 8.39; N, 8.22. Found [%]: C, 70.43; H, 8.50; N, 8.33.

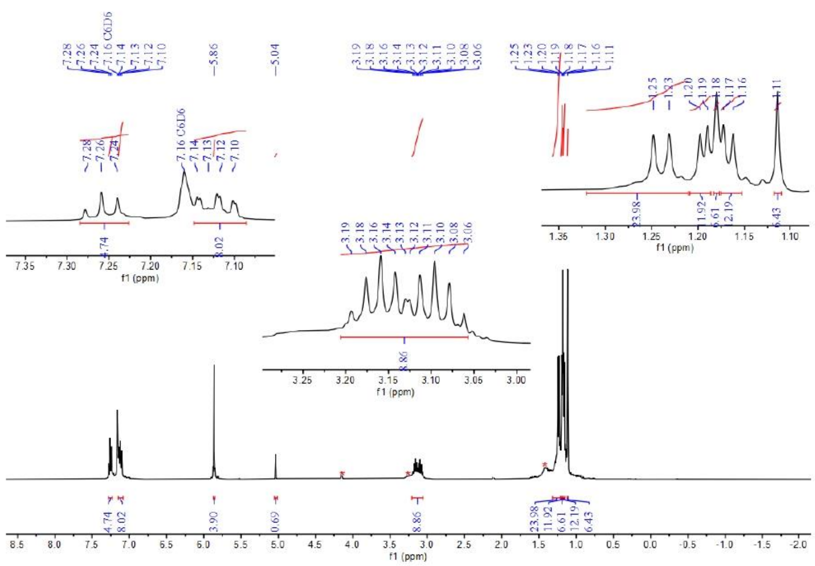

Figure S6. ^{1}H NMR spectrum of compound **3**. The resonances of IPrNH, resulting from minor complex decomposition in solution, are marked with asterisks *.

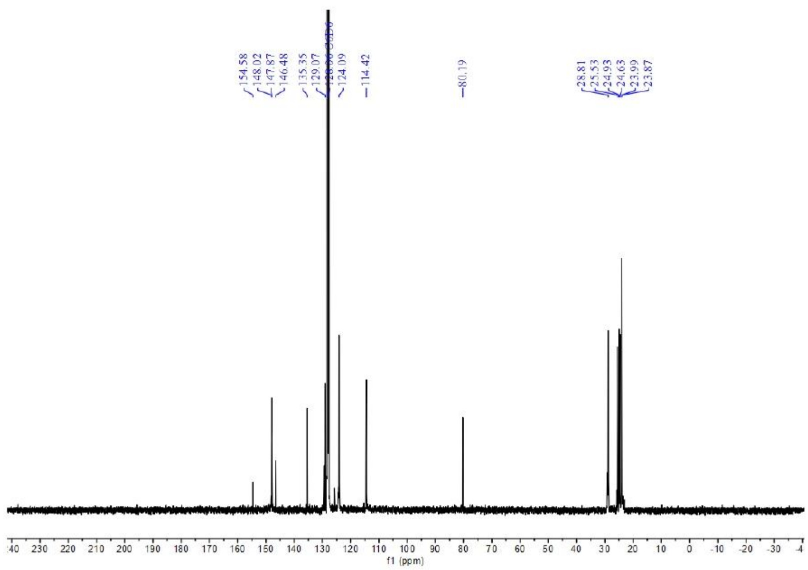

Figure S7. ^{13}C NMR spectrum of compound **3**.

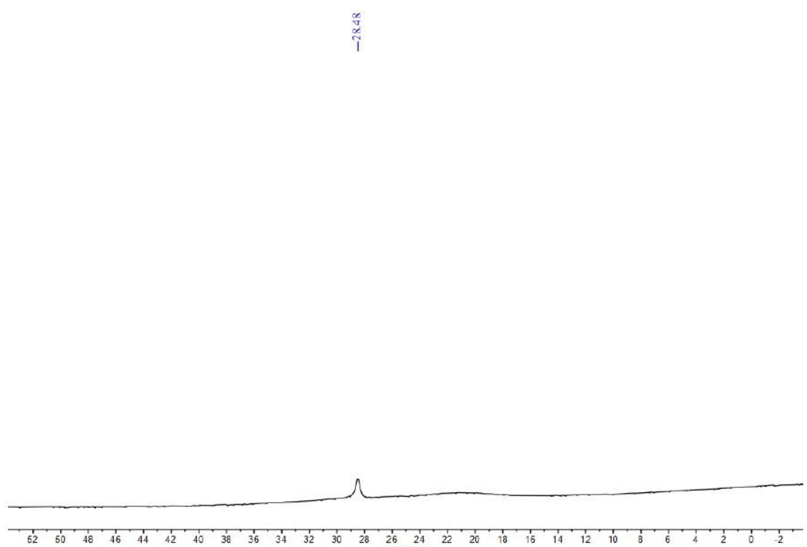

Figure S8. ^{11}B NMR spectrum of compound **3**.

S8

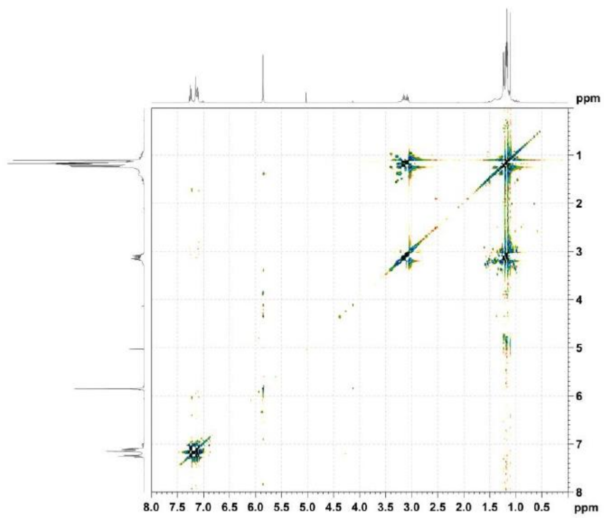

Figure S9. $^1H/^1H$ COSY NMR spectrum of compound **3**.

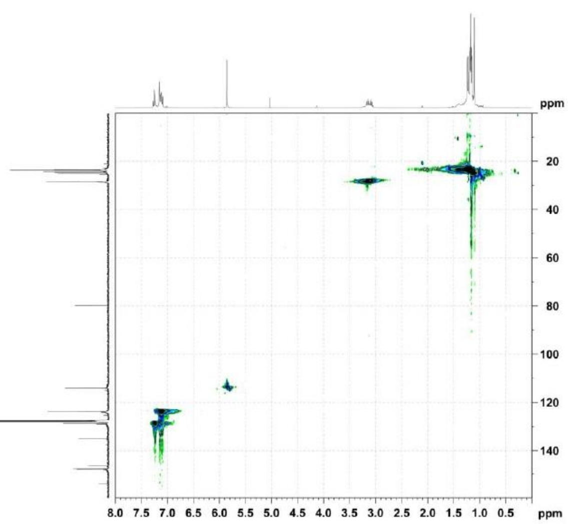

Figure S10. $^1H/^{13}C$ HSQC NMR spectrum of compound **3**.

S9

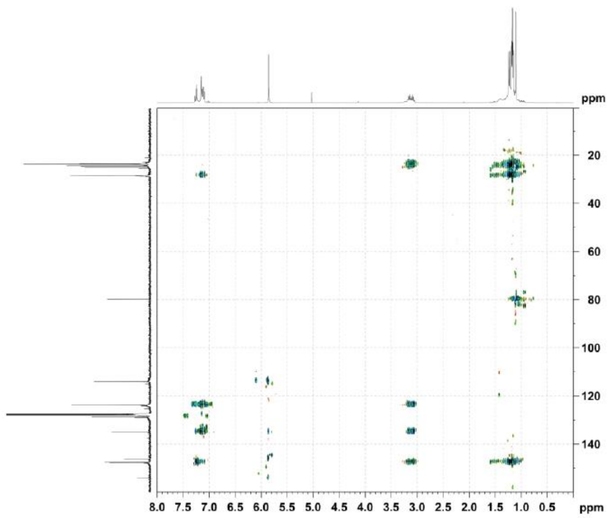

Figure S11. ^{1}H/^{13}C HMBC NMR spectrum of compound **3**.

Synthesis of compound 4

To the solution of **2** (120 mg, 134 μmol) in C_6H_6 (1.2 mL) in a Schlenk tube, bromotrimethylsilane (TMSBr) (18 μL, 134 μmol, 1.0 eq.) was added at room temperature. The reaction mixture was stirred for 20 min. After the reaction, unidentified precipitate was removed by filtration. Then the solvent was removed from the filtrate *in vacuo* to afford **4** as an orange solid (65 mg, 46%).

^{1}H NMR (400 MHz, C_6D_6) δ = 7.24 (t, J = 7.7 Hz, 4H, Ar*H*), 7.13 (d, J = 7.7 Hz, 8H, Ar*H*), 5.87 (s, 4H, NC*H*), 3.25 (septet, J = 6.8 Hz, 4H, C*H*(CH$_3$)$_2$), 3.09 (septet, J = 6.8 Hz, 4H, C*H*(CH$_3$)$_2$), 1.36 (d, J = 6.8 Hz, 12H, CH(C*H*$_3$)$_2$), 1.22 (d, J = 6.8 Hz, 12H, CH(C*H*$_3$)$_2$), 1.13 (d, J = 6.8 Hz, 12H, CH(C*H*$_3$)$_2$), 1.11 (d, J = 6.8 Hz, 12H, CH(C*H*$_3$)$_2$), 0.03 (s, 9H, Si(C*H*$_3$)$_3$).

^{13}C NMR (101 MHz, C_6D_6) δ = 148.0 (N*C*N), 147.7 (N*C*Ar), 147.5 (N*C*Ar), 146.3 (N*C*Ar), 135.5 (Ar*C*), 129.3 (Ar*C*), 124.4 (Ar*C*), 123.9 (Ar*C*), 115.8 (N*C*H), 113.8 (N*C*H), 28.9 (*C*H(CH$_3$)$_2$), 28.7 (*C*H(CH$_3$)$_2$), 25.4 (CH(*C*H$_3$)$_2$), 24.4 (CH(*C*H$_3$)$_2$), 23.9 (CH(*C*H$_3$)$_2$), 23.7 (CH(*C*H$_3$)$_2$), 23.5 (CH(*C*H$_3$)$_2$), 3.5 (Si(*C*H$_3$)$_3$).

Anal. Calcd. [%] for $C_{57}H_{81}BrGeN_6OSi$: C, 65.39; H, 7.80; N, 8.03. Found [%]: C, 65.30; H, 7.91; N, 8.13.

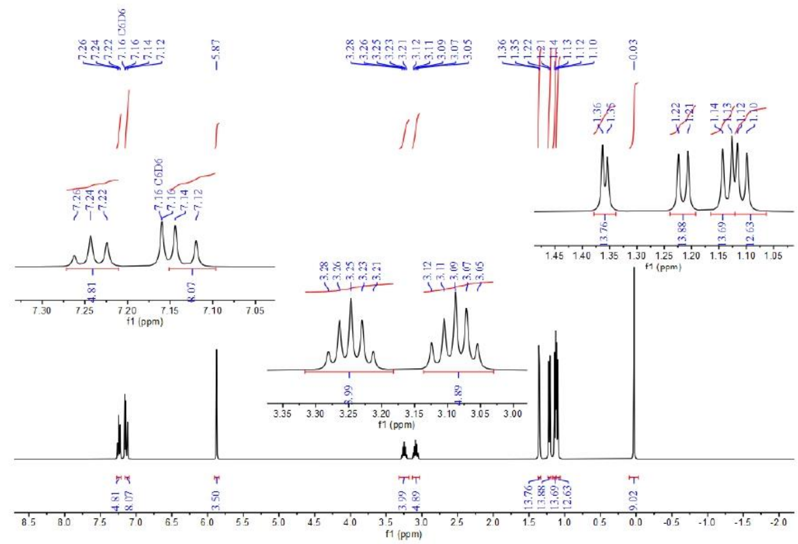

Figure S12. ^{1}H NMR spectrum of compound **4**.

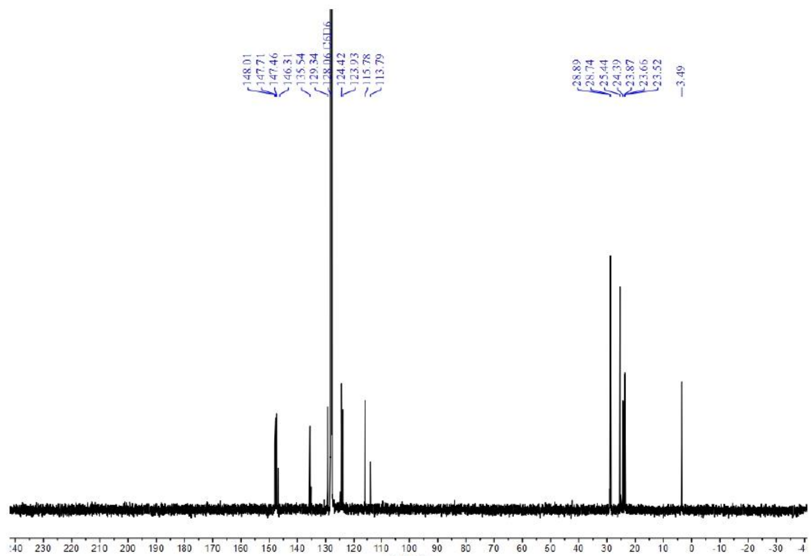

Figure S13. ^{13}C NMR spectrum of compound **4**.

S11

Synthesis of compound 5

To the solution of **2** (200 mg, 224 μmol) in toluene (2.0 mL) in a Schlenk tube, phenylsilane ($PhSiH_3$) (28 μL, 224 μmol, 1.0 eq.) was added at room temperature. The reaction mixture was stirred for 30 min. The solvent was removed *in vacuo* to afford **5** as an orange solid (180 mg, 80%).

^{1}H NMR (400 MHz, C_6D_6) δ = 7.63 – 7.61 (m, 2H, Ar$\underline{H}$), 7.28 – 7.22 (m, 7H, Ar$\underline{H}$), 7.13 – 7.06 (m, 8H, Ar$\underline{H}$), 5.88 (s, 4H, NC$\underline{H}$), 5.09 (s, 2H, Si$\underline{H_2}$), 4.78 (s, 1H, Ge$\underline{H}$), 3.18 – 3.04 (m, 8H, C$\underline{H}$(CH_3)$_2$), 1.15 – 1.11 (m, 48H, CH(C$\underline{H_3}$)$_2$).

^{13}C NMR (101 MHz, C_6D_6) δ = 154.6 (N$\underline{C}$N), 148.2 (N$\underline{C}$Ar), 147.9 (N$\underline{C}$Ar), 147.1 (N$\underline{C}$Ar), 138.7 ($SiH_2$$\underline{C}$), 135.0 ($SiH_2C\underline{C}$H), 134.8 (Ar$\underline{C}$), 129.2 (Ar$\underline{C}$), 124.0 (Ar$\underline{C}$), 114.4 (N$\underline{C}$H), 28.9 ($\underline{C}$H($CH_3$)$_2$), 28.7 ($\underline{C}$H($CH_3$)$_2$), 24.9 (CH($\underline{C}H_3$)$_2$), 23.8 (CH($\underline{C}H_3$)$_2$), 23.4 (CH($\underline{C}H_3$)$_2$).

Anal. Calcd. [%] for $C_{60}H_{80}GeN_6OSi$: C, 71.92; H, 8.05; N, 8.39. Found [%]: C, 71.87; H, 8.15; N, 8.44.

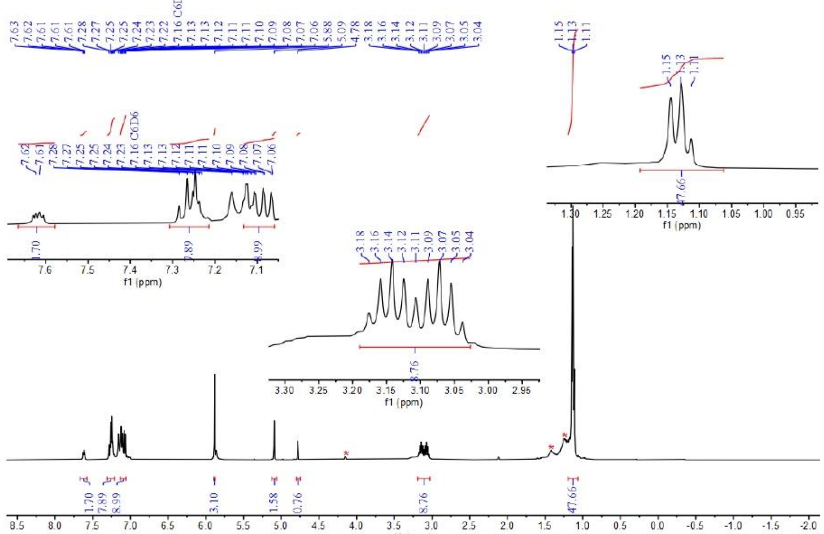

Figure S14. ^{1}H NMR spectrum of compound **5**. The resonances of IPrNH, resulting from minor complex decomposition in solution, are marked with asterisks *.

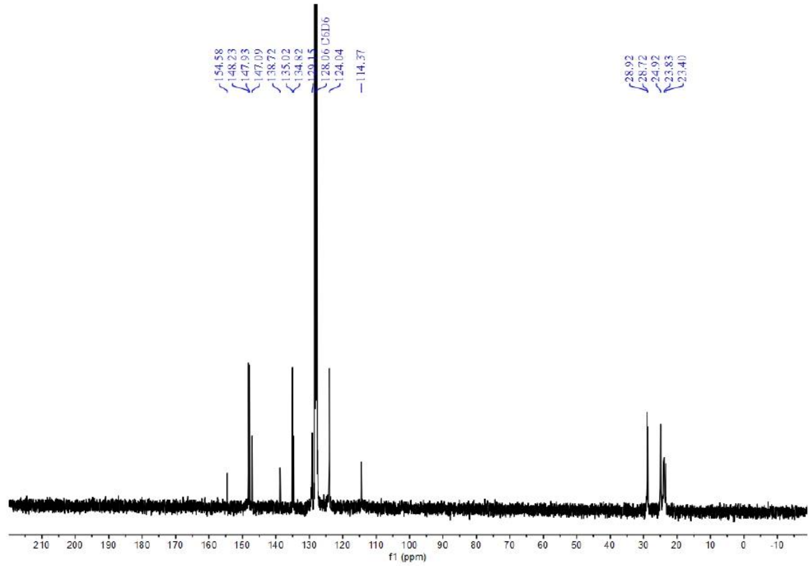

Figure S15. ^{13}C NMR spectrum of compound **5**.

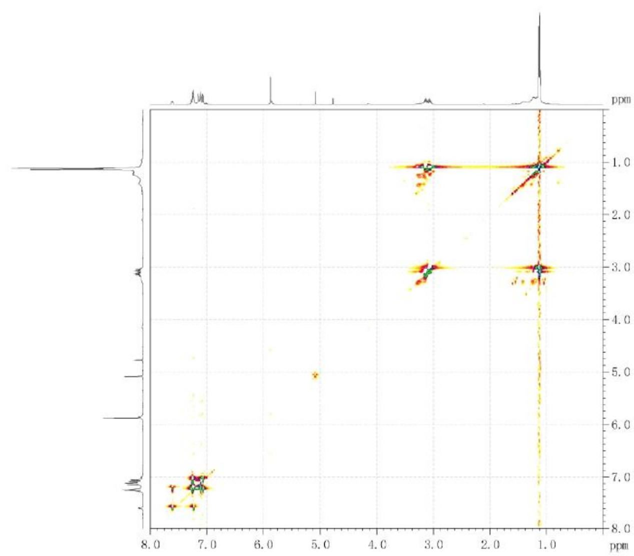

Figure S16. $^{1}H/^{1}H$ COSY NMR spectrum of compound **5**.

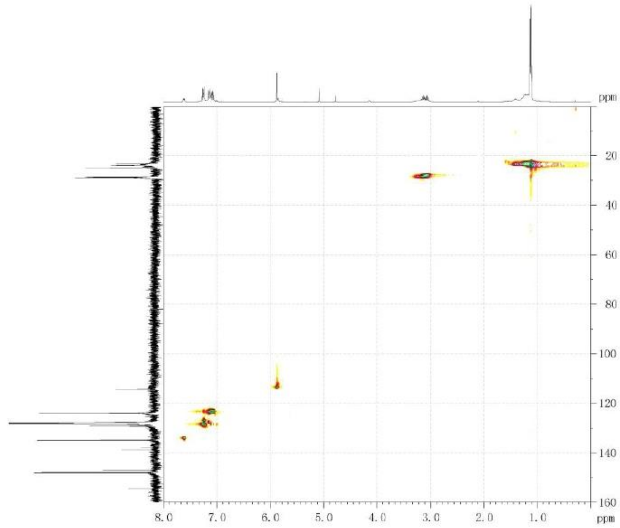

Figure S17. $^{1}H/^{13}C$ HSQC NMR spectrum of compound **5**.

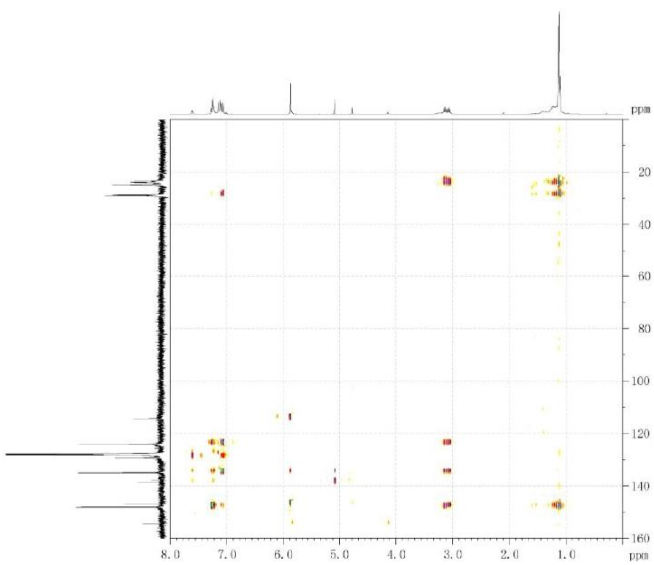

Figure S18. $^{1}H/^{13}C$ HMBC NMR spectrum of compound **5**.

Synthesis of compound 6

To the solution of **2** (200 mg, 224 µmol) in toluene (2.0 mL) in a Schlenk tube, benzaldehyde (PhCHO) (23 µL, 224 µmol, 1.0 eq.) was added at room temperature. The reaction mixture was stirred for 30 min. The solvent was removed *in vacuo* to afford **6** as an orange solid (155 mg, 70%).

^{1}H NMR (400 MHz, C_6D_6) δ = 7.47 (d, J = 6.9 Hz, 2H, Ar$\underline{H}$), 7.28 – 7.22 (m, 7H, Ar$\underline{H}$), 7.13 – 7.09 (m, 8H, Ar$\underline{H}$), 6.01 (s, 2H, NC$\underline{H}$), 5.96 (s, 2H, NC$\underline{H}$), 5.10 (s, 1H, OC$\underline{H}$), 3.07 (septet, J = 6.8 Hz, 8H, C$\underline{H}$(CH_3)$_2$), 1.19 (d, J = 6.8 Hz, 12H, CH(C$\underline{H}_3$)$_2$), 1.14 (d, J = 6.8 Hz, 12H, CH(C$\underline{H}_3$)$_2$), 1.11 (d, J = 6.8 Hz, 12H, CH(C$\underline{H}_3$)$_2$), 0.96 (d, J = 6.8 Hz, 12H, CH(C$\underline{H}_3$)$_2$).

^{13}C NMR (101 MHz, C_6D_6) δ = 154.6 (N$\underline{C}$N), 148.3 (N$\underline{C}$Ar), 148.0 (N$\underline{C}$Ar), 147.8 (N$\underline{C}$Ar), 147.7 (N$\underline{C}$Ar), 146.2 (N$\underline{C}$Ar), 134.5 (Ar$\underline{C}$), 134.0 (Ar$\underline{C}$), 129.2 (Ar$\underline{C}$), 127.2 (Ar$\underline{C}$), 124.1 (Ar$\underline{C}$), 114.9 (N$\underline{C}$H), 99.7 (O$\underline{C}$HO), 29.0 ($\underline{C}$H(CH_3)$_2$), 25.4 (CH($\underline{C}H_3$)$_2$), 25.1 (CH($\underline{C}H_3$)$_2$), 24.0 (CH($\underline{C}H_3$)$_2$), 23.2 (CH($\underline{C}H_3$)$_2$).

Anal. Calcd. [%] for $C_{61}H_{78}GeN_6O_2$: C, 73.27; H, 7.86; N, 8.40. Found [%]: C, 72.55; H, 8.00; N, 8.40.

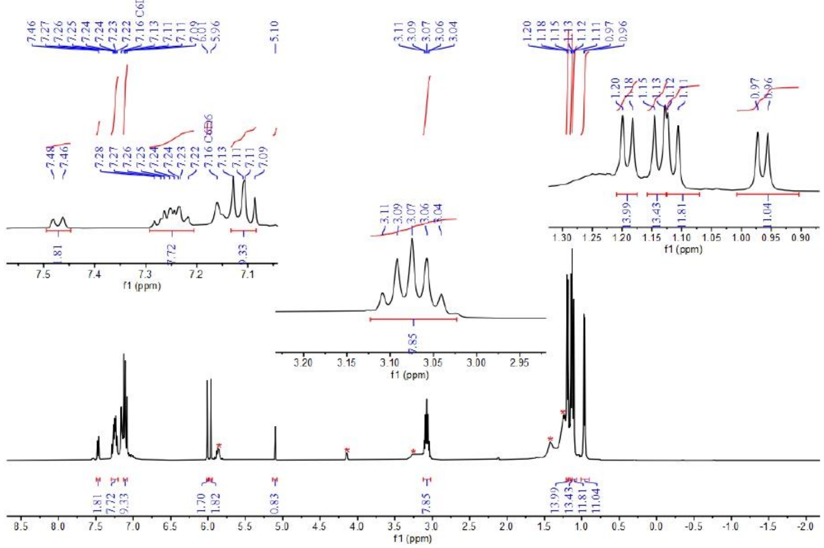

Figure S19. ^{1}H NMR spectrum of compound **6**. The resonances of IPrNH, resulting from minor complex decomposition in solution, are marked with asterisks *.

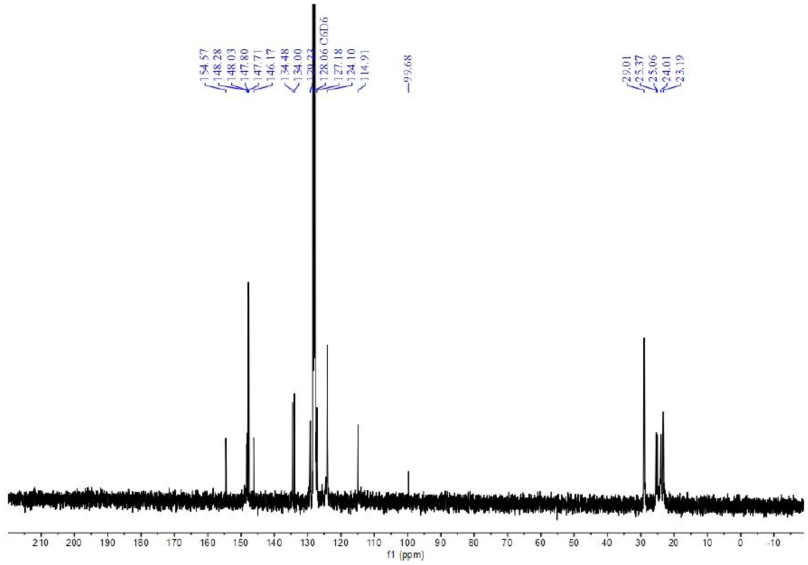

Figure S20. ^{13}C NMR spectrum of compound **6**.

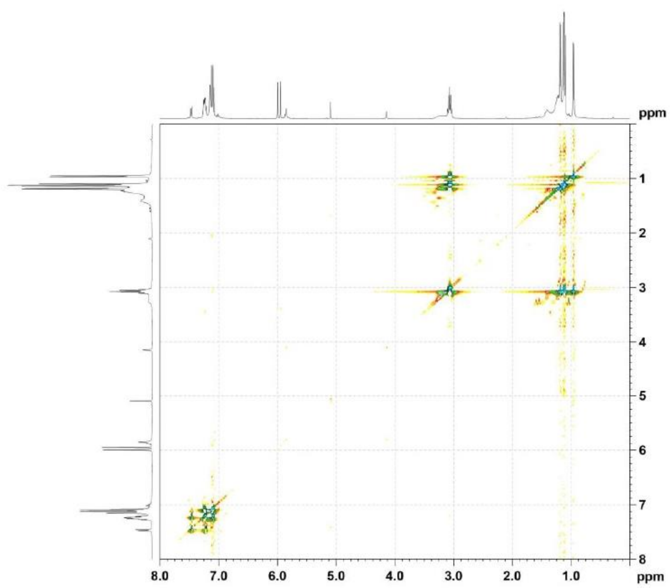

Figure S21. ^{1}H/^{1}H COSY NMR spectrum of compound **6**.

S16

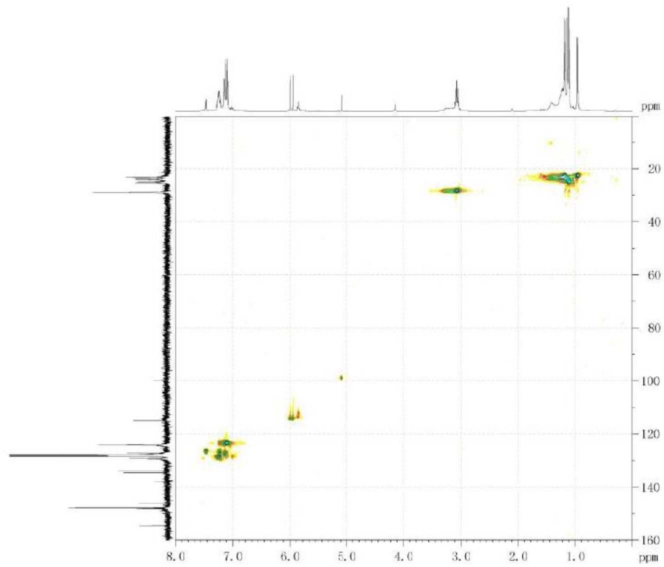

Figure S22. $^{1}H/^{13}C$ HSQC NMR spectrum of compound **6**.

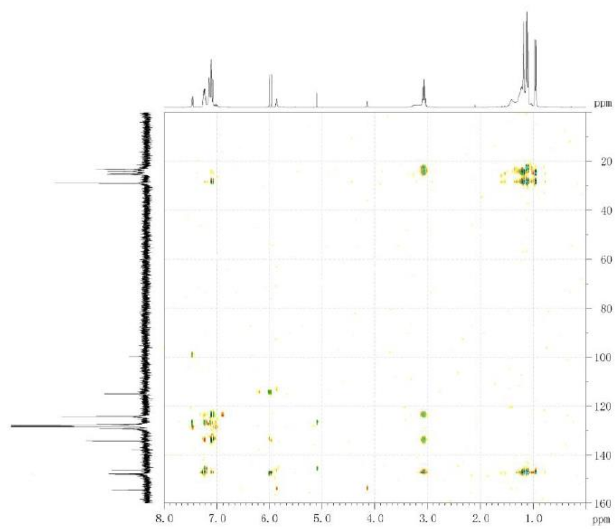

Figure S23. $^{1}H/^{13}C$ HMBC NMR spectrum of compound **6**.

Synthesis of compound 7

S17

To the solution of **2** (200 mg, 224 µmol) in toluene (2.0 mL) in a Schlenk tube, phenylacetylene (PhCCH) (25 µL, 224 µmol, 1.0 eq.) was added at room temperature. The reaction mixture was stirred for 30 min. The solvent was removed *in vacuo* to afford **7** as an orange solid (180 mg, 81%).

^{1}H NMR (400 MHz, C_6D_6) δ = 7.42 (d, J = 7.0 Hz, 2H, Ar<u>*H*</u>), 7.29 – 7.18 (m, 7H, Ar<u>*H*</u>), 7.13 – 7.10 (m, 8H, Ar<u>*H*</u>), 5.86 (s, 4H, NC<u>*H*</u>), 3.19 – 3.10 (m, 8H, C<u>*H*</u>(CH_3)$_2$), 1.26 (d, J = 6.8 Hz, 12H, CH(C<u>*H*</u>$_3$)$_2$), 1.23 (d, J = 6.8 Hz, 12H, CH(C<u>*H*</u>$_3$)$_2$), 1.17 (d, J = 6.8 Hz, 12H, CH(C<u>*H*</u>$_3$)$_2$), 1.15 (d, J = 6.8 Hz, 12H, CH(C<u>*H*</u>$_3$)$_2$), -0.77 (s, 1H, GeO<u>*H*</u>).

^{13}C NMR (101 MHz, C_6D_6) δ = 154.6 (N<u>*C*</u>N), 148.3 (N<u>*C*</u>Ar), 148.2 (N<u>*C*</u>Ar), 145.6 (N<u>*C*</u>Ar), 135.1 (Ar<u>*C*</u>), 132.4 (Ar<u>*C*</u>), 129.3 (Ar<u>*C*</u>), 124.0 (Ar<u>*C*</u>), 114.3 (N<u>*C*</u>H), 98.0 (GeC<u>*C*</u>Ph), 96.6 (Ge<u>*C*</u>CPh), 29.0 (<u>*C*</u>H(CH_3)$_2$), 24.6 (CH(<u>*C*</u>H$_3$)$_2$), 23.9 (CH(<u>*C*</u>H$_3$)$_2$).

Anal. Calcd. [%] for $C_{62}H_{78}GeN_6O$: C, 74.77; H, 7.89; N, 8.44. Found [%]: C, 74.97; H, 7.85; N, 7.94.

LIFDI-MS: calculated for $C_{62}H_{78}GeN_6O$: 996.54489. Found: 996.54934.

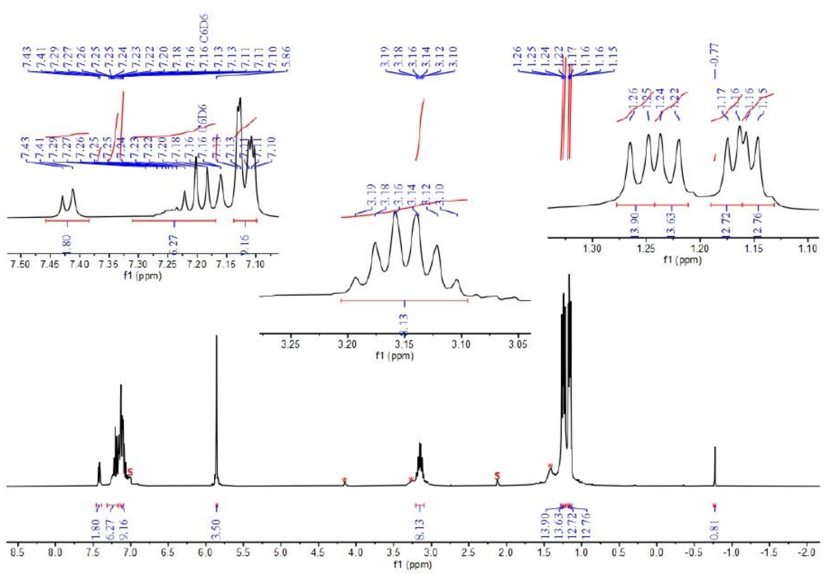

Figure S24. ^{1}H NMR spectrum of compound **7**. The respective resonances of IPrNH, resulting from minor complex decomposition in solution, are marked with asterisks * and residual toluene with an S.

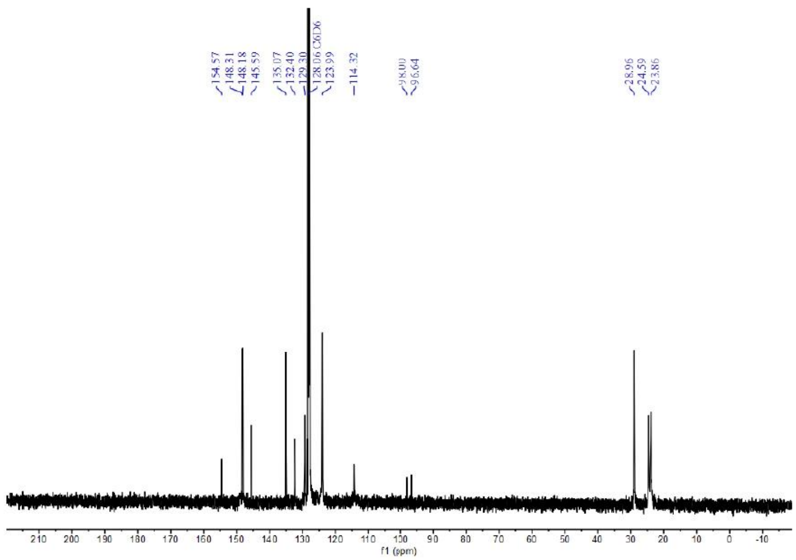

Figure S25. ^{13}C NMR spectrum of compound **7**.

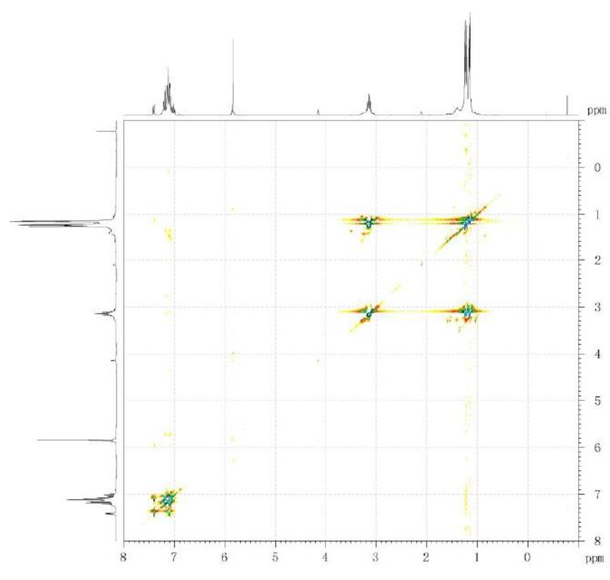

Figure S26. $^{1}H/^{1}H$ COSY NMR spectrum of compound **7**.

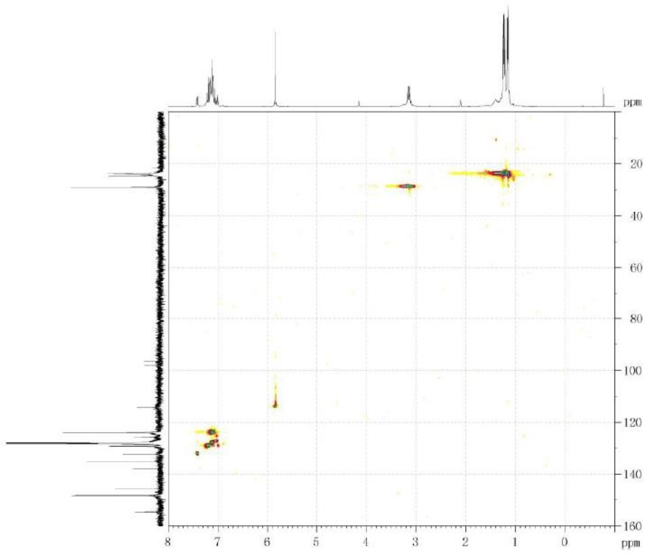

Figure S27. $^{1}H/^{13}C$ HSQC NMR spectrum of compound **7**.

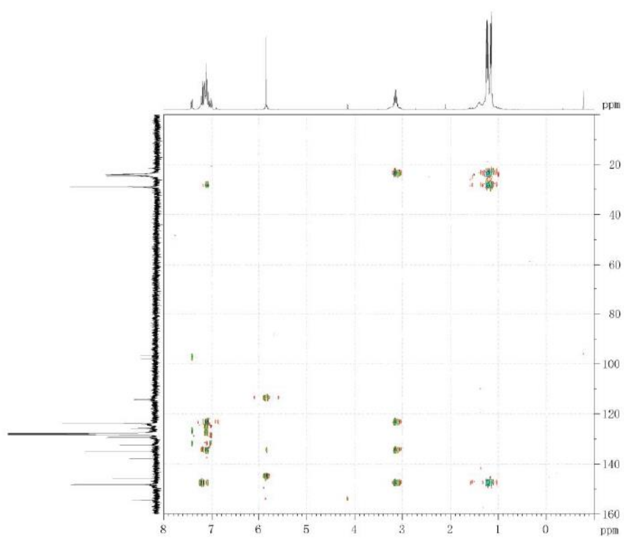

Figure S28. $^{1}H/^{13}C$ HMBC NMR spectrum of compound **7**.

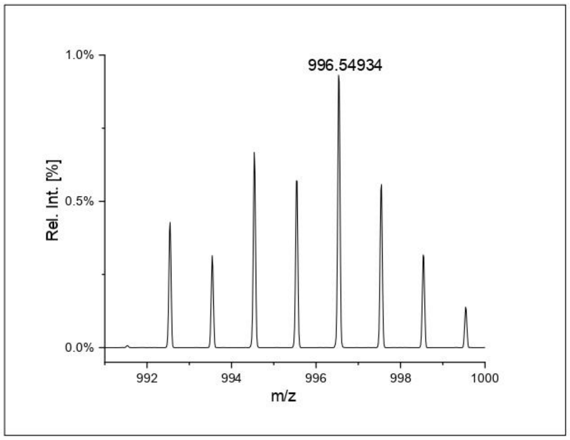

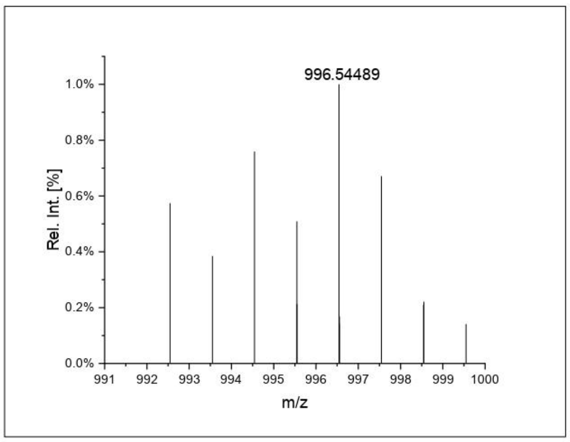

Figure S29. LIFDI-MS spectrum: expanded region of the compound signal showing the isotopic pattern of compound **7**. Measured (top) and calculated (bottom).

Reaction of 2 and 2,6-dimethylphenyl isocyanide (CNXyl)

To the mixture of **2** (40 mg, 45 µmol) and 2,6-dimethylphenyl isocyanide (CNXyl) (3 mg, 22 µmol, 0.5 eq.) in a J. Young PTFE tube, C_6D_6 (0.4 mL) was added at room temperature. The reaction mixture was heated at 80 °C. After 2.0 h, the completion of the reaction was confirmed by ^1H NMR spectroscopy.

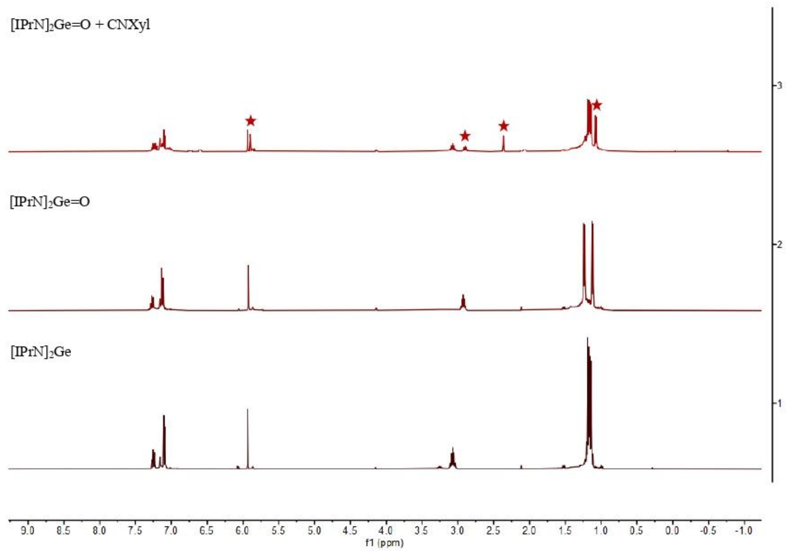

Figure S30. ^{1}H NMR spectrum of germylene **1**, germanone **2**, as well as the product mixture of germylene **1** and [2+2] cycloaddition product **8** (★).

Synthesis of compound 8

To the solution of **2** (40 mg, 45 µmol) in C_6D_6 (0.4 mL) in a J. Young PTFE tube, 2,6-dimethylphenyl isocyanate (7 µL, 45 µmol, 1.0 eq.) was added at room temperature. After 30 min, the completion of the reaction was confirmed by ^{1}H NMR. The solvent was removed *in vacuo* to afford **8** as an orange solid (44 mg, 90%).

^{1}H NMR (400 MHz, C_6D_6) δ = 7.22 (t, J = 7.7 Hz, 4H, Ar*H*), 7.14 (d, J = 7.7 Hz, 8H, Ar*H*), 7.02 – 6.97 (m, 3H, Ar*H*), 5.90 (s, 4H, NC*H*), 2.90 (septet, J = 6.8 Hz, 8H, C*H*(CH_3)$_2$), 2.37 (s, 6H, ArC*H*$_3$), 1.22 – 1.13 (m, 24H, CH(C*H*$_3$)$_2$), 1.07 (d, J = 6.8 Hz, 24H, CH(C*H*$_3$)$_2$).

^{13}C NMR (101 MHz, C_6D_6) δ = 154.6 (N*C*N), 153.0 (O*C*N), 148.6 (N*C*Ar), 147.2 (N*C*Ar), 133.3 (Ar*C*), 130.9 (Ar*C*), 129.8 (Ar*C*), 124.5 (Ar*C*), 115.1 (N*C*H), 29.0 (*C*H(CH_3)$_2$), 25.2 (CH(*C*H$_3$)$_2$), 24.0 (CH(*C*H$_3$)$_2$), 23.4 (CH(*C*H$_3$)$_2$), 23.2 (CH(*C*H$_3$)$_2$), 19.9 (Ar*C*H$_3$).

Anal. Calcd. [%] for $C_{63}H_{81}GeN_7O_2$: C, 72.69; H, 7.84; N, 9.42. Found [%]: C, 72.87; H, 7.85; N, 9.64.

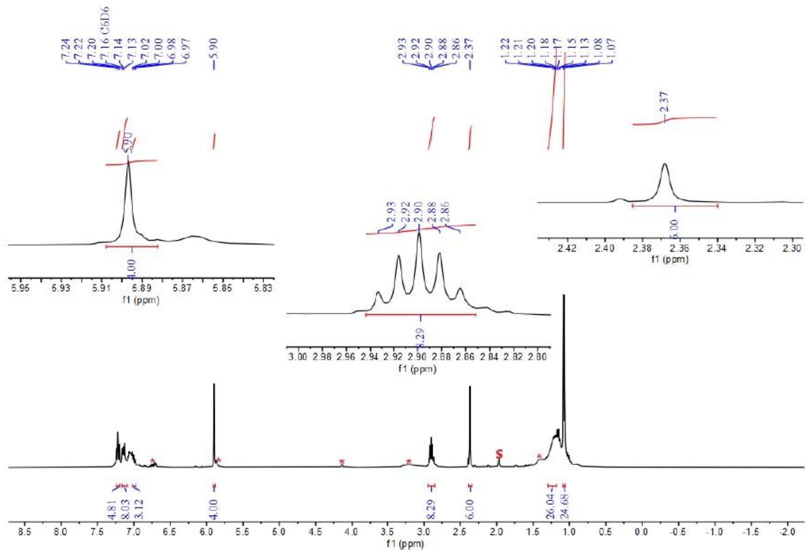

Figure S31. ^{1}H NMR spectrum of compound **8**. The respective resonances of IPrNH, resulting from minor complex decomposition in solution, are marked with asterisks * and residual 2,6-dimethylphenyl isocyanate with an S.

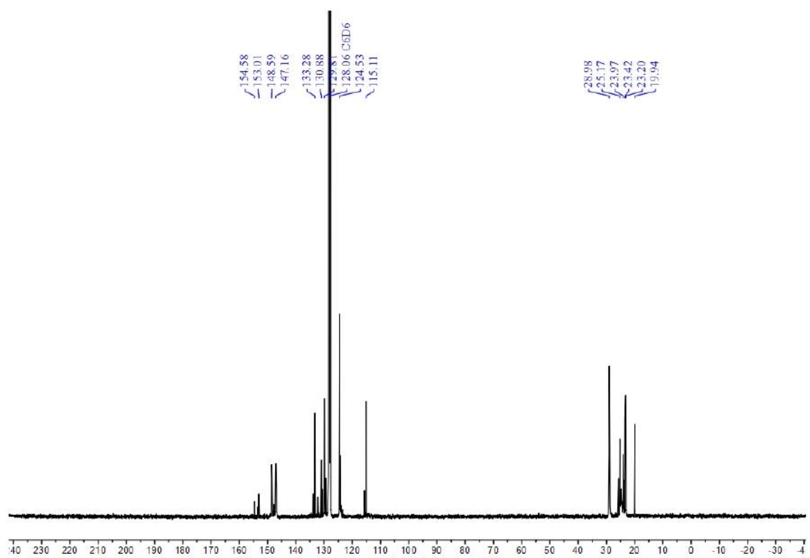

Figure S32. ^{13}C NMR spectrum of compound **8**.

S23

Reaction of 2 and methanol (MeOH)

To the solution of **2** (40 mg, 45 μmol) in C_6D_6 (0.4 mL) in a J. Young PTFE tube, methanol (MeOH) (2 μL, 45 μmol, 1.0 eq.) was added at room temperature. The color rapidly changed from orange to yellow. The product was confirmed by ^{1}H NMR spectrum as the free ligand IPrNH.

2. X-ray Crystallographic Data

General Information

The X-ray intensity data of **2** was collected on an X-ray single crystal diffractometer equipped with a CMOS detector (Bruker Photon-100), an IMS microsource with MoKα radiation (λ = 0.71073 Å) and a Helios mirror optic by using the APEX III software package.[S3] The measurement was performed on single crystals coated with the perfluorinated ether Fomblin® Y. The crystal was fixed on the top of a microsampler, transferred to the diffractometer and frozen under a stream of cold nitrogen. A matrix scan was used to determine the initial lattice parameters. Reflections were merged and corrected for Lorenz and polarization effects, scan speed, and background using SAINT.[S4] Absorption corrections, including odd and even ordered spherical harmonics were performed using SADABS.[S4] Space group assignments were based upon systematic absences, E statistics, and successful refinement of the structures. Structures were solved by direct methods with the aid of successive difference Fourier maps, and were refined against all data using the APEX III software in conjunction with SHELXL-2014[S5] and SHELXLE.[S6] All H atoms were placed in calculated positions and refined using a riding model, with methylene and aromatic C–H distances of 0.99 and 0.95 Å, respectively, and Uiso(H) = 1.2·U_{eq}(C). Full-matrix least-squares refinements were carried out by minimizing $\Sigma w(Fo^2–Fc^2)^2$ with SHELXL-97[S7] weighting scheme. Neutral atom scattering factors for all atoms and anomalous dispersion corrections for the non-hydrogen atoms were taken from International Tables for Crystallography.[S8] The image of the crystal structure was generated by Mercury.[S9] The CCDC number 2053427 (**2**) contains the supplementary crystallographic data for the structure. The data can be obtained free of charge from the Cambridge Crystallographic Data Centre *via* https://www.ccdc.cam.ac.uk/structures/.

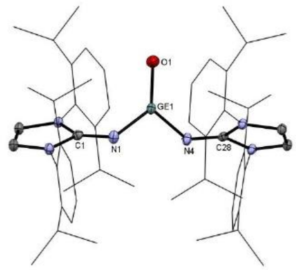

Figure S33. Molecular structure of **2**. Thermal ellipsoids are shown at 50% probability level. Hydrogen atoms are omitted for clarity. Selected bond lengths [Å] and angles [°]: Ge1–O1 1.6494(10), Ge1–N1 1.7819(12), Ge1–N4 1.7825(12), N1–C1 1.2872(18), N4–C28 1.2914(18), O1–Ge1–N1 125.94(6), O1–Ge1–N4 125.41(6), N1–Ge1–N4 108.65(6), Ge1–N1–C1 127.81(10), Ge1–N4–C28 125.02(10).

Table S1. Crystal data and structure refinement for compound **2**.

Compound #	2
Chemical formula	$C_{54}H_{72}GeN_6O$
Formula weight	893.79 g/mol
Temperature	100 K
Wavelength	0.71073 Å
Crystal size	0.356 x 0.230 x 0.180 mm
Crystal habit	clear light-yellow block
Crystal system	monoclinic
Space group	P 21/c
Unit cell dimensions	a = 21.8129(7) Å; α = 90°
	b = 11.8549(4) Å; β = 104.710(1)°
	c = 19.9092(7) Å; γ = 90°
Volume	4979.6(3) $Å^3$
Z	4
Density (calculated)	1.192 g/cm^3
Radiation source	IMS microsource
Theta range for data collection	1.97 to 25.35°
Index ranges	-26<=h<=26, -14<=k<=14, -23<=l<=23
Reflections collected	161254
Independent reflections	9095
Completeness	0.999
Absorption correction	Multi-Scan
Max. and min. transmission	0.7099 and 0.7452
Refinement method	Full-matrix least-squares on F^2
Function minimized	$\Sigma w(F_o^2 - F_c^2)^2$
Data / restraints / parameters	9095 / 0 / 575
Goodness-of-fit on F^2	1.035
Final R indices [I>2sigma(I)]	R1 = 0.0248, wR2 = 0.0613
R indices (all data)	R1 = 0.0288, wR2 = 0.0644
Largest diff. peak and hole	0.264 and -0.454 $eÅ^{-3}$

3. Computational Section

DFT calculations were performed at the ωB97X-D/def2-TZVPP//B97-D/def2-SVP level of theory.[S10-S13] Stationary points on the potential energy surface (PES) were characterized by harmonic vibrational frequency calculations. Electronic structure analysis was carried out at the same level of theory as the geometry optimization. All calculations were carried out using GAUSSIAN 09 program.[S14]

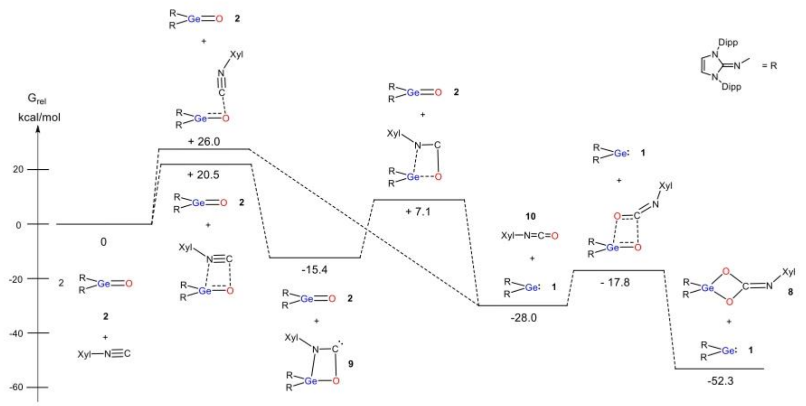

Figure S34. DFT-derived mechanism of the reaction of **2** and XylNC.

Table S2. NBO-Analysis of the central Ge in **2**.

2	Occupation	Atom	Polarization	*s*-character	*p*-character	*d*-character
Bond	1.93	Ge	22.59%	37.15%	62.34%	0.50%
		O	77.41%	19.00%	80.93%	0.08%
Bond	1.90	Ge	20.92%	31.40%	67.81%	0.79%
		N	79.08%	18.95%	81.01%	0.04%
Bond	1.90	Ge	20.92%	31.40%	67.81%	0.79%
		N	79.08%	18.95%	81.01%	0.04%

Table S3. Calculated Ge=O, Ge-N bond lengths [Å], NPA charges of Ge and O atoms, Wiberg Bond Index (WBI) and Mayer Bond Order (MBO) in **2**.

Compound	Bond length [Å]		NPA charge		WBI//MBO	
	Ge–O	Ge-N	Ge	O	Ge-O	Ge-N
2	1.670	1.808	+1.89	-1.02	1.30//1.75	0.76//1.03

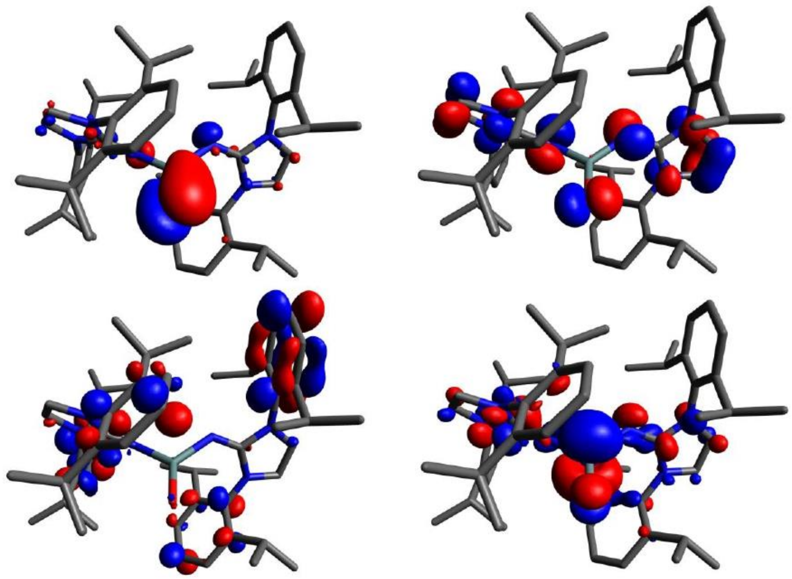

Figure S35. HOMO-3 (top left, -5.25 eV), HOMO (top right, –4.24 eV), LUMO (bottom left, –1.15 eV), and LUMO+9 (bottom right, –0.266 eV) of **2**.

Table S4. Cartesian coordinates of XylNC in Å.

Atomtype	X Coordinate [Å]	Y Coordinate [Å]	Z Coordinate [Å]
C	1.246100	-0.240301	0.000000
C	0.000000	0.441018	0.000000
C	-1.246099	-0.240301	0.000000
C	-1.217775	-1.646492	0.000000
C	0.000000	-2.344903	0.000000
C	1.217775	-1.646491	0.000000
N	0.000000	1.827038	0.000000
C	0.000003	3.015154	0.000000
C	-2.537743	0.539967	0.000000
H	-2.167176	-2.197283	0.000000
H	0.000001	-3.442216	0.000000
H	2.167175	-2.197284	0.000000
C	2.537742	0.539969	0.000000
H	-3.412645	-0.132335	0.000000
H	-2.601678	1.201617	0.885196
H	-2.601678	1.201617	-0.885196
H	3.412645	-0.132332	0.000000
H	2.601676	1.201619	-0.885196
H	2.601676	1.201619	0.885196

Table S5. Cartesian coordinates of **2** in Å.

Atomtype	X Coordinate [Å]	Y Coordinate [Å]	Z Coordinate [Å]
Ge	-0.000106	0.001422	-0.939312
O	-0.000129	0.003686	-2.609495
N	1.447517	0.177812	0.128748
N	2.299415	2.445959	-0.258881
N	3.592444	0.990213	0.780327
N	-1.447689	-0.177963	0.128311
N	-3.592511	-0.992426	0.777705
N	-2.299141	-2.445264	-0.265143
C	2.339843	1.113664	0.176532
C	3.498816	3.095730	0.057362
H	3.662552	4.138583	-0.210068
C	4.297127	2.197177	0.701092
H	5.299395	2.294388	1.116624
C	1.206844	3.000128	-1.002796
C	0.027015	3.373794	-0.301034
C	-1.038030	3.893158	-1.060261
H	-1.970092	4.178464	-0.562911
C	-0.931203	4.031630	-2.452394
H	-1.779483	4.429789	-3.023936
C	0.234089	3.637042	-3.119507
H	0.291244	3.722206	-4.210871
C	1.323857	3.094972	-2.411963
C	-0.053512	3.239142	1.220525
H	0.487734	2.315805	1.495978
C	-1.487747	3.081573	1.750331
H	-1.463737	2.862385	2.832346
H	-2.009004	2.248450	1.249816
H	-2.082302	4.005242	1.621860
C	0.660954	4.426719	1.904994
H	0.648842	4.301646	3.004725
H	0.148559	5.377388	1.662053
H	1.713905	4.511974	1.582303
C	2.574278	2.620337	-3.148487
H	3.184104	2.043356	-2.429819
C	2.242484	1.670065	-4.317486
H	1.589451	0.851798	-3.964628
H	3.178566	1.250456	-4.734130
H	1.728567	2.204358	-5.139321
C	3.421270	3.824224	-3.615304
H	3.711987	4.473162	-2.767902
H	2.853384	4.444026	-4.335437
H	4.344652	3.478358	-4.117693
C	4.088014	-0.246987	1.305281

C	3.952325	-0.500960	2.693795
C	4.422889	-1.735949	3.177883
H	4.329692	-1.972361	4.243896
C	4.993863	-2.679529	2.310754
H	5.344675	-3.641244	2.707268
C	5.111206	-2.405071	0.941962
H	5.552182	-3.154392	0.273154
C	4.665254	-1.179223	0.408798
C	3.244184	0.502541	3.603308
H	3.366374	1.503177	3.148370
C	1.727353	0.203926	3.643845
H	1.539631	-0.765353	4.142942
H	1.300389	0.146039	2.628272
H	1.191372	0.988008	4.210903
C	3.833987	0.572058	5.023861
H	3.369512	1.404012	5.585203
H	4.927802	0.733596	5.004140
H	3.636048	-0.354224	5.595676
C	4.771428	-0.894858	-1.088440
H	4.485026	0.159343	-1.252536
C	6.213741	-1.061559	-1.609375
H	6.923581	-0.431178	-1.041872
H	6.270052	-0.773655	-2.676057
H	6.554821	-2.111192	-1.531346
C	3.776520	-1.764786	-1.885227
H	4.022223	-2.839074	-1.781725
H	3.808948	-1.506777	-2.960331
H	2.744638	-1.611730	-1.529913
C	-2.339870	-1.114078	0.173624
C	-4.296927	-2.199342	0.695409
H	-5.299172	-2.297828	1.110696
C	-3.498427	-3.096078	0.049384
H	-3.661928	-4.138290	-0.220670
C	-4.088385	0.243337	1.305747
C	-4.666062	1.177576	0.411634
C	-5.112316	2.401976	0.947866
H	-5.553645	3.152787	0.280967
C	-4.994859	2.673116	2.317310
H	-5.345920	3.633744	2.716232
C	-4.423482	1.727586	3.182045
H	-4.330208	1.961412	4.248621
C	-3.952594	0.493939	2.694861
C	-4.772486	0.896792	-1.086264
H	-4.485796	-0.156923	-1.252960
C	-6.214970	1.064282	-1.606475
H	-6.924483	0.432321	-1.040324
H	-6.271427	0.778910	-2.673830

H	-6.556368	2.113619	-1.525863
C	-3.778033	1.768929	-1.881197
H	-4.024032	2.842891	-1.775055
H	-3.810642	1.513494	-2.956908
H	-2.746019	1.615327	-1.526503
C	-3.243962	-0.511561	3.601778
H	-3.365876	-1.511108	3.144374
C	-3.833504	-0.584830	5.022251
H	-3.368681	-1.418051	5.581419
H	-4.927274	-0.746655	5.002308
H	-3.635753	0.340067	5.596370
C	-1.727230	-0.212510	3.642799
H	-1.539768	0.755613	4.144229
H	-1.300452	-0.151980	2.627302
H	-1.190876	-0.997787	4.207849
C	-1.206374	-2.997342	-1.010329
C	-1.323118	-3.088434	-2.419768
C	-0.233127	-3.628414	-3.128567
H	-0.290063	-3.710640	-4.220167
C	0.932108	-4.024609	-2.462307
H	1.780554	-4.421099	-3.034763
C	1.038652	-3.889876	-1.069787
H	1.970658	-4.176396	-0.573027
C	-0.026608	-3.372711	-0.309361
C	-2.573457	-2.611978	-3.155253
H	-3.183530	-2.037060	-2.435142
C	-3.420154	-3.814713	-3.625558
H	-3.710938	-4.466029	-2.780006
H	-2.852012	-4.432430	-4.347278
H	-4.343491	-3.467619	-4.127182
C	-2.241559	-1.658459	-4.321577
H	-1.588730	-0.841064	-3.966330
H	-3.177612	-1.237847	-4.737270
H	-1.727390	-2.190428	-5.144763
C	0.053640	-3.242232	1.212575
H	-0.487658	-2.319664	1.490489
C	1.487790	-3.086124	1.743048
H	1.463610	-2.870037	2.825682
H	2.009088	-2.251552	1.244999
H	2.082396	-4.009400	1.612018
C	-0.660926	-4.431700	1.893646
H	-0.648985	-4.309670	2.993721
H	-0.148490	-5.381690	1.648156
H	-1.713828	-4.516068	1.570558

Table S6. Cartesian coordinates of transition state (+20.5 kcal/mol) in **Figure S34** in Å.

Atomtype	X Coordinate [Å]	Y Coordinate [Å]	Z Coordinate [Å]
C	3.689761	-3.420462	-2.044970
C	2.664797	-2.866531	-1.221499
C	2.490140	-3.305272	0.123367
C	3.347061	-4.301279	0.624017
C	4.364007	-4.850379	-0.173182
C	4.528863	-4.408166	-1.494840
N	1.851118	-1.832949	-1.666986
C	1.455375	-1.283705	-2.699818
O	0.433094	0.104119	-2.375297
Ge	-0.123342	0.500039	-0.767345
N	-1.553514	-0.218067	0.087971
C	-2.721178	-0.642349	-0.289898
N	-3.277306	-0.906777	-1.552910
C	-4.602570	-1.327641	-1.423868
C	-4.902941	-1.353120	-0.096079
N	-3.761674	-0.950503	0.601501
C	-2.534831	-1.017071	-2.780142
C	-1.980376	-2.277895	-3.113714
C	-1.302902	-2.380262	-4.341613
C	-1.181176	-1.272586	-5.191095
C	-1.732815	-0.037131	-4.831680
C	-2.415807	0.119190	-3.612313
C	-3.711372	-0.857661	2.033957
C	-4.348653	0.240427	2.659733
C	-4.406223	0.253931	4.068163
C	-3.830496	-0.776701	4.818606
C	-3.172875	-1.836373	4.175851
C	-3.097323	-1.904748	2.772214
C	-2.136257	-3.490663	-2.196730
C	-3.245322	-4.429983	-2.720733
C	-3.035841	1.454718	-3.207963
C	-2.131906	2.657055	-3.534249
C	-4.974114	1.374464	1.850232
C	-4.445951	2.753431	2.292964
C	-2.389294	-3.059152	2.060024
C	-1.351999	-3.781717	2.938585
C	1.448753	-2.657863	0.997825
C	3.876118	-2.945254	-3.464034
N	1.059495	0.825941	0.549232
C	1.970097	1.698399	0.824273
N	2.254056	2.963883	0.295345
C	3.271729	3.580007	1.040909
C	3.656636	2.709865	2.015552
N	2.883245	1.555829	1.879245
C	1.559695	3.607678	-0.782512

C	1.922259	3.293967	-2.119600
C	1.280277	4.013145	-3.147115
C	0.330720	5.000714	-2.855213
C	-0.016535	5.285231	-1.527566
C	0.588154	4.593526	-0.460156
C	2.996643	2.250029	-2.425675
C	4.410861	2.839653	-2.215079
C	0.178534	4.849986	0.991465
C	-0.873024	3.811461	1.441813
C	2.958968	0.372358	2.686352
C	1.914122	0.112109	3.605711
C	1.972840	-1.093517	4.333557
C	3.034498	-1.989225	4.158830
C	4.070588	-1.695907	3.258866
C	4.057418	-0.510327	2.500609
C	0.769046	1.094290	3.840601
C	0.829195	1.669803	5.272796
C	5.150729	-0.190116	1.478514
C	6.505651	-0.850285	1.792965
C	-0.602452	0.459941	3.545419
C	4.699168	-0.549161	0.044905
C	-0.334814	6.279105	1.249736
C	2.876518	1.637023	-3.831482
C	-0.821664	-4.265177	-1.983857
C	-4.437014	1.616153	-3.837798
C	-6.515796	1.318763	1.914967
C	-3.396300	-4.086359	1.491614
H	-5.816275	-1.628584	0.428839
H	-5.196171	-1.587651	-2.299320
H	-4.904858	1.085921	4.580164
H	-3.882261	-0.751599	5.914815
H	-2.712831	-2.622995	4.782743
H	-4.677398	1.236178	0.795396
H	-4.873827	3.550973	1.656562
H	-3.347070	2.795085	2.213715
H	-4.723270	2.982453	3.338756
H	-6.962720	2.112362	1.286660
H	-6.870484	1.464564	2.953106
H	-6.897563	0.343931	1.560446
H	-1.838195	-2.611770	1.212459
H	-0.650189	-3.070654	3.408853
H	-0.762109	-4.479547	2.318519
H	-1.836961	-4.376529	3.736083
H	-4.121237	-3.625561	0.800683
H	-3.962037	-4.566651	2.312788
H	-2.858960	-4.877877	0.936592
H	-1.608691	0.823699	-5.498265

H	-0.631960	-1.370199	-6.136078
H	-0.852731	-3.336249	-4.632532
H	-3.169684	1.438109	-2.109396
H	-2.059626	2.832370	-4.624333
H	-1.111393	2.501768	-3.144497
H	-2.540163	3.579589	-3.081248
H	-4.923114	2.545219	-3.482720
H	-5.093772	0.764110	-3.583281
H	-4.360734	1.668010	-4.940794
H	-2.458562	-3.126953	-1.206012
H	-4.197045	-3.888459	-2.870433
H	-3.426765	-5.254794	-2.005481
H	-2.951367	-4.873835	-3.691032
H	-0.481860	-4.757329	-2.914049
H	-0.969871	-5.058332	-1.226799
H	-0.013601	-3.600468	-1.642514
H	4.409887	2.798963	2.797469
H	3.618894	4.582250	0.793403
H	4.891273	-2.409582	3.135257
H	3.058651	-2.927443	4.728612
H	1.171730	-1.328787	5.045211
H	5.313562	0.903069	1.503568
H	6.828978	-0.652957	2.832057
H	7.280641	-0.459780	1.107687
H	6.465687	-1.945698	1.644990
H	5.374882	-0.092488	-0.702196
H	3.670841	-0.213114	-0.166872
H	4.717368	-1.642705	-0.092986
H	0.896246	1.941055	3.145988
H	0.038120	2.431055	5.414152
H	1.807717	2.143217	5.478484
H	0.671269	0.877130	6.028699
H	-0.834334	-0.345170	4.265531
H	-0.645175	0.047438	2.523736
H	-1.404556	1.215441	3.637419
H	1.522915	3.794424	-4.191801
H	-0.156581	5.545789	-3.673807
H	-0.770077	6.053570	-1.322695
H	2.862071	1.424000	-1.705324
H	4.560446	3.210365	-1.186150
H	4.588071	3.678830	-2.914914
H	5.175909	2.064473	-2.409688
H	1.846414	1.296180	-4.023114
H	3.530375	0.749751	-3.902503
H	3.195004	2.350681	-4.616359
H	1.074269	4.709398	1.625168
H	-1.130170	3.955144	2.508372

H	-0.518192	2.775773	1.315439
H	-1.797088	3.927975	0.844817
H	-0.463523	6.440871	2.335926
H	-1.320254	6.453334	0.778212
H	0.367171	7.042715	0.866917
H	3.221106	-4.635353	1.662284
H	5.029059	-5.622701	0.234998
H	5.325328	-4.835111	-2.119384
H	1.387949	-3.150921	1.980381
H	1.680469	-1.589977	1.161467
H	0.450622	-2.676223	0.525752
H	3.011604	-3.226467	-4.095998
H	3.925177	-1.840678	-3.513053
H	4.793472	-3.366050	-3.913049

Table S7. Cartesian coordinates of intermediate (-15.4 kcal/mol) in **Figure S34** in Å.

Atomtype	X Coordinate [Å]	Y Coordinate [Å]	Z Coordinate [Å]
C	-2.743531	-1.882633	2.960178
C	-2.353738	-0.535580	3.182426
C	-1.365829	-0.172789	4.131890
C	-0.755164	-1.204566	4.870705
C	-1.119482	-2.541167	4.669162
C	-2.102619	-2.874647	3.726996
N	-2.928501	0.509338	2.381776
C	-2.270204	1.042881	1.265922
N	-3.029553	2.169659	0.918253
C	-4.063258	2.357887	1.838199
C	-3.998435	1.340542	2.745453
C	-2.742795	2.928973	-0.264448
C	-1.572555	3.727301	-0.292748
C	-1.249445	4.368231	-1.505886
C	-2.058677	4.220299	-2.638746
C	-3.223747	3.440503	-2.579441
C	-3.592512	2.776882	-1.393757
C	-0.689823	3.932248	0.936285
C	0.778992	3.559355	0.666229
C	-4.823735	1.870067	-1.331274
C	-4.419160	0.393850	-1.534224
N	-1.158804	0.718338	0.711314
Ge	-0.209561	-0.622644	0.042168
O	-0.620157	-2.509541	0.439356
C	-0.937844	1.278888	4.335894
C	-1.030581	1.709958	5.813963
C	-3.842058	-2.230472	1.954212
C	-3.777002	-3.676277	1.431954

N	1.479828	0.021866	-0.027294
C	2.607034	-0.404868	-0.499880
N	3.059973	-1.674870	-0.902669
C	4.401164	-1.605446	-1.300872
C	4.803334	-0.311527	-1.186767
N	3.723936	0.424535	-0.689230
C	2.402337	-2.924540	-0.626834
C	1.796454	-3.641696	-1.690688
C	1.221229	-4.888648	-1.383490
C	1.232409	-5.390570	-0.075475
C	1.827212	-4.658262	0.956631
C	2.437407	-3.415970	0.703236
C	3.821771	1.820909	-0.361594
C	4.114124	2.198044	0.977381
C	4.365638	3.560800	1.225594
C	4.322644	4.508633	0.192395
C	3.985391	4.117493	-1.107387
C	3.711086	2.767672	-1.407537
C	1.744536	-3.080315	-3.113028
C	0.493720	-3.527629	-3.896118
C	3.117618	-2.655133	1.840545
C	4.248918	-3.489846	2.477637
C	4.147219	1.159801	2.102905
C	5.445399	0.319912	2.088560
C	3.316365	2.356802	-2.824062
C	4.544579	2.334035	-3.759501
C	3.010387	-3.446185	-3.922724
C	2.104408	-2.183610	2.903870
C	3.958578	1.770407	3.503344
C	2.202536	3.258884	-3.394533
C	0.475176	1.514694	3.767711
C	-5.239309	-1.959083	2.561181
C	-5.934257	2.259730	-2.323749
C	-0.818788	5.380573	1.458623
H	5.762703	0.161625	-1.390092
H	4.946994	-2.498877	-1.598294
H	4.598891	3.894571	2.241840
H	4.534702	5.563326	0.410560
H	3.927582	4.870063	-1.902668
H	3.290546	0.482346	1.925034
H	3.794791	0.964690	4.241732
H	3.091375	2.449475	3.541315
H	4.855278	2.333165	3.825986
H	5.425763	-0.421185	2.909318
H	6.326666	0.972693	2.237354
H	5.579624	-0.232291	1.144779
H	2.912158	1.329882	-2.773040

H	1.334301	3.298490	-2.714129
H	1.861265	2.868646	-4.371119
H	2.559438	4.292386	-3.561901
H	5.320120	1.639386	-3.389528
H	4.997381	3.341338	-3.833534
H	4.254223	2.012979	-4.777862
H	1.817727	-5.053917	1.979729
H	0.756211	-6.355330	0.141023
H	0.729413	-5.466715	-2.172135
H	3.592681	-1.754576	1.418614
H	1.587993	-3.038191	3.377043
H	1.329992	-1.533849	2.465358
H	2.617516	-1.609909	3.698987
H	4.783195	-2.894030	3.241867
H	4.983453	-3.813139	1.716909
H	3.853365	-4.395196	2.974959
H	1.708753	-1.978022	-3.017887
H	3.931651	-3.039630	-3.474784
H	2.933299	-3.049709	-4.953110
H	3.115979	-4.546007	-3.988020
H	0.592515	-4.573566	-4.243919
H	0.358733	-2.892203	-4.789649
H	-0.414960	-3.452921	-3.280750
H	-4.747062	3.202718	1.762537
H	-4.593833	1.141708	3.635286
H	-3.844865	3.335781	-3.475149
H	-1.782443	4.717368	-3.577918
H	-0.347398	4.989389	-1.559469
H	-5.253169	1.959854	-0.316515
H	-6.200831	3.330034	-2.243839
H	-6.841576	1.659611	-2.125607
H	-5.634058	2.055467	-3.368554
H	-4.062747	0.234976	-2.565285
H	-5.283092	-0.275197	-1.361162
H	-3.605292	0.089442	-0.855110
H	-1.052608	3.262518	1.733395
H	-0.215770	5.512424	2.377472
H	-1.869498	5.635299	1.693397
H	-0.453835	6.108251	0.708736
H	1.241031	4.225351	-0.085254
H	0.869004	2.517524	0.317609
H	1.373685	3.658398	1.591934
H	-2.359931	-3.927255	3.574200
H	-0.625105	-3.334835	5.244298
H	0.025444	-0.957315	5.600432
H	-3.714712	-1.553497	1.087192
H	-5.360481	-0.909620	2.876604

H	-5.403953	-2.604911	3.444859
H	-6.029895	-2.183975	1.820349
H	-2.787143	-3.907655	1.004975
H	-4.534344	-3.816476	0.639372
H	-4.011913	-4.404821	2.231508
H	-1.630240	1.925966	3.769750
H	0.759945	2.577253	3.881777
H	0.523200	1.259913	2.695449
H	1.219896	0.901460	4.306726
H	-0.794309	2.786340	5.913429
H	-0.312910	1.154232	6.446329
H	-2.044648	1.538008	6.220181
C	-1.207756	-2.751199	-0.713626
N	-1.169204	-1.610667	-1.446079
C	-1.788023	-1.327227	-2.684995
C	-1.360136	-0.173745	-3.409829
C	-1.982500	0.148377	-4.630204
C	-3.006524	-0.644623	-5.161409
C	-3.424268	-1.772656	-4.445102
C	-2.852109	-2.132192	-3.208740
C	-0.271908	0.738322	-2.895658
H	-1.646572	1.044300	-5.169025
H	-3.477913	-0.384205	-6.117602
H	-4.238016	-2.394233	-4.841991
C	-3.424270	-3.326948	-2.482245
H	-0.033776	1.512022	-3.642005
H	-0.574368	1.268311	-1.971946
H	0.660312	0.190665	-2.667825
H	-2.698190	-4.155524	-2.409179
H	-3.669820	-3.077652	-1.435034
H	-4.337766	-3.687082	-2.991087

Table S8. Cartesian coordinates of transition state (+7.1 kcal/mol) in **Figure S34** in Å.

Atomtype	X Coordinate [Å]	Y Coordinate [Å]	Z Coordinate [Å]
C	2.852759	2.843245	-2.721088
C	1.788390	1.958023	-2.350124
C	1.397638	0.916509	-3.244304
C	2.073355	0.772165	-4.470711
C	3.108798	1.636620	-4.845327
C	3.480323	2.663959	-3.969156
N	1.133545	2.060102	-1.101801
C	1.095999	3.085535	-0.262045
O	0.616744	2.865142	0.875945
Ge	0.191741	0.710870	0.329820
N	-1.441578	-0.061030	-0.027533

C	-2.584286	0.377238	-0.443685
N	-3.105864	1.674538	-0.641991
C	-4.429048	1.602469	-1.094073
C	-4.755980	0.289128	-1.220885
N	-3.650988	-0.463744	-0.814776
C	-2.528011	2.903362	-0.169525
C	-2.001137	3.830166	-1.107250
C	-1.530301	5.059112	-0.608238
C	-1.564325	5.347690	0.762227
C	-2.074897	4.411624	1.667098
C	-2.577514	3.174751	1.222572
C	-3.686019	-1.898999	-0.756020
C	-4.001757	-2.533876	0.476222
C	-4.206605	-3.926893	0.452860
C	-4.095985	-4.658995	-0.738747
C	-3.736822	-4.016641	-1.927919
C	-3.508303	-2.625972	-1.957458
C	-1.936094	3.518912	-2.604040
C	-3.214164	3.983807	-3.341019
C	-3.190551	2.196937	2.224946
C	-2.177920	1.740717	3.294588
C	-4.099910	-1.730719	1.777177
C	-3.950566	-2.596305	3.041966
C	-3.092972	-1.940924	-3.258166
C	-1.927825	-2.678365	-3.949554
C	0.297108	-0.058542	-2.907573
C	3.345882	3.952824	-1.823068
N	1.238236	-0.751964	0.501919
C	2.272369	-1.224797	1.097594
N	2.803326	-0.985802	2.374198
C	3.848044	-1.887167	2.633902
C	4.021395	-2.655969	1.520622
N	3.083895	-2.241772	0.572202
C	2.222053	-0.073082	3.315491
C	2.619969	1.291353	3.295410
C	1.985056	2.162660	4.201604
C	1.006299	1.695834	5.090092
C	0.639717	0.344347	5.098138
C	1.240458	-0.569752	4.211084
C	3.714467	1.777556	2.341944
C	5.114426	1.323590	2.820910
C	0.801981	-2.032706	4.171567
C	-0.458836	-2.187250	3.296002
C	2.885542	-2.748939	-0.753849
C	1.770926	-3.586878	-0.998696
C	1.535878	-3.987124	-2.329663
C	2.379749	-3.571175	-3.367180

C	3.489490	-2.755916	-3.095080
C	3.767300	-2.326631	-1.783473
C	0.851171	-4.066942	0.120766
C	0.962023	-5.596467	0.303443
C	4.928237	-1.381053	-1.471679
C	6.124683	-1.527334	-2.429470
C	-0.606766	-3.630433	-0.109579
C	4.432436	0.081264	-1.447093
C	0.582151	-2.638335	5.571686
C	3.726445	3.301081	2.126002
C	-0.701400	4.131044	-3.298235
C	-4.457499	2.797657	2.872027
C	-5.413526	-0.920691	1.876762
C	-4.295266	-1.789119	-4.215155
H	-5.679998	-0.192375	-1.537107
H	-5.020982	2.502430	-1.249649
H	-4.456717	-4.455651	1.378245
H	-4.272991	-5.742349	-0.731813
H	-3.624876	-4.602019	-2.848339
H	-3.252099	-1.018836	1.762085
H	-3.835476	-1.946074	3.928237
H	-3.070403	-3.257791	2.989038
H	-4.846430	-3.223867	3.210705
H	-5.433899	-0.348368	2.823014
H	-6.286105	-1.601635	1.870724
H	-5.531200	-0.201311	1.051019
H	-2.734509	-0.927709	-3.002439
H	-1.072388	-2.804328	-3.263970
H	-1.585331	-2.103866	-4.829976
H	-2.233793	-3.677831	-4.311404
H	-5.109443	-1.203993	-3.751021
H	-4.702235	-2.781161	-4.489906
H	-3.990719	-1.273905	-5.145945
H	-2.086122	4.641609	2.739541
H	-1.173029	6.305837	1.127213
H	-1.109842	5.796090	-1.300395
H	-3.513030	1.296635	1.677665
H	-1.814595	2.590617	3.900817
H	-1.295045	1.259150	2.841073
H	-2.647431	1.011475	3.981959
H	-4.931914	2.061910	3.548748
H	-5.197929	3.085576	2.102777
H	-4.217379	3.699150	3.466544
H	-1.868919	2.418595	-2.700791
H	-4.123040	3.483450	-2.968812
H	-3.130731	3.770107	-4.423714
H	-3.348495	5.075651	-3.218816

H	-0.829972	5.218541	-3.458566
H	-0.555014	3.666069	-4.289803
H	0.214772	3.976104	-2.709021
H	4.724139	-3.461760	1.311056
H	4.356956	-1.899363	3.596733
H	4.137881	-2.439276	-3.918902
H	2.173937	-3.885031	-4.399007
H	0.676695	-4.631904	-2.551353
H	5.292269	-1.626467	-0.456568
H	6.455367	-2.578988	-2.517327
H	6.975607	-0.924324	-2.061837
H	5.880684	-1.156412	-3.442546
H	4.130312	0.397921	-2.459324
H	5.232250	0.760705	-1.096308
H	3.555364	0.205425	-0.790992
H	1.188460	-3.600318	1.062195
H	0.334063	-5.928083	1.152444
H	2.005356	-5.907233	0.500773
H	0.614229	-6.132332	-0.600330
H	-1.033433	-4.102855	-1.012670
H	-0.688275	-2.535836	-0.212627
H	-1.239063	-3.936412	0.742980
H	2.244658	3.225578	4.206448
H	0.517480	2.397549	5.778284
H	-0.134536	-0.001822	5.792341
H	3.520626	1.300533	1.361469
H	5.196641	0.228676	2.911365
H	5.343119	1.770545	3.807358
H	5.888189	1.660691	2.105350
H	2.737700	3.677264	1.819066
H	4.458050	3.553204	1.337070
H	4.045583	3.833242	3.042643
H	1.608704	-2.615417	3.691102
H	-0.753892	-3.251057	3.233084
H	-0.294018	-1.816284	2.271143
H	-1.301264	-1.620828	3.732776
H	0.396503	-3.725481	5.487641
H	-0.297880	-2.197480	6.076748
H	1.461776	-2.485073	6.224015
H	1.769201	-0.041323	-5.142653
H	3.621105	1.512143	-5.807819
H	4.294722	3.346490	-4.246786
H	0.006075	-0.634540	-3.799888
H	0.616794	-0.784607	-2.135882
H	-0.602265	0.447640	-2.517803
H	2.590253	4.751375	-1.704642
H	3.545873	3.591314	-0.798943

H	4.272238	4.399862	-2.228578

Table S9. Cartesian coordinates of **1** in Å.

Atomtype	X Coordinate [Å]	Y Coordinate [Å]	Z Coordinate [Å]
C	-0.112632	-3.480924	-0.229350
C	-1.260114	-3.111545	-0.985391
C	-1.349271	-3.325565	-2.383705
C	-0.278337	-3.987406	-3.017203
C	0.852596	-4.378837	-2.291027
C	0.938828	-4.116076	-0.914832
N	-2.345553	-2.465682	-0.315609
C	-2.336414	-1.099523	0.054557
N	-3.610787	-0.909635	0.621016
C	-4.353896	-2.095159	0.582724
C	-3.575651	-3.053004	0.004166
C	-4.041675	0.323489	1.201589
C	-4.586962	1.323850	0.360988
C	-4.996055	2.532335	0.959574
C	-4.869461	2.729350	2.340656
C	-4.321985	1.724800	3.152898
C	-3.891855	0.503474	2.601853
N	-1.392058	-0.236695	-0.033366
Ge	-0.000286	0.001582	-1.248779
N	1.391023	0.237637	-0.032370
C	2.335547	1.100101	0.057341
N	2.345228	2.466799	-0.310836
C	3.575284	3.053358	0.010460
C	4.353011	2.094464	0.587979
N	3.609590	0.909071	0.624213
C	1.260856	3.113208	-0.981794
C	0.112075	3.481680	-0.227299
C	-0.938693	4.116620	-0.914049
C	-0.850499	4.380138	-2.289976
C	0.281837	3.989837	-3.014592
C	1.352140	3.328196	-2.379825
C	4.040619	-0.325497	1.201606
C	3.893523	-0.508010	2.601857
C	4.323892	-1.730684	3.149703
C	4.868918	-2.734133	2.334422
C	4.992873	-2.534588	0.953478
C	4.583498	-1.324645	0.358018
C	0.043433	3.193313	1.272070
C	0.845393	4.247147	2.068930
C	2.546388	2.832465	-3.192769
C	3.400317	4.009124	-3.709939

C	3.208473	0.558499	3.456382
C	3.799923	0.692270	4.871513
C	4.691222	-1.124609	-1.151947
C	3.692470	-2.037989	-1.892796
C	-4.696599	1.126856	-1.149241
C	-3.696795	2.040059	-1.888973
C	-3.204294	-0.563967	3.453145
C	-1.682238	-0.296571	3.507936
C	-2.542026	-2.828741	-3.198162
C	-2.097048	-1.902801	-4.350178
C	-0.046068	-3.193352	1.270268
C	-0.849577	-4.247296	2.065416
C	-1.389966	3.071185	1.810756
C	2.103718	1.905900	-4.345180
C	1.685732	0.294686	3.509771
C	6.132733	-1.324801	-1.662259
C	-6.138091	1.330445	-1.658158
C	-3.796000	-0.703561	4.867642
C	-3.396448	-4.004665	-3.716201
C	1.386601	-3.072030	1.811115
H	3.776890	4.101594	-0.207426
H	5.366663	2.138464	0.985283
H	-1.847322	4.398527	-0.372838
H	-1.684432	4.876566	-2.802942
H	0.328465	4.178093	-4.094324
H	0.520402	2.210369	1.431146
H	-1.364619	2.745139	2.865130
H	-1.968129	2.321668	1.244677
H	-1.931088	4.035702	1.784278
H	0.838772	3.997650	3.147338
H	0.395870	5.251487	1.946553
H	1.898041	4.298378	1.738262
H	3.183345	2.230420	-2.520240
H	1.481517	1.075357	-3.964231
H	2.988715	1.478614	-4.854142
H	1.514490	2.454333	-5.104286
H	3.758564	4.641396	-2.876482
H	2.814234	4.652218	-4.394011
H	4.282269	3.637227	-4.265363
H	4.218359	-1.910420	4.225667
H	5.190621	-3.684117	2.780884
H	5.410168	-3.330915	0.324519
H	3.349721	1.530617	2.949378
H	1.472619	-0.625900	4.084837
H	1.264932	0.166391	2.498009
H	1.162759	1.133669	4.005950
H	3.348236	1.559139	5.388956

H	4.896041	0.836666	4.843610
H	3.588780	-0.200175	5.490569
H	4.404793	-0.080499	-1.371488
H	6.841705	-0.658233	-1.136604
H	6.191071	-1.107676	-2.745730
H	6.473590	-2.366852	-1.513610
H	3.942926	-3.105420	-1.740969
H	3.710728	-1.835983	-2.980785
H	2.665994	-1.873096	-1.524808
H	-5.367726	-2.139984	0.979482
H	-3.776888	-4.100956	-0.215412
H	-5.415008	3.329657	0.332984
H	-5.190907	3.678276	2.789547
H	-4.214231	1.902569	4.228979
H	-4.412080	0.082677	-1.371030
H	-6.847958	0.664636	-1.132751
H	-6.197654	1.114679	-2.741830
H	-6.476916	2.372962	-1.508184
H	-3.944787	3.107561	-1.733684
H	-3.716988	1.841176	-2.977509
H	-2.670189	1.871877	-1.522790
H	-3.342943	-1.534818	2.943056
H	-3.342416	-1.570924	5.382610
H	-4.891747	-0.850563	4.838823
H	-3.587306	0.187476	5.489549
H	-1.471545	0.623028	4.085501
H	-1.261248	-0.164896	2.496675
H	-1.157646	-1.135616	4.002273
H	-0.323380	-4.174981	-4.097118
H	1.687051	-4.875436	-2.802975
H	1.846535	-4.398678	-0.372431
H	-3.179164	-2.225961	-2.526450
H	-3.756370	-4.636428	-2.883086
H	-2.810063	-4.648434	-4.399379
H	-4.277328	-3.632031	-4.272834
H	-1.474305	-1.072954	-3.968595
H	-2.981000	-1.474518	-4.860109
H	-1.507683	-2.451978	-5.108640
H	-0.522889	-2.210313	1.429160
H	1.359767	-2.746747	2.865693
H	1.965853	-2.322312	1.246420
H	1.927463	-4.036694	1.784758
H	-0.844450	-3.998342	3.143959
H	-0.400236	-5.251736	1.943195
H	-1.901751	-4.297960	1.733162

Table S10. Cartesian coordinates of XylNCO in Å.

Atomtype	X Coordinate [Å]	Y Coordinate [Å]	Z Coordinate [Å]
C	1.044490	1.118249	0.000295
C	-0.005879	0.162204	0.001213
C	0.257325	-1.235915	0.000766
C	1.600529	-1.655187	-0.000834
C	2.651976	-0.726033	-0.001882
C	2.370181	0.648805	-0.001315
N	-1.314413	0.643211	0.003148
C	-2.496829	0.384429	-0.000896
C	-0.880216	-2.228682	0.001957
H	1.819238	-2.731142	-0.001239
H	3.692436	-1.074391	-0.003101
H	3.191144	1.377749	-0.002104
C	0.720762	2.593571	0.000966
H	-0.507110	-3.266988	0.002248
H	-1.529887	-2.100846	0.890371
H	-1.530980	-2.101891	-0.885823
H	1.638434	3.206913	0.000418
H	0.115074	2.868349	-0.883999
H	0.116418	2.867848	0.886996
O	-3.672239	0.260409	-0.003428

Table S11. Cartesian coordinates of transition state (-17.8 kcal/mol) in **Figure S34** in Å.

Atomtype	X Coordinate [Å]	Y Coordinate [Å]	Z Coordinate [Å]
C	5.437682	-2.312524	0.888437
C	4.080206	-2.729307	0.779035
C	3.711763	-3.794428	-0.090018
C	4.720557	-4.385896	-0.876047
C	6.057599	-3.967236	-0.797049
C	6.410062	-2.940142	0.091415
N	3.155636	-2.069552	1.584871
C	2.185526	-1.31009	1.482896
O	1.408035	-0.560385	2.052955
Ge	0.142031	-0.261673	-0.059524
O	1.489577	-1.281386	-0.36523
C	2.285249	-4.279199	-0.167247
C	5.791402	-1.172536	1.813371
N	0.142753	1.497236	-0.357599
C	0.868185	2.218518	-1.16111
N	1.339761	1.965579	-2.455391
C	1.972349	3.103632	-2.966
C	1.918185	4.072185	-2.008414
N	1.252555	3.53189	-0.903321

C	1.343907	0.666277	-3.068193
C	2.561002	-0.054866	-3.113062
C	2.525968	-1.355768	-3.65142
C	1.326939	-1.913586	-4.105901
C	0.134899	-1.174521	-4.059123
C	0.116088	0.136937	-3.548633
C	3.876825	0.523881	-2.597795
C	4.490983	-0.349997	-1.491435
C	-1.15077	0.993767	-3.55292
C	-1.093838	2.034567	-4.694863
C	0.986322	4.21944	0.328229
C	-0.020111	5.219454	0.332934
C	-0.246497	5.906265	1.541224
C	0.483838	5.588391	2.694255
C	1.449404	4.572242	2.66893
C	1.72736	3.860726	1.48498
C	-0.876195	5.46747	-0.912211
C	-1.996438	4.404395	-1.019392
C	2.786356	2.755076	1.436154
C	3.105775	2.136278	2.807768
N	-1.503015	-0.863524	0.152975
C	-2.371877	-1.363631	0.961679
N	-2.446387	-1.389346	2.359832
C	-3.636161	-2.012116	2.764979
C	-4.317664	-2.378827	1.645364
N	-3.552297	-1.985029	0.543762
C	-1.490677	-0.820135	3.268683
C	-0.681476	-1.696871	4.035708
C	0.228746	-1.115262	4.937193
C	0.336741	0.276392	5.051812
C	-0.475188	1.120163	4.282979
C	-1.421797	0.591833	3.38418
C	-4.004922	-2.013359	-0.815375
C	-3.556224	-3.047505	-1.670182
C	-4.069989	-3.074979	-2.982613
C	-4.990622	-2.112405	-3.416885
C	-5.391444	-1.077098	-2.559307
C	-4.895595	-0.994633	-1.24493
C	-0.760833	-3.211356	3.83371
C	-0.295488	-4.029941	5.051382
C	-2.384266	1.491321	2.606043
C	-3.78379	1.492087	3.264207
C	-2.527431	-4.079165	-1.214374
C	-1.193328	-3.891921	-1.968372
C	-5.211646	0.203904	-0.348843
C	-6.687945	0.639112	-0.398097

C	0.024457	-3.631527	2.572059
C	-1.878855	2.92849	2.422494
C	-3.057489	-5.521562	-1.351076
C	-4.26769	1.380653	-0.692709
C	-1.462977	6.887587	-0.997214
C	4.079747	3.248379	0.747477
C	-2.445578	0.174743	-3.630313
C	4.86637	0.754586	-3.760009
H	-3.875128	-2.128302	3.821188
H	-5.278931	-2.874659	1.516387
H	-0.369125	2.204923	4.384487
H	1.07073	0.709761	5.743387
H	0.880759	-1.754381	5.541488
H	-2.489684	1.066701	1.593276
H	-2.572083	3.483076	1.767614
H	-0.883716	2.946654	1.950768
H	-1.829051	3.478715	3.380231
H	-4.486246	2.104615	2.66713
H	-3.732291	1.923971	4.281948
H	-4.20603	0.475226	3.343537
H	-1.821215	-3.472288	3.659214
H	-0.284133	-3.063034	1.678682
H	-0.124554	-4.708145	2.364498
H	1.104009	-3.454832	2.716768
H	-0.804496	-3.71043	5.979586
H	0.795486	-3.940052	5.209468
H	-0.511582	-5.10197	4.888218
H	-6.079676	-0.307495	-2.927657
H	-5.382732	-2.15426	-4.441292
H	-3.740224	-3.861772	-3.672203
H	-4.995235	-0.084473	0.694934
H	-4.488979	1.775182	-1.702077
H	-3.210728	1.064161	-0.672463
H	-4.398693	2.205337	0.032198
H	-6.872195	1.435911	0.346532
H	-7.366724	-0.205423	-0.17729
H	-6.963865	1.04862	-1.388044
H	-2.32484	-3.902258	-0.143189
H	-4.005098	-5.657163	-0.797047
H	-2.317097	-6.240632	-0.952918
H	-3.242795	-5.786407	-2.409323
H	-1.324179	-4.062157	-3.05425
H	-0.437223	-4.609045	-1.599825
H	-0.792255	-2.875104	-1.823796
H	2.293081	5.094675	-1.998347
H	2.419992	3.099915	-3.958763
H	1.991832	4.326865	3.587701

H	0.287658	6.129417	3.629106
H	-1.01358	6.686556	1.589637
H	2.367884	1.938552	0.823249
H	3.88589	3.630632	-0.270226
H	4.805302	2.417348	0.664067
H	4.549954	4.059066	1.336418
H	3.636968	2.848793	3.468077
H	3.76099	1.257969	2.671409
H	2.189942	1.784559	3.311618
H	-0.22567	5.336559	-1.796435
H	-1.952367	7.034556	-1.977748
H	-0.681709	7.661168	-0.879799
H	-2.233535	7.059313	-0.222138
H	-2.755407	4.568568	-0.232327
H	-1.606037	3.380054	-0.894575
H	-2.503509	4.474931	-2.000436
H	3.447614	-1.948947	-3.678797
H	1.313827	-2.940757	-4.492511
H	-0.792207	-1.633061	-4.416185
H	3.670037	1.508251	-2.14317
H	4.438623	1.420765	-4.533327
H	5.1309	-0.201782	-4.249313
H	5.801663	1.212637	-3.386029
H	3.763964	-0.48892	-0.677394
H	5.405896	0.123772	-1.090014
H	4.769822	-1.354435	-1.855432
H	-1.180412	1.546298	-2.596127
H	-3.319361	0.839275	-3.524171
H	-2.49712	-0.578286	-2.826532
H	-2.551283	-0.343993	-4.601237
H	-1.985865	2.689195	-4.663609
H	-1.073174	1.528225	-5.678856
H	-0.198027	2.676255	-4.620607
H	4.443771	-5.200423	-1.559459
H	6.823885	-4.447561	-1.41927
H	7.454858	-2.609057	0.1646
H	6.883082	-1.01185	1.859967
H	5.318094	-0.231475	1.469856
H	5.40992	-1.351857	2.836187
H	2.187623	-5.113443	-0.884801
H	1.93794	-4.633663	0.820803
H	1.614966	-3.454465	-0.468822

Table S12. Cartesian coordinates of **8** in **Figure S34** in Å.

Atomtype	X Coordinate [Å]	Y Coordinate [Å]	Z Coordinate [Å]
C	-0.668694	-1.522222	3.917608
C	-1.514142	-0.665109	3.170289
C	-1.470451	0.750091	3.289955
C	-0.544952	1.294104	4.200189
C	0.277302	0.464688	4.975962
C	0.213204	-0.925928	4.838356
N	-2.469342	-1.2481	2.265089
C	-2.399217	-1.248933	0.864881
N	-3.605752	-1.825903	0.462125
C	-4.385069	-2.164087	1.572519
C	-3.684211	-1.809513	2.683054
N	-1.517996	-0.797974	0.02581
Ge	0.127034	-0.147167	0.150768
N	0.270482	1.531388	-0.37785
C	1.046062	2.181062	-1.18958
N	1.563952	1.843527	-2.444263
C	2.257275	2.934649	-2.98184
C	2.199328	3.951824	-2.075695
N	1.468642	3.489871	-0.976597
C	1.560937	0.507677	-2.974667
C	2.766898	-0.234732	-2.947055
C	2.718996	-1.569435	-3.394764
C	1.517572	-2.139916	-3.826723
C	0.338818	-1.378832	-3.856428
C	0.334365	-0.033402	-3.444337
C	1.214843	4.201399	0.243571
C	1.906516	3.799449	1.416352
C	1.623263	4.506319	2.601456
C	0.701858	5.563273	2.611179
C	0.025677	5.930296	1.439351
C	0.256964	5.246796	0.229829
C	4.087672	0.360064	-2.4602
C	4.721322	-0.461964	-1.324487
C	-0.913062	0.845284	-3.550511
C	-2.224791	0.053029	-3.623311
C	2.941651	2.671492	1.380819
C	4.292626	3.19258	0.840178
C	-0.546839	5.546697	-1.038186
C	-1.714195	4.541749	-1.186312
C	-4.100944	-1.800507	-0.884492
C	-4.85267	-0.670201	-1.296892
C	-5.384161	-0.683126	-2.599976
C	-5.156628	-1.766018	-3.460809
C	-4.381402	-2.854283	-3.038777
C	-3.838824	-2.896963	-1.738938

C	-5.004818	0.558536	-0.400755
C	-6.453088	1.078783	-0.3254
C	-2.945053	-4.052964	-1.299743
C	-3.577802	-5.432736	-1.569061
C	-2.425491	1.641714	2.493056
C	-1.884766	3.057844	2.244042
C	-0.693022	-3.039245	3.735734
C	-1.568941	-3.71449	4.816233
O	1.132599	-0.569202	1.695599
C	1.923854	-1.392649	0.968804
O	1.519991	-1.33058	-0.332161
N	2.878536	-2.07114	1.479179
C	5.06702	0.536648	-3.641211
C	-0.790479	1.80652	-4.755878
C	3.121741	1.941355	2.722824
C	-1.058862	6.995066	-1.127558
C	-4.029191	1.668547	-0.853902
C	-1.556171	-3.927158	-1.963782
C	-3.814359	1.700946	3.168856
C	0.716425	-3.667782	3.734635
H	2.740543	2.86848	-3.955395
H	2.609716	4.960381	-2.100769
H	-0.58971	-1.844533	-4.199658
H	1.493595	-3.192219	-4.137611
H	3.629626	-2.178622	-3.365863
H	-0.964527	1.460237	-2.633946
H	-3.082688	0.745187	-3.591799
H	-2.325082	-0.64087	-2.772299
H	-2.310661	-0.523466	-4.563172
H	-1.668506	2.478921	-4.801626
H	-0.745725	1.235237	-5.702828
H	0.115844	2.434492	-4.69158
H	3.886698	1.363409	-2.04599
H	4.035061	-0.536554	-0.467833
H	5.656776	0.018939	-0.982653
H	4.969803	-1.492591	-1.631954
H	4.62969	1.161426	-4.442823
H	5.327455	-0.442874	-4.084663
H	6.004742	1.015029	-3.300183
H	-0.704338	6.746253	1.473133
H	0.500112	6.101025	3.546783
H	2.129428	4.225712	3.531184
H	0.123085	5.38923	-1.90356
H	-2.483023	4.734339	-0.415741
H	-1.37776	3.498302	-1.063593
H	-2.193025	4.647109	-2.178269
H	-1.509281	7.175078	-2.12113

H	-0.243549	7.726777	-0.977959
H	-1.843494	7.198894	-0.374749
H	2.574758	1.911365	0.672261
H	4.180451	3.648621	-0.1603
H	5.016782	2.360164	0.758357
H	4.717294	3.95536	1.520426
H	3.613492	2.581784	3.480233
H	3.757102	1.049827	2.575501
H	2.153531	1.587325	3.115009
H	-5.367695	-2.618653	1.453502
H	-3.9284	-1.89106	3.740222
H	-4.18752	-3.682696	-3.730676
H	-5.572311	-1.752474	-4.476641
H	-5.964967	0.176867	-2.954236
H	-2.7968	-3.963816	-0.208003
H	-4.577925	-5.516795	-1.10454
H	-2.935182	-6.232726	-1.156246
H	-3.689079	-5.627577	-2.652434
H	-1.643407	-3.995982	-3.065182
H	-0.886825	-4.737853	-1.622567
H	-1.085924	-2.960912	-1.714526
H	-4.714329	0.272959	0.625187
H	-6.520427	1.905118	0.407027
H	-7.152824	0.281696	-0.012733
H	-6.799325	1.474115	-1.298833
H	-4.294948	2.035988	-1.863082
H	-2.991785	1.294435	-0.883719
H	-4.069992	2.526105	-0.157819
H	0.882543	-1.559691	5.430281
H	0.990716	0.911371	5.680301
H	-0.461619	2.380573	4.304776
H	-1.151138	-3.242851	2.748775
H	-2.610574	-3.349526	4.8018
H	-1.154237	-3.513028	5.822429
H	-1.589156	-4.811005	4.66871
H	1.413935	-3.120853	3.078712
H	0.657334	-4.718415	3.394001
H	1.149794	-3.682756	4.752753
H	-2.560375	1.180631	1.499953
H	-2.571759	3.602819	1.574206
H	-0.893014	3.033045	1.763517
H	-1.81051	3.646462	3.176738
H	-4.514294	2.298392	2.553801
H	-3.739373	2.176387	4.165412
H	-4.252082	0.69604	3.299691
C	3.705058	-2.956493	0.781407
C	5.11075	-2.809793	0.990093

C	6.001834	-3.662919	0.318721
C	5.530361	-4.67704	-0.53118
C	4.148166	-4.8554	-0.685232
C	3.21663	-4.020531	-0.03445
C	5.611028	-1.724091	1.91465
H	7.082286	-3.530826	0.469595
H	6.235796	-5.339768	-1.049353
H	3.771441	-5.671698	-1.318027
C	1.735721	-4.276715	-0.196491
H	1.546053	-5.320794	-0.506483
H	1.190673	-4.089984	0.747331
H	1.294019	-3.59964	-0.949198
H	6.704422	-1.789757	2.060767
H	5.374656	-0.717216	1.519442
H	5.10782	-1.785704	2.898053

Table S13. Cartesian coordinates of transition state (26.0 kcal/mol) in **Figure S34** in Å.

Atomtype	X Coordinate [Å]	Y Coordinate [Å]	Z Coordinate [Å]
C	4.178517	3.696842	-0.380802
C	3.219506	2.762032	-0.859488
C	3.135178	2.416323	-2.242146
C	4.05433	3.014307	-3.124409
C	5.0115	3.933064	-2.665708
C	5.066818	4.27413	-1.304607
N	2.372595	2.189117	0.083631
C	1.397379	1.468623	0.14662
O	0.800312	0.887413	1.941782
Ge	0.027426	0.121504	0.560185
N	-1.640385	0.34147	-0.090072
C	-2.529099	1.280355	-0.075985
N	-2.599185	2.545034	0.538637
C	-3.822617	3.162146	0.249372
C	-4.532757	2.323311	-0.553406
N	-3.757036	1.17945	-0.752858
C	-1.550787	3.195956	1.273864
C	-0.782615	4.193251	0.62103
C	0.209778	4.847821	1.375841
C	0.429857	4.511964	2.717973
C	-0.33729	3.515471	3.335351
C	-1.343083	2.834987	2.627175
C	-4.148193	0.072077	-1.573543
C	-5.070391	-0.869946	-1.046325
C	-5.471244	-1.929236	-1.882286
C	-4.973451	-2.043916	-3.189336
C	-4.064224	-1.101841	-3.683522

C	-3.631042	-0.022982	-2.887198
C	-1.043343	4.595527	-0.830844
C	-1.830234	5.923817	-0.895302
C	-2.207547	1.761764	3.286191
C	-1.463631	0.95777	4.364517
C	-5.543277	-0.763003	0.403714
C	-4.499269	-1.414031	1.338049
C	-2.638634	0.993921	-3.44615
C	-1.267509	0.343346	-3.721506
C	2.092587	1.448756	-2.739887
C	4.214889	4.039999	1.089437
N	0.561788	-1.483462	-0.038439
C	1.435708	-2.3694	0.285105
N	2.12589	-3.159438	-0.655599
C	2.88183	-4.142254	-0.015301
C	2.726732	-3.965239	1.327292
N	1.875262	-2.868473	1.521876
C	2.084833	-2.860093	-2.053701
C	3.218635	-2.245647	-2.655586
C	3.110374	-1.871992	-4.008452
C	1.922091	-2.086591	-4.725282
C	0.827562	-2.706706	-4.111092
C	0.886403	-3.115723	-2.763611
C	4.488806	-1.9786	-1.839213
C	5.76441	-1.855771	-2.691923
C	-0.292738	-3.852011	-2.128764
C	-0.491709	-5.227029	-2.805028
C	1.348268	-2.486812	2.80071
C	2.029862	-1.504146	3.564376
C	1.509172	-1.200788	4.835902
C	0.350571	-1.829827	5.313251
C	-0.316268	-2.780289	4.529771
C	0.175108	-3.137307	3.258342
C	3.304341	-0.844232	3.040249
C	4.542259	-1.707401	3.377087
C	-0.558099	-4.165035	2.396247
C	-1.820325	-3.539077	1.768944
C	0.246283	4.694205	-1.667341
C	-3.507758	2.385755	3.841291
C	-6.944478	-1.34941	0.650436
C	-3.195757	1.695583	-4.703045
C	3.505647	0.598553	3.536285
C	-0.894254	-5.455998	3.169812
C	-1.589154	-3.021585	-2.153171
C	4.340435	-0.740474	-0.923761
H	-5.521654	2.420124	-1.000168
H	-4.062307	4.145191	0.650861

S53

H	-6.178894	-2.679034	-1.511089
H	-5.295384	-2.879653	-3.82417
H	-3.676246	-1.205931	-4.704349
H	-5.590068	0.311161	0.662303
H	-4.774701	-1.264227	2.399736
H	-3.491237	-0.998978	1.169262
H	-4.446271	-2.501245	1.145278
H	-7.276032	-1.112386	1.678434
H	-6.950462	-2.451731	0.555536
H	-7.689613	-0.941464	-0.057551
H	-2.484585	1.774162	-2.679692
H	-0.838451	-0.080621	-2.798755
H	-0.561903	1.091416	-4.127093
H	-1.352106	-0.471654	-4.463891
H	-4.172768	2.171456	-4.497523
H	-3.33596	0.981486	-5.536576
H	-2.494688	2.478858	-5.04919
H	-0.133912	3.246766	4.377033
H	1.216997	5.024579	3.286281
H	0.822621	5.625079	0.903883
H	-2.497808	1.043204	2.4988
H	-1.268713	1.563938	5.270425
H	-0.502525	0.588315	3.969294
H	-2.073959	0.090799	4.678237
H	-4.154434	1.603815	4.283995
H	-4.083062	2.899626	3.049505
H	-3.274066	3.125675	4.630796
H	-1.671803	3.810821	-1.291187
H	-2.788393	5.858469	-0.350004
H	-2.049718	6.19795	-1.944857
H	-1.240209	6.743423	-0.442752
H	0.887786	5.533701	-1.341466
H	-0.000218	4.862789	-2.73242
H	0.841408	3.772902	-1.589674
H	3.447766	-4.885065	-0.576631
H	3.108116	-4.536888	2.172125
H	3.95787	-1.392836	-4.510196
H	1.85477	-1.771329	-5.77486
H	-0.091256	-2.880755	-4.684344
H	4.633656	-2.84932	-1.173782
H	5.890048	-2.718993	-3.371367
H	6.651281	-1.799525	-2.034019
H	5.757721	-0.934219	-3.304309
H	4.392462	0.190042	-1.514935
H	5.157853	-0.71174	-0.179419
H	3.382662	-0.73891	-0.379278
H	-0.045271	-4.040264	-1.070325

H	-1.304062	-5.787802	-2.304433
H	0.429904	-5.837505	-2.760899
H	-0.769795	-5.111721	-3.87016
H	-1.913916	-2.809417	-3.187479
H	-1.459585	-2.064903	-1.62115
H	-2.408879	-3.577998	-1.661807
H	2.002436	-0.443616	5.454225
H	-0.047218	-1.56044	6.300148
H	-1.230811	-3.252408	4.908564
H	3.209396	-0.798937	1.94132
H	4.463397	-2.726381	2.960274
H	4.666269	-1.794049	4.473856
H	5.458597	-1.242419	2.965264
H	2.60713	1.19996	3.324171
H	4.367877	1.049917	3.009878
H	3.735995	0.631956	4.61886
H	0.111362	-4.45378	1.566317
H	-2.346287	-4.273992	1.130032
H	-1.562494	-2.668559	1.142378
H	-2.521276	-3.207458	2.557184
H	-1.330058	-6.207483	2.484723
H	-1.635231	-5.273751	3.970676
H	0.008239	-5.893342	3.635948
H	5.8131	4.996853	-0.949522
H	5.716123	4.388099	-3.373658
H	4.009827	2.755938	-4.190685
H	3.233156	4.419282	1.42923
H	4.413295	3.138793	1.699455
H	4.989106	4.796089	1.308084
H	2.154608	0.469244	-2.233231
H	1.071118	1.820351	-2.538494
H	2.188369	1.273577	-3.824468

4. References

[S1] D. Franz, E. Irran, S. Inoue, *Dalton Trans.* **2014**, *43*, 4451-4461.

[S2] J. Kouvetakis, A. Haaland, D. J. Shorokhov, H. V. Volden, G. V. Girichev, V. I. Sokolov, P. Matsunaga, *J. Am. Chem. Soc.* **1998**, *120*, 6738-6744.

[S3] *APEX suite of crystallographic software*, APEX 3 version 2015.5-2; Bruker AXS Inc.: Madison, Wisconsin, USA, 2015.

[S4] *SAINT*, Version 7.56a and SADABS Version 2008/1; Bruker AXS Inc.: Madison, Wisconsin, USA, 2008.

[S5] G. M. Sheldrick, *SHELXL-2014*, University of Göttingen, Göttingen, Germany, 2014.

[S6] C. B. Hübschle, G. M. Sheldrick, B. Dittrich, *J. Appl. Cryst.* **2011**, *44*, 1281-1284.

[S7] G. M. Sheldrick, *SHELXL-97*, University of Göttingen, Göttingen, Germany, 1998.

[S8] A. J. C. Wilson, *International Tables for Crystallography*, Vol. C, Tables 6.1.1.4 (pp. 500-502), 4.2.6.8 (pp. 219-222), and 4.2.4.2 (pp. 193-199); Kluwer Academic Publishers: Dordrecht, The Netherlands, 1992.

[S9] C. F. Macrae, I. J. Bruno, J. A. Chisholm, P. R. Edgington, P. McCabe, E. Pidcock, L. Rodriguez-Monge, R. Taylor, J. van de Streek, P. A. Wood, *J. Appl. Cryst.* **2008**, *41*, 466-470.

[S10] F. Weigend, R. Ahlrichs, *Phys. Chem. Chem. Phys.* **2005**, *7*, 3297-3305.

[S11] A. D. Becke, *J. Chem. Phys.* **1997**, *107*, 8554-8560.

[S12] S. Grimme, *J. Comput. Chem.* **2006**, *27*, 1787-1799.

[S13] J.-D. Chai, M. Head-Gordon, *Phys. Chem. Chem. Phys.* **2008**, *10*, 6615-6620.

[S14] Gaussian 09, Revision B.01, M. J. Frisch, G. W. Trucks, H. B. Schlegel, G. E. Scuseria, M. A. Robb, J. R. Cheeseman, G. Scalmani, V. Barone, B. Mennucci, G. A. Petersson, H. Nakatsuji, M. Caricato, X. Li, H. P. Hratchian, A. F. Izmaylov, J. Bloino, G. Zheng, J. L. Sonnenberg, M. Hada, M. Ehara, K. Toyota, R. Fukuda, J. Hasegawa, M. Ishida, T. Nakajima, Y. Honda, O. Kitao, H. Nakai, T. Vreven, J. A. Montgomery, Jr., J. E. Peralta, F. Ogliaro, M. Bearpark, J. J. Heyd, E. Brothers, K. N. Kudin, V. N. Staroverov, R. Kobayashi, J. Normand, K. Raghavachari, A. Rendell, J. C. Burant, S. S. Iyengar, J. Tomasi, M. Cossi, N. Rega, J. M. Millam, M. Klene, J. E. Knox, J. B. Cross, V. Bakken, C. Adamo, J. Jaramillo, R. Gomperts, R. E. Stratmann, O. Yazyev, A. J. Austin, R. Cammi, C. Pomelli, J. W. Ochterski, R. L. Martin, K. Morokuma, V. G. Zakrzewski, G. A. Voth, P. Salvador, J. J. Dannenberg, S. Dapprich, A. D. Daniels, Ö. Farkas, J. B. Foresman, J. V. Ortiz, J. Cioslowski, and D. J. Fox, Gaussian, Inc., Wallingford CT, 2009.

9.2 Supporting Information for Chapter 5

Supporting Information

Isolation and Reactivity of Tetrylene-Tetrylone-Iron Complexes Supported by Bis(*N*-Heterocyclic Imine) Ligands

Xuan-Xuan Zhao,[†] *Tibor Szilvási,*[‡] *Franziska Hanusch,*[†] *John A. Kelly,*[†] *Shiori Fujimori,*[†] *and Shigeyoshi Inoue**[,†]

[†]Department of Chemistry, WACKER-Institute of Silicon Chemistry and Catalysis Research Center, Technische Universität München, Lichtenbergstraße 4, 85748 Garching bei München, Germany

[‡]Department of Chemical and Biological Engineering, University of Alabama, Tuscaloosa, AL 35487, USA

Table of Contents

1. Experimental Section

General Considerations

All experiments and manipulations were carried out under dry oxygen-free argon atmosphere using standard Schlenk techniques or in a glovebox. All glass junctions were coated with PTFE-based grease Merkel Triboflon III. All the solvents were dried and freshly distilled under Ar atmosphere prior to use by standard techniques. The ^{1}H, $^{13}C\{^{1}H\}$, $^{119}Sn\{^{1}H\}$ NMR spectra were recorded on Bruker 400 MHz spectrometer. Chemical shifts are referenced to (residual) solvent signals. Abbreviations: s = singlet, br. = broadened, d = doublet, t = triplet, m = multiplet. ATRFT-IR spectra were recorded on a Bruker Alpha FT-IR spectrometer (diamond ATR, located inside an argon-filled glovebox) in a range of 400 – 4000 cm^{-1}. UV-Vis spectra were taken on an Agilent Cary 60 spectrophotometer (Unisoku Scientific Instruments Co.). Elemental analysis (EA) was conducted with a EURO EA (HEKA tech) instrument equipped with a CHNS combustion analyzer. Liquid Injection Field Desorption Ionization Mass Spectrometry (LIFDI-MS) was measured directly from an inert atmosphere glovebox with a Thermo Fisher Scientific Exactive Plus Orbitrap equipped with an ion source from Linden CMS or recorded at a TOF LCT 700 from Waters equipped with an ion source from Linden CMS GmbH. Unless otherwise stated, all commercially available chemicals were purchased from *abcr GmbH*, *Sigma-Aldrich Chemie GmbH* or *Tokyo Chemical Industry Co., Ltd.*, and used without further purification. The starting materials IPrNLi (IPrN = bis(2,6-diisopropylphenyl)imidazolin-2-imino)[S1], $GeCl_2$•dioxane[S2], $SnCl_2$•dioxane[S3], Collman's reagent ($Na_2Fe(CO)_4$)[S4], $K[Fe(CO)_2(\eta^5\text{-}C_5H_5)]$[S5], $Li[Fe(CO)_2(\eta^5\text{-}C_5H_5)]$[S6] were prepared according to the literature procedures, respectively.

Synthetic Procedures

Synthesis of chloro(imino)germylene 1

IPrNLi (4.0 g, 9.77 mmol) dissolved in THF (200 mL) was added dropwise to a solution of $GeCl_2$•dioxane (2.26 g, 9.77 mmol, 1.0 eq.) in THF (100 mL) at room temperature. The reaction mixture was stirred for 2 h. The volatiles were removed *in vacuo* and the solid residue was dissolved in dichloromethane (DCM) and the solution was concentrated by slow evaporation of the solvent until formation of the crystalline product commenced. The crystals were separated from the liquid phase to afford colorless **1** after drying *in vacuo* (4.83 g, 97%).

^1H NMR (400 MHz, $CDCl_3$) δ = 7.25 (t, J = 7.7 Hz, 4H, Ar*H*), 7.04 (d, J = 7.7 Hz, 8H, Ar*H*), 6.29 (s, 4H, NC*H*), 3.05 – 2.96 (m, 8H, C*H*(CH_3)$_2$), 1.34 – 1.27 (m, 24H, CH(C*H*$_3$)$_2$), 1.07 – 0.98 (m, 24H, CH(C*H*$_3$)$_2$).

$^{13}C\{^1H\}$ NMR (101 MHz, $CDCl_3$) δ = 150.2 (N*C*N), 147.9 (N*C*Ar), 133.1 (Ar*C*), 130.7 (Ar*C*), 125.0 (Ar*C*), 118.1 (N*C*H), 28.2 (*C*H(CH_3)$_2$), 26.7 (CH(*C*H$_3$)$_2$), 25.8 (CH(*C*H$_3$)$_2$), 23.2 (CH(*C*H$_3$)$_2$), 22.8 (CH(*C*H$_3$)$_2$).

Anal. Calcd. [%] for $C_{54}H_{72}Cl_2Ge_2N_6$: C, 63.50; H, 7.11; N, 8.23. Found [%]: C, 63.37; H, 7.15; N, 7.98.

LIFDI-MS: calculated for $C_{54}H_{72}Cl_2Ge_2N_6$: 1022.36191. Found: 1022.35879.

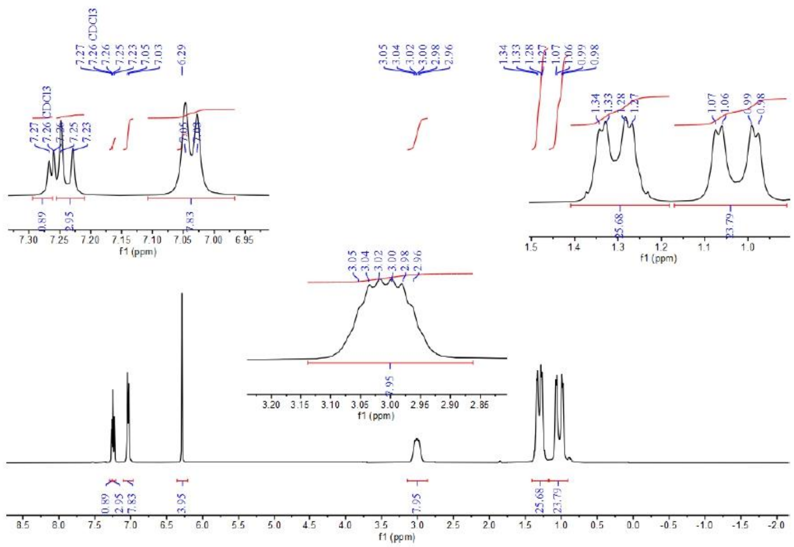

Figure S1. ^{1}H NMR spectrum of chloro(imino)germylene **1** in $CDCl_3$.

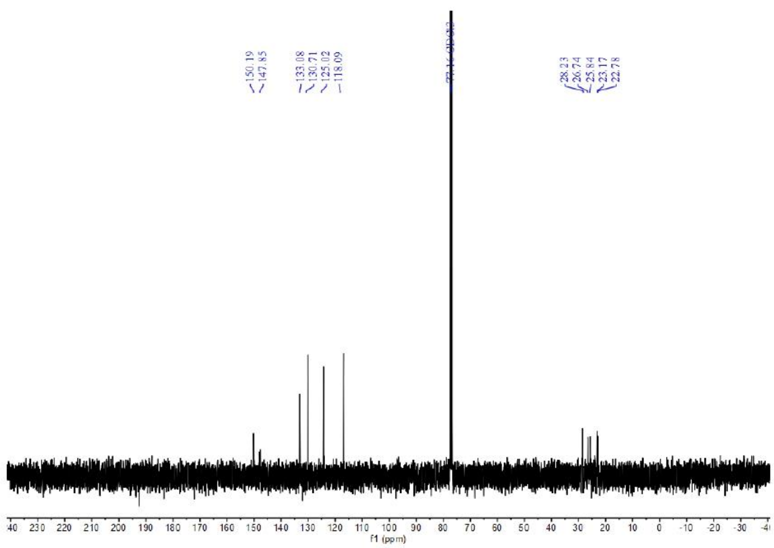

Figure S2. $^{13}C\{^{1}H\}$ NMR spectrum of chloro(imino)germylene **1** in $CDCl_3$.

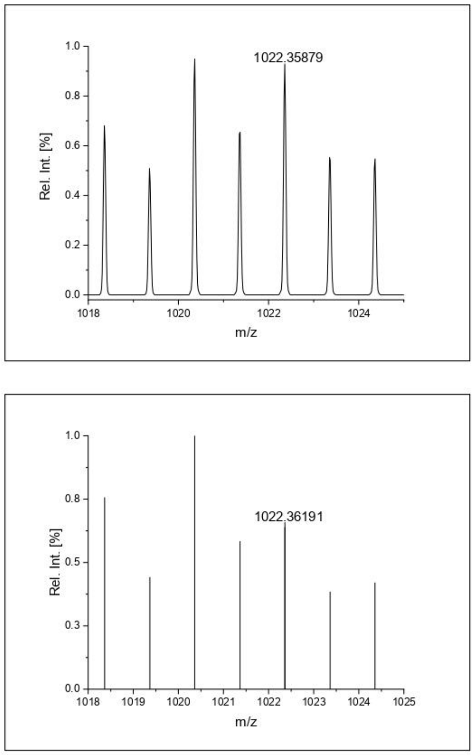

Figure S3. LIFDI-MS spectrum: expanded region of the compound signal showing the isotopic pattern of chloro(imino)germylene **1**. Measured (top) and calculated (bottom).

Synthesis of chloro(imino)stannylene 2

IPrNLi (4.0 g, 9.77 mmol) dissolved in THF (200 mL) was added dropwise to a solution of $SnCl_2$•dioxane (2.71 g, 9.77 mmol, 1.0 eq.) in THF (100 mL) at room temperature. The reaction mixture was stirred for 2 h. The volatiles were removed *in vacuo* and the solid residue was dissolved in DCM and the solution was concentrated by slow evaporation of the solvent until formation of the crystalline product commenced. The crystals were separated from the liquid phase to afford colorless **2** after drying *in vacuo* (3.65 g, 67%).

^{1}H NMR (400 MHz, $CDCl_3$) δ = 7.24 (t, J = 7.7 Hz, 4H, Ar<u>*H*</u>), 7.10 – 7.07 (m, 8H, Ar<u>*H*</u>), 6.25 (s, 4H, NC<u>*H*</u>), 3.06 (septet, J = 6.8 Hz, 4H, C<u>*H*</u>(CH_3)$_2$), 2.99 (septet, J = 6.8 Hz, 4H, C<u>*H*</u>(CH_3)$_2$), 3.10 – 2.96 (m, 8H, C<u>*H*</u>(CH_3)$_2$), 1.36 (d, J = 6.8 Hz, 12H, CH(C<u>*H*</u>$_3$)$_2$), 1.32 (d, J = 6.8 Hz, 12H, CH(C<u>*H*</u>$_3$)$_2$), 1.09 (d, J = 6.8 Hz, 12H, CH(C<u>*H*</u>$_3$)$_2$), 1.00 (d, J = 6.8 Hz, 12H, CH(C<u>*H*</u>$_3$)$_2$).

$^{13}C\{^{1}H\}$ NMR (101 MHz, $CDCl_3$) δ = 148.3 (N<u>*C*</u>N),133.5 (Ar<u>*C*</u>), 130.2 (Ar<u>*C*</u>), 124.9 (Ar<u>*C*</u>), 124.8 (Ar<u>*C*</u>), 116.0 (N<u>*C*</u>H), 28.5 (<u>*C*</u>H(CH_3)$_2$), 26.5 (CH(<u>*C*</u>H$_3$)$_2$), 25.4 (CH(<u>*C*</u>H$_3$)$_2$), 23.3 (CH(<u>*C*</u>H$_3$)$_2$), 23.1 (CH(<u>*C*</u>H$_3$)$_2$).

$^{119}Sn\{^{1}H\}$ NMR (149 MHz, $CDCl_3$) δ = 133.1.

Anal. Calcd. [%] for $C_{54}H_{72}Cl_2N_6Sn_2$: C, 58.25; H, 6.52; N, 7.55. Found [%]: C, 58.13; H, 6.56; N, 7.32.

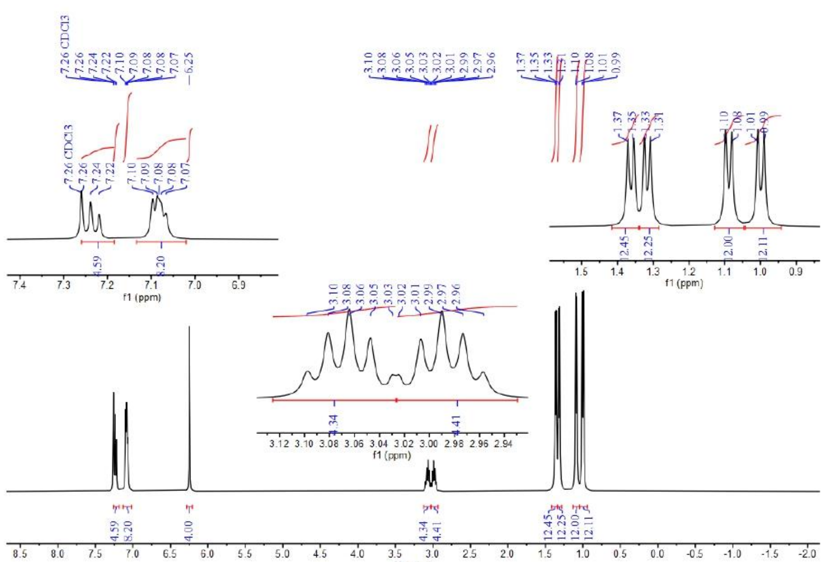

Figure S4. ^{1}H NMR spectrum of chloro(imino)stannylene **2** in $CDCl_3$.

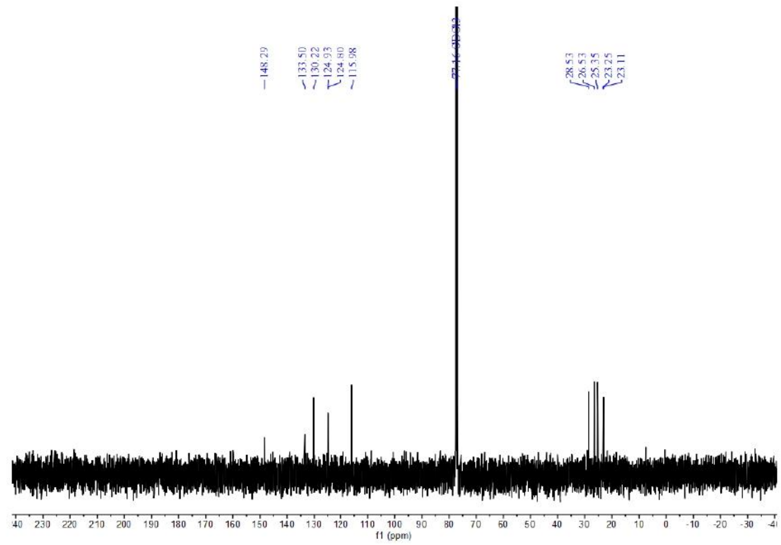

Figure S5. $^{13}C\{^1H\}$ NMR spectrum of chloro(imino)stannylene **2** in $CDCl_3$.

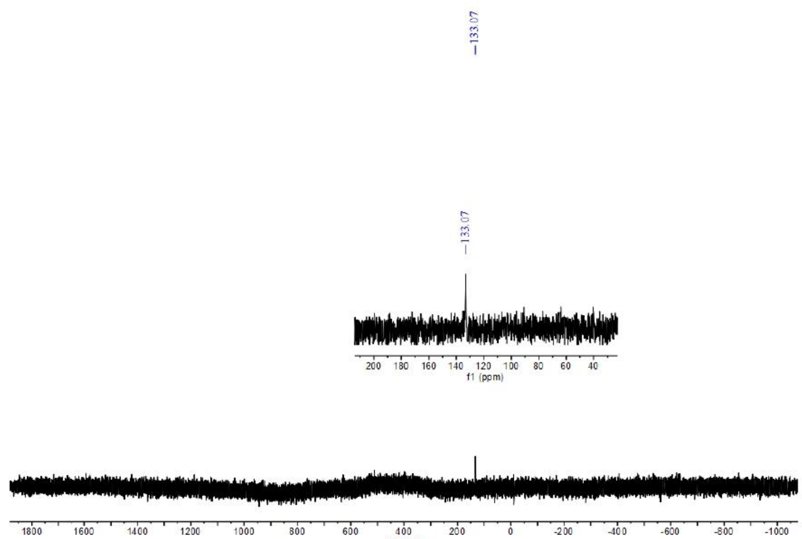

Figure S6. $^{119}Sn\{^1H\}$ NMR spectrum of chloro(imino)stannylene **2** in $CDCl_3$.

S7

Synthesis of compound 3

A THF solution of $Na_2Fe(CO)_4$ (42 mg, 196 µmol, 1.0 eq.), which was prepared from the reaction of $Fe(CO)_5$ (196 µmol) with 2 equiv. of $NaC_{10}H_8$ in a solution of THF (10 mL), was added dropwise to a suspension of **1** (200 mg, 196 µmol, 1.0 eq.) in THF (15 mL) at room temperature. The reaction mixture was stirred for 12 h. The solvent was removed *in vacuo* and the solid residue was extracted with toluene (10 mL × 3). After filtration, the solvent was removed from the filtrate *in vacuo* to afford an orange crude solid, and **3** was obtained as red crystals from a recrystallization of the remaining solid from Et_2O at -30 °C (180 mg, 82%).

^{1}H NMR (400 MHz, C_6D_6) δ = 7.24 (t, J = 7.7 Hz, 4H, Ar$\underline{H}$), 7.06 (d, J = 7.7 Hz, 8H, Ar$\underline{H}$), 5.92 (s, 4H, NC$\underline{H}$), 3.22 (br. s, 8H, C$\underline{H}$(CH_3)$_2$), 1.32 (d, J = 6.8 Hz, 24H, CH(C$\underline{H}_3$)$_2$), 1.00 (d, J = 6.8 Hz, 24H, CH(C$\underline{H}_3$)$_2$).

^{13}C{^{1}H} NMR (101 MHz, C_6D_6) δ = 217.7 ($\underline{C}$O), 148.2 (N$\underline{C}$N), 145.5 (N$\underline{C}$Ar), 132.8 (Ar$\underline{C}$), 130.3 (Ar$\underline{C}$), 124.7 (Ar$\underline{C}$), 116.6 (N$\underline{C}$H), 28.4 ($\underline{C}$H(CH_3)$_2$), 26.1 (CH($\underline{C}H_3$)$_2$), 23.2 (CH($\underline{C}H_3$)$_2$).

IR in the solid state: *v*(CO) = 1975, 1909, 1877, and 1862 cm^{-1}.

IR in toluene: *v*(CO) = 2022, 1998, 1919 and 1881 cm^{-1}.

Anal. Calcd. [%] for $C_{58}H_{72}FeGe_2N_6O_4$: C, 62.29; H, 6.49; N, 7.51. Found [%]: C, 61.76; H, 6.39; N, 7.11.

LIFDI-MS: calculated for $C_{58}H_{72}FeGe_2N_6O_4$: 1120.33880. Found: 1120.33636.

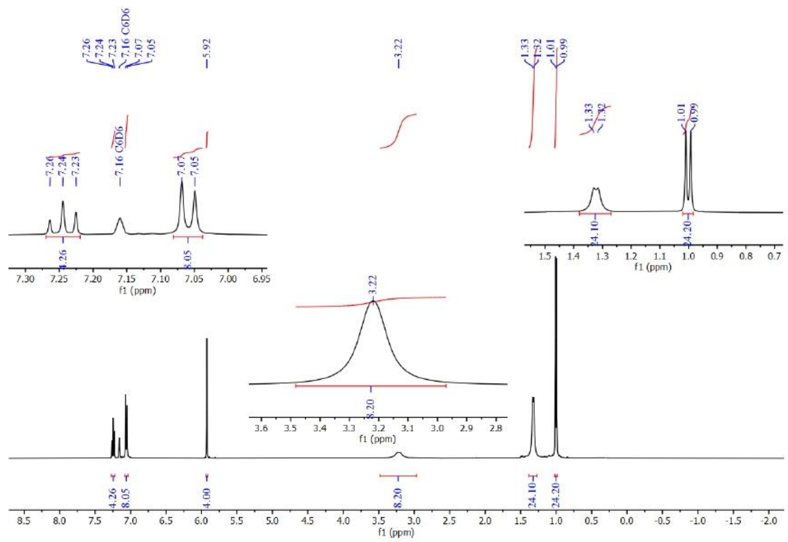

Figure S7. ^{1}H NMR spectrum of compound **3** in C_6D_6.

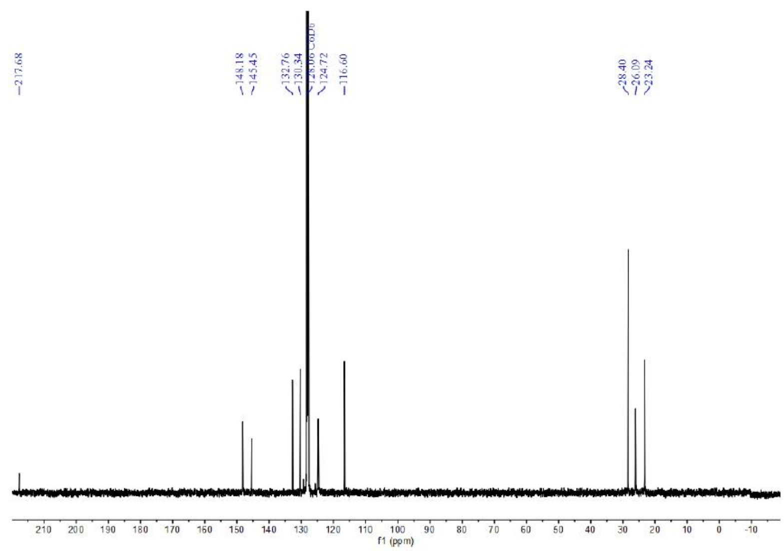

Figure S8. $^{13}C\{^{1}H\}$ NMR spectrum of compound **3** in C_6D_6.

S9

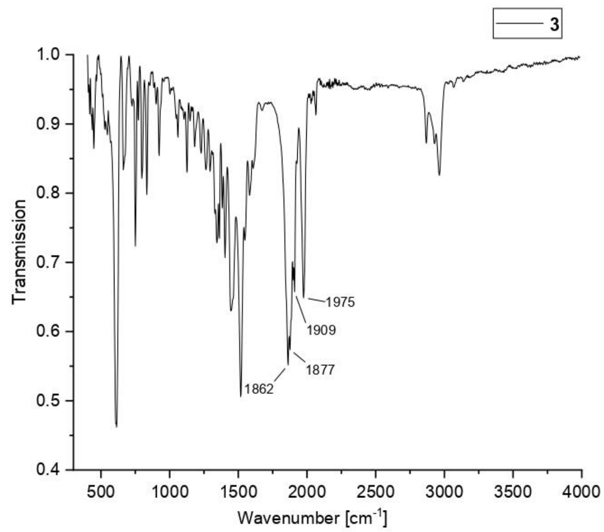

Figure S9. IR spectrum of compound **3** in the solid state.

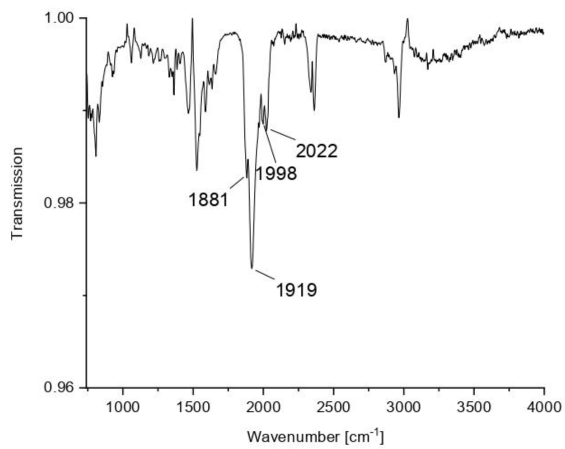

Figure S10. IR spectrum of compound **3** in toluene (5.0×10^{-3} M).

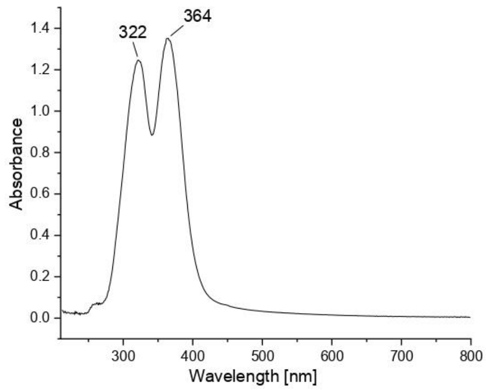

Figure S11. UV-Vis spectrum of compound **3** (THF, 2.0 × 10^{-4} M).

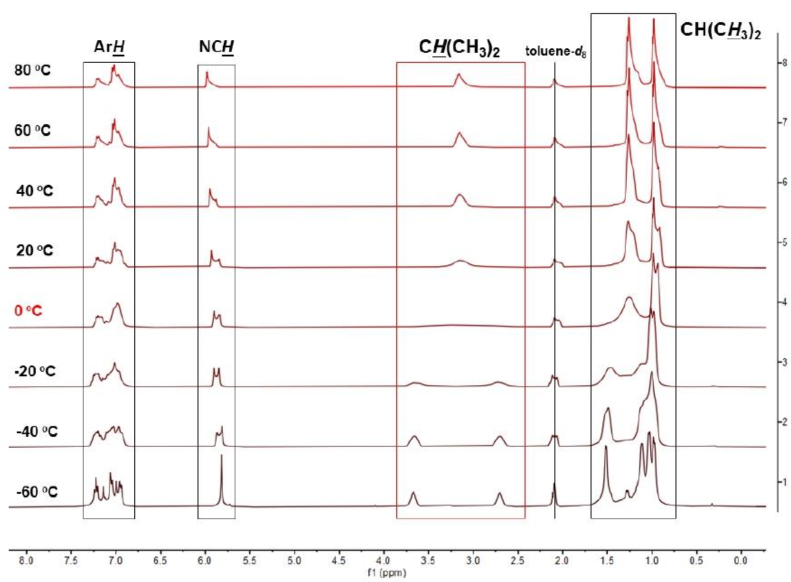

Figure S12. A stacked plot of variable temperature (VT) ^{1}H NMR spectra of compound **3** in toluene-d_8 from -60 °C to +80 °C.

Kinetic study for compound 3

Calculations of the exchange rates (k, s^{-1}) were performed by line shape analysis (LSA)[S7] of the experimental ^{1}H NMR signals of the isopropyl methine protons; the enthalpic ($\Delta H^‡$) and entropic ($\Delta S^‡$) contributions to the transition state of $\Delta H^‡$ and $\Delta S^‡$ were derived from Eyring plot.[S8] The value of $\Delta G^‡$ at 273 K was also calculated.

Table S1. The temperatures (K) and calculated exchange rate constants (k, s^{-1}).

T/K	213	233	253	273	293	313	333	353
k/s^{-1}	8	59	200	844	4029	8722	29529	70310

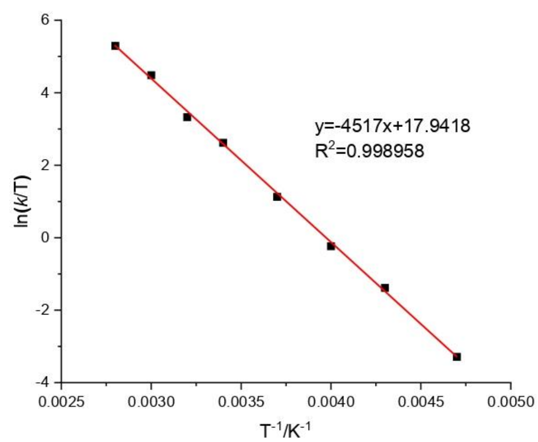

Figure S13. Eyring plot of ln(k/T) against 1/T with linear regression (y=-4517x+17.9418).

$\Delta H^‡$ = -aR = -(-4517×1.9872×10^{-3}) kcal mol^{-1} = 8.98 kcal mol^{-1}

$\Delta S^‡$ = R[b-(k_B/h)] = 1.9872×(17.9418-23.7600) cal mol^{-1}K^{-1} = -11.56 cal mol^{-1}K^{-1}

$\Delta G^‡$ = $\Delta H^‡$-T$\Delta S^‡$ = 8.98-273×(-11.56×10^{-3}) kcal mol^{-1} = 12.14 kcal mol^{-1}

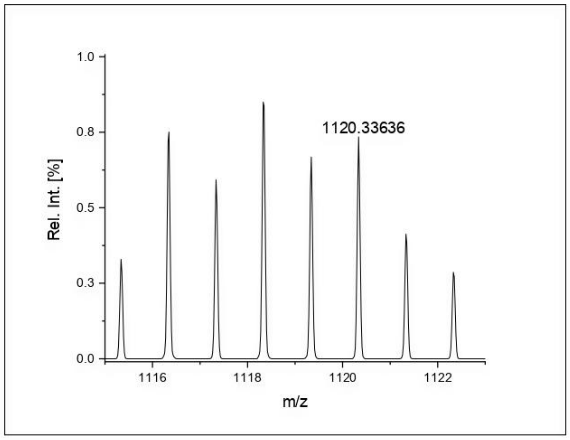

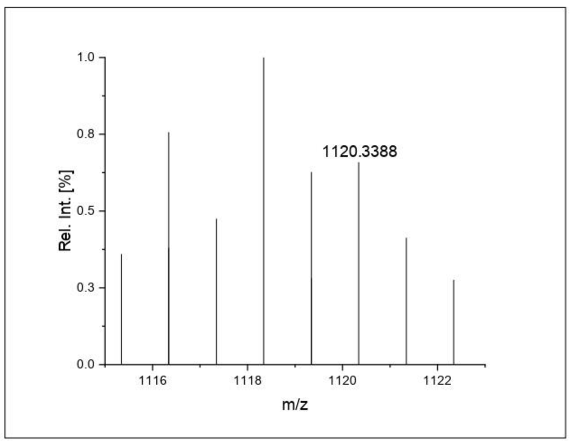

Figure S14. LIFDI-MS spectrum: expanded region of the compound signal showing the isotopic pattern of compound **3**. Measured (top) and calculated (bottom).

Synthesis of compound 4

A THF solution of $Na_2Fe(CO)_4$ (38 mg, 180 µmol, 1.0 eq.), which was prepared from the reaction of $Fe(CO)_5$ (180 µmol) with 2 equiv. of $NaC_{10}H_8$ in a solution of THF (10 mL), was added dropwise to a suspension of **2** (200 mg, 180 µmol, 1.0 eq.) in THF (15 mL) at room temperature. The reaction mixture was stirred for 12 h. The solvent was removed *in vacuo* and the solid residue was extracted with toluene (10 mL × 3). After filtration, the solvent was removed from the filtrate *in vacuo* to afford an orange crude solid, and **4** was obtained as red crystals from a recrystallization of the remaining solid from Et_2O at -30 °C (161 mg, 74%).

^{1}H NMR (400 MHz, C_6D_6) δ = 7.22 (t, J = 7.7 Hz, 4H, Ar*H*), 7.13 – 7.01 (m, 8H, Ar*H*), 5.98 (s, 4H, NC*H*), 3.65 (br. s, 4H, C*H*(CH_3)$_2$), 2.89 (br. s, 4H, C*H*(CH_3)$_2$), 1.54 – 1.49 (m, 12H, CH(C*H*$_3$)$_2$), 1.26 – 1.24 (m, 12H, CH(C*H*$_3$)$_2$), 1.07 – 0.95 (m, 24H, CH(C*H*$_3$)$_2$).

^{13}C{^{1}H} NMR (101 MHz, C_6D_6) δ = 216.9 (*C*O), 148.9 (N*C*N), 148.4 (N*C*Ar), 146.9 (N*C*Ar), 133.0 (Ar*C*), 130.1 (Ar*C*), 129.3 (Ar*C*), 125.7 (Ar*C*), 124.2 (Ar*C*), 115.6 (N*C*H), 28.6 (*C*H(CH_3)$_2$), 28.1 (*C*H(CH_3)$_2$), 26.8 (CH(*C*H$_3$)$_2$), 25.4 (CH(*C*H$_3$)$_2$), 23.8 (CH(*C*H$_3$)$_2$), 22.9 (CH(*C*H$_3$)$_2$).

^{119}Sn{^{1}H} NMR (149 MHz, C_6D_6) δ = 357.3.

IR in the solid state: *ν*(CO) = 1976, 1899, and 1870 cm^{-1}.

IR in toluene: *ν*(CO) = 2025, 1985 and 1917 cm^{-1}.

Anal. Calcd. [%] for $C_{58}H_{72}FeN_6O_4Sn_2$: C, 57.55; H, 6.00; N, 6.94. Found [%]: C, 57.43; H, 6.03; N, 6.73.

LIFDI-MS: calculated for $C_{58}H_{72}FeN_6O_4Sn_2$: 1212.30084. Found: 1212.29963.

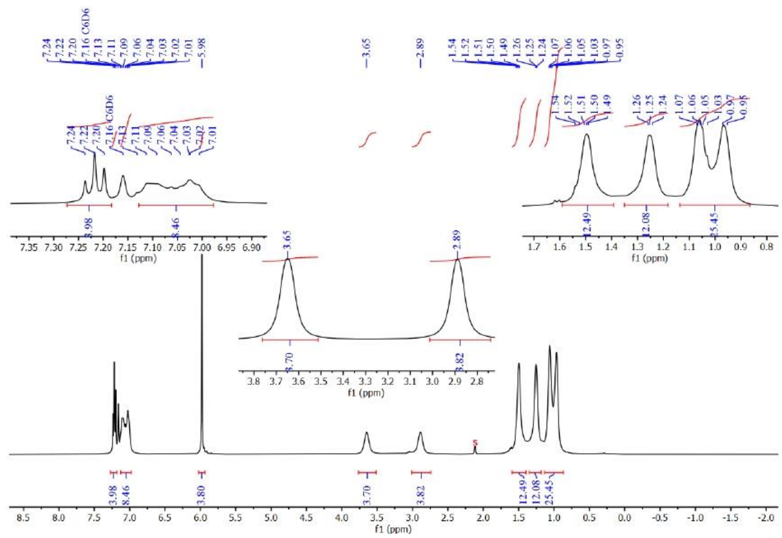

Figure S15. ^{1}H NMR spectrum of compound **4** in C_6D_6. The resonances of residual toluene are marked with an S.

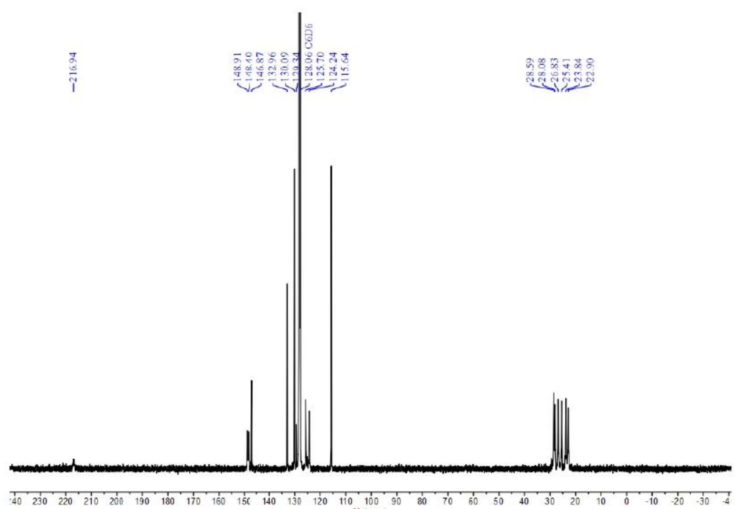

Figure S16. $^{13}C\{^{1}H\}$ NMR spectrum of compound **4** in C_6D_6.

S15

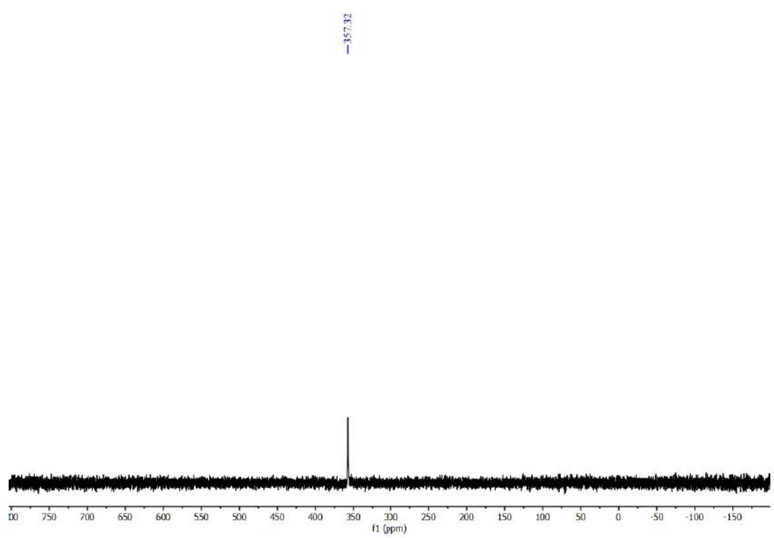

Figure S17. $^{119}Sn\{^1H\}$ NMR spectrum of compound **4** in C_6D_6.

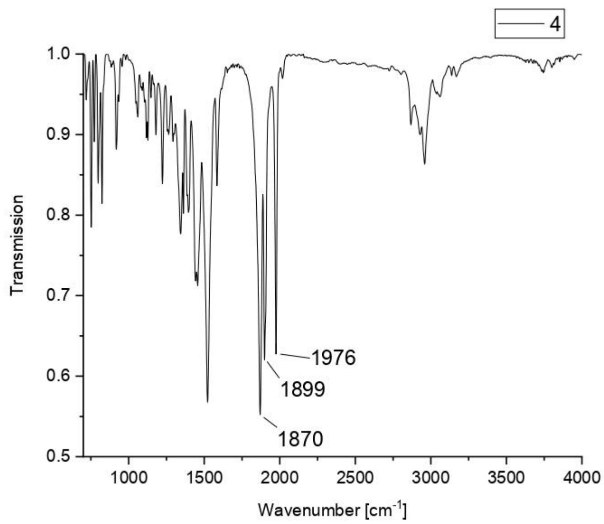

Figure S18. IR spectrum of compound **4** in the solid state.

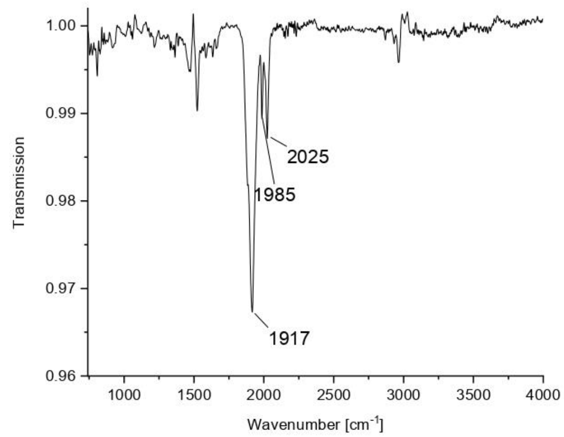

Figure S19. IR spectrum of compound **4** in toluene (5.0×10^{-3} M).

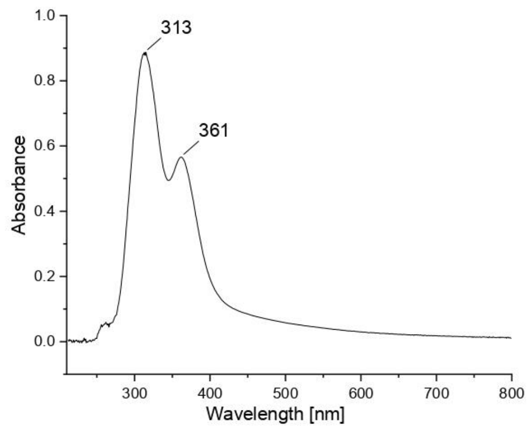

Figure S20. UV-Vis spectrum of compound **4** (THF, 2.0×10^{-4} M).

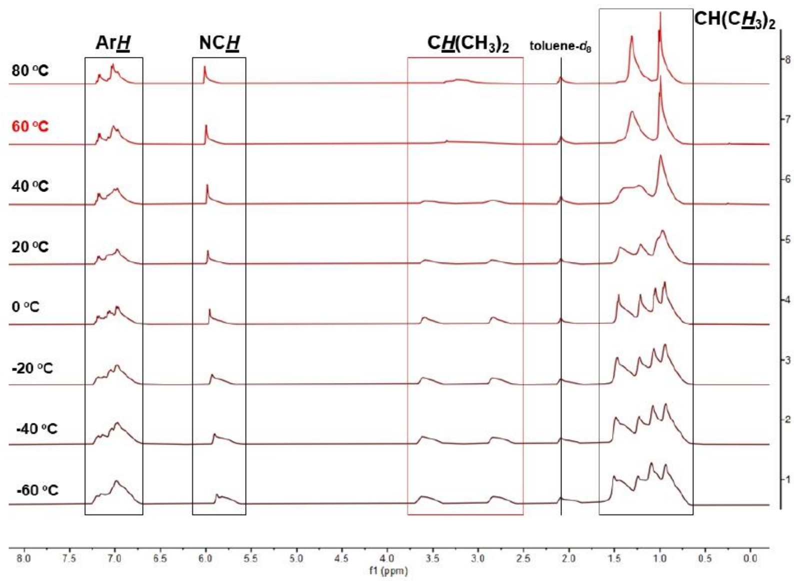

Figure S21. A stacked plot of variable temperature (VT) ^{1}H NMR spectra of compound **4** in toluene-d_8 from -60 °C to +80 °C.

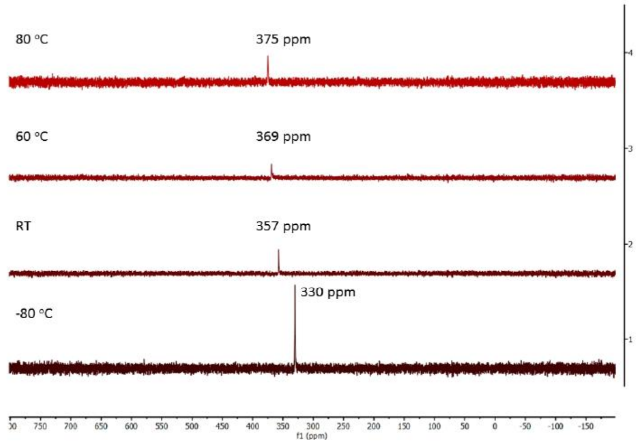

Figure S22. A stacked plot of variable temperature (VT) ^{119}Sn NMR spectra of compound **4** in toluene-d_8 from -80 °C to +80 °C.

Kinetic study for compound 4

Calculations of the exchange rates (k, s^{-1}) were performed by line shape analysis (LSA)[S7] of the experimental ^{1}H NMR signals of the isopropyl methine protons; the enthalpic ($\Delta H^‡$) and entropic ($\Delta S^‡$) contributions to the transition state of $\Delta H^‡$ and $\Delta S^‡$ were derived from Eyring plot.[S8] The value of $\Delta G^‡$ at 333 K was also calculated.

Table S2. The temperatures (K) and calculated exchange rate constants (k, s^{-1}).

T/K	213	233	253	273	293	313	333	353
k/s^{-1}	6	55	230	1115	6700	17345	58004	153559

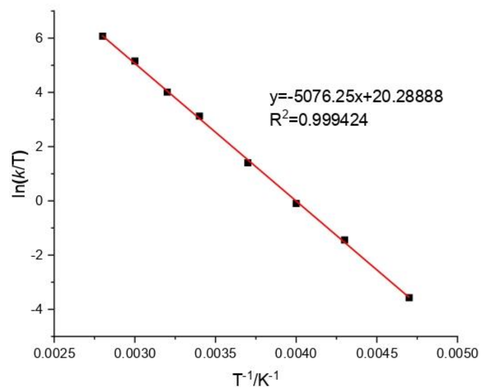

Figure S23. Eyring plot of ln(*k*/T) against 1/T with linear regression (y=-5076.25x+20.28888).

$\Delta H^{\ddagger}$ = -aR = -(-5076.25×1.9872×10^{-3}) kcal mol^{-1} = 10.09 kcal mol^{-1}

$\Delta S^{\ddagger}$ = R[b-(k_B/h)] = 1.9872×(20.28888-23.7600) cal mol^{-1}K^{-1} = -6.90 cal mol^{-1}K^{-1}

$\Delta G^{\ddagger}$ = $\Delta H^{\ddagger}$-T$\Delta S^{\ddagger}$ = 10.09-333×(-6.90×10^{-3}) kcal mol^{-1} = 12.39 kcal mol^{-1}

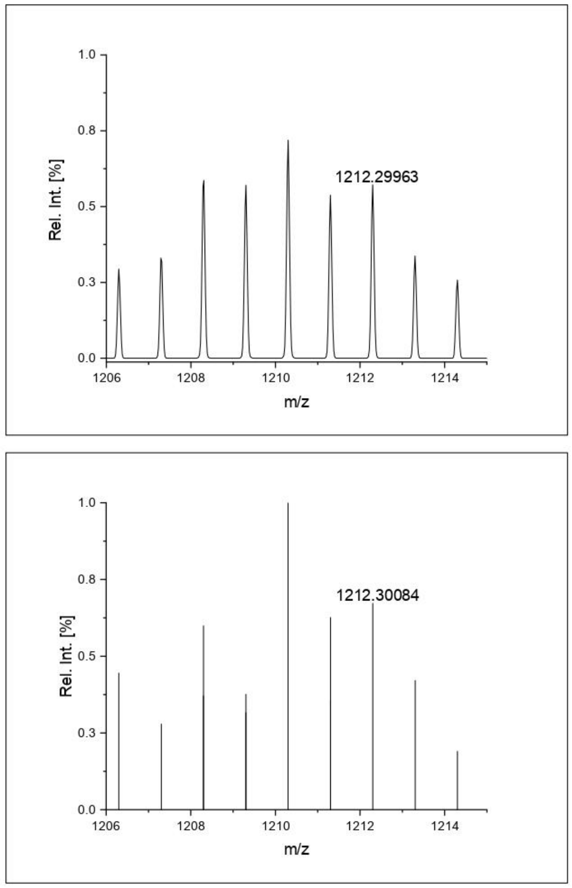

Figure S24. LIFDI-MS spectrum: expanded region of the compound signal showing the isotopic pattern of compound **4**. Measured (top) and calculated (bottom).

Synthesis of compound 7

$GaCl_3$ (16 mg, 90 µmol, 2.0 eq.) dissolved in benzene (2 mL) was added dropwise to a solution of **3** (50 mg, 45 µmol, 1.0 eq.) in benzene (4 mL) at room temperature. The reaction mixture was stirred for 2 h. The solvent was removed *in vacuo* and the solid residue was washed with toluene (3 mL × 3) and dried *in vacuo* to give pure **7** (46 mg, 86%) as an orange powder. Yellow crystals of **7** suitable for single crystal X-ray analysis were obtained in a saturated fluorobenzene solution at –30°C for several days.

^1H NMR (400 MHz, CD_3CN) δ = 7.56 (t, J = 7.7 Hz, 4H, Ar$\underline{H}$), 7.33 (d, J = 7.7 Hz, 8H, Ar$\underline{H}$), 7.12 (s, 4H, NC$\underline{H}$), 2.41 (septet, J = 6.8 Hz, 8H, C$\underline{H}(CH_3)_2$), 1.14 (d, J = 6.8 Hz, 24H, $CH(C\underline{H}_3)_2$), 1.10 (d, J = 6.8 Hz, 24H, $CH(C\underline{H}_3)_2$).

$^{13}C\{^1H\}$ NMR (101 MHz, CD_3CN) δ = 150.1 (N$\underline{C}$N), 147.5 (N$\underline{C}$Ar), 133.6 (N$\underline{C}$Ar), 131.3 (N$\underline{C}$Ar), 126.9 (Ar$\underline{C}$), 120.6 (Ar$\underline{C}$), 29.9 ($\underline{C}H(CH_3)_2$), 25.4 ($CH(\underline{C}H_3)_2$), 23.0 ($CH(\underline{C}H_3)_2$).

Anal. Calcd. [%] for $C_{54}H_{72}Cl_5GaGe_2N_6$: C, 54.16; H, 6.06; N, 7.02. Found [%]: C, 54.10; H, 6.15; N, 6.95.

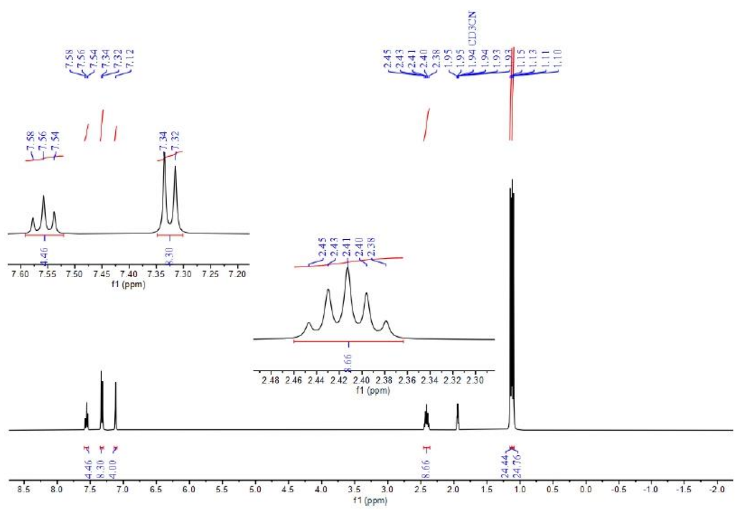

Figure S25. ^1H NMR spectrum of compound **7** in CD_3CN.

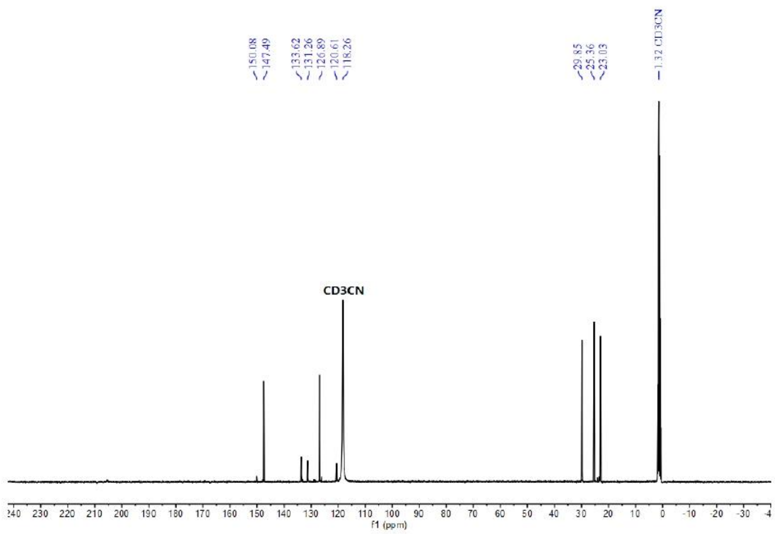

Figure S26. $^{13}C\{^1H\}$ NMR spectrum of compound **7** in CD_3CN.

Synthesis of compound 8

$GaCl_3$ (15 mg, 82 µmol, 2.0 eq.) dissolved in benzene (2 mL) was added dropwise to a solution of **4** (50 mg, 41 µmol, 1.0 eq.) in benzene (4 mL) at room temperature. The reaction mixture was stirred for 2 h. The solvent was removed *in vacuo* and the solid residue was washed with toluene (3 mL × 3) and dried *in vacuo* to give pure **8** (48 mg, 89%) as an orange powder. Crystals of **8** suitable for single crystal X-ray analysis were obtained in a saturated fluorobenzene solution at –30°C for several days.

^1H NMR (400 MHz, CD_3CN) δ = 7.45 (t, J = 7.7 Hz, 4H, Ar*H*), 7.29 (d, J = 7.7 Hz, 8H, Ar*H*), 6.89 (s, 4H, NC*H*), 2.62 (septet, J = 6.8 Hz, 8H, C*H*(CH_3)$_2$), 1.18 (d, J = 6.8 Hz, 24H, CH(C*H*$_3$)$_2$), 1.11 (d, J = 6.8 Hz, 24H, CH(C*H*$_3$)$_2$).

$^{13}C\{^1H\}$ NMR (101 MHz, CD_3CN) δ = 152.3 (N*C*N), 148.4 (N*C*Ar), 132.9 (Ar*C*), 132.6 (Ar*C*), 127.2 (Ar*C*), 29.7 (*C*H(CH_3)$_2$), 25.3 (CH(*C*H$_3$)$_2$), 23.4 (CH(*C*H$_3$)$_2$).

$^{119}Sn\{^1H\}$ NMR (149 MHz, THF-d_8) δ = 139.6.

Anal. Calcd. [%] for $C_{54}H_{72}Cl_5GaN_6Sn_2$: C, 50.29; H, 5.63; N, 6.52. Found [%]: C, 50.22; H, 5.75; N, 6.47.

LIFDI-MS (positive ion mode): calculated for $[M\text{-}GaCl_4]^+$: 1079.3551 Found: 1079.0481.

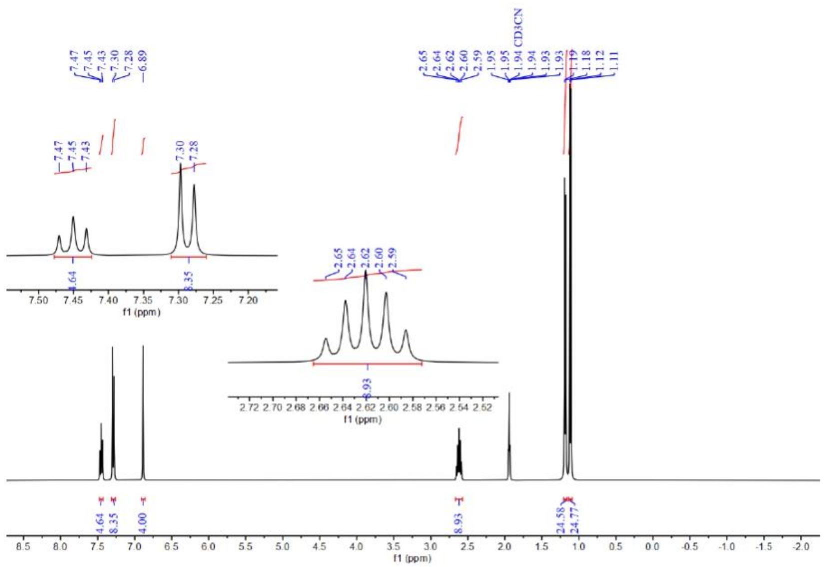

Figure S27. ^1H NMR spectrum of compound **8** in CD_3CN.

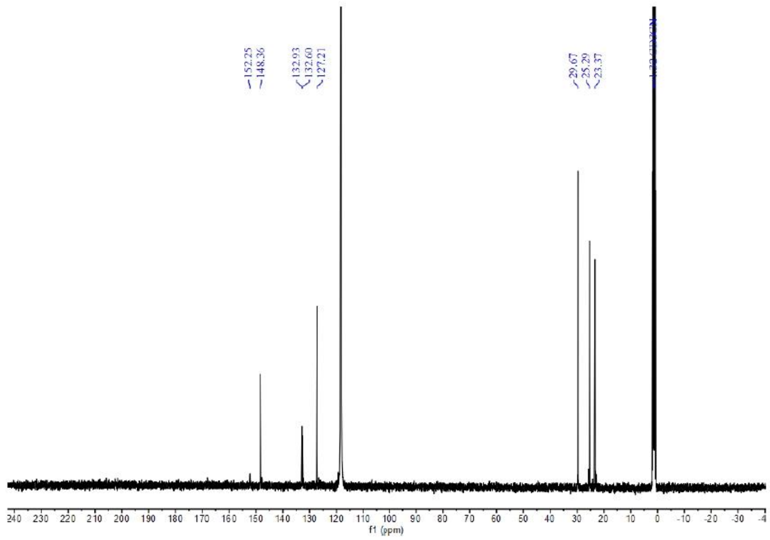

Figure S28. $^{13}C\{^1H\}$ NMR spectrum of compound **8** in CD_3CN.

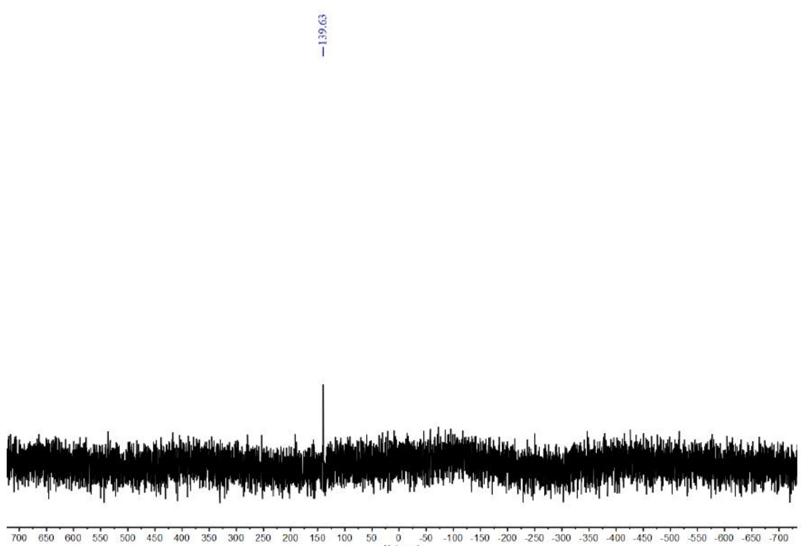

Figure S29. $^{119}Sn\{^1H\}$ NMR spectrum of compound **8** in THF-d_8.

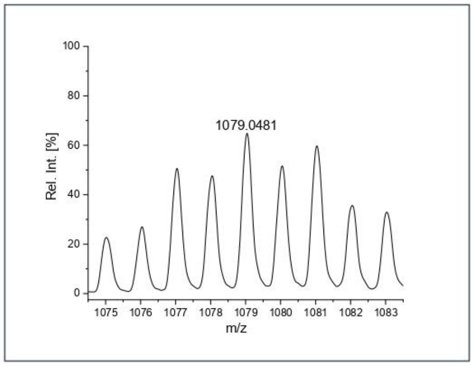

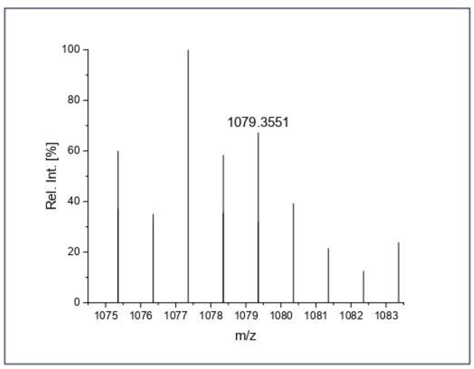

Figure S30. LIFDI-MS spectrum: expanded region of the compound signal showing the isotopic pattern of compound **8**. Measured (top) and calculated (bottom).

Synthesis of compound D

IPrNLi (78 mg, 190 µmol, 1.0 eq.) dissolved in THF (5 mL) was added dropwise to a solution of $GeCl_2$•dioxane (44 mg, 190 µmol, 1.0 eq.) in THF (2 mL) at room temperature.

The reaction mixture was stirred for 2 h. Then the solution of K[Fe(CO)$_2$(η^5-C_5H_5)] (FpK) (62 mg, 285 µmol, 1.5 eq.) in THF (2 mL) was gradually added. The reaction mixture was stirred for 12 h at room temperature. The solvent was removed *in vacuo* and the solid residue was extracted with toluene (2 mL × 3). After filtration, the solvent was removed from the filtrate *in vacuo* to afford **D** as an orange solid (52 mg, 62%). The ^{1}H NMR spectrum of **D** is identical to that reported in the literature.[S9]

Synthesis of compound 11

5 mL toluene was added to a flask containing **2** (300 mg, 0.27 mmol) and freshly prepared potassium graphite (KC_8) (73 mg, 0.54 mmol, 2.0 eq.) at room temperature with vigorous stirring. Gradually the solution turned dark orange and the stirring was continued for 24h at RT. The resulted solution was filtered, and the solid residue was extracted with toluene (2 mL × 3). After filtration, the solvent was removed from the filtrate *in vacuo* to afford **11** as a yellow solid (200 mg, 80%).

^{1}H NMR (400 MHz, C_6D_6) δ = 7.24 (t, J = 7.7 Hz, 4H, Ar*H*), 7.12 (d, J = 7.7 Hz, 8H, Ar*H*), 5.98 (s, 4H, NC*H*), 3.14 (septet, J = 6.8 Hz, 8H, C*H*(CH$_3$)$_2$), 1.19 (d, J = 6.8 Hz, 24H, CH(C*H*$_3$)$_2$), 1.18 (d, J = 6.8 Hz, 24H, CH(C*H*$_3$)$_2$).

^{13}C{^{1}H} NMR (101 MHz, C_6D_6) δ = 154.6 (N*C*N), 148.8 (N*C*Ar), 148.5 (N*C*Ar), 135.1 (Ar*C*), 129.0 (Ar*C*), 124.2 (Ar*C*), 113.2 (N*C*H), 28.9 (*C*H(CH$_3$)$_2$), 24.5 (CH(*C*H$_3$)$_2$), 24.0 (CH(*C*H$_3$)$_2$), 23.6 (CH(*C*H$_3$)$_2$).

^{119}Sn{^{1}H} NMR (149 MHz, C_6D_6) δ = 459.2.

Anal. Calcd. [%] for $C_{54}H_{72}N_6Sn$: C, 70.20; H, 7.86; N, 9.10. Found [%]: C, 70.12; H, 7.64; N, 9.08.

LIFDI-MS: Due to decomposition, compound **11** was not observed in the mass spectrum.

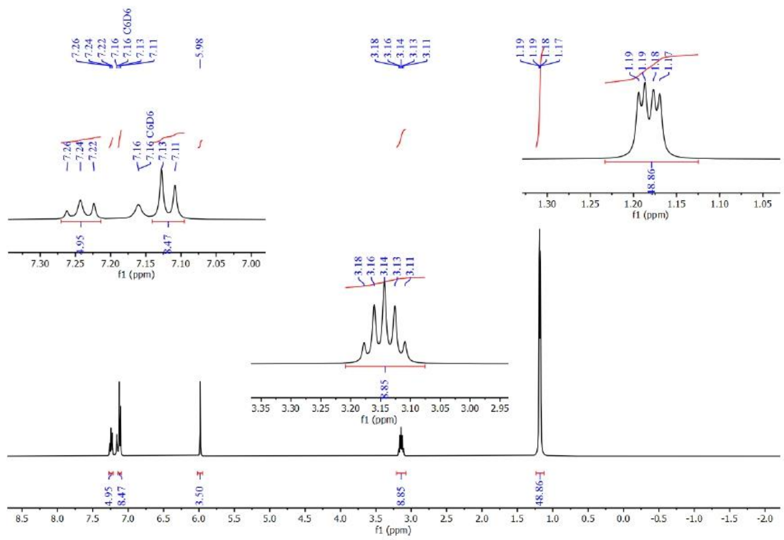

Figure S31. [1]H NMR spectrum of compound **11** in C_6D_6.

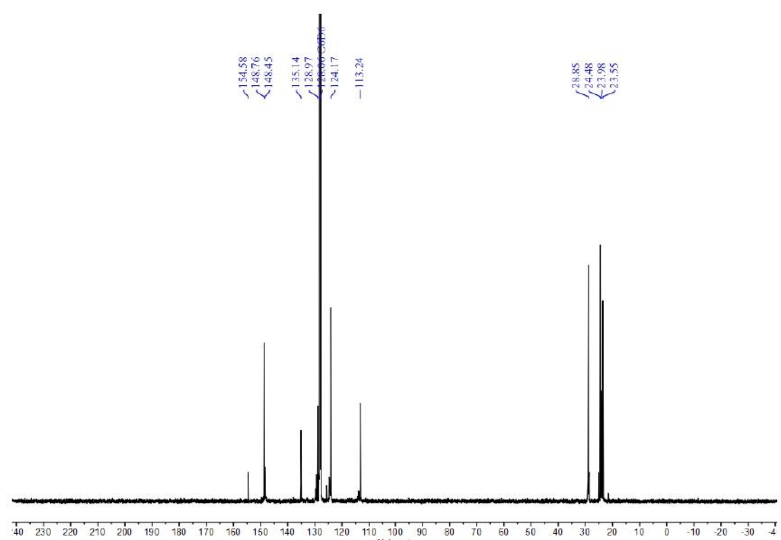

Figure S32. $^{13}C\{^1H\}$ NMR spectrum of compound **11** in C_6D_6.

S28

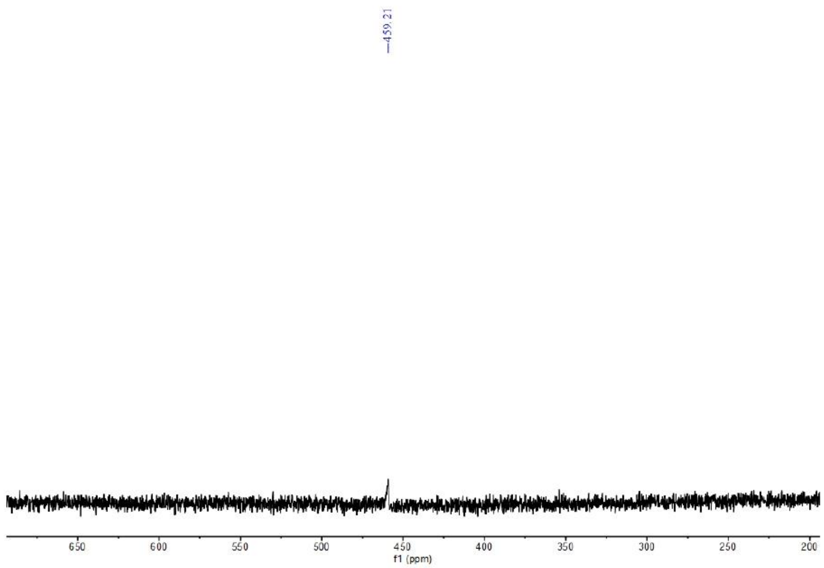

Figure S33. $^{119}Sn\{^1H\}$ NMR spectrum of compound **11** in C_6D_6.

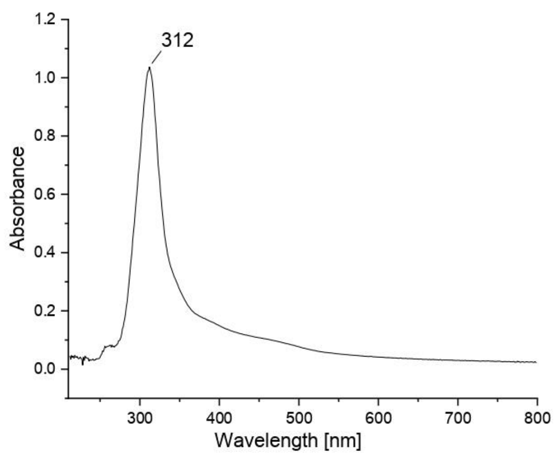

Figure S34. UV-Vis spectrum of compound **11** (THF, 1.0×10^{-3} M).

Synthesis of compound 12

IPrNLi (190 mg, 463 μmol, 1.0 eq.) dissolved in THF (10 mL) was added dropwise to a solution of $SnCl_2$•dioxane (129 mg, 463 μmol, 1.0 eq.) in THF (5 mL) at room temperature. The reaction mixture was stirred for 2 h. Then the solution of FpK (150 mg, 695 μmol, 1.5 eq.) in THF (5 mL) was gradually added. The reaction mixture was stirred for 12 h at room temperature. The solvent was removed *in vacuo* and the solid residue was extracted with toluene (5 mL × 3). After filtration, the solvent was removed from the filtrate *in vacuo* to afford **12** as a dark-red solid (154 mg, 60%). Crystals suitable for X-ray crystallography were obtained by cooling (-30 °C) a saturated solution of **12** in Et_2O.

^{1}H NMR (400 MHz, C_6D_6) δ = 7.22 – 7.17 (m, 4H, Ar$\underline{H}$), 7.09 (d, J = 7.7 Hz, 8H, Ar$\underline{H}$), 5.95 (s, 4H, NC$\underline{H}$), 3.96 (s, 5H, η^5-$C_5\underline{H}_5$), 3.51 (br. s, 4H, C$\underline{H}$(CH_3)$_2$), 3.00 (br. s, 4H, C$\underline{H}$(CH_3)$_2$), 1.42 – 1.32 (m, 24H, CH(C$\underline{H}_3$)$_2$), 1.15 (d, J = 6.8 Hz, 24H, CH(C$\underline{H}_3$)$_2$).

^{13}C{^{1}H} NMR (101 MHz, C_6D_6) δ = 222.6 ($\underline{C}$O), 154.9 (N$\underline{C}$N), 148.8 (N$\underline{C}$Ar), 144.8 (N$\underline{C}$Ar), 136.2 (Ar$\underline{C}$), 129.0 (Ar$\underline{C}$), 128.6 (Ar$\underline{C}$), 125.1 (Ar$\underline{C}$), 124.7 (Ar$\underline{C}$), 124.1 (Ar$\underline{C}$), 114.5 (N$\underline{C}$H), 83.2 (η^5-$\underline{C}_5H_5$), 29.0 ($\underline{C}$H(CH_3)$_2$), 28.5 ($\underline{C}$H(CH_3)$_2$), 25.6 (CH($\underline{C}H_3$)$_2$), 24.0 (CH($\underline{C}H_3$)$_2$), 22.3 (CH($\underline{C}H_3$)$_2$).

^{119}Sn{^{1}H} NMR (149 MHz, C_6D_6) δ = 314.0.

IR: ν(CO) = 2006 and 1925 cm^{-1}.

Anal. Calcd. [%] for $C_{61}H_{77}FeLiN_6O_2Sn$: C, 66.14; H, 7.01; N, 7.59. Found [%]: C, 66.00; H, 7.05; N, 7.36.

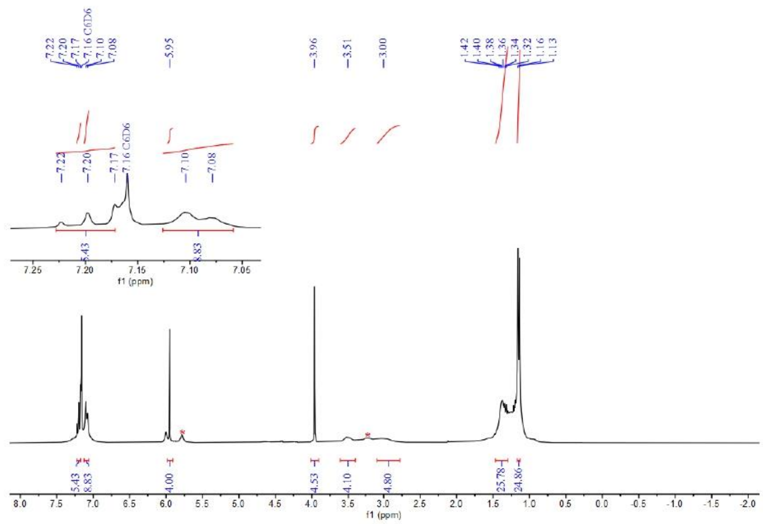

Figure S35. ^{1}H NMR spectrum of compound **12** in C_6D_6. The resonances of IPrNH, resulting from minor complex decomposition in solution, are marked with asterisks*.

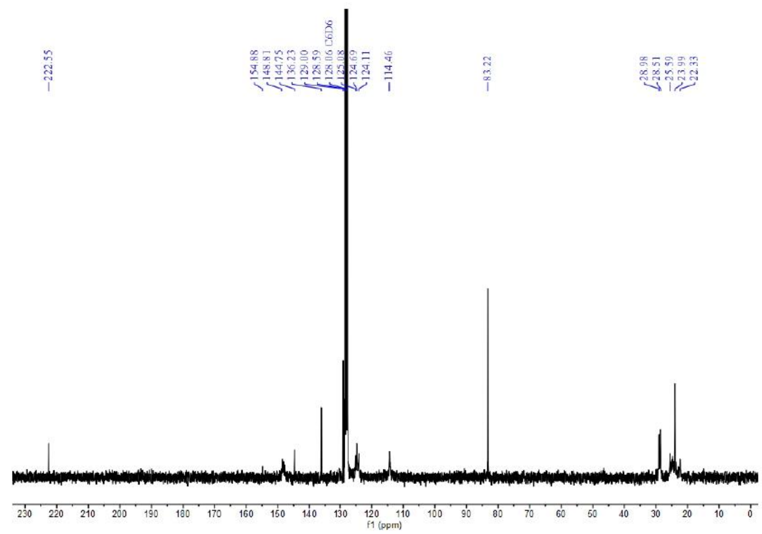

Figure S36. $^{13}C\{^1H\}$ NMR spectrum of compound **12** in C_6D_6.

S31

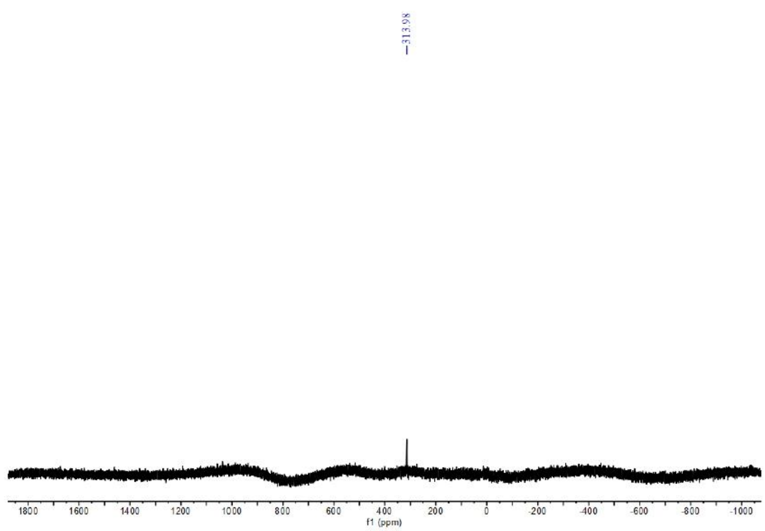

Figure S37. $^{119}Sn\{^{1}H\}$ NMR spectrum of compound **12** in C_6D_6.

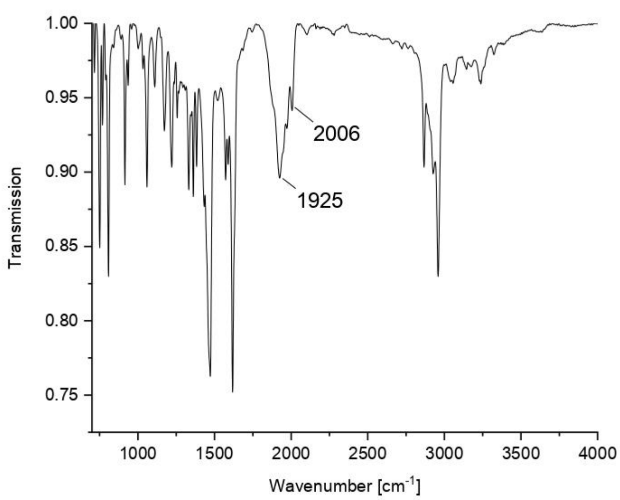

Figure S38. IR spectrum of compound **12** in the solid state.

S32

Synthesis of compound 13

LiI (12 mg, 90 µmol, 1.0 eq.) dissolved in THF (2 mL) was added dropwise to a solution of **12** (100 mg, 90 µmol, 1.0 eq.) in THF (6 mL) at room temperature. The reaction mixture was stirred for 12 h at room temperature. The solvent was removed *in vacuo* and the solid residue was extracted with toluene (4 mL × 3). After filtration, the solvent was removed from the filtrate *in vacuo* to afford **13** as a yellow solid (69 mg, 72%). Crystals suitable for X-ray crystallography were obtained by cooling (-30 °C) a saturated solution of **13** in Et_2O.

^{1}H NMR (400 MHz, C_6D_6) δ = 7.19 – 7.17 (m, 4H, Ar*H*), 7.05 (d, J = 7.7 Hz, 8H, Ar*H*), 5.97 (s, 4H, NC*H*), 3.22 (septet, J = 6.8 Hz, 8H, C*H*(CH_3)$_2$), 1.30 (d, J = 6.8 Hz, 24H, CH(C*H*$_3$)$_2$), 1.11 (d, J = 6.8 Hz, 24H, CH(C*H*$_3$)$_2$).

^{13}C{^{1}H} NMR (101 MHz, C_6D_6) δ = 154.6 (N*C*N), 148.8 (N*C*Ar), 148.4 (N*C*Ar), 135.1 (Ar*C*), 129.6 (Ar*C*), 128.6 (Ar*C*), 124.7 (Ar*C*), 114.0 (N*C*H), 29.0 (*C*H(CH_3)$_2$), 28.6 (*C*H(CH_3)$_2$), 25.2 (CH(*C*H$_3$)$_2$), 24.3 (CH(*C*H$_3$)$_2$), 24.2 (CH(*C*H$_3$)$_2$).

^{119}Sn{^{1}H} NMR (149 MHz, C_6D_6) δ = 61.6.

Anal. Calcd. [%] for $C_{54}H_{72}ILiN_6Sn$: C, 61.32; H, 6.86; N, 7.95. Found [%]: C, 61.25; H, 6.72; N, 8.03.

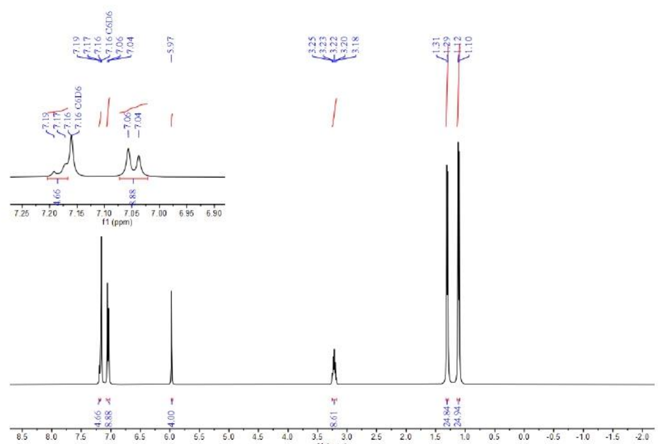

Figure S39. ^{1}H NMR spectrum of compound **13** in C_6D_6.

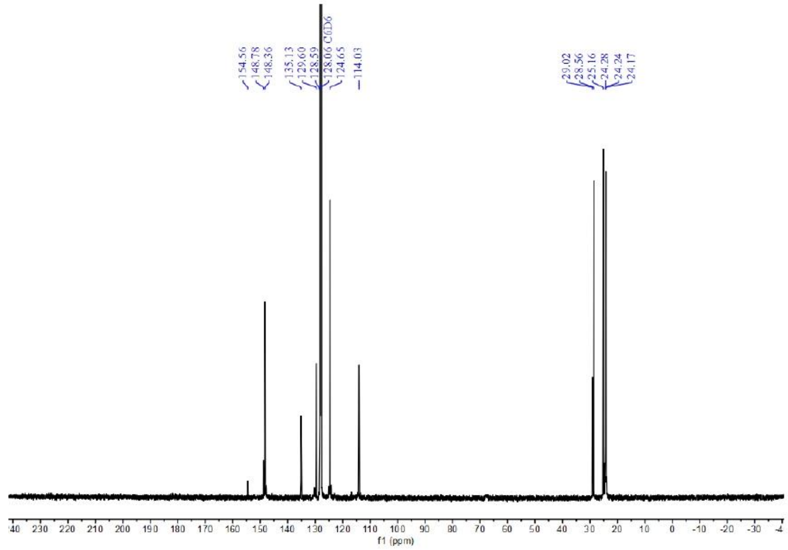

Figure S40. $^{13}C\{^{1}H\}$ NMR spectrum of compound **13** in C_6D_6.

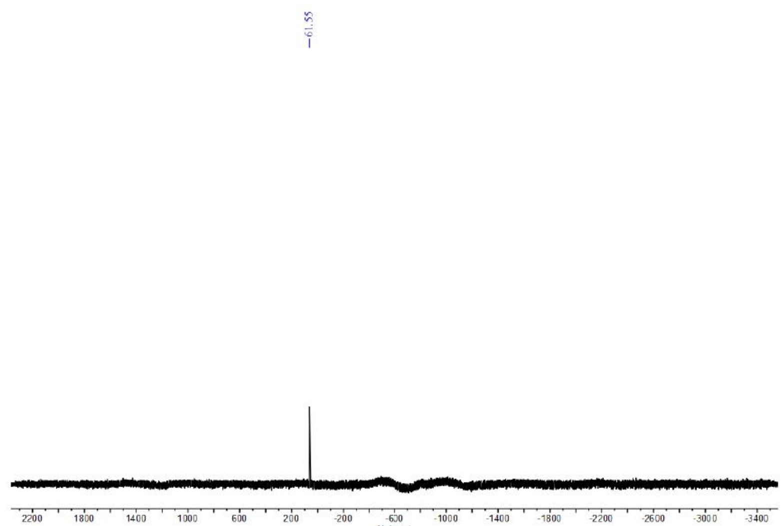

Figure S41. $^{119}Sn\{^{1}H\}$ NMR spectrum of compound **13** in C_6D_6.

2. X-ray Crystallographic Data

General Information

The X-ray intensity data of compounds **1**, **3**, **4**, **7**, **12**, and **13** were collected on an X-ray single crystal diffractometer equipped with a CMOS detector (Bruker Photon-100), an IMS microsource with MoKα radiation (λ = 0.71073 Å) and a Helios mirror optic by using the APEX III software package.[S10] The measurements were performed on single crystals coated with the perfluorinated ether Fomblin® Y. The crystals were fixed on the top of a microsampler, transferred to the diffractometer and frozen under a stream of cold nitrogen. A matrix scan was used to determine the initial lattice parameters. Reflections were merged and corrected for Lorenz and polarization effects, scan speed, and background using SAINT.[S11] Absorption corrections, including odd and even ordered spherical harmonics were performed using SADABS.[S11] Space group assignments were based upon systematic absences, E statistics, and successful refinement of the structures. Structures were solved by direct methods with the aid of successive difference Fourier maps, and were refined against all data using the APEX III software in conjunction with SHELXL-2014[S12] and SHELXLE.[S13] All H atoms were placed in calculated positions and refined using a riding model, with methylene and aromatic C–H distances of 0.99 and 0.95 Å, respectively, and Uiso(H) = 1.2·Ueq(C). Full-matrix least-squares refinements were carried out by minimizing $\Sigma w(Fo^2–Fc^2)^2$ with SHELXL-97[S14] weighting scheme. Neutral atom scattering factors for all atoms and anomalous dispersion corrections for the non-hydrogen atoms were taken from International Tables for Crystallography.[S15] The images of the crystal structure were generated by Mercury.[S16] The CCDC number 2086600 (**1**), 2053426 (**3**), 2053428 (**4**), 2053429 (**12**) and 2178695 (**13**) contain the supplementary crystallographic data for the structures. The data can be obtained free of charge from the Cambridge Crystallographic Data Centre *via* https://www.ccdc.cam.ac.uk/structures/.

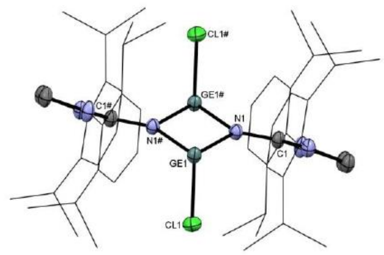

Figure S42. Molecular structure of **1**. Thermal ellipsoids are shown at 30% probability level. Hydrogen atoms are omitted for clarity. Selected bond lengths [Å] and angles [°]: Ge1–Cl1 2.385(7), Ge1–N1 1.956(7), N1–C1 1.305(13), Ge1–N1# 2.003(7), Cl1–Ge1–N1 94.0(3), Cl1–Ge1–N1# 89.5(3), N1–Ge1–N1# 79.5(3), Ge1–N1–C1 131.2(6), Ge1–N1#–C1# 127.6(6), Ge1–N1–Ge1# 100.5(4).

Due to crystal fragmentation upon freezing in 100K and 150K cold N_2-stream, the data collection was performed at 200K causing enhanced thermal movement and therefore resulting in large atomic displacement parameters and required modeling as a whole molecule two part disorder. The structural discussion is limited to the $(NGeCl)_2$ core, due to enlarged ADP within the IDipp groups.

Table S3. Crystal data and structure refinement for compound **1**.

Chemical formula	$C_{54}H_{72}Cl_2Ge_2N_6$
Formula weight	1021.30
Radiation source	IMS microsource (Mo)
Temperature (K)	200
Wavelength (Å)	0.71073
Crystal system (Space group)	Monoclinic, $P2_1/n$
Unit cell dimensions	a = 12.7576(4) Å, α = 90° b = 13.8870(5) Å, β = 104.258(1)° c = 15.6125(5) Å, γ = 90°
Volume (Å^3)	2680.78(15)
Z	2

Density Dx (g/cm^3)	1.265
Absorption coefficient μ (mm^{-1})	1.261
Absorption correction	Multi-Scan
F(000)	1072
Theta (max) (°)	25.35
Index ranges	–15<=h<=15, –16<=k<=16, –18<=l<=18
Absorption Correction Tmin, Tmax	0.6970, 0.7452
Coverage of independent reflections (%)	100
Refinement method	Full-matrix least-squares on F^2
Data / Parameter / Restraints	4896 / 594 / 1717
Goodness-of-fit on F^2	1.051
Final R indices (I>2σ(I))	R1(all) = 0.0423, wR2(all) = 0.0912 R1 = 0.0362, wR2 = 0.0870

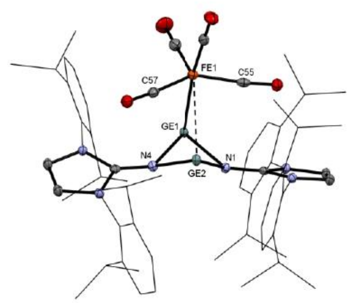

Figure 43. Molecular structure of **3**. Thermal ellipsoids are shown at 50% probability level. Hydrogen atoms and solvent molecules are omitted for clarity. Selected bond lengths [Å] and angles [°]: Ge1–Fe1 2.6968(6), Ge2···Fe1 2.9670(5), Ge1–N1 2.0601(12), Ge1–N4 2.0219(12), Ge2–N1 1.9585(12), Ge2–N4 1.9888(13), C1–N1 1.3066(18), C4–N4 1.3042(18), Fe1–Ge1–N1 92.37(4), Fe1–Ge1–N4 91.80(4), N1–Ge1–N4 76.16(5), N1–Ge2–N4 79.26(5), Ge1–N1–Ge2 87.03(5), Ge1–N4–Ge2 87.27(5), Ge1–N1–C1 132.59(9), Ge1–N4–C4 134.85(10), Ge2–N1–C1 126.98(9), Ge2–N4–C4 125.76(9), C55–Fe1–C57 144.23.

Table S4. Crystal data and structure refinement for compound **3•(Et$_2$O)**.

Chemical formula	$C_{58}H_{72}FeGe_2N_6O_4$•($C_4H_{10}O$)
Formula weight	1192.41
Radiation source	IMS microsource (Mo)
Temperature (K)	100
Wavelength (Å)	0.71073
Crystal system (Space group)	Monoclinic, P2$_1$/n
Unit cell dimensions	a = 22.314(2) Å, α = 90° b = 12.6702(12) Å, β = 109.642(3)° c = 22.970(2) Å, γ = 90°
Volume (Å^3)	6116.3(10)
Z	4
Density Dx (g/cm^3)	1.295
Absorption coefficient μ (mm^{-1})	1.262
Absorption correction	Multi-Scan
F(000)	2504
Theta (max) (°)	25.35
Index ranges	–26<=h<=26, –15<=k<=15, –27<=l<=27
Absorption Correction Tmin, Tmax	0.7024, 0.7452
Coverage of independent reflections (%)	99.9
Refinement method	Full-matrix least-squares on F^2
Data / Parameter / Restraints	11191 / 763 / 195
Goodness-of-fit on F^2	0.999
Final R indices (I>2σ(I))	R1(all) = 0.0229, wR2(all) = 0.0517 R1 = 0.0212, wR2 = 0.0508

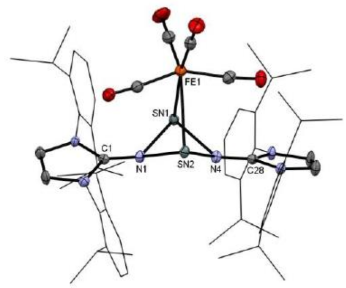

Figure 44. Molecular structure of **4**. Thermal ellipsoids are shown at 50% probability level. Hydrogen atoms are omitted for clarity. Selected bond lengths [Å] and angles [°]: Sn1–Fe1 2.8511(10), Sn2–Fe1 2.9432(10), Sn1–N1 2.204(3), Sn1–N4 2.240(3), Sn2–N1 2.237(3), Sn2–N4 2.180(3), N1–C1 1.291(5), N4–C28 1.300(5), Sn1–Fe1–Sn2 64.65(2), Fe1–Sn1–N1 86.97(8), Fe1–Sn1–N4 87.21(8), Fe1–Sn2–N1 84.13(8), Fe1–Sn2–N4 86.03(9), Sn1–N1–Sn2 88.51(11), Sn1–N4–Sn2 89.05(10), N1–Sn1–N4 75.80(10), N1–Sn2–N4 76.35(11), Sn1–N1–C1 130.2(2), Sn1–N4–C28 129.6(3), Sn2–N1–C1 129.5(2), Sn2–N4–C28 129.7(3).

Table S5. Crystal data and structure refinement for compound **4**.

Chemical formula	$C_{58}H_{72}FeN_6O_4Sn_2$
Formula weight	1210.49
Radiation source	IMS microsource (Mo)
Temperature (K)	100
Wavelength (Å)	0.71073
Crystal system (Space group)	Orthorhombic, $Pna2_1$
Unit cell dimensions	a = 39.133(3) Å, α = 90° b = 13.1762(10) Å, β = 90° c = 12.2656(9) Å, γ = 90°
Volume (Å^3)	6324.4(8)
Z	4
Density Dx (g/cm^3)	1.271
Absorption coefficient μ (mm^{-1})	1.054

Absorption correction	Multi-Scan
F(000)	2480.0
Theta (max) (°)	25.35
Index ranges	–46<=h<=47, –15<=k<=15, –14<=l<=14
Absorption Correction Tmin, Tmax	0.7009, 0.7452
Coverage of independent reflections (%)	99.9
Refinement method	Full-matrix least-squares on F^2
Data / Parameter / Restraints	11567 / 746 / 232
Goodness-of-fit on F^2	1.028
Final R indices (I>2σ(I))	R1(all) = 0.0254, wR2(all) = 0.0536 R1 = 0.0220, wR2 = 0.0514

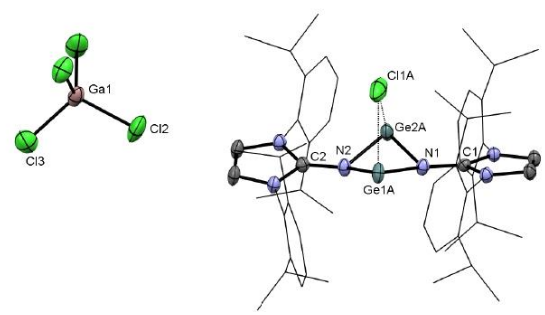

Figure 45. Molecular structure of **7**. Thermal ellipsoids are shown at 50% probability level. Hydrogen atoms are omitted for clarity. Selected bond lengths [Å] and angles [°]: Cl1A–Ge1A 2.647, Cl1A–Ge2A 2.602, Ge1A–N1 1.963(2), Ge1A–N2 1.990(3), Ge2A–N1 1.987(4), Ge2A–N2 1.960(3), C1–N1 1.323(3), C2–N2 1.324(4), N1–Ge1A–N2 77.7(1), N1–Ge2A–N2 77.8(1), Ge1A–N1–Ge2A 94.4(1), Ge1A–N2–Ge2A 94.4(1), Ge1A–N1–C1 127.7(2), Ge1A–N2–C2 126.2(2), Ge2A–N1–C1 128.3(2), Ge2A–N2–C2 127.6(2), Cl1A–Ge1A–N1 78.81, Cl1A–Ge1A–N2 78.35, Cl1A–Ge2A–N1 79.53, Cl1A–Ge2A–N2 79.98.

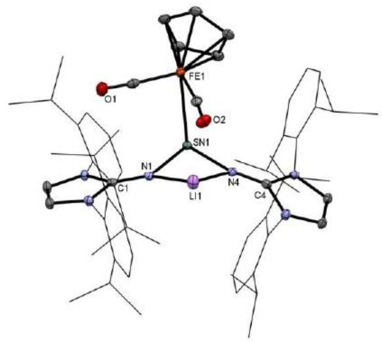

Figure 46. Molecular structure of **12**. Thermal ellipsoids are shown at 50% probability level. Hydrogen atoms and solvent molecules are omitted for clarity. Selected bond lengths [Å] and angles [°]: Sn1–Fe1 2.7671(6), Sn1–N1 2.1763(11), Sn1–N4 2.1717(11), Li1–N1 1.950(3), Li1–N4 1.945(3), C1–N1 1.2713(18), C4–N4 1.2650(18), Fe1–Sn1–N1 96.24(3), Fe1–Sn1–N4 100.66(3), Sn1–N1–C1 129.16(9), Sn1–N4–C4 132.68(9), Li1–N1–C1 141.33(12), Li1–N4–C4 134.92(12), Sn1–N1–Li1 89.40(9), Sn1–N4–Li1 89.66(9), N1–Sn1–N4 81.83(4), N1–Li1–N4 93.94(11).

Table S6. Crystal data and structure refinement for compound **12•(Et$_2$O)**.

Chemical formula	$C_{61}H_{77}FeLiN_6O_2Sn\bullet(C_4H_{10}O)$
Formula weight	1181.91
Radiation source	IMS microsource (Mo)
Temperature (K)	100
Wavelength (Å)	0.71073
Crystal system (Space group)	Monoclinic, $P2_1/n$
Unit cell dimensions	a = 13.3328(5) Å, α = 90° b = 24.6779(10) Å, β = 107.878(1)° c = 19.4551(8) Å, γ = 90°
Volume (Å^3)	6092.1(4)
Z	4

Density Dx (g/cm^3)	1.289
Absorption coefficient μ (mm^{-1})	0.697
Absorption correction	Multi-Scan
F(000)	2488
Theta (max) (°)	25.35
Index ranges	–16<=h<=16, –29<=k<=29, –23<=l<=23
Tmin, Tmax	0.7049, 0.7452
Coverage of independent reflections (%)	99.9
Refinement method	Full-matrix least-squares on F^2
Data / Parameter / Restraints	11135 / 712 / 0
Goodness-of-fit on F^2	1.079
Final R indices (I>2σ(I))	R1(all) = 0.0194, wR2(all) = 0.0471 R1 = 0.0190, wR2 = 0.0468

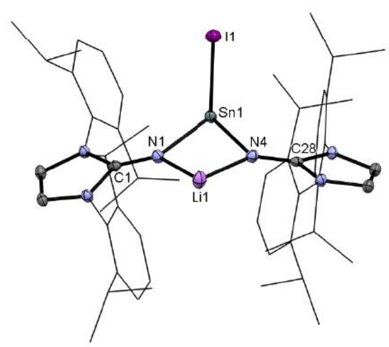

Figure 47. Molecular structure of **13**. Thermal ellipsoids are shown at 50% probability level. Hydrogen atoms and solvent molecules are omitted for clarity. Selected bond lengths [Å] and angles [°]: Sn1–I1 3.0218(6), Sn1–N1 2.136(2), Sn1–N4 2.136(2), Li1–N1 1.944(4), Li1–N4 1.923(4), C1–N1 1.273(3), C28–N4 1.278(2), I1–Sn1–N1 98.13(5), I1–Sn1–N4 88.86(5), Sn1–N1–C1 135.8(1), Sn1–N4–C28 130.7(1), Li1–N1–C1 131.0(2), Li1–N4–C28 135.7(2), Sn1–N1–Li1 93.0(1), Sn1–N4–Li1 93.6(1), N1–Sn1–N4 80.48(6), N1–Li1–N4 91.1(2).

Table S7. Crystal data and structure refinement for compound **13•(Et_2O)**.

Chemical formula	$C_{54}H_{72}ILiN_6Sn$•($C_4H_{10}O$)
Formula weight	1131.82
Radiation source	IMS microsource (Mo)
Temperature (K)	100.00
Wavelength (Å)	0.71073
Crystal system (Space group)	Monoclinic, $P2_1/c$
Unit cell dimensions	a = 12.2143(5) Å, α = 90° b = 23.3867(8) Å, β = 103.999(2)° c = 20.3571(9) Å, γ = 90°
Volume (Å^3)	5642.3(4)
Z	4
Density Dx (g/cm^3)	1.332
Absorption coefficient μ (mm^{-1})	1.043
Absorption correction	Multi-Scan
F(000)	2344.0
Theta (max) (°)	26.144
Index ranges	–15<=h<=15, –28<=k<=28, –25<=l<=25
Absorption Correction Tmin, Tmax	0.695, 0.745
Coverage of independent reflections (%)	99.4
Refinement method	Full-matrix least-squares on F^2
Data / Parameters / Restraints	11178 / 631 / 0
Goodness-of-fit on F^2	1.055
Final R indices (I>2σ(I))	R1(all) = 0.0303, wR2(all) = 0.0497 R1 = 0.0228, wR2 = 0.0470

3. Computational Section

DFT calculations were performed at the ωB97X-D/def2-TZVPP//B97-D/def2-SVP level of theory.[S17-S20] Stationary points on the potential energy surface (PES) were characterized by harmonic vibrational frequency calculations. Electronic structure analysis was carried out at the same level of theory as the geometry optimization. Calculations of molecules were carried out using GAUSSIAN 09 program.[S21] Solid state calculations of bulk LiCl, KCl, Ge, Sn, and the corresponding reference states in the gas phase were carried out with the Vienna Ab initio Simulation Package (VASP) [S22-S23] at the PBE-D3 level of theory[S24-S25]. To describe electron-ion interactions, we used projector augmented-wave (PAW) potentials with valence electron wave functions expanded using a plane-wave basis set with a cutoff energy of 520 eV.[S26-S27] The Brillouin zone was sampled *via* a $24 \times 24 \times 24$ Gamma-centered Monkhorst-Pack k-point mesh in the primitive unit cell of the bulk materials whereas the reference gas-phase calculation used Gamma-point only in a 25 Å x 26 Å x 27 Å unit cell.[S28] Each structure was relaxed until the Hellmann-Feynman forces acting upon each atom were less than or equal to 0.01 eV/Å.

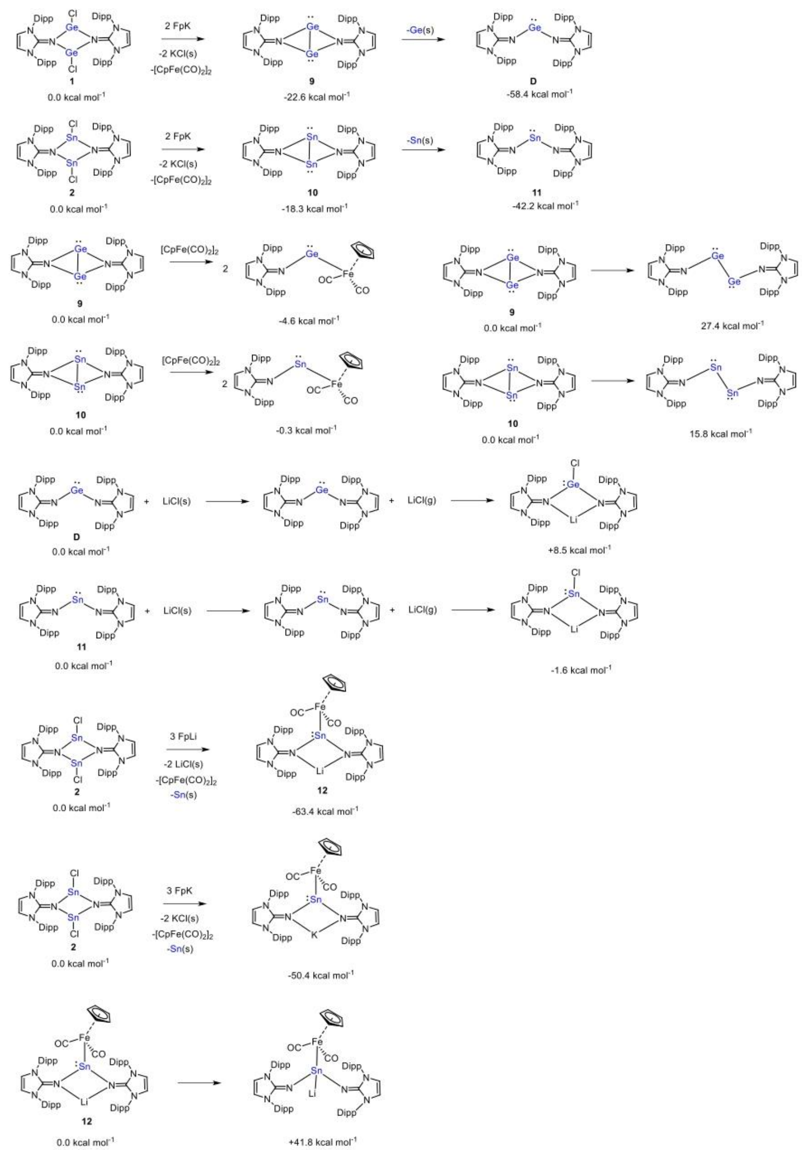

Figure S48. DFT-derived internal energy for various (hypothetical) chemical transformations.

S45

Table S8. NBO-Analysis of the central Ge atoms in **3**.

3	Occupation	Atom	Polarization	*s*-character	*p*-character	*d*-character
Bond	1.92	Ge1	34.50%	20.68%	50.82%	28.50%
		Fe	65.50%	67.93%	32.07%	0.00%
Lone Pair	1.97	Ge1	-	93.27%	6.73%	0.00%
Empty Orbital	0.28	Ge1	-	5.07%	94.82%	0.11%
Empty Orbital	0.24	Ge1	-	0.03%	99.74%	0.23%
Lone Pair	1.97	Ge2	-	92.72%	7.28%	0.00%
Empty Orbital	0.52	Ge2	-	2.21%	97.68%	0.11%
Empty Orbital	0.30	Ge2	-	5.50%	94.39%	0.11%
Empty Orbital	0.24	Ge2	-	0.00%	99.76%	0.24%

Table S9. NBO-Analysis of the central Sn atoms in **4**.

4	Occupation	Atom	Polarization	*s*-character	*p*-character	*d*-character
Bond	1.60	Sn1	11.98%	2.39%	97.14%	0.47%
		Fe	88.02%	2.95%	7.33%	89.72%
Lone Pair	1.96	Sn1	-	89.90%	10.10%	0.00%
Empty Orbital	0.34	Sn1	-	8.99%	90.84%	0.18%
Empty Orbital	0.28	Sn1	-	0.00%	99.52%	0.47%
Bond	1.51	Sn2	33.71%	2.90%	96.99%	0.11%
		Fe	66.29%	5.23%	42.23%	52.54%
Lone Pair	1.96	Sn2	-	90.19%	9.81%	0.00%
Empty Orbital	0.32	Sn2	-	7.44%	92.36%	0.20%
Empty Orbital	0.28	Sn2	-	0.00%	99.60%	0.40%

Table S10. Calculated E = Ge, Sn-related bond lengths [Å], NPA charges of Ge, Sn, and Fe atoms, Wiberg Bond Index (WBI) and Mayer Bond Order (MBO) in **3** and **4**.

Compound	Bond length [Å]		NPA charge		WBI//MBO	
	E–N	E-Fe	E	Fe	E–N	E-Fe
3	2.061/2.043	2.842/3.043	+0.87/+0.82	-1.40	0.51/0.48// 0.65/0.61	0.51/0.36// 0.58/0.40
4	2.271/2.330	3.053/3.165	+0.93/+0.95	-1.44	0.40/0.38// 0.54/0.51	0.48/0.41// 0.54/0.45

Table S11. NBO-Analysis of the central Ge atoms in **5**.

5	Occupation	Atom	Polarization	*s*-character	*p*-character	*d*-character
Bond	1.61	Ge1	38.66%	7.73%	92.22%	0.05%
		Fe	61.34%	10.53%	44.91%	44.55%
Lone Pair	1.95	Ge1	-	88.51%	11.49%	0.00%
Empty Orbital	0.31	Ge1	-	3.91%	95.99%	0.09%
Empty Orbital	0.29	Ge1	-	0.00%	99.73%	0.26%
Lone Pair	1.98	Ge2	-	88.18%	11.80%	0.02%
Empty Orbital	0.33	Ge2	-	13.08%	86.67%	0.25%
Empty Orbital	0.28	Ge2	-	0.06%	99.35%	0.59%
Bond	1.62	N	90.41%	0.06%	99.91%	0.04%
		Ge2	9.59%	0.20%	98.60%	1.20%

Table S12. NBO-Analysis of the central Sn atoms in **6**.

6	Occupation	Atom	Polarization	*s*-character	*p*-character	*d*-character
Bond	1.57	Sn1	33.99%	5.53%	94.43%	0.04%
		Fe	66.01%	10.32%	45.86%	43.82%
Lone Pair	1.96	Sn1	-	92.06%	7.94%	0.00%
Empty Orbital	0.28	Sn1	-	2.50%	97.43%	0.07%
Empty Orbital	0.26	Sn1	-	0.02%	99.78%	0.20%
Lone Pair	1.98	Sn2	-	92.97%	7.02%	0.02%
Empty Orbital	0.30	Sn2	-	1.42%	98.26%	0.31%
Empty Orbital	0.27	Sn2	-	6.89%	92.90%	0.21%
Empty Orbital	0.24	Sn2	-	0.04%	99.68%	0.28%

Table S13. Calculated E = Ge, Sn-related bond lengths [Å], NPA charges of Ge, Sn, and Fe atoms, Wiberg Bond Index (WBI) and Mayer Bond Order (MBO) in **5** and **6**.

Compound	Bond length [Å]		NPA charge		WBI//MBO	
	E–N	E-Fe	E	Fe	E-N	E-Fe
5	2.233/2.208/ 1.936/1.907	2.524/4.384	+0.74/+1.04	-1.57	0.35/0.38/0.64/0.68// 0.41/0.44/0.85/0.90	0.74/0.02// 0.86/0.03
6	2.467/2.457 2.175/2.144/	2.715/4.371	+0.87/+1.20	-1.58	0.29/0.31/0.50/0.53/// 0.37/0.40/0.75/0.80	0.66/0.05// 0.77/0.05

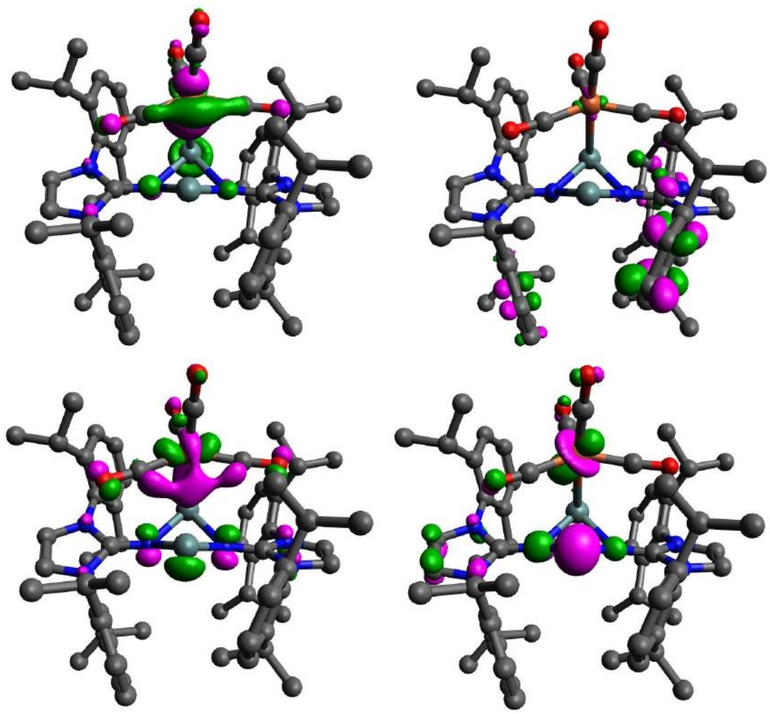

Figure S49. HOMO (top left, –3.70 eV), HOMO-1 (bottom left, –3.85 eV), HOMO-5 (bottom right, –5.18 eV), and LUMO (top right, –1.52 eV) of **3**. Hydrogens are omitted for clarity.

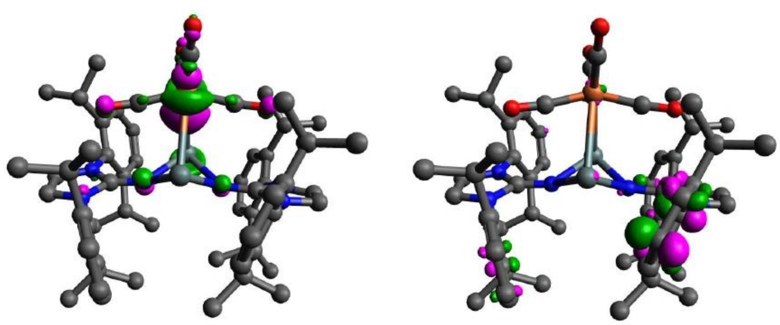

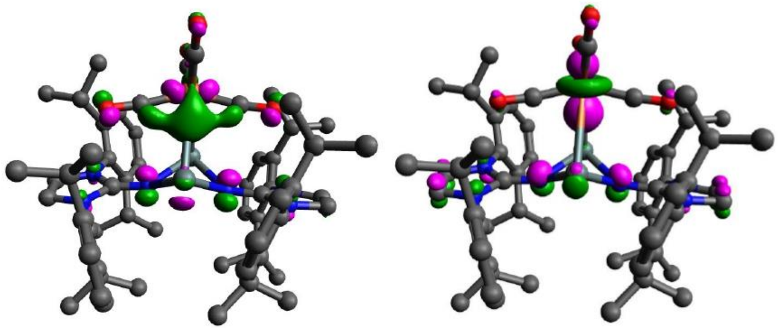

Figure S50. HOMO (top left, –3.76 eV), HOMO-1 (bottom left, –3.82 eV), HOMO-5 (bottom right, –4.98 eV), and LUMO (top right, –1.54 eV) of **4**. Hydrogens are omitted for clarity.

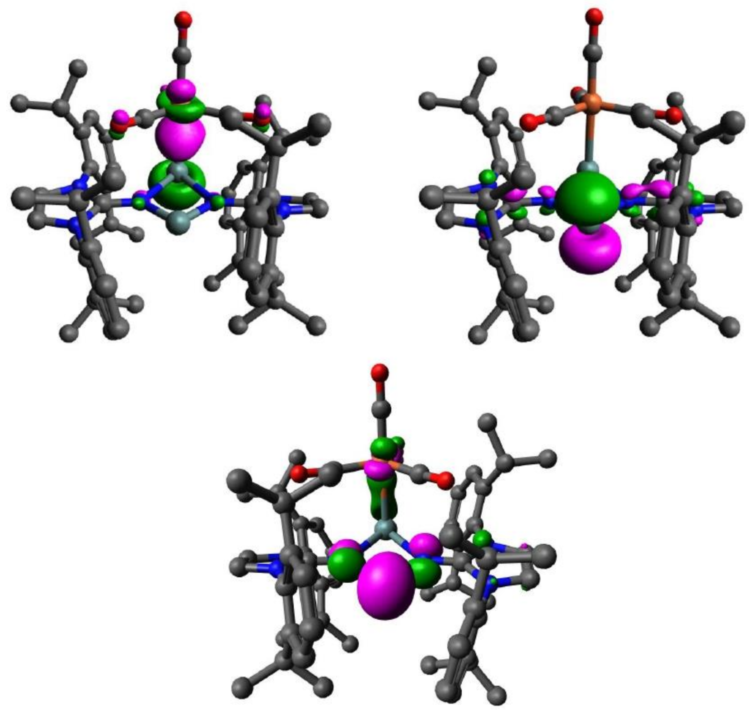

Figure S51. HOMO (top left, –3.38 eV), HOMO-6 (bottom, –5.00 eV), and LUMO (top right, –2.39 eV) of **5**. Hydrogens are omitted for clarity.

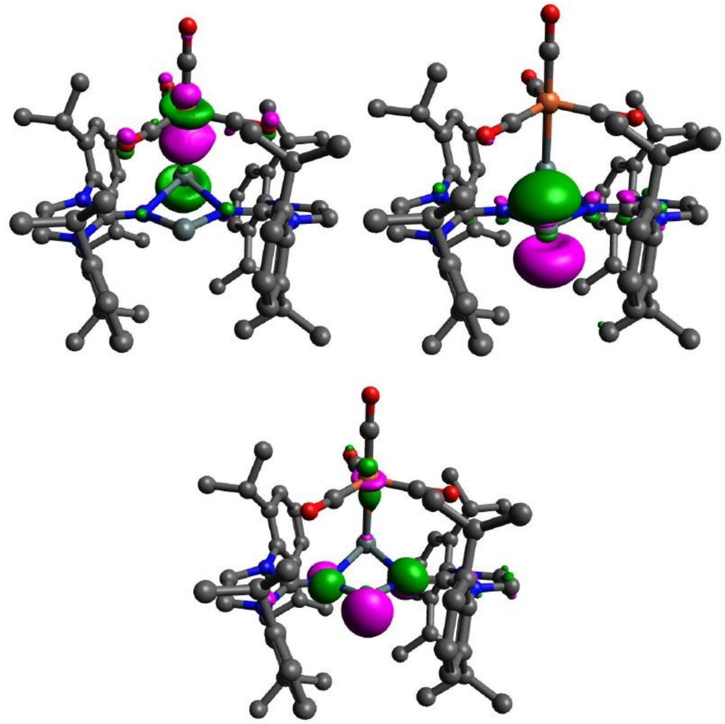

Figure S52. HOMO (top left, –3.48 eV), HOMO-7 (bottom, –5.07 eV), and LUMO (top right, –2.47 eV) of **6**. Hydrogens are omitted for clarity.

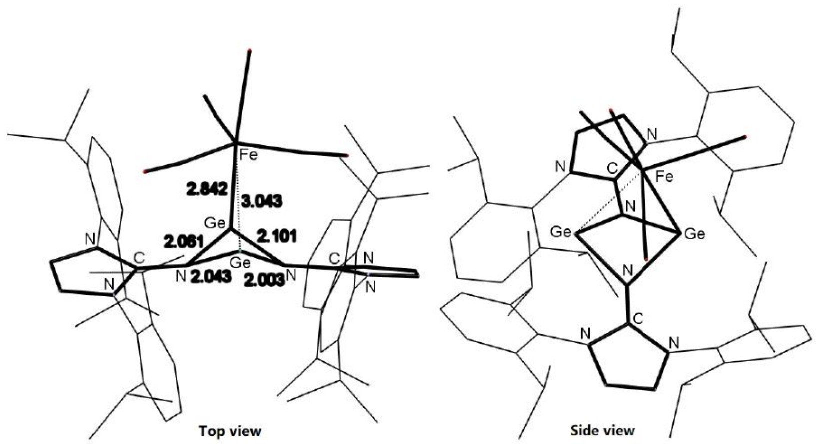

Figure S53. Optimized geometry of **3** with calculated bond lengths given in [Å]. Hydrogens are omitted for clarity.

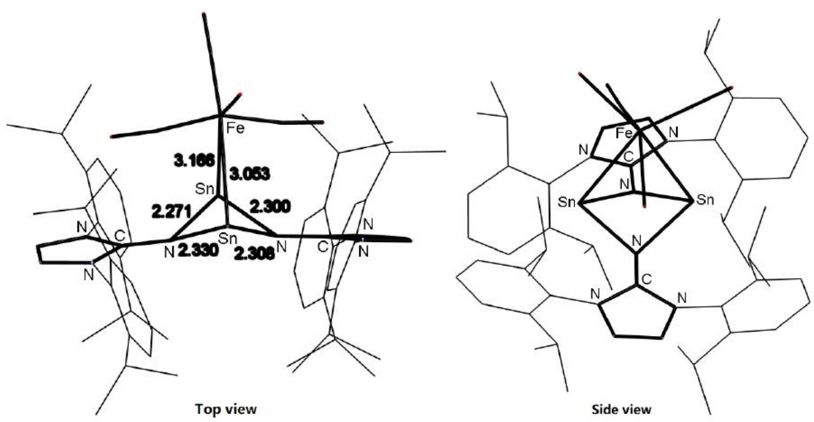

Figure S54. Optimized geometry of **4** with calculated bond lengths given in [Å]. Hydrogens are omitted for clarity.

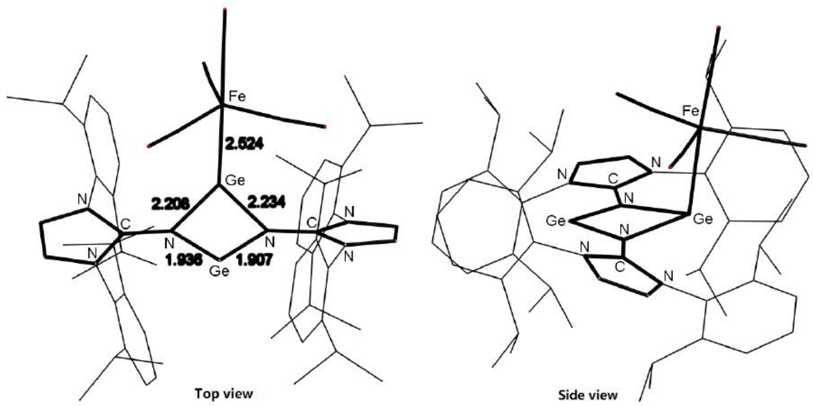

Figure S55. Optimized geometry of **5** with calculated bond lengths given in [Å]. Hydrogens are omitted for clarity.

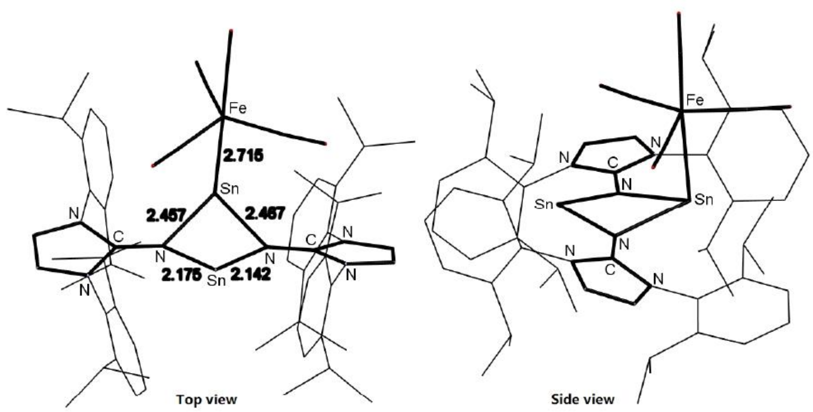

Figure S56. Optimized geometry of **6** with calculated bond lengths given in [Å]. Hydrogens are omitted for clarity.

Table S14. Cartesian coordinates of LiCl in Å.

Atomtype	X Coordinate [Å]	Y Coordinate [Å]	Z Coordinate [Å]
Li	0	0	-1.724358
Cl	0	0	0.304298

Table S15. Cartesian coordinates of KCl in Å.

Atomtype	X Coordinate [Å]	Y Coordinate [Å]	Z Coordinate [Å]
K	0	0	1.273513
Cl	0	0	-1.423338

Table S16. Cartesian coordinates of FpK in Å.

Atomtype	X Coordinate [Å]	Y Coordinate [Å]	Z Coordinate [Å]
C	1.866718	-1.151266	0.789244
C	2.444713	-0.709621	-0.458668
C	2.444682	0.709598	-0.458651
C	1.866659	1.151201	0.789285
C	1.529159	-0.000043	1.573675
Fe	0.435153	-0.00006	-0.260231
C	-0.644904	-1.221141	-0.785029
O	-1.497033	-2.00823	-1.062654
C	-0.644734	1.221199	-0.785008
O	-1.496713	2.008483	-1.062521
K	-2.668336	0.000003	0.923701
H	2.796439	-1.357572	-1.264333
H	1.715448	-2.193401	1.081558
H	1.136974	-0.000051	2.593404
H	1.715398	2.193323	1.081647
H	2.796353	1.357612	-1.26429

Table S17. Cartesian coordinates of Fp in Å.

Atomtype	X Coordinate [Å]	Y Coordinate [Å]	Z Coordinate [Å]
C	1.735139	0.733414	-0.820143
C	1.475266	1.133881	0.541165
C	1.358917	-0.034989	1.352371
C	1.483577	-1.162997	0.481851
C	1.743739	-0.692395	-0.855314
Fe	-0.176268	-0.002116	-0.221405
C	-1.344138	1.299471	-0.056109
O	-2.090694	2.179455	0.095648
C	-1.360491	-1.290107	-0.053872
O	-2.120239	-2.159423	0.094929
H	1.386937	2.165613	0.890251

H	1.883621	1.409617	-1.665351
H	1.896311	-1.323387	-1.734175
H	1.403103	-2.211636	0.778441
H	1.148389	-0.063128	2.423053

Table S18. Cartesian coordinates of **1** in Å.

Atomtype	X Coordinate [Å]	Y Coordinate [Å]	Z Coordinate [Å]
C	-3.265417	2.496461	2.085073
C	-3.281016	2.074937	0.732507
C	-3.080706	2.967896	-0.356088
C	-2.840023	4.31978	-0.045038
C	-2.816183	4.760585	1.286114
C	-3.033644	3.861676	2.336709
N	-3.534244	0.689198	0.446794
C	-2.578348	-0.278032	0.115598
N	-3.324896	-1.451055	-0.065991
C	-4.68452	-1.197189	0.155105
C	-4.812399	0.118317	0.471245
N	-1.282963	-0.136831	0.000163
Ge	0.168494	-1.574254	0.255596
Cl	0.549398	-2.211155	-2.000272
C	-2.862614	-2.615064	-0.777016
C	-2.44701	-3.757806	-0.045789
C	-2.004257	-4.871085	-0.784785
C	-1.983111	-4.844627	-2.186
C	-2.414984	-3.70928	-2.881148
C	-2.868278	-2.568588	-2.193289
C	-2.542973	-3.799537	1.480185
C	-3.9292	-4.33184	1.911881
C	-3.319861	-1.328068	-2.965117
C	-2.12932	-0.613596	-3.639791
C	-3.171766	2.478882	-1.805147
C	-2.379026	3.338381	-2.805898
C	-3.541465	1.526304	3.233651
C	-4.995502	1.697521	3.731059
N	1.293243	0.087467	0.018429
Ge	-0.111624	1.526567	-0.21999
Cl	0.155612	2.160563	2.069694
C	2.579716	0.268271	0.142
N	3.501823	-0.551475	0.792042
C	4.773718	0.03094	0.751866

C	4.671808	1.196119	0.057529
N	3.334586	1.342049	-0.334372
C	3.191999	-1.808343	1.417785
C	2.611112	-1.794718	2.713429
C	2.328232	-3.038337	3.308621
C	2.598489	-4.238224	2.636021
C	3.153632	-4.222473	1.349727
C	3.458593	-3.00746	0.704431
C	2.312832	-0.480404	3.430372
C	3.54127	-0.01883	4.245379
C	4.061716	-2.991972	-0.700364
C	5.60456	-3.07845	-0.637222
C	2.857448	2.351901	-1.243355
C	2.710303	3.684242	-0.775249
C	2.264012	4.652164	-1.698052
C	1.957552	4.30412	-3.01764
C	2.097868	2.977362	-3.451434
C	2.555651	1.969224	-2.583001
C	3.023789	4.083739	0.666257
C	4.430923	4.716593	0.765182
C	2.721599	0.524597	-3.058626
C	4.20866	0.180683	-3.303795
C	1.972819	5.041306	1.265081
C	1.878355	0.173198	-4.295915
C	3.512039	-4.106069	-1.612531
C	1.052336	-0.536344	4.311376
C	-1.422241	-4.614872	2.152716
C	-4.427366	-1.659479	-3.986955
C	-4.645175	2.352351	-2.255881
C	-2.550873	1.658975	4.407466
H	5.423072	1.933046	-0.217487
H	5.624152	-0.439907	1.240957
H	-5.68705	0.717275	0.717698
H	-5.428639	-1.982122	0.030193
H	2.142121	5.690633	-1.370269
H	1.600492	5.071254	-3.717164
H	1.844838	2.726011	-4.48633
H	3.006337	3.162838	1.276523
H	0.954208	4.637449	1.14773
H	2.024994	6.046243	0.804277
H	2.159879	5.164729	2.347722
H	4.666246	4.973905	1.815232
H	4.47753	5.646577	0.166622

H	5.222324	4.041986	0.393783
H	2.350716	-0.133896	-2.255535
H	1.908674	-0.918578	-4.456097
H	2.25728	0.665547	-5.212633
H	0.819757	0.454284	-4.154001
H	4.824738	0.341955	-2.401943
H	4.625121	0.800331	-4.121334
H	4.30736	-0.88262	-3.593313
H	3.341864	-5.169583	0.832493
H	2.361391	-5.196876	3.11548
H	1.876546	-3.069776	4.306103
H	2.109557	0.287336	2.664997
H	1.194401	-1.173688	5.205246
H	0.187432	-0.917346	3.738842
H	0.801249	0.481654	4.656533
H	3.782908	-0.751829	5.039218
H	3.338753	0.957532	4.724672
H	4.433074	0.094919	3.602238
H	-2.662589	5.038636	-0.851587
H	-2.618338	5.817856	1.504871
H	-3.004067	4.220293	3.37183
H	-2.732269	1.466548	-1.839104
H	-5.216544	1.66906	-1.604484
H	-4.696136	1.955602	-3.287586
H	-5.141995	3.341072	-2.241293
H	-1.335853	3.48223	-2.47363
H	-2.845176	4.331163	-2.952517
H	-2.359729	2.837584	-3.791224
H	-3.439626	0.499954	2.836405
H	-2.754552	0.871878	5.157995
H	-2.655108	2.633985	4.919775
H	-1.510868	1.560974	4.056675
H	-5.223173	0.966416	4.529878
H	-5.728933	1.55643	2.91676
H	-5.144188	2.713621	4.14366
H	-2.378495	-3.697319	-3.976917
H	-1.616226	-5.717347	-2.741243
H	-1.664056	-5.769458	-0.25817
H	-2.458305	-2.757303	1.842136
H	-1.472929	-4.48585	3.250037
H	-0.424503	-4.286213	1.813708
H	-1.524563	-5.697267	1.947295
H	-4.073263	-5.368077	1.550729

H	-4.749038	-3.714391	1.504558
H	-4.019191	-4.335813	3.014925
H	3.789969	-2.025358	-1.163106
H	3.853026	-3.933746	-2.650371
H	3.885	-5.10274	-1.30832
H	2.409749	-4.11123	-1.614731
H	6.033945	-3.035993	-1.656108
H	6.046228	-2.256114	-0.049252
H	5.916697	-4.033432	-0.1727
H	-3.759867	-0.615124	-2.246626
H	-2.479211	0.29937	-4.157665
H	-1.362434	-0.338443	-2.897659
H	-1.641926	-1.270138	-4.383535
H	-4.794924	-0.731173	-4.464099
H	-4.053267	-2.320622	-4.790824
H	-5.284966	-2.163269	-3.503387

Table S19. Cartesian coordinates of **9** in Å.

Atomtype	X Coordinate [Å]	Y Coordinate [Å]	Z Coordinate [Å]
C	3.250717	2.572253	-1.747522
C	3.274693	2.059378	-0.424229
C	2.949601	2.853224	0.703642
C	2.580165	4.193606	0.477277
C	2.561754	4.725571	-0.818677
C	2.904532	3.925957	-1.918399
N	3.582238	0.676003	-0.219772
C	2.598777	-0.305839	0.027175
N	3.338467	-1.436904	0.420551
C	4.710482	-1.146628	0.4039
C	4.858615	0.151911	0.022879
N	1.314269	-0.195907	-0.071137
Ge	-0.167243	-1.523041	-0.728219
C	2.764018	-2.688845	0.807717
C	2.829201	-3.775635	-0.098853
C	2.278298	-5.007421	0.308486
C	1.660087	-5.138538	1.556928
C	1.575329	-4.038347	2.424675
C	2.12178	-2.78989	2.073026
C	3.459312	-3.63282	-1.483371
C	2.490349	-4.055607	-2.607506
C	2.043832	-1.578979	3.005376

C	0.944566	-1.687907	4.074269
C	2.947749	2.274013	2.116296
C	1.504898	2.111148	2.632919
C	3.605905	1.683771	-2.937913
C	2.717998	1.930534	-4.172518
Ge	0.146102	0.963325	-1.254366
N	-1.288102	0.07046	-0.070701
C	-2.553775	0.343291	-0.081055
N	-3.156	1.605801	0.11525
C	-4.551006	1.484872	0.046297
C	-4.84826	0.180496	-0.205512
N	-3.640324	-0.527784	-0.280217
C	-2.477252	2.698031	0.753776
C	-1.99976	3.778548	-0.031165
C	-1.353763	4.836995	0.638036
C	-1.188173	4.816399	2.029714
C	-1.668228	3.737115	2.783568
C	-2.320828	2.654332	2.162917
C	-2.247417	3.826554	-1.537185
C	-1.0975	4.477406	-2.328307
C	-2.816271	1.46967	2.992316
C	-3.68496	1.91019	4.188066
C	-3.51908	-1.897536	-0.679108
C	-3.26895	-2.881308	0.315181
C	-3.16928	-4.220512	-0.105948
C	-3.298662	-4.562842	-1.460529
C	-3.512178	-3.570967	-2.425396
C	-3.616285	-2.214436	-2.056711
C	-3.125319	-2.475966	1.781945
C	-4.508742	-2.258289	2.435422
C	-3.784171	-1.136119	-3.125055
C	-2.593077	-1.13217	-4.106985
C	4.79066	-4.409725	-1.566639
C	3.406611	-1.288438	3.67477
C	5.101577	1.835705	-3.295284
C	-2.279498	-3.456973	2.610692
C	-5.132013	-1.280335	-3.862537
C	-3.587479	4.537053	-1.837185
C	3.806183	3.107135	3.089676
C	-1.634658	0.589641	3.448776
H	5.447497	-1.902467	0.672174
H	5.751177	0.766486	-0.087828
H	-5.803451	-0.320739	-0.358308

H	-5.199488	2.344261	0.212503
H	2.321053	-5.868375	-0.369855
H	1.226553	-6.102047	1.855221
H	1.067903	-4.158755	3.387165
H	3.688424	-2.563544	-1.639911
H	1.540547	-3.493508	-2.545542
H	2.253567	-5.134978	-2.557419
H	2.946705	-3.860435	-3.596481
H	5.263283	-4.272348	-2.557805
H	4.625268	-5.493602	-1.415445
H	5.503888	-4.067752	-0.793711
H	1.782286	-0.712093	2.373703
H	0.845808	-0.724758	4.605741
H	1.179415	-2.460753	4.831105
H	-0.03183	-1.92605	3.62213
H	4.206901	-1.128095	2.932783
H	3.705083	-2.129344	4.329929
H	3.337516	-0.376351	4.29768
H	2.293998	4.824544	1.327212
H	2.267058	5.771224	-0.976301
H	2.876247	4.355561	-2.926249
H	3.444191	0.636985	-2.619292
H	2.907974	2.92223	-4.624906
H	1.646081	1.867235	-3.91188
H	2.931782	1.171418	-4.947859
H	5.322827	2.876526	-3.600557
H	5.374134	1.165852	-4.133061
H	5.749051	1.590221	-2.434375
H	-2.968724	-5.009354	0.626544
H	-3.212296	-5.613551	-1.766929
H	-3.581336	-3.848159	-3.484632
H	-2.595082	-1.507475	1.794603
H	-5.099475	-1.499625	1.892886
H	-4.39115	-1.91293	3.480542
H	-5.086184	-3.202572	2.447852
H	-1.29665	-3.633216	2.138166
H	-2.78813	-4.431052	2.742515
H	-2.11111	-3.042499	3.621402
H	-3.789304	-0.154084	-2.61988
H	-2.700167	-0.305548	-4.835213
H	-2.538765	-2.078532	-4.677898
H	-1.637115	-0.999167	-3.564971
H	-5.258262	-0.468074	-4.603252

H	-5.98187	-1.239193	-3.155716
H	-5.189855	-2.243377	-4.404639
H	-1.523944	3.727616	3.870639
H	-0.676151	5.648385	2.530976
H	-0.969708	5.68652	0.062705
H	-2.341776	2.779412	-1.881573
H	-1.259119	4.333814	-3.412986
H	-0.125509	4.028258	-2.057903
H	-1.043661	5.568357	-2.148704
H	-3.556177	5.585691	-1.484129
H	-4.435292	4.035894	-1.337036
H	-3.7881	4.546461	-2.925595
H	3.397058	1.26688	2.071781
H	1.503501	1.617823	3.622922
H	1.006638	3.09129	2.735494
H	0.905237	1.500398	1.937938
H	3.850402	2.611069	4.077818
H	4.840214	3.226825	2.715998
H	3.381398	4.116936	3.244644
H	-3.457727	0.84352	2.348524
H	-2.002906	-0.293539	4.003063
H	-1.04918	0.239878	2.581849
H	-0.959218	1.154583	4.117249
H	-4.101487	1.022864	4.701377
H	-3.097716	2.477576	4.934548
H	-4.526689	2.548184	3.860615

Table S20. Cartesian coordinates of **2** in Å.

Atomtype	X Coordinate [Å]	Y Coordinate [Å]	Z Coordinate [Å]
C	3.101408	-2.461994	2.293636
C	3.300648	-2.206241	0.912738
C	3.204247	-3.220712	-0.07942
C	2.908642	-4.527071	0.356469
C	2.712152	-4.803937	1.716965
C	2.806875	-3.784936	2.672985
N	3.64137	-0.873376	0.503417
C	2.733136	0.140174	0.138956
N	3.567846	1.246777	-0.122753
C	4.912739	0.904102	0.067629
C	4.956461	-0.397439	0.455106
N	1.434939	0.075926	0.06254

Sn	-0.075366	1.789326	0.269202
Cl	-0.450773	2.377429	-2.185401
C	3.16842	2.416163	-0.855489
C	2.915059	3.624257	-0.152187
C	2.537163	4.74902	-0.911038
C	2.413707	4.669051	-2.305182
C	2.687436	3.470481	-2.974396
C	3.08224	2.320189	-2.267421
C	3.117481	3.713429	1.361888
C	4.562807	4.160734	1.681782
C	3.39333	1.020408	-3.009708
C	2.119746	0.378765	-3.597832
C	3.442595	-2.904249	-1.558971
C	2.612843	-3.774678	-2.522788
C	3.243058	-1.347997	3.33089
C	4.694795	-1.292372	3.861867
N	-1.40093	-0.022799	0.004072
Sn	0.06209	-1.733501	-0.219273
Cl	-0.45265	-2.334291	2.214415
C	-2.695029	-0.119535	0.060429
N	-3.605186	0.742225	0.694609
C	-4.913195	0.268249	0.543991
C	-4.856481	-0.877957	-0.183905
N	-3.512131	-1.121592	-0.492856
C	-3.257363	1.95338	1.380384
C	-2.688668	1.861373	2.681776
C	-2.369424	3.066561	3.335591
C	-2.601246	4.306527	2.720963
C	-3.156265	4.36951	1.436794
C	-3.492711	3.195729	0.731622
C	-2.446992	0.501316	3.333572
C	-3.749115	-0.051754	3.954484
C	-4.123431	3.277573	-0.658709
C	-5.639766	3.559491	-0.543369
C	-3.061393	-2.181667	-1.350604
C	-3.088241	-3.517803	-0.863416
C	-2.659658	-4.539395	-1.735984
C	-2.209671	-4.244468	-3.027104
C	-2.185423	-2.917819	-3.483022
C	-2.614639	-1.854738	-2.665527
C	-3.584238	-3.867454	0.540402
C	-5.048826	-4.36249	0.488818
C	-2.599437	-0.408054	-3.16402

C	-4.025169	0.101916	-3.476063
C	-2.707277	-4.917215	1.253907
C	-1.676205	-0.173035	-4.37105
C	-3.460656	4.327918	-1.572129
C	-1.308367	0.499736	4.366995
C	2.107358	4.634609	2.073505
C	4.470397	1.227377	-4.095269
C	4.944106	-3.009155	-1.911036
C	2.250622	-1.461509	4.503756
H	-5.645461	-1.539213	-0.534707
H	-5.757724	0.790952	0.988285
H	5.797112	-1.039885	0.711204
H	5.709163	1.62063	-0.126436
H	-2.670697	-5.579587	-1.391587
H	-1.872014	-5.054042	-3.687349
H	-1.826853	-2.710092	-4.496142
H	-3.545073	-2.944362	1.146442
H	-1.648455	-4.612867	1.273253
H	-2.794597	-5.913562	0.780409
H	-3.0403	-5.022781	2.303047
H	-5.422526	-4.571614	1.508946
H	-5.116836	-5.298044	-0.098846
H	-5.726525	-3.627144	0.021499
H	-2.190621	0.216209	-2.350904
H	-1.573882	0.912658	-4.539998
H	-2.074525	-0.633391	-5.296214
H	-0.662558	-0.571217	-4.187552
H	-4.697154	0.020155	-2.604244
H	-4.473249	-0.470567	-4.311259
H	-3.983387	1.167201	-3.771285
H	-3.326058	5.345681	0.968561
H	-2.340827	5.233415	3.248603
H	-1.924986	3.03777	4.336109
H	-2.132997	-0.199511	2.541509
H	-1.575113	1.056173	5.286376
H	-0.38538	0.939602	3.946728
H	-1.079134	-0.54137	4.651978
H	-4.099443	0.599148	4.778975
H	-3.571509	-1.064557	4.362223
H	-4.557731	-0.124549	3.205404
H	2.819021	-5.336552	-0.376203
H	2.469019	-5.826275	2.033855
H	2.627815	-4.01755	3.727988

H	3.136109	-1.854018	-1.720974
H	5.557415	-2.329592	-1.295665
H	5.110166	-2.748261	-2.973674
H	5.305655	-4.042361	-1.748724
H	1.54065	-3.770412	-2.256488
H	2.963948	-4.823745	-2.531888
H	2.712956	-3.387821	-3.553826
H	3.034911	-0.392474	2.814555
H	2.30271	-0.548378	5.12591
H	2.496319	-2.316571	5.161959
H	1.218997	-1.585959	4.136763
H	4.809383	-0.46621	4.589173
H	5.426525	-1.135748	3.050395
H	4.950894	-2.238991	4.375184
H	2.574321	3.41909	-4.063606
H	2.092182	5.550268	-2.874572
H	2.326616	5.698184	-0.405547
H	2.988391	2.692278	1.769864
H	2.224913	4.544866	3.16949
H	1.065517	4.372459	1.816221
H	2.27127	5.697478	1.814579
H	4.752635	5.170026	1.269421
H	5.308562	3.471817	1.248849
H	4.726469	4.198852	2.775583
H	-3.992224	2.292519	-1.142955
H	-3.886508	4.251078	-2.590149
H	-3.652287	5.358103	-1.216293
H	-2.373115	4.165064	-1.649188
H	-6.108316	3.568303	-1.54565
H	-6.160328	2.804118	0.07062
H	-5.811499	4.548048	-0.076001
H	3.813175	0.304987	-2.281659
H	2.36443	-0.590462	-4.073656
H	1.363914	0.215476	-2.813326
H	1.659531	1.0346	-4.358923
H	4.741135	0.257201	-4.553494
H	4.107896	1.887807	-4.905155
H	5.387296	1.678587	-3.672298

Table S21. Cartesian coordinates of **10** in Å.

Atomtype	X Coordinate [Å]	Y Coordinate [Å]	Z Coordinate [Å]

C	3.419241	2.786761	-1.602454
C	3.31219	2.263884	-0.286738
C	2.801374	3.030779	0.79239
C	2.365103	4.341256	0.51763
C	2.467771	4.880148	-0.772043
C	3.003592	4.115017	-1.817792
N	3.676736	0.90359	-0.046993
C	2.729407	-0.138388	0.125161
N	3.523052	-1.229603	0.553699
C	4.874759	-0.860377	0.609911
C	4.967162	0.448818	0.251303
N	1.454122	-0.10323	-0.052879
Sn	-0.055081	-1.674152	-0.823791
C	3.012762	-2.510148	0.931695
C	3.214169	-3.610689	0.060202
C	2.730958	-4.871608	0.465415
C	2.047693	-5.022771	1.677159
C	1.831022	-3.914007	2.51024
C	2.309019	-2.636633	2.162478
C	3.93544	-3.456371	-1.278152
C	3.112814	-4.018997	-2.455779
C	2.107936	-1.422542	3.071583
C	0.973512	-1.594864	4.093649
C	2.705611	2.458388	2.204112
C	1.238883	2.21604	2.608202
C	3.989412	1.943821	-2.741605
C	3.180868	2.060965	-4.048517
Sn	0.124786	1.202247	-1.338895
N	-1.383304	0.037584	-0.059873
C	-2.660783	0.217501	-0.053657
N	-3.369361	1.429374	0.174802
C	-4.75185	1.197388	0.128496
C	-4.950204	-0.119271	-0.147164
N	-3.693375	-0.729659	-0.256399
C	-2.789737	2.555428	0.849863
C	-2.44313	3.715602	0.109347
C	-1.894931	4.804491	0.816394
C	-1.698449	4.739734	2.203007
C	-2.054549	3.586158	2.91405
C	-2.608845	2.472001	2.254532
C	-2.730282	3.809655	-1.388537
C	-1.70951	4.666496	-2.160714
C	-2.993892	1.221474	3.043937

C	-3.943659	1.541287	4.216267
C	-3.496453	-2.088853	-0.653331
C	-3.164161	-3.05423	0.337073
C	-3.01841	-4.391314	-0.079824
C	-3.179999	-4.750051	-1.426418
C	-3.474475	-3.776292	-2.389131
C	-3.629781	-2.423498	-2.025102
C	-2.993748	-2.634069	1.797427
C	-4.364331	-2.463278	2.490671
C	-3.922287	-1.36605	-3.087806
C	-2.853435	-1.356412	-4.200911
C	5.337264	-4.101407	-1.223536
C	3.416615	-1.034782	3.797662
C	5.474628	2.296445	-2.980182
C	-2.089909	-3.578091	2.607492
C	-5.341446	-1.545333	-3.668357
C	-4.163206	4.336677	-1.633602
C	3.436087	3.34501	3.23397
C	-1.74117	0.461618	3.519979
H	5.639823	-1.57349	0.913586
H	5.828512	1.112959	0.191627
H	-5.867302	-0.690427	-0.287316
H	-5.464719	1.994861	0.3341
H	2.882094	-5.742028	-0.184784
H	1.667937	-6.009425	1.973017
H	1.277494	-4.052352	3.444515
H	4.070151	-2.375402	-1.462596
H	2.106466	-3.563879	-2.493391
H	2.987863	-5.115455	-2.380976
H	3.624372	-3.807464	-3.413658
H	5.874327	-3.954532	-2.179925
H	5.260416	-5.189881	-1.038591
H	5.950209	-3.665601	-0.413373
H	1.818922	-0.583047	2.415193
H	0.787941	-0.636232	4.609082
H	1.226823	-2.343484	4.8687
H	0.035888	-1.902261	3.60355
H	4.238289	-0.828755	3.091409
H	3.738826	-1.847242	4.477047
H	3.257932	-0.122947	4.404364
H	1.936174	4.945132	1.326671
H	2.122814	5.904135	-0.965967
H	3.079816	4.549302	-2.821562

H	3.944548	0.887493	-2.417873
H	3.260979	3.070942	-4.493048
H	2.110058	1.844846	-3.880074
H	3.563908	1.341886	-4.796511
H	5.577738	3.354734	-3.287817
H	5.904862	1.662483	-3.7788
H	6.075326	2.151343	-2.064146
H	-2.755643	-5.164195	0.649935
H	-3.057336	-5.798155	-1.729174
H	-3.573655	-4.066	-3.442549
H	-2.496896	-1.647835	1.788054
H	-4.999615	-1.732324	1.961357
H	-4.227924	-2.103875	3.528519
H	-4.904299	-3.428795	2.528453
H	-1.110376	-3.711588	2.11379
H	-2.553533	-4.572668	2.751085
H	-1.917447	-3.155436	3.61392
H	-3.887206	-0.376906	-2.597814
H	-3.056763	-0.536385	-4.915624
H	-2.851373	-2.303566	-4.772957
H	-1.842487	-1.204193	-3.777723
H	-5.564283	-0.750649	-4.405429
H	-6.108602	-1.503245	-2.873109
H	-5.439029	-2.521421	-4.180753
H	-1.893845	3.54576	3.998293
H	-1.263175	5.59694	2.733471
H	-1.613822	5.714801	0.275587
H	-2.685536	2.779654	-1.791471
H	-1.860972	4.543387	-3.249185
H	-0.673392	4.371108	-1.917504
H	-1.828774	5.743481	-1.935198
H	-4.275862	5.356005	-1.216989
H	-4.922696	3.689773	-1.162011
H	-4.379577	4.382975	-2.717999
H	3.213468	1.478738	2.205452
H	1.190006	1.740271	3.605145
H	0.672074	3.162837	2.652925
H	0.73617	1.554555	1.883333
H	3.423226	2.860692	4.228882
H	4.490184	3.515036	2.945441
H	2.94829	4.332537	3.338875
H	-3.543929	0.543605	2.370303
H	-2.029368	-0.467491	4.045477

H	-1.100203	0.193866	2.663595
H	-1.145843	1.07684	4.219691
H	-4.270875	0.604459	4.705734
H	-3.450513	2.163613	4.986574
H	-4.843366	2.081351	3.867287

Table S22. Cartesian coordinates of **3** in Å.

Atomtype	X Coordinate [Å]	Y Coordinate [Å]	Z Coordinate [Å]
C	-1.443923	4.162477	-0.320945
C	-1.950142	3.298606	0.684882
C	-1.685589	3.501154	2.064567
C	-0.868324	4.589834	2.422744
C	-0.343836	5.44836	1.44796
C	-0.632474	5.237822	0.093
N	-2.8089	2.200778	0.321937
C	-2.414592	0.852786	0.313037
N	-3.617111	0.134681	0.350227
C	-4.700175	1.023993	0.382226
C	-4.205137	2.289621	0.36408
C	-3.76496	-1.29769	0.36253
C	-3.402172	-2.008261	1.543129
C	-3.532394	-3.410141	1.526495
C	-4.034086	-4.076736	0.401301
C	-4.437151	-3.351736	-0.723907
C	-4.313163	-1.949728	-0.774996
N	-1.183784	0.413789	0.306808
Ge	0.324444	1.100036	-0.887426
N	1.328713	-0.185034	0.275316
C	2.609231	-0.433593	0.314742
N	3.242256	-1.528928	0.908928
C	4.629808	-1.431148	0.73226
C	4.884801	-0.270499	0.069224
N	3.657598	0.352874	-0.185484
C	2.589123	-2.560266	1.67118
C	2.494063	-3.865286	1.124703
C	1.853125	-4.856093	1.897158
C	1.325228	-4.560304	3.156683
C	1.441336	-3.264594	3.683158
C	2.079493	-2.238251	2.962822
C	3.505271	1.712123	-0.631002
C	3.305086	2.715406	0.355071

C	3.050885	4.028475	-0.0825
C	3.041208	4.342764	-1.448088
C	3.309897	3.350801	-2.399163
C	3.545513	2.014505	-2.017117
C	3.075957	-4.231556	-0.236805
C	4.310678	-5.144734	-0.072594
C	2.247914	-0.836637	3.553816
C	3.707729	-0.585356	3.998044
C	3.862881	0.963555	-3.074174
C	5.263676	1.215289	-3.675319
C	-2.975831	-1.264561	2.811901
C	-2.203643	-2.133347	3.818424
C	-4.836969	-1.193263	-1.995528
C	-6.382646	-1.140076	-1.957517
C	-1.819006	3.98005	-1.788605
C	-3.084012	4.804138	-2.1215
Ge	-0.337757	-1.464036	0.245521
Fe	-0.31407	-1.337309	-2.593191
C	-0.192219	-1.396097	-4.361759
O	-0.103067	-1.454167	-5.521945
C	1.421692	-1.629969	-2.385442
O	2.567874	-1.874067	-2.320934
C	-1.109427	-2.893575	-2.262339
O	-1.595817	-3.944497	-2.107066
C	-1.528083	-0.039915	-2.628948
O	-2.374398	0.770129	-2.749352
C	2.025992	-4.875346	-1.16492
C	1.294422	-0.534554	4.721206
C	2.784266	0.88887	-4.174064
C	-4.20526	-0.624855	3.499512
C	-4.364169	-1.789551	-3.336945
C	-0.676508	4.323792	-2.763987
H	5.296223	-2.20925	1.100706
H	5.821157	0.182331	-0.254055
H	-5.723636	0.656716	0.409734
H	-4.70707	3.255035	0.403637
H	1.763719	-5.872157	1.494988
H	0.820347	-5.342147	3.738708
H	1.026305	-3.057255	4.674105
H	3.407634	-3.304812	-0.727655
H	1.131517	-4.238097	-1.263981
H	1.702276	-5.866259	-0.794663
H	2.45252	-5.015624	-2.174843

H	4.75832	-5.36748	-1.059428
H	4.035594	-6.106503	0.401048
H	5.086063	-4.670964	0.558558
H	2.001908	-0.119748	2.750806
H	1.365486	0.532623	4.995044
H	1.548793	-1.123354	5.622759
H	0.247783	-0.745148	4.45152
H	4.425258	-0.713094	3.170527
H	3.988259	-1.283999	4.809008
H	3.816527	0.44655	4.381441
H	2.860146	4.814153	0.658107
H	2.831059	5.369904	-1.772547
H	3.324022	3.611085	-3.464022
H	3.88724	-0.018246	-2.577262
H	2.750414	1.813808	-4.780511
H	1.783404	0.715835	-3.741262
H	2.99808	0.046445	-4.856673
H	5.306271	2.190613	-4.196955
H	5.513317	0.425757	-4.40881
H	6.045339	1.218468	-2.892092
H	-3.238851	-3.99454	2.403774
H	-4.112915	-5.171157	0.403979
H	-4.837391	-3.883735	-1.593595
H	-2.299336	-0.447462	2.508631
H	-4.738858	0.068727	2.8275
H	-3.892434	-0.054602	4.394467
H	-4.916904	-1.408134	3.822337
H	-1.323821	-2.612152	3.353678
H	-2.844585	-2.922222	4.255163
H	-1.853781	-1.506101	4.657904
H	-4.453851	-0.161049	-1.951563
H	-4.678566	-1.130167	-4.166658
H	-4.804252	-2.787594	-3.52033
H	-3.267517	-1.883866	-3.36955
H	-6.769458	-0.540923	-2.803432
H	-6.76434	-0.697215	-1.019334
H	-6.808083	-2.158574	-2.037683
H	-0.636044	4.761679	3.480713
H	0.295214	6.289671	1.746824
H	-0.220318	5.919651	-0.658806
H	-2.075637	2.91832	-1.937465
H	-0.94368	3.986632	-3.782194
H	0.266757	3.828669	-2.472167

H	-0.492962	5.414335	-2.815907
H	-2.898822	5.884746	-1.967734
H	-3.938581	4.510489	-1.486268
H	-3.376161	4.649247	-3.177066
C	3.379004	2.408655	1.847199
H	3.584467	1.333274	1.966777
C	4.552446	3.160017	2.511361
C	2.046851	2.706682	2.555306
H	2.08964	2.382004	3.610743
H	1.813409	3.785677	2.540368
H	1.211568	2.17966	2.066423
H	4.62985	2.880785	3.579305
H	5.513079	2.917319	2.020521
H	4.40981	4.255815	2.457769
C	-2.255629	2.581742	3.143425
H	-2.964893	1.886966	2.664658
C	-1.147261	1.724626	3.783822
C	-3.052978	3.363387	4.207551
H	-1.575773	1.034157	4.532529
H	-0.626267	1.125313	3.018767
H	-0.397288	2.356093	4.293967
H	-3.521724	2.661697	4.922946
H	-2.403005	4.045569	4.787033
H	-3.853164	3.968676	3.743083

Table S23. Cartesian coordinates of **4** in Å.

Atomtype	X Coordinate [Å]	Y Coordinate [Å]	Z Coordinate [Å]
C	-3.078677	-2.649434	1.483442
C	-3.54454	-1.993583	0.307405
C	-3.866279	-2.713819	-0.875943
C	-3.648429	-4.106876	-0.876818
C	-3.151503	-4.763484	0.254493
C	-2.882019	-4.042225	1.426505
N	-3.717462	-0.568714	0.341242
C	-2.68631	0.396506	0.326323
N	-3.383965	1.627846	0.389015
C	-4.765308	1.399203	0.454016
C	-4.969851	0.057121	0.412043
N	-1.402481	0.207851	0.296015
Sn	-0.160011	-1.69238	-0.120032
Fe	0.055971	-0.654865	-2.983438

C	0.336195	0.126922	-4.552739
O	0.536612	0.61959	-5.589736
C	-2.80006	2.879419	0.785996
C	-2.541049	3.081612	2.16639
C	-1.969032	4.308561	2.557609
C	-1.678355	5.302142	1.612181
C	-1.973804	5.094068	0.25759
C	-2.544924	3.88488	-0.185628
C	-2.931932	3.688663	-1.648245
C	-4.35477	4.235174	-1.904564
C	-4.497839	-2.052911	-2.096907
C	-6.008102	-2.379952	-2.146109
C	-2.857088	-1.867826	2.777209
C	-4.205577	-1.580196	3.478432
Sn	0.207586	1.521958	-0.689997
N	1.426218	-0.063299	0.386628
C	2.714664	-0.151808	0.520311
N	3.689326	0.858783	0.358782
C	4.972089	0.334177	0.571826
C	4.837839	-0.977278	0.903178
N	3.471795	-1.283937	0.886202
C	3.42927	2.241374	0.06966
C	2.876912	3.078724	1.088134
C	2.624349	4.423901	0.75758
C	2.932156	4.932406	-0.514505
C	3.501252	4.102705	-1.484497
C	3.755304	2.740829	-1.218417
C	4.374937	1.867698	-2.302941
C	3.582667	1.946198	-3.622058
C	2.916414	-2.494474	1.416414
C	2.89178	-3.66182	0.612216
C	2.297676	-4.818058	1.156125
C	1.753135	-4.814728	2.44776
C	1.837466	-3.663502	3.244995
C	2.439525	-2.487768	2.756008
C	3.564494	-3.701401	-0.754526
C	2.688008	-4.34003	-1.846767
C	-1.936536	4.319939	-2.639517
C	-3.819668	-2.461374	-3.417344
C	-1.896403	-2.563641	3.753716
C	4.924237	-4.427201	-0.647632
C	5.855449	2.245348	-2.521121
C	-0.324657	-2.329429	-3.435576

O	-0.566568	-3.427866	-3.751352
C	-1.544535	0.082118	-2.729835
O	-2.620534	0.556043	-2.703209
C	1.780879	-0.801614	-2.57694
O	2.940328	-0.920516	-2.436053
H	-5.46934	2.224333	0.541846
H	-5.88818	-0.524911	0.427771
H	-1.756058	4.487813	3.618421
H	-1.228941	6.250071	1.934779
H	-1.756896	5.884207	-0.469642
H	-2.959983	2.603644	-1.842714
H	-4.397155	5.323679	-1.705776
H	-5.101614	3.741072	-1.25985
H	-4.648129	4.063572	-2.957279
H	-1.992995	5.425561	-2.632451
H	-2.169106	3.982573	-3.665954
H	-0.894259	4.030776	-2.411592
H	-3.871987	-4.681463	-1.782825
H	-2.978979	-5.846856	0.227622
H	-2.505128	-4.57468	2.305233
H	-4.383676	-0.962389	-1.99659
H	-6.529016	-2.082879	-1.217723
H	-6.165467	-3.467035	-2.282034
H	-6.488619	-1.855676	-2.993966
H	-4.239388	-1.867284	-4.249348
H	-3.984117	-3.529776	-3.652853
H	-2.734448	-2.280451	-3.383313
H	-2.399827	-0.89911	2.504614
H	-4.041969	-0.971035	4.387123
H	-4.691642	-2.527032	3.781474
H	-4.902497	-1.028889	2.825043
H	-2.32995	-3.497879	4.15813
H	-1.69854	-1.898609	4.61319
H	-0.931045	-2.804813	3.27411
H	5.580928	-1.734296	1.148185
H	5.858422	0.953426	0.448163
H	2.262032	-5.733228	0.553972
H	1.279972	-5.721956	2.844712
H	1.44422	-3.680552	4.268698
H	3.765056	-2.662296	-1.060117
H	1.700915	-3.854556	-1.911318
H	2.527282	-5.420219	-1.669454
H	3.175275	-4.230939	-2.83258

H	5.441538	-4.420607	-1.625573
H	4.787367	-5.481252	-0.338091
H	5.583199	-3.939843	0.095112
H	3.740839	4.505078	-2.475615
H	2.724591	5.985014	-0.74529
H	2.174439	5.092157	1.497369
H	4.338962	0.821225	-1.963757
H	3.65776	2.946714	-4.088025
H	2.515305	1.719811	-3.459589
H	3.972374	1.205947	-4.343894
H	5.951735	3.292407	-2.867032
H	6.310015	1.589711	-3.28756
H	6.442047	2.143889	-1.5888
C	2.588927	-1.264678	3.659843
H	3.176007	-0.510818	3.113947
C	1.222544	-0.629712	3.971752
C	3.375042	-1.591753	4.947464
H	1.347361	0.315595	4.530926
H	0.683743	-0.411452	3.034558
H	0.598838	-1.305083	4.583233
H	3.541464	-0.670422	5.537081
H	2.823741	-2.304648	5.589276
H	4.360825	-2.035538	4.715449
C	2.574628	2.523913	2.483527
H	2.059198	1.560185	2.332535
C	3.868708	2.256834	3.287186
C	1.624376	3.40334	3.31001
H	1.317006	2.86055	4.221613
H	2.114382	4.340514	3.63969
H	0.714654	3.663613	2.742354
H	3.618753	1.825517	4.27478
H	4.541037	1.54961	2.775675
H	4.41878	3.20198	3.455793
C	-2.879549	2.022789	3.214518
H	-3.347071	1.169834	2.699586
C	-1.609372	1.488952	3.897879
C	-3.910975	2.543491	4.237444
H	-4.175007	1.744205	4.955291
H	-3.509788	3.398164	4.814168
H	-4.838147	2.87601	3.735336
H	-1.851897	0.638416	4.561065
H	-0.888666	1.142825	3.139589
H	-1.119931	2.268064	4.510282

Table S24. Cartesian coordinates of **D** in Å.

Atomtype	X Coordinate [Å]	Y Coordinate [Å]	Z Coordinate [Å]
C	-1.599942	-3.201766	-2.368775
C	-1.354945	-3.114269	-0.975213
C	-0.134653	-3.540123	-0.385589
C	0.830571	-4.115037	-1.232956
C	0.58934	-4.26035	-2.608336
C	-0.611652	-3.808149	-3.170066
N	-2.339725	-2.496059	-0.143171
C	-2.281924	-1.123448	0.195062
N	-3.550002	-0.866495	0.749445
C	-4.324591	-2.033833	0.764835
C	-3.581758	-3.034273	0.211535
N	-1.306173	-0.30161	0.077507
Ge	0.009003	-0.025362	-1.205935
N	1.462662	0.178152	-0.058922
C	2.42646	1.022641	-0.021598
N	2.440351	2.391571	-0.379347
C	3.69583	2.95365	-0.112998
C	4.482335	1.977373	0.420992
N	3.724941	0.801325	0.475674
C	1.318408	3.091066	-0.925536
C	1.318079	3.405354	-2.307583
C	0.227045	4.137287	-2.817125
C	-0.839546	4.503624	-1.988161
C	-0.843492	4.137759	-0.632535
C	0.234121	3.43167	-0.066303
C	2.435867	2.939158	-3.238094
C	3.266394	4.129113	-3.762474
C	0.255827	3.034605	1.41029
C	1.190054	3.957587	2.225334
C	4.10922	-0.38934	1.17136
C	4.826834	-1.39413	0.474938
C	5.205262	-2.545169	1.192507
C	4.878389	-2.688118	2.548869
C	4.155119	-1.68758	3.210851
C	3.752559	-0.518169	2.537416
C	5.095749	-1.260809	-1.022819
C	6.446656	-1.853409	-1.464985
C	2.899376	0.533271	3.244052

C	3.495992	0.979611	4.593522
C	-3.975909	0.433789	1.166174
C	-4.270896	1.40456	0.172715
C	-4.679064	2.679227	0.611855
C	-4.797245	2.967596	1.97921
C	-4.492747	1.99398	2.940454
C	-4.062707	0.709282	2.554987
C	-4.177055	1.051149	-1.31349
C	-5.41268	0.241971	-1.768477
C	-3.612921	-0.336708	3.576649
C	-2.071204	-0.323533	3.70162
C	0.09007	-3.375657	1.116211
C	1.569194	-3.248214	1.508621
C	-2.867835	-2.626011	-2.999049
C	-3.793211	-3.74512	-3.520128
C	3.924718	-1.884954	-1.817275
C	1.449133	0.025872	3.405129
C	-1.138463	2.967359	2.051495
C	1.883135	2.080354	-4.395594
C	-3.954354	2.264652	-2.231299
C	-4.274938	-0.190976	4.958012
C	-0.599042	-4.521449	1.890995
C	-2.543643	-1.600503	-4.105574
H	5.512746	2.002448	0.774549
H	3.90548	3.999653	-0.334034
H	-3.817738	-4.08302	0.034058
H	-5.333747	-2.038273	1.175563
H	5.756042	-3.344558	0.683718
H	5.179267	-3.594644	3.090075
H	3.883945	-1.821968	4.265054
H	5.113712	-0.180415	-1.259431
H	2.9599	-1.440738	-1.517988
H	3.868134	-2.973585	-1.625867
H	4.064473	-1.733586	-2.904915
H	6.635455	-1.613488	-2.527976
H	6.460256	-2.956164	-1.374775
H	7.283906	-1.452225	-0.864068
H	2.859311	1.42793	2.598584
H	0.814402	0.813195	3.851639
H	1.412686	-0.858504	4.07011
H	1.022373	-0.249897	2.425821
H	4.537096	1.334322	4.477581
H	3.496431	0.157481	5.33401

H	2.894376	1.805074	5.018717
H	-1.7053	4.400919	-0.011025
H	-1.687632	5.063235	-2.403445
H	0.204917	4.403033	-3.881286
H	3.113043	2.293636	-2.651133
H	1.242271	2.67596	-5.072742
H	1.280828	1.238718	-4.006894
H	2.714938	1.669005	-4.998482
H	2.639021	4.818866	-4.358691
H	4.090608	3.77464	-4.410259
H	3.706245	4.708847	-2.929824
H	1.788803	-4.444004	-0.81787
H	1.356179	-4.71365	-3.25006
H	-0.774996	-3.900453	-4.251057
H	-0.396581	-2.428181	1.409832
H	-1.678906	-4.573135	1.662577
H	-0.486414	-4.371575	2.981818
H	-0.144543	-5.496663	1.629843
H	2.059634	-2.430508	0.953378
H	2.131227	-4.186083	1.339361
H	1.65092	-3.013516	2.583813
H	-3.420011	-2.081645	-2.21353
H	-3.474766	-1.122098	-4.464464
H	-2.056272	-2.078745	-4.975909
H	-1.868088	-0.811902	-3.726953
H	-4.722127	-3.317693	-3.943364
H	-4.072503	-4.442946	-2.709178
H	-3.294954	-4.332155	-4.315184
H	-4.574619	2.245812	4.003434
H	-5.120883	3.966657	2.299419
H	-4.910169	3.458904	-0.122121
H	-3.290446	0.404985	-1.434112
H	-3.747624	1.918583	-3.260967
H	-3.092179	2.866742	-1.89626
H	-4.845771	2.919562	-2.278268
H	-6.333873	0.847607	-1.669562
H	-5.538068	-0.678295	-1.171758
H	-5.306837	-0.053567	-2.829668
H	0.665991	2.010931	1.453909
H	-1.054748	2.561822	3.074917
H	-1.60951	3.964759	2.13635
H	-1.810086	2.303524	1.482328
H	1.245712	3.609428	3.274451

H	2.216699	3.968825	1.819578
H	0.807282	4.996383	2.228827
H	-3.896903	-1.330289	3.183357
H	-1.72305	-1.16814	4.326126
H	-1.577706	-0.383664	2.716732
H	-1.73804	0.614855	4.181904
H	-4.007897	-1.053515	5.596292
H	-3.928568	0.71919	5.483251
H	-5.377128	-0.143439	4.881813

Table S25. Cartesian coordinates of **12** in Å.

Atomtype	X Coordinate [Å]	Y Coordinate [Å]	Z Coordinate [Å]
C	3.64632	2.084165	-1.928594
C	3.77637	1.62947	-0.587259
C	3.853109	2.536299	0.503252
C	3.770346	3.917245	0.234991
C	3.627562	4.382985	-1.076348
C	3.575736	3.474699	-2.142888
N	3.824052	0.223912	-0.301992
C	2.683757	-0.523269	0.133905
N	3.266619	-1.750294	0.577538
C	4.661481	-1.711215	0.437052
C	5.001411	-0.499391	-0.080257
N	1.46836	-0.129429	0.152906
Sn	-0.40815	-1.303958	-0.232112
Fe	-0.589615	-0.585125	-3.122467
C	-2.087418	0.214349	-2.813495
O	-3.072817	0.842539	-2.698769
C	2.577671	-2.738671	1.357934
C	2.260394	-3.988646	0.7657
C	1.619142	-4.960034	1.560631
C	1.285646	-4.693005	2.892216
C	1.600689	-3.450349	3.46104
C	2.256258	-2.451202	2.716884
C	2.618752	-4.298932	-0.685695
C	1.498134	-5.055866	-1.427121
C	2.647425	-1.119958	3.361986
C	1.783324	-0.735838	4.574312
C	4.067506	2.055474	1.935339
C	2.981045	2.576595	2.892832

C	3.605201	1.098693	-3.098629
C	3.008139	1.6961	-4.386502
Li	0.431528	1.537687	0.017743
N	-1.303948	0.59366	0.41314
C	-2.51683	0.948886	0.619198
N	-2.949698	2.30005	0.748988
C	-4.320733	2.361455	1.008653
C	-4.79457	1.08531	1.031966
N	-3.717105	0.210603	0.812805
C	-1.987951	3.35192	0.860151
C	-1.661029	4.12943	-0.284418
C	-0.599749	5.050516	-0.170024
C	0.107494	5.196058	1.033303
C	-0.252129	4.442663	2.159634
C	-1.30596	3.508641	2.096593
C	-2.469808	3.991223	-1.570317
C	-1.66166	4.24807	-2.85527
C	-1.700604	2.705369	3.333169
C	-2.240391	3.628864	4.445674
C	-3.813844	-1.216508	0.919158
C	-3.298444	-1.862939	2.082234
C	-3.397662	-3.265303	2.155134
C	-4.012998	-4.005583	1.135485
C	-4.545542	-3.35127	0.021207
C	-4.452292	-1.950466	-0.115258
C	-2.702771	-1.051903	3.234305
C	-3.810793	-0.334736	4.040111
C	-5.062922	-1.273423	-1.337652
C	-4.613915	-1.94062	-2.653239
C	3.945231	-5.086822	-0.774297
C	4.140036	-1.112293	3.763572
C	5.012034	0.534068	-3.407673
C	-1.825769	-1.881643	4.185739
C	-6.603929	-1.243351	-1.236129
C	-3.702934	4.924076	-1.521098
C	-0.34212	-1.095566	-5.187421
C	0.171493	0.809886	-2.513119
O	0.591567	1.8364	-2.085025
C	5.481316	2.423646	2.432998
C	-0.547141	1.824229	3.84545
H	5.28655	-2.550768	0.738068
H	5.980781	-0.078468	-0.305317
H	-5.803728	0.706586	1.186275

H	-4.835811	3.310029	1.154259
H	1.367738	-5.934383	1.126675
H	0.775816	-5.456151	3.494687
H	1.333502	-3.262678	4.505919
H	2.776281	-3.327626	-1.191406
H	0.523105	-4.554516	-1.296542
H	1.401107	-6.095384	-1.062567
H	1.71988	-5.10858	-2.508516
H	4.208595	-5.286994	-1.830307
H	3.852929	-6.059047	-0.253321
H	4.781468	-4.533441	-0.312936
H	2.485272	-0.3382	2.599958
H	2.011511	0.299455	4.882794
H	1.979442	-1.388105	5.446446
H	0.711055	-0.788792	4.335121
H	4.801787	-1.275038	2.896971
H	4.341495	-1.90338	4.510781
H	4.409253	-0.138566	4.214401
H	3.823532	4.632337	1.065139
H	3.556645	5.460768	-1.273045
H	3.460212	3.862744	-3.159318
H	2.961863	0.256261	-2.778182
H	3.662346	2.484837	-4.803352
H	2.006606	2.122389	-4.213624
H	2.926505	0.916684	-5.165166
H	5.7013	1.351434	-3.693954
H	4.960614	-0.17979	-4.251959
H	5.445063	0.002024	-2.546001
H	-2.993258	-3.796171	3.022443
H	-4.080343	-5.098353	1.217148
H	-5.039545	-3.934771	-0.764888
H	-2.053748	-0.281079	2.78299
H	-4.418953	0.332099	3.406479
H	-3.360567	0.279517	4.843022
H	-4.484724	-1.075096	4.511979
H	-1.020821	-2.409782	3.645034
H	-2.42059	-2.628712	4.744765
H	-1.362947	-1.218274	4.937553
H	-4.703921	-0.232759	-1.362264
H	-4.925686	-1.324389	-3.516121
H	-5.058315	-2.946403	-2.778298
H	-3.515796	-2.038561	-2.683984
H	-7.03923	-0.720832	-2.109083

H	-6.941689	-0.722565	-0.32151
H	-7.018418	-2.269519	-1.20969
H	0.297328	4.572693	3.100187
H	0.944757	5.903331	1.091774
H	-0.309821	5.650722	-1.039471
H	-2.838848	2.952491	-1.609624
H	-2.265845	3.958124	-3.734389
H	-0.729051	3.660973	-2.868265
H	-1.405471	5.319074	-2.971803
H	-3.386597	5.983967	-1.470031
H	-4.338784	4.717793	-0.64252
H	-4.320767	4.791631	-2.429265
H	4.002817	0.957093	1.935808
H	3.119113	2.147406	3.901957
H	3.011781	3.677925	2.990551
H	1.974727	2.296381	2.540858
H	5.647898	2.028516	3.453098
H	6.258499	2.001489	1.769635
H	5.620373	3.521041	2.464301
H	-2.522167	2.029197	3.046944
H	-0.895761	1.179331	4.672197
H	-0.166141	1.17144	3.041007
H	0.291956	2.431769	4.230645
H	-2.58288	3.029322	5.310525
H	-1.458267	4.324905	4.804474
H	-3.093399	4.23304	4.085175
C	0.874291	-1.331399	-4.475858
C	0.630825	-2.319601	-3.463249
C	-0.74509	-2.692861	-3.535134
C	-1.344401	-1.928357	-4.595096
H	-2.397008	-1.962087	-4.884844
H	-1.253925	-3.421909	-2.900842
H	1.374605	-2.710242	-2.770731
H	1.829429	-0.839613	-4.658617
H	-0.488199	-0.394945	-6.011687

Table S26. Cartesian coordinates of **11** in Å.

Atomtype	X Coordinate [Å]	Y Coordinate [Å]	Z Coordinate [Å]
C	2.260158	3.52096	-1.669224
C	1.793603	3.204778	-0.367016

C	0.518388	3.623316	0.104686
C	-0.258404	4.431742	-0.748066
C	0.213431	4.810571	-2.015031
C	1.457683	4.357962	-2.471032
N	2.5895	2.349284	0.455037
C	2.387119	0.941099	0.468197
N	3.573271	0.448256	1.063241
C	4.428103	1.503958	1.403356
C	3.828603	2.668701	1.024301
N	1.382807	0.260758	0.076773
Sn	-0.019772	0.368647	-1.451232
N	-1.637192	-0.051925	-0.204608
C	-2.474001	-0.990343	0.005773
N	-2.464331	-2.347608	-0.427102
C	-3.564717	-3.038839	0.098371
C	-4.298603	-2.157417	0.834315
N	-3.656096	-0.915385	0.782503
C	-1.49647	-2.875712	-1.333704
C	-1.606843	-2.547794	-2.715383
C	-0.621932	-3.049988	-3.58979
C	0.429336	-3.843253	-3.109672
C	0.521186	-4.150965	-1.745248
C	-0.436141	-3.675187	-0.826999
C	-2.773367	-1.694865	-3.222774
C	-4.061009	-2.538333	-3.357905
C	-0.316382	-3.954996	0.671036
C	0.416349	-5.269494	0.998498
C	-4.148135	0.305098	1.339364
C	-4.81483	1.223999	0.491039
C	-5.261525	2.436151	1.054258
C	-5.070638	2.71122	2.414287
C	-4.421105	1.780667	3.239374
C	-3.937986	0.565591	2.718626
C	-5.035903	0.931858	-0.991774
C	-6.52637	1.009839	-1.38171
C	-3.131619	-0.4112	3.571985
C	-3.577366	-0.469356	5.044395
C	3.817024	-0.947686	1.251494
C	4.072846	-1.754692	0.110811
C	4.255018	-3.136011	0.315974
C	4.201888	-3.687973	1.604348
C	3.954867	-2.870834	2.715815
C	3.74468	-1.48638	2.562284

C	4.18917	-1.122546	-1.277055
C	5.565168	-0.440277	-1.449065
C	3.348071	-0.597189	3.741565
C	1.811535	-0.434136	3.775809
C	0.034699	3.204434	1.493284
C	-1.494798	3.206423	1.644152
C	3.569234	2.950114	-2.215597
C	4.652134	4.043537	-2.327075
C	-4.171629	1.85845	-1.872569
C	-1.623791	-0.090658	3.460033
C	0.35845	-2.768719	1.394488
C	-2.477764	-0.95359	-4.538824
C	3.910796	-2.095877	-2.434735
C	3.877304	-1.083986	5.102371
C	0.704075	4.075468	2.580197
C	3.366213	2.224232	-3.562135
H	-5.223978	-2.292938	1.393839
H	-3.722067	-4.097142	-0.108534
H	4.168073	3.70094	1.105486
H	5.384916	1.324966	1.893226
H	-5.768845	3.1717	0.417227
H	-5.427708	3.659597	2.836717
H	-4.272638	2.015366	4.299525
H	-4.705085	-0.104278	-1.180286
H	-3.108276	1.766301	-1.593618
H	-4.476191	2.91603	-1.752696
H	-4.280336	1.591139	-2.941105
H	-6.660942	0.720121	-2.441371
H	-6.924283	2.035395	-1.263649
H	-7.139982	0.333881	-0.757698
H	-3.278844	-1.420841	3.14638
H	-1.026293	-0.873476	3.96007
H	-1.397775	0.874816	3.951401
H	-1.300036	-0.018525	2.407315
H	-4.664604	-0.650553	5.135741
H	-3.34155	0.467811	5.58348
H	-3.043935	-1.284715	5.567707
H	1.358087	-4.760948	-1.389208
H	1.190724	-4.21864	-3.805565
H	-0.670705	-2.815792	-4.658429
H	-2.962555	-0.919747	-2.458138
H	-2.410113	-1.647852	-5.397925
H	-1.533172	-0.383051	-4.478615

H	-3.295325	-0.242114	-4.757359
H	-3.923743	-3.338772	-4.109956
H	-4.904825	-1.900493	-3.684053
H	-4.342388	-3.006735	-2.399447
H	-1.249317	4.766238	-0.423741
H	-0.406127	5.448397	-2.658929
H	1.801826	4.634983	-3.4753
H	0.366887	2.160982	1.642866
H	1.805919	4.026403	2.516033
H	0.403563	3.730362	3.587921
H	0.398068	5.134234	2.474461
H	-1.97433	2.560497	0.888008
H	-1.921188	4.225346	1.577681
H	-1.773468	2.806316	2.633259
H	3.935877	2.19418	-1.500259
H	4.308194	1.736628	-3.876426
H	3.069051	2.923667	-4.365809
H	2.584765	1.446712	-3.481785
H	5.6046	3.613943	-2.691558
H	4.840474	4.518607	-1.346987
H	4.341124	4.836014	-3.034343
H	3.90377	-3.322148	3.712665
H	4.348067	-4.767287	1.74199
H	4.444674	-3.793287	-0.539619
H	3.415688	-0.338366	-1.337741
H	3.87017	-1.538368	-3.38897
H	2.944392	-2.61374	-2.299255
H	4.706131	-2.859215	-2.53678
H	6.380314	-1.187429	-1.398806
H	5.741298	0.316019	-0.663766
H	5.623621	0.067833	-2.430362
H	-1.344919	-4.043158	1.069918
H	0.368786	-2.949659	2.485168
H	1.402214	-2.643128	1.058437
H	-0.157221	-1.81544	1.20217
H	0.328609	-5.48606	2.079259
H	0.000626	-6.127469	0.43752
H	1.496945	-5.195998	0.773568
H	3.776996	0.406457	3.567695
H	1.511659	0.307996	4.539645
H	1.409197	-0.119062	2.79807
H	1.336825	-1.399025	4.031678
H	3.662442	-0.329223	5.881428

H	3.387122	-2.023928	5.419205
H	4.969107	-1.258535	5.079374

Table S27. Cartesian coordinates of germylenoid of **D** shown in **Figure S48** in Å.

Atomtype	X Coordinate [Å]	Y Coordinate [Å]	Z Coordinate [Å]
C	3.547995	2.243088	-1.519341
C	3.430102	1.809277	-0.173236
C	2.99447	2.67618	0.869215
C	2.719701	4.016489	0.535024
C	2.868919	4.475851	-0.783335
C	3.277779	3.600297	-1.79654
N	3.64949	0.431456	0.133692
C	2.569425	-0.479194	0.224404
N	3.206281	-1.726323	0.37148
C	4.598677	-1.56849	0.391238
C	4.872294	-0.241383	0.236664
N	1.329369	-0.151886	0.202818
Ge	-0.254505	-1.200946	-0.36696
N	-1.294781	0.419891	0.046361
C	-2.548982	0.661814	-0.080383
N	-3.662962	-0.178659	-0.276332
C	-4.848811	0.567701	-0.248673
C	-4.516684	1.880489	-0.087634
N	-3.121157	1.952035	-0.0108
C	-3.583505	-1.608765	-0.325509
C	-3.477631	-2.251053	-1.589053
C	-3.389642	-3.656106	-1.596357
C	-3.386781	-4.389024	-0.40016
C	-3.468909	-3.730579	0.83254
C	-3.565748	-2.326767	0.895838
C	-3.452471	-1.440157	-2.884625
C	-4.887169	-1.126736	-3.367367
C	-3.612451	-1.622323	2.250394
C	-4.900269	-1.972258	3.024751
C	-2.315423	3.110043	0.21318
C	-1.574327	3.646863	-0.878796
C	-0.726185	4.741302	-0.613533
C	-0.625715	5.282426	0.677643
C	-1.358045	4.731853	1.737162
C	-2.206835	3.624308	1.531314

C	-1.708552	3.049651	-2.28325
C	-3.029884	3.502135	-2.945366
C	-2.907506	2.930142	2.700302
C	-3.37549	3.896126	3.8046
C	2.491742	-2.914554	0.731157
C	2.060573	-3.79395	-0.295339
C	1.324308	-4.930443	0.088881
C	0.999512	-5.158031	1.434073
C	1.411758	-4.258486	2.426543
C	2.171631	-3.11868	2.097352
C	2.372055	-3.491287	-1.760985
C	3.758121	-4.050553	-2.152951
C	2.57095	-2.108973	3.174314
C	1.352392	-1.265587	3.61166
C	2.852824	2.151792	2.299057
C	1.843463	2.943325	3.149018
C	3.972828	1.285393	-2.630648
C	5.482194	1.445048	-2.92214
C	-0.513065	3.34801	-3.205779
C	-1.995843	1.822628	3.280189
C	-2.349717	-1.93005	3.080473
C	-2.643528	-2.107941	-4.011118
C	1.285853	-3.984592	-2.734283
C	3.255752	-2.776197	4.384215
C	4.230213	2.0882	2.996021
C	3.142186	1.441973	-3.919093
H	-5.139871	2.772413	-0.030086
H	-5.821056	0.085911	-0.343487
H	5.823224	0.28768	0.188617
H	5.262105	-2.420628	0.534978
H	-0.127898	5.172398	-1.422106
H	0.042479	6.134006	0.859902
H	-1.250785	5.153846	2.742658
H	-1.745286	1.949595	-2.174295
H	0.452052	3.087253	-2.73488
H	-0.475148	4.414181	-3.502273
H	-0.598836	2.742232	-4.124506
H	-3.139153	3.029022	-3.939327
H	-3.040925	4.600673	-3.082856
H	-3.906739	3.220069	-2.337058
H	-3.808827	2.430787	2.300797
H	-2.538232	1.240675	4.049151
H	-1.103173	2.26954	3.756708

H	-1.651929	1.130433	2.491754
H	-3.982058	4.723934	3.392667
H	-2.522553	4.337664	4.354009
H	-3.989438	3.351814	4.54588
H	-3.447216	-4.311822	1.762806
H	-3.30565	-5.483488	-0.431664
H	-3.302634	-4.187484	-2.54999
H	-2.947028	-0.484329	-2.653362
H	-3.152162	-3.009793	-4.403452
H	-1.630837	-2.376081	-3.66696
H	-2.529415	-1.400071	-4.85201
H	-5.432842	-2.063672	-3.591842
H	-4.857892	-0.518042	-4.291193
H	-5.464756	-0.567292	-2.611548
H	2.372803	4.710354	1.307123
H	2.646174	5.523695	-1.022786
H	3.369627	3.968397	-2.824729
H	2.467447	1.119787	2.22526
H	4.936797	1.456058	2.430047
H	4.12929	1.661935	4.012409
H	4.668308	3.100478	3.088379
H	0.875017	3.059369	2.630022
H	2.216817	3.954187	3.401829
H	1.659246	2.413768	4.101736
H	3.80415	0.257817	-2.261242
H	3.432662	0.658622	-4.64356
H	3.315866	2.419859	-4.407525
H	2.065275	1.323427	-3.711105
H	5.807416	0.720318	-3.692217
H	6.092212	1.280596	-2.015589
H	5.699651	2.464064	-3.296334
H	1.130585	-4.437019	3.471715
H	0.40583	-6.039672	1.709284
H	0.969656	-5.630237	-0.675534
H	2.41199	-2.390693	-1.86319
H	1.474455	-3.571518	-3.741464
H	0.284224	-3.648188	-2.413997
H	1.280581	-5.088414	-2.820137
H	3.775043	-5.152737	-2.049665
H	4.559143	-3.635217	-1.515651
H	3.993198	-3.800159	-3.204965
H	-3.624537	-0.533537	2.06959
H	-2.35208	-1.348809	4.021453

H	-2.289144	-3.002832	3.343577
H	-1.438516	-1.669536	2.516604
H	-4.937267	-1.421924	3.984356
H	-5.801724	-1.709881	2.440281
H	-4.948178	-3.053879	3.25383
H	3.305498	-1.412757	2.731544
H	1.659147	-0.49597	4.346043
H	0.898946	-0.758088	2.742432
H	0.581942	-1.902724	4.084772
H	3.605535	-2.005893	5.097333
H	2.561255	-3.440893	4.931772
H	4.127259	-3.380142	4.07038
Li	0.345998	1.466739	-0.21957
Cl	0.092476	-0.299438	-2.693445

Table S28. Cartesian coordinates of stannylenoid of **11** shown in **Figure S48** in Å.

Atomtype	X Coordinate [Å]	Y Coordinate [Å]	Z Coordinate [Å]
C	3.03491	-2.979086	1.929269
C	3.351325	-2.237075	0.761599
C	3.382634	-2.823448	-0.534789
C	3.089421	-4.198028	-0.63009
C	2.777876	-4.95163	0.510594
C	2.752304	-4.350863	1.776361
N	3.611848	-0.837378	0.889572
C	2.662715	0.170825	0.599258
N	3.410264	1.368753	0.775434
C	4.72564	1.084036	1.158551
C	4.845927	-0.270706	1.241163
C	2.924347	2.613296	0.272856
C	3.214741	2.968712	-1.06898
C	2.705266	4.193938	-1.548638
C	1.913514	5.012311	-0.734085
C	1.602849	4.62085	0.578053
C	2.096544	3.412766	1.106791
C	4.026737	2.05759	-1.986889
C	3.204184	1.615713	-3.214956
C	1.784993	2.961466	2.533531
C	2.937106	3.34552	3.488694
N	1.428803	0.116824	0.268279
Sn	0.023228	-1.518506	-0.274779

Cl	0.141379	-0.655708	-2.742205
C	3.714874	-1.981321	-1.770769
C	3.184432	-2.571429	-3.088559
C	2.941288	-2.287469	3.291032
C	3.287543	-3.207871	4.476206
N	-1.436504	0.130208	0.044493
C	-2.688808	0.175828	-0.22228
N	-3.649991	-0.850008	-0.412295
C	-4.926412	-0.30496	-0.602753
C	-4.810627	1.051954	-0.584656
N	-3.460805	1.359106	-0.374469
C	-3.375199	-2.241017	-0.22447
C	-3.116765	-3.057907	-1.359922
C	-2.843294	-4.420996	-1.132798
C	-2.802815	-4.945733	0.16705
C	-3.045131	-4.118444	1.27085
C	-3.339203	-2.75179	1.098992
C	-2.914412	2.667759	-0.212197
C	-2.120889	3.215974	-1.259501
C	-1.575483	4.500843	-1.060542
C	-1.821943	5.216264	0.120134
C	-2.604932	4.656832	1.138446
C	-3.157107	3.367089	1.000867
C	-3.137321	-2.476584	-2.773771
C	-2.145134	-3.160571	-3.732651
C	-3.59671	-1.865073	2.31581
C	-2.349647	-1.774115	3.218422
C	-1.913417	2.449682	-2.568179
C	-0.642936	2.856744	-3.336141
C	-3.931325	2.701196	2.139975
C	-2.986219	1.811838	2.981024
C	-4.564472	-2.518965	-3.366637
C	-4.834859	-2.338337	3.106287
C	-3.160359	2.578589	-3.472351
C	-4.6969	3.689912	3.037342
C	5.23518	-1.721836	-1.880103
C	1.543163	-1.653562	3.483146
C	0.438111	3.486125	3.059567
C	5.358569	2.719124	-2.397764
Li	0.034338	1.394377	-0.142716
H	-5.558639	1.833005	-0.718416
H	-5.801464	-0.941362	-0.727132
H	5.45266	1.875889	1.337211

S88

H	5.690437	-0.894845	1.531983
H	-0.948784	4.949696	-1.837607
H	-1.390926	6.217477	0.25011
H	-2.772455	5.225378	2.059961
H	-1.795804	1.379145	-2.320719
H	0.254534	2.855786	-2.690557
H	-0.735996	3.863687	-3.787222
H	-0.458241	2.130915	-4.146415
H	-3.022058	1.985607	-4.395849
H	-3.327419	3.634697	-3.75986
H	-4.068243	2.209867	-2.963289
H	-4.681358	2.029925	1.68373
H	-3.566809	1.211206	3.706306
H	-2.274121	2.437963	3.549061
H	-2.402971	1.124637	2.343637
H	-5.337649	4.368597	2.444403
H	-4.011079	4.310711	3.644345
H	-5.340942	3.135166	3.744728
H	-3.005325	-4.537338	2.284337
H	-2.572496	-6.008274	0.319533
H	-2.637412	-5.079754	-1.983318
H	-2.828183	-1.418306	-2.691341
H	-2.467638	-4.186779	-3.99474
H	-1.131244	-3.195806	-3.300544
H	-2.081459	-2.582161	-4.67181
H	-4.919745	-3.564654	-3.445717
H	-4.57164	-2.076979	-4.381081
H	-5.286515	-1.958619	-2.748551
H	0.956382	5.25987	1.187543
H	1.515566	5.956354	-1.128131
H	2.917636	4.496623	-2.581527
H	1.723418	1.8572	2.512558
H	3.89445	2.903729	3.160643
H	2.727136	2.98624	4.514149
H	3.058603	4.445096	3.526507
H	-0.385094	3.291035	2.349433
H	0.465458	4.576091	3.249001
H	0.189705	2.993405	4.017285
H	4.27845	1.144059	-1.422837
H	3.795708	0.913883	-3.832534
H	2.934848	2.478421	-3.853816
H	2.274454	1.100374	-2.915842
H	5.957742	2.023913	-3.015573

H	5.958414	2.998331	-1.511422
H	5.184871	3.635599	-2.993554
H	2.499104	-4.957213	2.653134
H	2.544962	-6.019742	0.409787
H	3.089846	-4.687792	-1.609295
H	3.212645	-1.005298	-1.639316
H	3.335408	-1.841113	-3.903588
H	2.101957	-2.775548	-3.033508
H	3.720646	-3.498927	-3.367997
H	5.782808	-2.674753	-2.011639
H	5.634594	-1.213146	-0.98658
H	5.447825	-1.080491	-2.75631
H	-3.812251	-0.845375	1.954971
H	-2.542018	-1.107449	4.079495
H	-2.064497	-2.76709	3.614435
H	-1.493092	-1.365766	2.655568
H	-5.043762	-1.647016	3.94491
H	-5.730407	-2.377517	2.458659
H	-4.680726	-3.347653	3.532814
H	3.676256	-1.46067	3.293463
H	1.481844	-1.138361	4.461128
H	1.317384	-0.919787	2.690004
H	0.758758	-2.433007	3.456189
H	3.354398	-2.61511	5.407309
H	2.510046	-3.978267	4.638682
H	4.253113	-3.724695	4.323741

Table S29. Cartesian coordinates of insertion isomer of **12** shown in **Figure S48** in Å.

Atomtype	X Coordinate [Å]	Y Coordinate [Å]	Z Coordinate [Å]
C	0.787895	-2.733479	-4.227469
C	1.800028	-1.818778	-4.653928
C	2.721793	-1.676501	-3.571302
C	2.297057	-2.514908	-2.487701
C	1.097192	-3.175411	-2.896515
Fe	0.787874	-1.054196	-2.914292
C	1.354249	0.552921	-2.563888
O	1.807192	1.619444	-2.44949
Sn	0.03042	-1.118486	-0.296249
N	-1.430801	0.423973	-0.124123
C	-2.66884	0.503851	-0.368883

N	-3.397622	1.706394	-0.633125
C	-4.722596	1.430346	-0.97448
C	-4.920607	0.086552	-0.90179
N	-3.716732	-0.506478	-0.483224
C	-2.91818	3.020217	-0.315356
C	-2.084166	3.713238	-1.233918
C	-1.70705	5.030343	-0.908085
C	-2.131111	5.637474	0.283958
C	-2.927041	4.926536	1.188624
C	-3.328057	3.604236	0.909642
C	-3.591973	-1.846971	-0.033007
C	-3.517039	-2.101753	1.37316
C	-3.280583	-3.428609	1.801583
C	-3.158046	-4.48328	0.872054
C	-3.307244	-4.223786	-0.497047
C	-3.530576	-2.913499	-0.973182
C	-1.640637	3.046631	-2.535553
C	-2.796927	2.996591	-3.560258
C	-4.15781	2.831148	1.931854
C	-3.369659	2.627691	3.242504
C	-3.762279	-0.979694	2.38101
C	-3.301611	-1.309829	3.809684
C	-3.732138	-2.669122	-2.462977
C	-5.157528	-3.094088	-2.883169
N	1.563896	0.15698	0.434621
C	2.646775	0.053694	1.064302
N	3.719436	1.006769	1.101966
C	4.713179	0.608687	1.997919
C	4.358274	-0.587566	2.544648
N	3.122505	-0.964486	1.987618
C	3.719615	2.227989	0.353846
C	4.571848	2.351587	-0.775803
C	4.566322	3.566805	-1.486202
C	3.703432	4.609739	-1.126258
C	2.8461	4.458448	-0.030186
C	2.850001	3.280199	0.742256
C	5.458119	1.198755	-1.241976
C	6.919817	1.381465	-0.778161
C	1.943336	3.182942	1.963992
C	2.213061	4.325027	2.967818
C	2.263268	-1.954984	2.532973
C	2.412063	-3.312371	2.137983
C	1.542758	-4.27655	2.698615

C	0.546457	-3.903537	3.619735
C	0.398667	-2.550964	3.98451
C	1.240756	-1.55563	3.445479
C	3.490764	-3.716478	1.138274
C	4.781103	-4.149324	1.870671
C	1.110484	-0.102204	3.882586
C	1.920505	0.13938	5.174348
C	-0.810564	-0.511859	-3.290723
O	-1.871561	-0.145241	-3.630279
C	3.027616	-4.8185	0.165255
C	-0.339366	0.38369	4.020443
C	0.45792	3.125892	1.554618
C	5.403157	1.002579	-2.771879
C	-0.406284	3.703618	-3.175807
C	-5.526272	3.493049	2.188894
C	-5.263683	-0.601655	2.409932
C	-2.672394	-3.37009	-3.329099
H	4.859807	-1.194523	3.298036
H	5.59387	1.224776	2.177178
H	-5.807599	-0.507465	-1.120359
H	-5.412534	2.228229	-1.249504
H	1.651724	-5.331962	2.422418
H	-0.098589	-4.669125	4.073165
H	-0.356447	-2.273255	4.728818
H	3.727718	-2.806714	0.555109
H	2.042975	-4.579611	-0.276702
H	2.951896	-5.801904	0.666799
H	3.753038	-4.927555	-0.660859
H	5.565735	-4.424477	1.141067
H	4.584554	-5.029512	2.512573
H	5.175562	-3.34004	2.508512
H	1.552238	0.511973	3.086904
H	-0.34331	1.46268	4.252238
H	-0.885559	-0.1275	4.833281
H	-0.889273	0.245324	3.071714
H	2.977266	-0.15558	5.042311
H	1.497997	-0.435903	6.021116
H	1.897592	1.213163	5.439811
H	2.16019	5.271403	0.23927
H	3.692228	5.539896	-1.709696
H	5.225706	3.688753	-2.35385
H	5.064747	0.277922	-0.772212
H	5.958256	1.79749	-3.304614

H	4.360676	1.023064	-3.131691
H	5.868346	0.038548	-3.052932
H	7.347249	2.306691	-1.210549
H	7.546796	0.529799	-1.106636
H	6.994844	1.45758	0.320729
H	-3.2434	-3.658308	2.873114
H	-2.993231	-5.510308	1.225795
H	-3.246717	-5.052185	-1.212705
H	-3.191141	-0.09811	2.037301
H	-5.625793	-0.266505	1.424359
H	-5.43089	0.220948	3.128781
H	-5.869812	-1.469825	2.732437
H	-2.262427	-1.674791	3.836778
H	-3.952971	-2.067848	4.285173
H	-3.345932	-0.399193	4.432406
H	-3.629894	-1.585967	-2.637253
H	-2.763075	-3.033848	-4.377486
H	-2.785847	-4.471216	-3.320022
H	-1.661373	-3.113658	-2.978141
H	-5.324732	-2.868593	-3.95302
H	-5.932404	-2.568675	-2.295334
H	-5.303525	-4.181704	-2.734595
H	-3.235683	5.396629	2.131289
H	-1.823914	6.66657	0.51312
H	-1.06456	5.594113	-1.592224
H	-1.369797	2.00923	-2.269045
H	-0.050464	3.082407	-4.016823
H	0.426331	3.798437	-2.458547
H	-0.644002	4.705913	-3.583451
H	-3.114422	4.022235	-3.83284
H	-3.671728	2.453327	-3.168901
H	-2.467304	2.475096	-4.476983
H	2.193383	2.242869	2.482956
H	-0.184929	3.041804	2.449934
H	0.156282	4.047948	1.025373
H	0.255468	2.263949	0.896428
H	1.613149	4.175015	3.886397
H	3.280766	4.371284	3.254519
H	1.931458	5.309023	2.547687
H	-4.354955	1.830042	1.517594
H	-3.946587	2.003397	3.951221
H	-2.406107	2.129116	3.040898
H	-3.155493	3.59229	3.740251

H	-6.124292	2.887334	2.896895
H	-5.409609	4.502601	2.626485
H	-6.101565	3.594326	1.250273
H	-0.079739	-3.038788	-4.815425
H	0.512728	-3.881498	-2.302516
H	2.80187	-2.60668	-1.526467
H	3.589128	-1.016765	-3.558085
H	1.843123	-1.300484	-5.613649
Li	-0.736249	-3.101599	1.379767

Table S30. Cartesian coordinates of Ge-Fp monomer shown in **Figure S48** in Å.

Atomtype	X Coordinate [Å]	Y Coordinate [Å]	Z Coordinate [Å]
C	-3.505224	-1.481728	-0.794699
C	-2.791819	-1.360351	0.423524
C	-2.449538	-2.4813	1.222852
C	-2.901396	-3.74494	0.796627
C	-3.647835	-3.886145	-0.384053
C	-3.938297	-2.768127	-1.175477
N	-2.369188	-0.05356	0.836534
C	-1.151407	0.511043	0.4219
N	-1.289486	1.881467	0.695673
C	-2.54518	2.13298	1.261056
C	-3.210183	0.945796	1.345839
C	-0.293807	2.858753	0.367698
C	0.517865	3.381568	1.405977
C	1.480829	4.347163	1.055763
C	1.640541	4.754459	-0.27512
C	0.842968	4.20378	-1.287788
C	-0.143096	3.243666	-0.989842
C	0.403229	2.836619	2.829872
C	1.198047	1.515079	2.94749
C	-1.053164	2.662933	-2.073745
C	-0.404326	2.608683	-3.467661
N	-0.135965	-0.082845	-0.078569
Ge	0.86862	-0.830122	-1.372504
Fe	3.050604	-1.323027	-0.338476
C	3.294278	-2.95398	-1.739734
C	-1.627916	-2.294529	2.497643
C	-2.517278	-1.795302	3.659157
C	-3.765942	-0.281816	-1.704972

C	-3.028873	-0.440588	-3.051863
C	3.129697	0.396277	-0.066435
O	3.25703	1.53762	0.141597
C	2.223805	-1.612703	1.159034
O	1.7381	-1.817699	2.201396
C	-0.849478	-3.551862	2.920645
C	-5.273643	-0.029964	-1.909736
C	-2.399277	3.419832	-2.121184
C	0.834319	3.834999	3.919007
H	-2.835995	3.138345	1.563924
H	-4.207486	0.71014	1.715423
H	0.992595	4.527543	-2.32358
H	2.404784	5.500565	-0.528572
H	2.130675	4.772324	1.828005
H	-1.272729	1.61882	-1.793997
H	0.580388	2.107762	-3.430487
H	-0.265788	3.616951	-3.901675
H	-1.052069	2.039082	-4.158904
H	-3.073649	2.964207	-2.871093
H	-2.24088	4.479736	-2.397378
H	-2.910889	3.391762	-1.142854
H	-4.496886	-2.893737	-2.111496
H	-3.991403	-4.881204	-0.695811
H	-2.662579	-4.635368	1.388008
H	-3.353539	0.617747	-1.218155
H	-3.419319	-1.302379	-3.625284
H	-1.946002	-0.597534	-2.894337
H	-3.160096	0.466928	-3.670656
H	-5.759468	-0.881133	-2.423203
H	-5.433039	0.872659	-2.529533
H	-5.787632	0.120397	-0.942319
H	-0.661208	2.595755	3.012358
H	1.066738	1.068464	3.951193
H	0.87445	0.779029	2.19418
H	2.275445	1.701168	2.784853
H	0.594173	3.427841	4.918556
H	1.925358	4.016627	3.89769
H	0.322746	4.809294	3.808654
H	-0.878465	-1.511683	2.280759
H	-0.151862	-3.299196	3.73802
H	-1.523985	-4.349382	3.28747
H	-0.252092	-3.955372	2.083967
H	-1.905754	-1.622732	4.565009

H	-3.024939	-0.848145	3.406613
H	-3.292143	-2.546758	3.905296
C	3.957951	-1.795262	-2.237151
C	4.966539	-1.419813	-1.27821
C	4.941247	-2.352417	-0.201551
C	3.881039	-3.280779	-0.470623
H	3.575676	-4.105724	0.17765
H	5.571609	-2.332348	0.689422
H	5.63329	-0.558333	-1.363549
H	3.736524	-1.275213	-3.17182
H	2.477261	-3.49123	-2.226693

Table S31. Cartesian coordinates of Sn-Fp monomer shown in **Figure S48** in Å.

Atomtype	X Coordinate [Å]	Y Coordinate [Å]	Z Coordinate [Å]
C	1.130778	2.742019	1.626215
C	-0.035012	2.604478	0.82854
C	-0.275083	3.439957	-0.302435
C	0.667705	4.446647	-0.585551
C	1.803969	4.624587	0.218363
C	2.033371	3.77864	1.309151
N	-0.992092	1.596085	1.158299
C	-1.182708	0.408584	0.401837
N	-2.332229	-0.167577	0.980653
C	-2.789177	0.611715	2.047661
C	-1.964124	1.690049	2.165116
C	-3.021463	-1.293146	0.423036
C	-3.956105	-1.066719	-0.619565
C	-4.639842	-2.180865	-1.143355
C	-4.404933	-3.469931	-0.644657
C	-3.467751	-3.670174	0.378139
C	-2.748163	-2.58934	0.924749
C	-4.178546	0.325746	-1.205506
C	-3.507223	0.430176	-2.592296
C	-1.727358	-2.807325	2.036384
C	-0.761022	-3.969036	1.73394
N	-0.493428	-0.047633	-0.570655
Sn	1.234087	0.279553	-1.624869
Fe	2.798295	-1.596803	-0.52789
C	4.509175	-0.29925	-0.704334
C	-1.531888	3.261116	-1.155763

C	-2.759969	3.913048	-0.481473
C	1.411652	1.807573	2.79875
C	2.860301	1.278837	2.780642
C	1.872572	-1.441579	0.930191
O	1.304292	-1.404222	1.951694
C	1.648659	-2.711529	-1.220033
O	0.927959	-3.525233	-1.64715
C	-1.37731	3.766289	-2.600992
C	1.091862	2.492845	4.144818
C	-2.43634	-3.005068	3.393931
C	-5.667631	0.719365	-1.265568
H	-3.665189	0.318709	2.625491
H	-1.97594	2.52203	2.867832
H	-3.284201	-4.68392	0.75372
H	-4.950359	-4.326176	-1.062675
H	-5.361643	-2.037411	-1.956973
H	-1.117055	-1.892445	2.10966
H	-0.298881	-3.850954	0.73872
H	-1.273635	-4.949491	1.761987
H	0.045943	-3.991069	2.48884
H	-1.694798	-3.128582	4.20612
H	-3.078993	-3.906509	3.375156
H	-3.076626	-2.138075	3.64191
H	2.93161	3.9166	1.92279
H	2.519186	5.423668	-0.016541
H	0.514689	5.10748	-1.445224
H	0.745813	0.934495	2.693516
H	3.591808	2.071173	3.028091
H	3.114113	0.869475	1.78758
H	2.977053	0.468657	3.522956
H	1.728696	3.38645	4.291582
H	1.274772	1.798913	4.986905
H	0.037053	2.818239	4.19255
H	-3.679829	1.054775	-0.543565
H	-3.610669	1.454078	-2.99821
H	-2.433013	0.185362	-2.517719
H	-3.976382	-0.271201	-3.308391
H	-5.771867	1.764091	-1.615222
H	-6.233704	0.078304	-1.967269
H	-6.144627	0.638589	-0.271219
H	-1.722811	2.176875	-1.221259
H	-2.258562	3.466692	-3.19654
H	-1.310849	4.869767	-2.650693

H	-0.477668	3.341599	-3.083065
H	-3.669344	3.727831	-1.084072
H	-2.934834	3.502886	0.528112
H	-2.621091	5.00761	-0.393821
C	4.666072	-1.205034	0.402832
C	4.675678	-2.545811	-0.097193
C	4.478696	-2.469739	-1.509808
C	4.390694	-1.085622	-1.88991
H	4.256671	-0.708964	-2.906639
H	4.399461	-3.32026	-2.19122
H	4.771327	-3.45674	0.496492
H	4.762982	-0.914504	1.451274
H	4.500395	0.791647	-0.641948

Table S32. Cartesian coordinates of K analog of **12** shown in **Figure S48** in Å.

Atomtype	X Coordinate [Å]	Y Coordinate [Å]	Z Coordinate [Å]
C	0.740506	-4.081289	-1.905448
C	-0.057233	-4.21108	-3.095304
C	0.579441	-3.49259	-4.155242
C	1.75441	-2.888929	-3.606924
C	1.860389	-3.258907	-2.220724
Fe	0.05558	-2.145996	-2.574215
C	0.285533	-0.495861	-2.976101
O	0.407108	0.625721	-3.33717
Sn	0.204534	-1.221099	0.188734
N	1.594981	0.543378	0.014895
C	2.690136	0.817026	0.599065
N	3.236814	2.141875	0.801195
C	4.433305	2.095672	1.524161
C	4.713004	0.791452	1.784964
N	3.685595	-0.000155	1.24845
C	2.602163	3.341716	0.376687
C	1.890835	4.124357	1.330843
C	1.256923	5.300517	0.876665
C	1.328895	5.687494	-0.471004
C	2.043676	4.909021	-1.39598
C	2.689474	3.719559	-0.994392
C	3.911607	-1.382786	0.952359
C	4.654614	-1.70919	-0.212761
C	4.931935	-3.068101	-0.4616

C	4.480828	-4.065475	0.413011
C	3.749094	-3.721884	1.559297
C	3.454568	-2.376585	1.857353
C	1.814528	3.669708	2.790242
C	1.458177	4.794711	3.778516
C	3.4719	2.850328	-1.980919
C	3.047125	3.023189	-3.449834
C	5.120513	-0.634613	-1.194513
C	6.639779	-0.694056	-1.448892
C	2.731948	-1.98031	3.144456
C	3.753943	-1.66452	4.261031
N	-1.521707	0.205617	0.093739
C	-2.760654	0.030196	0.336046
N	-3.836314	0.915489	-0.044466
C	-5.079673	0.374456	0.298689
C	-4.85969	-0.798281	0.94915
N	-3.474776	-1.01022	1.019851
C	-3.65804	2.161774	-0.713901
C	-3.352569	3.323956	0.055927
C	-3.156354	4.54204	-0.62776
C	-3.262131	4.612142	-2.027424
C	-3.574925	3.463757	-2.766683
C	-3.7756	2.219211	-2.129872
C	-2.905651	-2.054266	1.815322
C	-3.071905	-3.40367	1.40452
C	-2.579581	-4.423656	2.244864
C	-1.93721	-4.119487	3.448053
C	-1.777955	-2.781407	3.837148
C	-2.255083	-1.723916	3.04213
C	-3.271002	3.246975	1.580814
C	-4.685687	3.297467	2.203392
C	-4.138828	0.984463	-2.945283
C	-5.623948	1.038142	-3.368206
C	-3.770384	-3.779227	0.100247
C	-5.143559	-4.432839	0.366687
C	-2.122387	-0.268542	3.497658
C	-1.051547	-0.050598	4.580183
C	-1.65485	-1.962091	-2.413831
O	-2.82725	-1.897145	-2.409125
C	-2.382957	4.337438	2.208422
C	-3.222705	0.779061	-4.167283
C	-2.889274	-4.69484	-0.772524
C	-3.478875	0.291898	3.983098

C	0.853036	2.472274	2.973844
C	4.992934	3.084535	-1.833998
C	4.320641	-0.711097	-2.510865
C	1.715593	-3.02581	3.632063
K	-0.273716	2.323446	-1.129638
H	-6.011733	0.87613	0.039784
H	-5.560617	-1.502665	1.394169
H	4.98155	3.002328	1.781212
H	5.577683	0.339749	2.270589
H	-2.919442	5.45178	-0.065339
H	-3.10683	5.570755	-2.540005
H	-3.665479	3.528808	-3.857707
H	-2.828057	2.265854	1.830809
H	-1.394508	4.400513	1.719457
H	-2.221071	4.120177	3.27967
H	-2.856009	5.33607	2.147888
H	-5.190391	4.245212	1.934753
H	-4.623274	3.23979	3.305776
H	-5.310624	2.457519	1.857047
H	-4.009448	0.107794	-2.29311
H	-3.441566	-0.197772	-4.633922
H	-2.157449	0.776944	-3.879337
H	-3.374173	1.56152	-4.935687
H	-5.818219	1.906857	-4.027026
H	-6.290144	1.122011	-2.490013
H	-5.898508	0.119912	-3.920545
H	-2.702714	-5.471508	1.944733
H	-1.554763	-4.924345	4.089162
H	-1.274213	-2.565802	4.7837
H	-3.935791	-2.854243	-0.474445
H	-3.353418	-4.83372	-1.76635
H	-2.756326	-5.695005	-0.318175
H	-1.894726	-4.24476	-0.921577
H	-5.653385	-4.665337	-0.587586
H	-5.805022	-3.771248	0.95542
H	-5.029373	-5.378543	0.930715
H	-1.80494	0.315413	2.613372
H	-3.367012	1.349046	4.289769
H	-3.841835	-0.280396	4.858349
H	-4.250393	0.249456	3.196489
H	-0.064907	-0.431136	4.260139
H	-1.322929	-0.540346	5.534732
H	-0.951422	1.028863	4.787861

H	0.701615	5.928045	1.581575
H	0.829232	6.607496	-0.801763
H	2.095443	5.230578	-2.442153
H	2.824433	3.306668	3.060284
H	-0.196855	2.787019	2.845991
H	0.96082	2.062327	3.993366
H	1.042555	1.662167	2.252499
H	2.121471	5.67213	3.664547
H	1.552911	4.423807	4.815541
H	0.412881	5.133642	3.649996
H	3.261334	1.801497	-1.707674
H	5.548947	2.41392	-2.515352
H	5.339785	2.882808	-0.806465
H	5.252806	4.129149	-2.09183
H	3.32328	4.018394	-3.847759
H	1.961706	2.875796	-3.590094
H	3.559782	2.267895	-4.072339
H	5.492371	-3.34877	-1.361851
H	4.695772	-5.120096	0.197648
H	3.404673	-4.515145	2.231665
H	4.911008	0.349845	-0.747423
H	4.623219	0.103664	-3.194939
H	3.238096	-0.619842	-2.317446
H	4.503184	-1.672557	-3.025977
H	6.934863	-1.633133	-1.953946
H	7.205775	-0.62407	-0.501595
H	6.950485	0.145549	-2.099054
H	2.178156	-1.046841	2.926727
H	0.982366	-3.276615	2.8458
H	1.157406	-2.627089	4.497558
H	2.211144	-3.956521	3.96787
H	4.359667	-2.56079	4.496005
H	3.231233	-1.351565	5.1852
H	4.440855	-0.852454	3.967613
H	-1.000483	-4.756365	-3.171366
H	0.21773	-3.39598	-5.180807
H	2.448134	-2.242488	-4.147506
H	2.653439	-2.965121	-1.534753
H	0.52086	-4.519565	-0.929683

Table S33. Cartesian coordinates of **5** in Å.

Atomtype	X Coordinate [Å]	Y Coordinate [Å]	Z Coordinate [Å]
C	3.490552	1.260731	-2.416183
C	3.772012	0.952382	-1.061644
C	4.143061	1.945847	-0.114066
C	4.203651	3.280381	-0.555323
C	3.892774	3.616396	-1.880362
C	3.548993	2.617021	-2.798604
N	3.639273	-0.403381	-0.59596
C	2.494485	-0.908506	0.02291
N	2.898714	-2.118213	0.584171
C	4.236966	-2.365379	0.267052
C	4.69604	-1.304774	-0.455721
N	1.298028	-0.369496	0.100377
Ge	-0.683749	-1.377721	0.312962
Fe	-1.065645	-2.055805	-2.087888
C	-1.599455	-0.395532	-2.34988
O	-1.934459	0.70283	-2.625516
C	2.102949	-2.916142	1.485182
C	1.666836	-4.204	1.080185
C	0.839904	-4.918238	1.972518
C	0.487135	-4.389225	3.217077
C	0.982745	-3.140037	3.619126
C	1.80318	-2.377144	2.770137
C	2.128809	-4.867399	-0.215134
C	0.978126	-5.491911	-1.027788
C	2.412645	-1.05391	3.239794
C	1.644752	-0.37793	4.387279
C	4.481714	1.599594	1.334885
C	3.660739	2.421955	2.348376
C	3.140306	0.188088	-3.439177
C	1.715633	0.372512	-3.99907
C	3.209287	-5.927215	0.105363
C	3.894483	-1.255063	3.633095
C	4.189465	0.142507	-4.571086
N	-1.032704	0.802439	0.265837
C	-2.145103	1.50253	0.311981
N	-2.283382	2.894689	0.241127

C	-3.625836	3.258708	0.354294
C	-4.342933	2.112595	0.501965
N	-3.448989	1.037234	0.48102
C	-1.198865	3.83201	0.304056
C	-0.694849	4.384635	-0.900856
C	0.388478	5.278031	-0.799441
C	0.959828	5.581629	0.444358
C	0.442596	5.019838	1.620244
C	-0.657476	4.141335	1.578936
C	-1.299346	4.010923	-2.250515
C	-0.235947	3.763848	-3.337684
C	-1.213287	3.532331	2.865292
C	-1.686911	4.620493	3.851151
C	-3.875785	-0.320401	0.721823
C	-3.585589	-0.905248	1.986432
C	-4.053584	-2.213777	2.214722
C	-4.797926	-2.895574	1.24433
C	-5.096741	-2.283134	0.023645
C	-4.640472	-0.984885	-0.272925
C	-2.866979	-0.116118	3.08557
C	-3.835605	0.8761	3.770431
C	-5.026443	-0.329514	-1.599229
C	-4.837005	-1.265849	-2.810457
C	-2.185376	-1.004603	4.139355
C	-6.490674	0.167461	-1.550228
C	-2.32024	5.079726	-2.698612
C	-1.397095	-2.606214	-3.747011
O	-1.595247	-2.951125	-4.843841
C	0.665052	-2.320086	-2.186537
O	1.817177	-2.513122	-2.354625
C	-2.042052	-3.316573	-1.274296
O	-2.646691	-4.190791	-0.78105
C	5.997127	1.746781	1.589905
C	-0.196906	2.578898	3.525399
H	4.729789	-3.281822	0.585308
H	5.672518	-1.099886	-0.892657
H	-5.409879	1.947254	0.630268
H	-3.930728	4.303828	0.328907
H	0.470592	-5.907373	1.679647
H	-0.168279	-4.958415	3.88872
H	0.718516	-2.756218	4.60925
H	2.584553	-4.095436	-0.853747
H	0.202682	-4.742696	-1.256608

H	0.506915	-6.339195	-0.495366
H	1.37019	-5.878674	-1.986465
H	3.603753	-6.36911	-0.828995
H	2.786484	-6.745921	0.718437
H	4.058569	-5.498363	0.670555
H	2.374874	-0.35069	2.391281
H	2.050241	0.634819	4.561377
H	1.74002	-0.938713	5.336159
H	0.574121	-0.281569	4.147192
H	4.490813	-1.659055	2.796846
H	3.974086	-1.95861	4.483164
H	4.34764	-0.293619	3.939528
H	4.485409	4.069007	0.152516
H	3.924259	4.666051	-2.199735
H	3.317591	2.887387	-3.835668
H	3.158847	-0.786687	-2.929277
H	1.61308	1.329397	-4.544953
H	0.959272	0.340943	-3.197106
H	1.472416	-0.450176	-4.6949
H	4.194858	1.079583	-5.160229
H	3.9611	-0.688834	-5.263474
H	5.209399	-0.011478	-4.170765
H	-3.831631	-2.713022	3.162791
H	-5.135645	-3.92125	1.436468
H	-5.670373	-2.833719	-0.729208
H	-2.064416	0.47072	2.606019
H	-4.290201	1.575865	3.048249
H	-3.29816	1.47575	4.529892
H	-4.65242	0.330088	4.279229
H	-1.503545	-1.730756	3.663246
H	-2.922754	-1.556195	4.752451
H	-1.599518	-0.375234	4.833702
H	-4.363599	0.539488	-1.753151
H	-4.955218	-0.692125	-3.748063
H	-5.590636	-2.07576	-2.820825
H	-3.832481	-1.718192	-2.799624
H	-6.755829	0.676105	-2.496332
H	-6.675944	0.872545	-0.720099
H	-7.181462	-0.686886	-1.417713
H	0.898213	5.266617	2.587144
H	1.819025	6.262724	0.497898
H	0.806995	5.721222	-1.709965
H	-1.841936	3.05992	-2.11947

H	-0.713716	3.32596	-4.232281
H	0.535477	3.056836	-2.986549
H	0.267455	4.699735	-3.647746
H	-1.827175	6.06184	-2.833628
H	-3.127565	5.204738	-1.95364
H	-2.783517	4.790795	-3.660477
H	4.230857	0.539761	1.501138
H	3.873543	2.079155	3.377636
H	3.905348	3.499071	2.296504
H	2.576825	2.315225	2.167769
H	6.246599	1.447624	2.62545
H	6.580531	1.112764	0.897216
H	6.322721	2.79463	1.447216
H	-2.099101	2.928789	2.605395
H	-0.636033	2.107658	4.423658
H	0.095893	1.771291	2.832948
H	0.718956	3.115811	3.834922
H	-2.153158	4.154266	4.739316
H	-0.843709	5.244361	4.202654
H	-2.431331	5.289004	3.380813
Ge	0.746618	1.43795	-0.155182

Table S34. Cartesian coordinates of **6** in Å.

Atomtype	X Coordinate [Å]	Y Coordinate [Å]	Z Coordinate [Å]
C	2.323216	-1.814479	2.951468
C	2.847511	-2.23351	1.693485
C	2.806529	-3.588815	1.273486
C	2.185577	-4.521806	2.130832
C	1.634433	-4.128064	3.353258
C	1.712884	-2.788114	3.762291
N	3.450291	-1.248141	0.83564
C	2.760187	-0.196568	0.209161
N	3.783369	0.591177	-0.35003
C	5.033068	0.01969	-0.093621
C	4.826358	-1.115547	0.629726
N	1.471328	-0.009061	0.19919
Sn	-0.303243	-1.719977	0.291218
Fe	-0.291761	-2.175745	-2.385669
C	1.456941	-2.018958	-2.257586
O	2.63381	-1.933968	-2.26855

C	3.582093	1.919005	-0.852807
C	3.551978	2.991679	0.082732
C	3.28446	4.284192	-0.407519
C	3.060638	4.504852	-1.774406
C	3.121335	3.437788	-2.679419
C	3.385314	2.12193	-2.243185
C	3.813033	2.775021	1.572378
C	2.651168	3.276226	2.450801
C	3.476357	0.981291	-3.249871
C	4.696854	1.177144	-4.175834
C	3.452081	-4.068273	-0.022828
C	4.761238	-4.828885	0.288899
C	2.478172	-0.372286	3.435929
C	3.88067	-0.160893	4.049888
N	-1.362822	0.497182	0.315373
C	-2.620121	0.840366	0.30565
N	-3.746444	0.014861	0.472147
C	-4.918514	0.776924	0.464565
C	-4.572779	2.080445	0.298041
N	-3.179227	2.133511	0.195316
C	-3.741001	-1.407979	0.679715
C	-3.346683	-1.908792	1.954086
C	-3.373054	-3.305167	2.13719
C	-3.773029	-4.16154	1.102341
C	-4.172452	-3.642443	-0.134215
C	-4.171491	-2.25511	-0.376762
C	-2.944206	-0.960402	3.088885
C	-2.062699	-1.619899	4.164013
C	-4.686201	-1.701881	-1.706477
C	-4.153333	-2.455206	-2.940662
C	-2.423513	3.344903	0.283382
C	-2.007954	3.779469	1.570891
C	-1.21045	4.938398	1.642078
C	-0.873462	5.652461	0.482132
C	-1.331814	5.22665	-0.772951
C	-2.104467	4.055355	-0.903995
C	-2.423259	3.039866	2.841208
C	-3.281205	3.941507	3.752751
C	-2.593491	3.566631	-2.26491
C	-1.557036	3.744909	-3.38966
C	-0.320966	-2.567834	-4.117157
O	-0.329557	-2.809969	-5.258626
C	-1.009979	-3.715858	-1.830625

S106

O	-1.466619	-4.751893	-1.521022
C	-1.222316	-0.684976	-2.519563
O	-1.819011	0.320944	-2.707628
C	-3.925771	4.258187	-2.631456
C	-6.23363	-1.712641	-1.719197
C	-4.189385	-0.317037	3.741776
C	2.178147	0.810211	-4.064237
C	2.507009	-4.932424	-0.881138
C	1.383416	0.079961	4.415842
C	5.152216	3.419721	1.990595
C	-1.213793	2.463297	3.600623
H	-5.176909	2.985616	0.260621
H	-5.891991	0.308819	0.591952
H	-0.861511	5.292462	2.620299
H	-0.250642	6.553149	0.558347
H	-1.063372	5.797919	-1.66862
H	-2.786001	2.483871	-2.17414
H	-3.787139	5.353154	-2.71792
H	-4.702816	4.073727	-1.868036
H	-4.301793	3.880494	-3.600636
H	-1.41451	4.809246	-3.657509
H	-1.898751	3.214228	-4.2963
H	-0.577235	3.323733	-3.103747
H	-4.467441	-4.327469	-0.935314
H	-3.760635	-5.24752	1.25723
H	-3.058188	-3.734359	3.093782
H	-4.340837	-0.655799	-1.789961
H	-6.671037	-1.158603	-0.869896
H	-6.607773	-2.752786	-1.66464
H	-6.613912	-1.26198	-2.655304
H	-4.4646	-1.92507	-3.859753
H	-4.557619	-3.483056	-3.000263
H	-3.053094	-2.50763	-2.924981
H	-2.34131	-0.150259	2.641427
H	-3.882998	0.401919	4.525706
H	-4.823563	-1.090878	4.214556
H	-4.804561	0.228487	3.005989
H	-2.622974	-2.371809	4.751457
H	-1.70795	-0.852969	4.876634
H	-1.180853	-2.110672	3.714514
H	5.526829	-1.856995	1.009959
H	5.948973	0.475727	-0.467413
H	2.132784	-5.573049	1.824848

H	1.144156	-4.868576	3.998254
H	1.287691	-2.500532	4.729107
H	3.705987	-3.182953	-0.625487
H	1.573087	-4.395105	-1.117373
H	2.250833	-5.885906	-0.381934
H	2.998201	-5.17934	-1.84009
H	5.263879	-5.128664	-0.649768
H	4.55539	-5.745893	0.873677
H	5.467737	-4.212456	0.876481
H	2.957065	3.621071	-3.748021
H	2.843315	5.518104	-2.135924
H	3.249655	5.129078	0.291202
H	3.627676	0.045569	-2.690289
H	1.951574	1.708565	-4.669892
H	1.313261	0.593716	-3.413481
H	2.274744	-0.050509	-4.749794
H	4.594501	2.088472	-4.796009
H	4.796702	0.313092	-4.858597
H	5.633805	1.267246	-3.59424
H	2.390482	0.282991	2.55451
H	1.482244	1.162078	4.613359
H	0.378879	-0.102847	4.000566
H	1.458434	-0.439304	5.390004
H	4.011583	0.891382	4.365425
H	4.015758	-0.80555	4.938902
H	4.680752	-0.40005	3.32741
H	3.907365	1.691638	1.749964
H	2.853825	3.058874	3.515332
H	2.49888	4.367016	2.35225
H	1.704497	2.776394	2.181542
H	5.362424	3.212814	3.056807
H	5.990029	3.021102	1.390065
H	5.127165	4.517353	1.853139
H	-3.054232	2.185157	2.546974
H	-3.629334	3.371836	4.634919
H	-2.701712	4.810467	4.118311
H	-4.168731	4.32597	3.216986
H	-1.553362	1.871113	4.470269
H	-0.623073	1.798341	2.948917
H	-0.554693	3.267028	3.976967
Sn	0.30823	1.681081	-0.417875

4. References

[S1] D. Franz, E. Irran, S. Inoue, *Dalton Trans.* **2014**, *43*, 4451-4461.

[S2] J. Kouvetakis, A. Haaland, D. J. Shorokhov, H. V. Volden, G. V. Girichev, V. I. Sokolov, P. Matsunaga, *J. Am. Chem. Soc.* **1998**, *120*, 6738-6744.

[S3] V. A. Kuznetsov, A. V. Pestov, *Polymer Science, Series B*, **2016**, *58*, 13-18.

[S4] H. Strong, P. J. Krusic, J. S. Filippo, S. Keenan, R. G. Finke, *Inorganic Syntheses*, **2007**, *28*, 203-207.

[S5] J. S. Plotkin, S. G. Shore, *Inorg. Chem.* **1981**, *20*, 284-285.

[S6] M. Okazaki, K. Satoh, T. Akagi, M. Iwata, K. A. Jung, R. Shiozawa, H. Okada, K. Ueno, H. Tobita, H. Ogino, *J. Organomet. Chem.* **2002**, *645*, 201-205.

[S7] J. Rohonczy, DNMR line shape analysis, Software Manual, version 1.1, Bruker BioSpin GmbH: Rheinstetten, **2007**.

[S8] J. Sandstrom, Dynamic NMR spectroscopy, Academic Press: London, **1982**.

[S9] M. W. Lui, C. Merten, M. J. Ferguson, R. McDonald, Y. Xu, E. Rivard, *Inorg. Chem.* **2015**, *54*, 2040-2049.

[S10] *APEX suite of crystallographic software*, APEX 3 version 2015.5-2; Bruker AXS Inc.: Madison, Wisconsin, USA, **2015**.

[S11] *SAINT*, Version 7.56a and SADABS Version 2008/1; Bruker AXS Inc.: Madison, Wisconsin, USA, **2008**.

[S12] G. M. Sheldrick, *SHELXL-2014*, University of Göttingen, Göttingen, Germany, **2014**.

[S13] C. B. Hübschle, G. M. Sheldrick, B. Dittrich, *J. Appl. Cryst.* **2011**, *44*, 1281-1284.

[S14] G. M. Sheldrick, *SHELXL-97*, University of Göttingen, Göttingen, Germany, **1998**.

[S15] A. J. C. Wilson, *International Tables for Crystallography*, Vol. C, Tables 6.1.1.4 (pp. 500-502), 4.2.6.8 (pp. 219-222), and 4.2.4.2 (pp. 193-199); Kluwer Academic Publishers: Dordrecht, The Netherlands, **1992**.

[S16] C. F. Macrae, I. J. Bruno, J. A. Chisholm, P. R. Edgington, P. McCabe, E. Pidcock, L. Rodriguez-Monge, R. Taylor, J. van de Streek, P. A. Wood, *J. Appl. Cryst.* **2008**, *41*, 466-470.

[S17] F. Weigend, R. Ahlrichs, *Phys. Chem. Chem. Phys.* **2005**, *7*, 3297-3305.

[S18] A. D. Becke, *J. Chem. Phys*. **1997**, *107*, 8554-8560.

[S19] S. Grimme, *J. Comput. Chem.* **2006**, *27*, 1787-1799.

[S20] J.-D. Chai, M. Head-Gordon, *Phys. Chem. Chem. Phys.* **2008**, *10*, 6615-6620.

[S21] Gaussian 09, Revision B.01, M. J. Frisch, G. W. Trucks, H. B. Schlegel, G. E. Scuseria, M. A. Robb, J. R. Cheeseman, G. Scalmani, V. Barone, B. Mennucci, G. A. Petersson, H. Nakatsuji, M. Caricato, X. Li, H. P. Hratchian, A. F. Izmaylov, J. Bloino, G. Zheng, J. L. Sonnenberg, M. Hada, M. Ehara, K. Toyota, R. Fukuda, J. Hasegawa, M. Ishida, T. Nakajima, Y. Honda, O. Kitao, H. Nakai, T. Vreven, J. A. Montgomery, Jr., J. E. Peralta, F. Ogliaro, M. Bearpark, J. J. Heyd, E. Brothers, K. N. Kudin, V. N. Staroverov, R. Kobayashi, J. Normand, K. Raghavachari, A. Rendell, J. C. Burant, S. S. Iyengar, J. Tomasi, M. Cossi, N. Rega, J. M. Millam, M. Klene, J. E. Knox, J. B. Cross, V. Bakken, C. Adamo, J. Jaramillo, R. Gomperts, R. E. Stratmann, O. Yazyev, A. J. Austin, R. Cammi, C. Pomelli, J. W. Ochterski, R. L. Martin, K. Morokuma, V. G. Zakrzewski, G. A. Voth, P. Salvador, J. J. Dannenberg, S. Dapprich, A. D. Daniels, Ö. Farkas, J. B. Foresman, J. V. Ortiz, J. Cioslowski, and D. J. Fox, Gaussian, Inc., Wallingford CT, **2009**.

[S22] G. Kresse, J. Furthmüller, *Comput. Mater. Sci.* **1996**, *6*, 15-50.

[S23] G. Kresse, J. Furthmüller, *Phys. Rev. B* **1996**, *54*, 11169-11186.

[S24] J. P. Perdew, K. Burke, M. Ernzerhof, *Phys. Rev. Lett*. **1996**, *77*, 3865.

[S25] S. Grimme, J. Antony, S. Ehrlich, H. Krieg, *J. Chem. Phys*. **2010**, *132*, 154104.

[S26] P. E. Blöchl, *Phys. Rev. B* **1994**, *50*, 17953-17979.

[S27] G. Kresse, D. Joubert, *Phys. Rev. B* **1999**, *59*, 1758-1775.

[S28] H. J. Monkhorst, J. D. Pack, *Phys. Rev. B* **1976**, *13*, 5188-5192.

9.3 Supporting Information for Chapter 6

Supporting Information

N-Heterocyclic Imine-Stabilized Binuclear Tin(II) Cations: Synthesis, Reactivity, and Catalytic Application

Xuan-Xuan Zhao,[†] *John A. Kelly,*[†] *Arseni Kostenko,*[†] *Shiori Fujimori,*[†] *and Shigeyoshi Inoue**[,†]

[†]School of Natural Sciences, Department of Chemistry, WACKER-Institute of Silicon Chemistry and Catalysis Research Center, Technische Universität München, Lichtenbergstraße 4, 85748 Garching bei München, Germany

Table of Contents

1. Experimental Section

General Considerations

All experiments and manipulations were carried out under dry oxygen-free argon atmosphere using standard Schlenk techniques or in a glovebox. All glass junctions were coated with PTFE-based grease Merkel Triboflon III. All the solvents were dried and freshly distilled under Ar atmosphere prior to use by standard techniques. The ^{1}H, ^{19}F, $^{13}C\{^{1}H\}$, $^{11}B\{^{1}H\}$ and $^{119}Sn\{^{1}H\}$ NMR spectra were recorded on Bruker 400 MHz spectrometer. Chemical shifts are referenced to (residual) solvent signals (CD_3CN: $\delta(^{1}H) = 1.94$ ppm and $\delta(^{13}C) = 1.32$ ppm; $CDCl_3$: $\delta(^{1}H) = 7.26$ ppm and $\delta(^{13}C) = 77.16$ ppm). Abbreviations: s = singlet, d = doublet, t = triplet, m = multiplet. Elemental analysis (EA) was conducted with a EURO EA (HEKA tech) instrument equipped with a CHNS combustion analyzer. Liquid Injection Field Desorption Ionization Mass Spectrometry (LIFDI-MS) was measured directly from an inert atmosphere glovebox with a Thermo Fisher Scientific Exactive Plus Orbitrap equipped with an ion source from Linden CMS. Unless otherwise stated, all commercially available chemicals were purchased from *abcr GmbH*, *Sigma-Aldrich Chemie GmbH* or *Tokyo Chemical Industry Co., Ltd.*, and used without further purification. The starting materials IPrNLi (IPrN = bis(2,6-diisopropylphenyl)imidazolin-2-imino),[S1] Cp*Sn[BF_4],[S2] and Cp*Sn[OTf],[S3] were prepared according to the literature procedures, respectively.

Synthesis of [IPrNSnOTf]$_2$, 1

IPrNLi (203 mg, 496 µmol) dissolved in THF (6 mL) was added dropwise to a solution of Cp*Sn[OTf] (200 mg, 496 µmol, 1.0 eq.) in THF (4 mL) at -78 ºC. The reaction mixture was stirred for 12 h followed by warming to room temperature. The solvent was removed *in vacuo* and the solid residue was washed with toluene (5 mL × 3) and dried *in vacuo* to give pure **1** (180 mg, 61%) as a white powder. Colorless crystals of **1** suitable for single crystal X-ray analysis were obtained from a saturated solution in CD_3CN at -30 ºC for several days.

^{1}H NMR (400 MHz, CD_3CN) δ = 7.42 (t, *J* = 7.7 Hz, 4H, Ar*H*), 7.29 (d, *J* = 7.7 Hz, 8H, Ar*H*), 6.88 (s, 4H, NC*H*), 2.67 – 2.56 (m, 8H, C*H*(CH_3)$_2$), 1.21 (d, *J* = 6.8 Hz, 24H, CH(C*H*$_3$)$_2$), 1.09 (d, *J* = 6.8 Hz, 24H, CH(C*H*$_3$)$_2$).

^{13}C{^{1}H} NMR (101 MHz, CD_3CN) δ = 153.3 (N*C*N), 148.5 (N*C*Ar), 133.4 (Ar*C*), 132.9 (Ar*C*), 129.9 (Ar*C*), 129.2 (Ar*C*), 127.5 (Ar*C*), 126.3 (Ar*C*), 118.3 (N*C*H), 68.3 (SO_3*C*F_3), 29.4 (*C*H(CH_3)$_2$), 26.2 (CH(*C*H$_3$)$_2$), 25.7 (CH(*C*H$_3$)$_2$), 23.1 (CH(*C*H$_3$)$_2$), 21.5 (CH(*C*H$_3$)$_2$).

^{119}Sn{^{1}H} NMR (149 MHz, CD_3CN) δ = 146.0.

^{19}F NMR (376 MHz, CD_3CN) δ = -79.4.

Anal. Calcd. [%] for $C_{56}H_{72}F_6N_6O_6S_2Sn_2$: C, 50.17; H, 5.41; N, 6.27. Found [%]: C, 50.10; H, 5.48; N, 6.35.

LIFDI-MS (positive ion mode): calculated for [M-OTf]$^+$: 1193.33826. Found: 1193.32344.

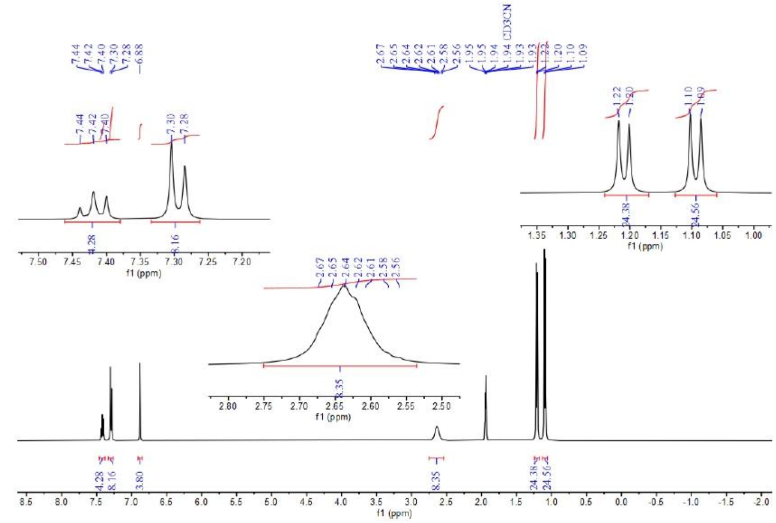

Figure S1. ^{1}H NMR spectrum of compound **1** in CD_3CN.

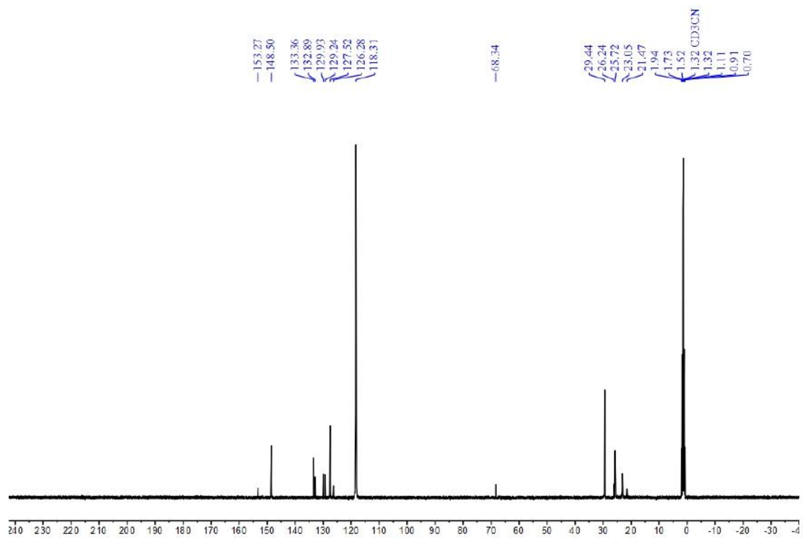

Figure S2. $^{13}C\{^{1}H\}$ NMR spectrum of compound **1** in CD_3CN.

S4

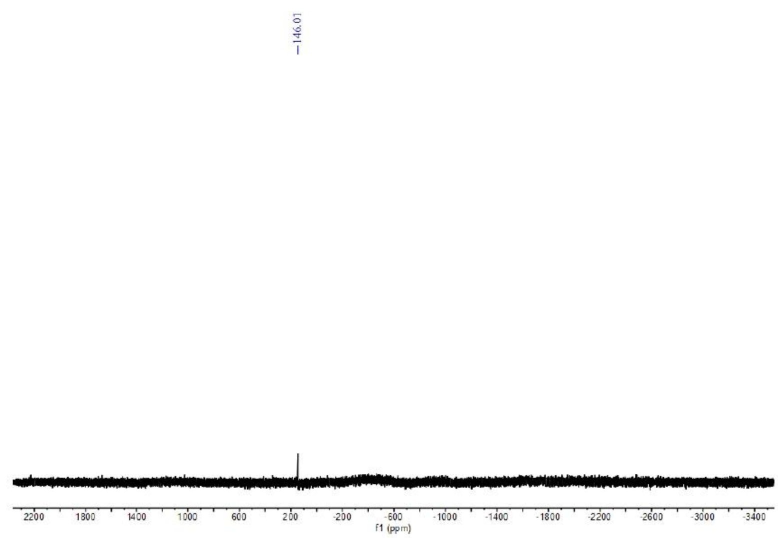

Figure S3. $^{119}Sn\{^{1}H\}$ NMR spectrum of compound **1** in CD_3CN.

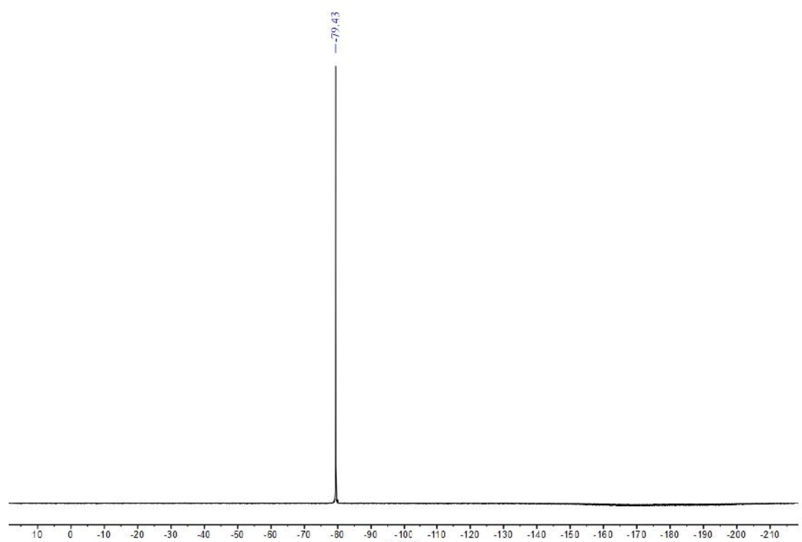

Figure S4. ^{19}F NMR spectrum of compound **1** in CD_3CN.

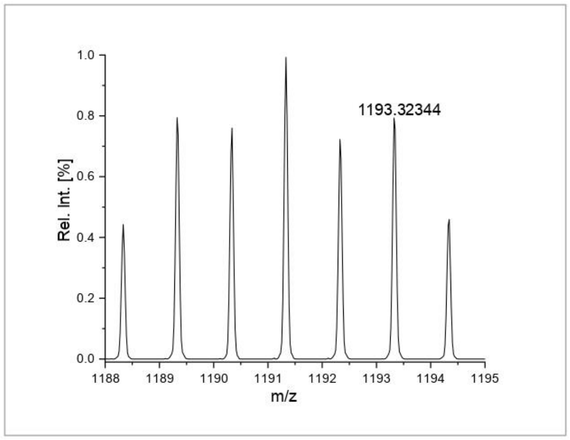

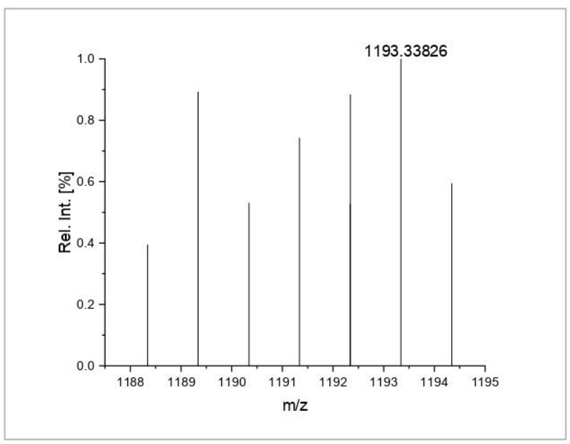

Figure S5. LIFDI-MS spectrum: expanded region of the compound signal showing the isotopic pattern of compound **1**. Measured (top) and calculated (bottom).

Synthesis of [IPrNSnBF$_4$]$_2$, 2

IPrNLi (223 mg, 543 µmol) dissolved in THF (6 mL) was added dropwise to a solution of Cp*Sn[BF$_4$] (185 mg, 543 µmol, 1.0 eq.) in THF (4 mL) at -78 °C. The reaction mixture was stirred for 12 h followed by warming to room temperature. The solvent was removed *in vacuo* and the solid residue was washed with toluene (5 mL × 3) and dried *in vacuo* to give pure **2** (174 mg, 53%) as a white powder. Colorless crystals of **2** suitable for single crystal X-ray analysis were obtained by slow diffusion of Et$_2$O into a saturated THF solution at -30 °C for several days.

^{1}H NMR (400 MHz, CD$_3$CN) δ = 7.43 (t, *J* = 7.7 Hz, 4H, Ar$\underline{H}$), 7.26 (d, *J* = 7.7 Hz, 8H, Ar$\underline{H}$), 6.83 (s, 4H, NC$\underline{H}$), 2.60 (septet, *J* = 6.8 Hz, 8H, C$\underline{H}$(CH$_3$)$_2$), 1.12 (d, *J* = 6.8 Hz, 48H, CH(C$\underline{H}_3$)$_2$).

^{13}C{^{1}H} NMR (101 MHz, CD$_3$CN) δ = 152.4 (N$\underline{C}$N), 148.3 (N$\underline{C}$Ar), 133.0 (Ar$\underline{C}$), 132.4 (Ar$\underline{C}$), 130.0 (Ar$\underline{C}$), 129.3 (Ar$\underline{C}$), 127.0 (Ar$\underline{C}$), 126.3 (Ar$\underline{C}$), 125.5 (Ar$\underline{C}$), 117.4 (N$\underline{C}$H), 29.8 ($\underline{C}$H(CH$_3$)$_2$), 25.0 (CH($\underline{C}$H$_3$)$_2$), 23.4 (CH($\underline{C}$H$_3$)$_2$).

^{119}Sn{^{1}H} NMR (149 MHz, CD$_3$CN) δ = 81.9 (d, *J* = 609.9 Hz).

^{11}B{^{1}H} NMR (128 MHz, CD$_3$CN) δ = -1.2.

^{19}F NMR (376 MHz, CD$_3$CN) δ = -41.2 (Sn$\underline{F}$), -152.5.

Anal. Calcd. [%] for $C_{54}H_{72}B_2F_8N_6Sn_2$: C, 53.33; H, 5.97; N, 6.91. Found [%]: C, 53.26; H, 6.05; N, 7.00.

LIFDI-MS: Due to decomposition, compound **2** was not observed in the mass spectrum.

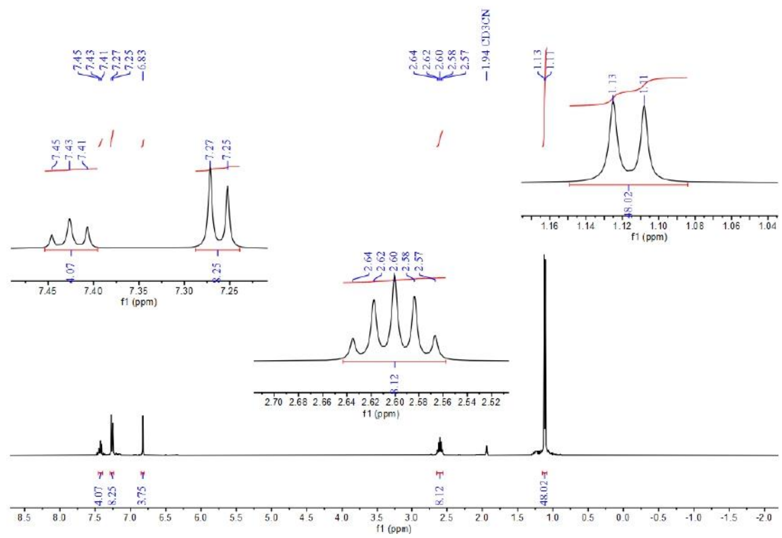

Figure S6. ^{1}H NMR spectrum of compound **2** in CD_3CN.

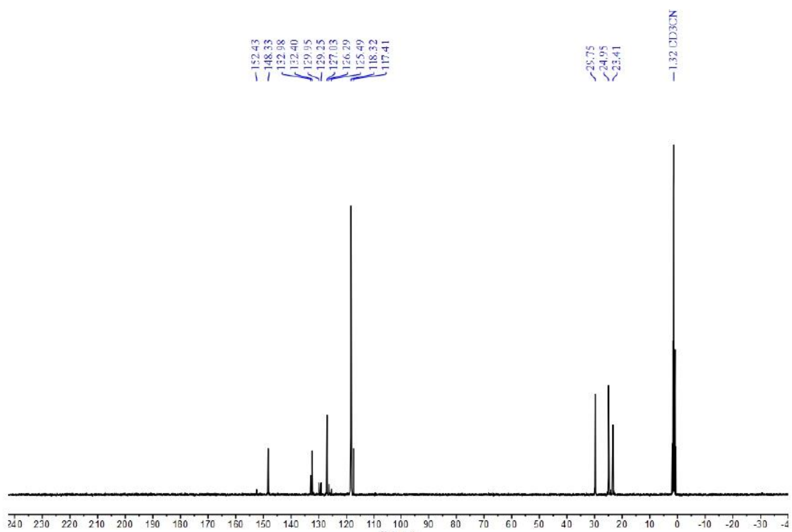

Figure S7. $^{13}C\{^{1}H\}$ NMR spectrum of compound **2** in CD_3CN.

S8

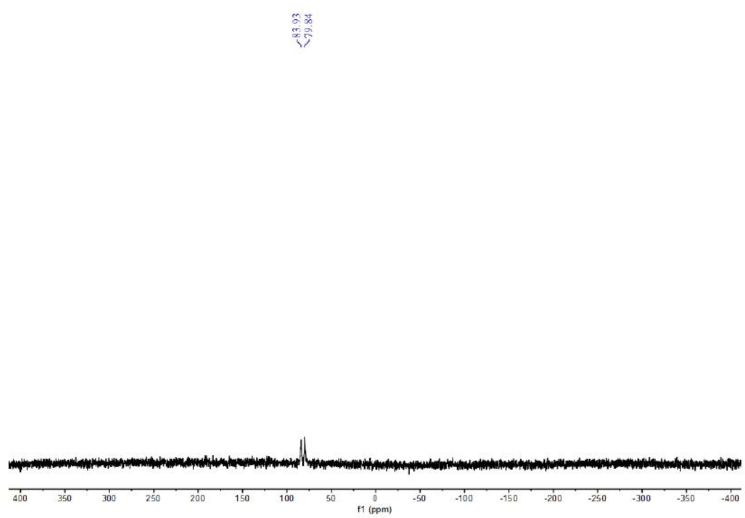

Figure S8. $^{119}Sn\{^{1}H\}$ NMR spectrum of compound **2** in CD_3CN.

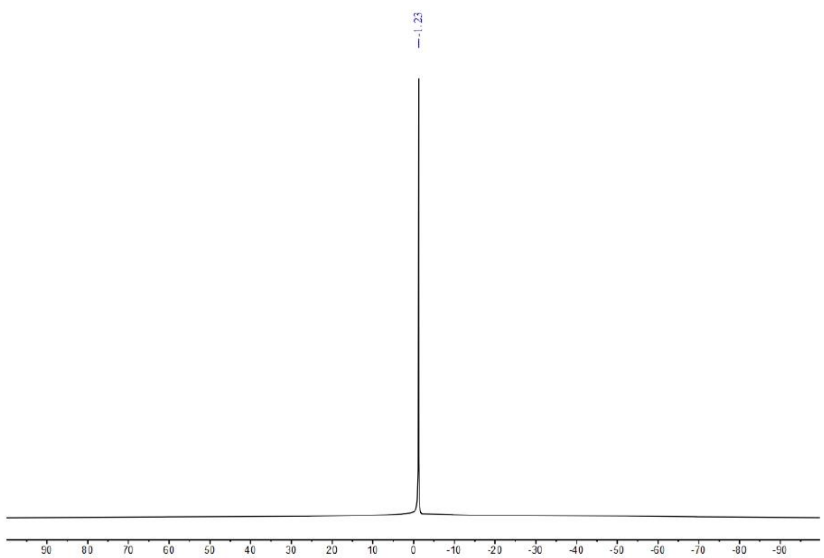

Figure S9. $^{11}B\{^{1}H\}$ NMR spectrum of compound **2** in CD_3CN.

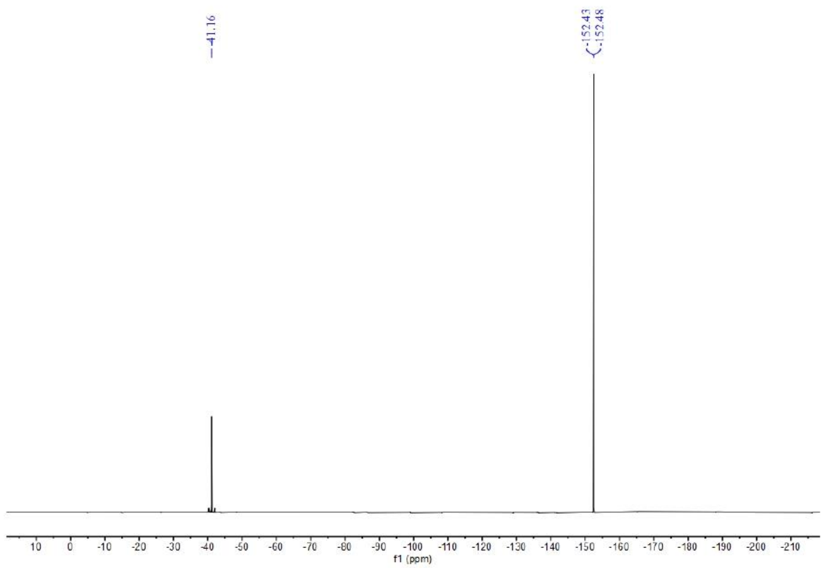

Figure S10. ^{19}F NMR spectrum of compound **2** in CD_3CN.

Reaction of 1 and K[BF$_4$]

0.4 mL CD_3CN were added to a J. Young PTFE tube containing **1** (40 mg, 30 μmol) and K[BF_4] (2 eq., 8 mg, 60 μmol) at room temperature. The obtained solution was well shaken. After 30 min, the completion of the reaction was confirmed by ^{1}H NMR. The reaction resulted in a product mixture (**1** (73%) and **2** (27%)).

Reaction of 2 and K[OTf]

0.4 mL CD_3CN were added to a J. Young PTFE tube containing **2** (40 mg, 33 μmol) and K[OTf] (2 eq., 12 mg, 66 μmol) at room temperature. The obtained solution was well shaken. After 30 min, the completion of the reaction was confirmed by ^{1}H NMR. The reaction resulted in a product mixture (**1** (73%) and **2** (27%)).

Synthesis of $[IPrNSnI]_2$, 3

LiI (11 mg, 82 µmol, 2.0 eq.) dissolved in CH_3CN (2 mL) was added dropwise to a solution of **2** (50 mg, 41 µmol, 1.0 eq.) in CH_3CN (4 mL) at room temperature. The reaction mixture was stirred for 2 h. The volatiles were removed *in vacuo* and the solid residue was dissolved in dichloromethane (DCM) and the solution was concentrated by slow evaporation of the solvent until formation of the crystalline product commenced. The crystals were separated from the liquid phase to afford colorless **3** after drying *in vacuo* (41 mg, 76%).

^{1}H NMR (400 MHz, $CDCl_3$) δ = 7.27 (t, J = 7.7 Hz, 4H, Ar$\underline{H}$), 7.12 (d, J = 7.7 Hz, 8H, Ar$\underline{H}$), 6.34 (s, 4H, NC$\underline{H}$), 3.22 – 3.17 (m, 8H, C$\underline{H}$(CH_3)$_2$), 1.39 (d, J = 6.8 Hz, 24H, CH(C$\underline{H}_3$)$_2$), 1.04 (d, J = 6.8 Hz, 24H, CH(C$\underline{H}_3$)$_2$).

$^{13}C\{^{1}H\}$ NMR (101 MHz, $CDCl_3$) δ = 148.3 (N$\underline{C}$N), 133.1 (Ar$\underline{C}$), 130.6 (Ar$\underline{C}$), 124.9 (Ar$\underline{C}$), 116.6 (N$\underline{C}$H), 28.3 ($\underline{C}$H(CH_3)$_2$), 26.1 (CH($\underline{C}H_3$)$_2$), 24.3 (CH($\underline{C}H_3$)$_2$).

Anal. Calcd. [%] for $C_{54}H_{72}I_2N_6Sn_2$: C, 50.03; H, 5.60; N, 6.48. Found [%]: C, 49.96; H, 5.68; N, 6.56.

LIFDI-MS: Due to decomposition, compound **3** was not observed in the mass spectrum.

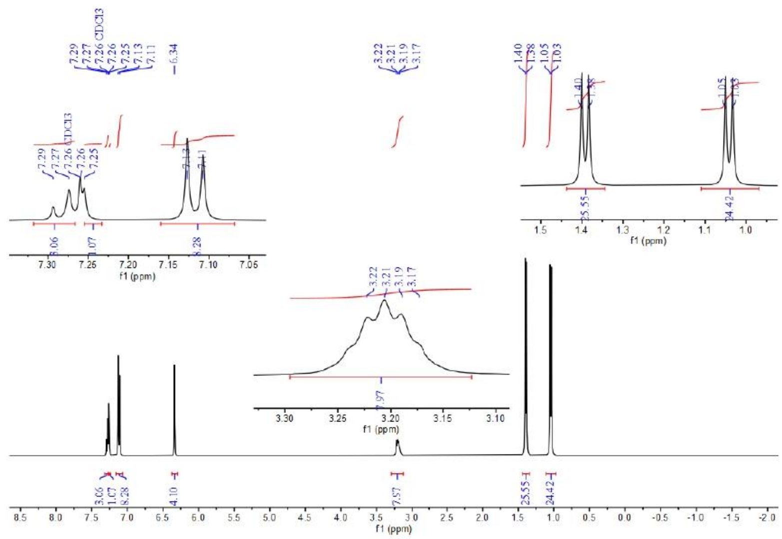

Figure S11. ^{1}H NMR spectrum of compound **3** in $CDCl_3$.

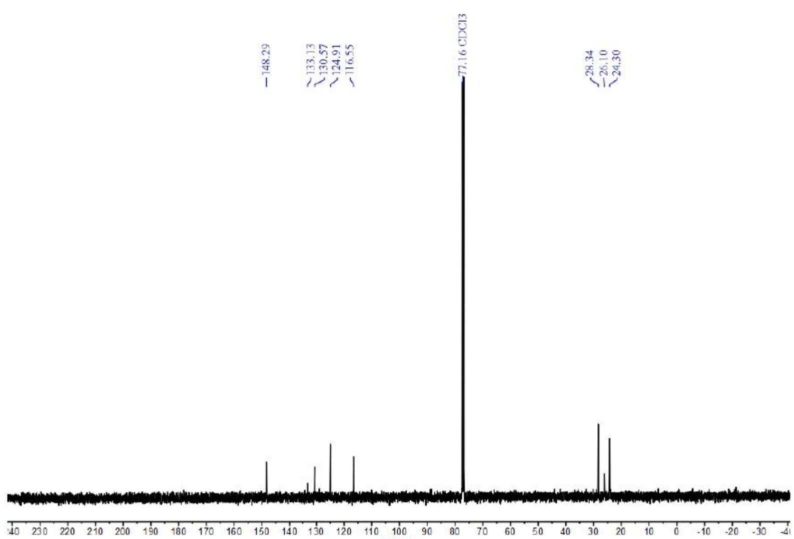

Figure S12. $^{13}C\{^{1}H\}$ NMR spectrum of compound **3** in $CDCl_3$.

Catalysis Studies

General procedures for catalytic hydroboration of aldehydes

Pinacolborane (HBpin, 1.0 mmol) was added to a solution of aldehyde (1.0 mmol) and 1,3,5-trimethoxybenzene (100 µmol) in CD_3CN (0.4 mL) in NMR tube. After shaking, 0.5 mol % of **1** or **2** or $Na[BF_4]$ or K[OTf] was added, and the obtained solution was well shaken again. The reactions were monitored regularly using ^{1}H NMR spectroscopy.

General procedures for catalytic hydroboration of ketones

Pinacolborane (HBpin, 500 µmol) was added to a solution of ketone (500 µmol) and 1,3,5-trimethoxybenzene (50 µmol) in CD_3CN (0.4 mL) in NMR tube. After shaking, 5 mol % of **2** was added, and the obtained solution was well shaken again. The reactions were monitored regularly using ^{1}H NMR spectroscopy.

Spectroscopic data of hydroboration products

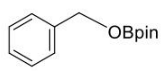

^{1}H NMR (400 MHz, CD_3CN): δ = 1.28 (s, 12H, Bpin-C*H*$_3$), 4.92 (s, 2H, C*H*$_2$-OBpin), 7.30 – 7.42 (m, 5H, Ar*H*).

^{13}C{^{1}H} NMR (101 MHz, CD_3CN): δ = 25.0 (Bpin-*C*H$_3$), 67.4 (*C*H$_2$-OBpin), 83.8 (BO*C*(CH$_3$)$_2$), 127.7 (Ar*C*), 128.4 (Ar*C*), 129.3 (Ar*C*), 140.5 (Ar*C*).

^{11}B{^{1}H} NMR (128 MHz, CD_3CN): δ = 22.6.

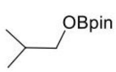

^{1}H NMR (400 MHz, CD_3CN): δ = 0.88 (d, *J* = 6.8 Hz, 6H, C*H*$_3$), 1.22 (s, 12H, Bpin-C*H*$_3$), 1.77 (septet, *J* = 6.8 Hz, 1H, C*H*(CH$_3$)$_2$), 3.57 (d, *J* = 6.5 Hz, 2H, C*H*$_2$-OBpin).

^{13}C{^{1}H} NMR (101 MHz, CD_3CN): δ = 19.1 (CH(*C*H$_3$)$_2$), 25.0 (Bpin-*C*H$_3$), 30.7 (*C*H(CH$_3$)$_2$), 71.9 (*C*H$_2$-OBPin), 83.3 (BO*C*(CH$_3$)$_2$).

^{11}B{^{1}H} NMR (128 MHz, CD_3CN): δ = 22.2.

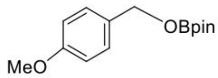

^{1}H NMR (400 MHz, CD_3CN): δ = 1.26 (s, 12H, Bpin-C$\underline{H}_3$), 3.78 (s, 3H, OC$\underline{H}_3$), 4.82 (s, 2H, C$\underline{H}_2$-OBpin), 6.91 (d, J = 8.8 Hz, 2H, Ar$\underline{H}$), 7.29 (d, J = 8.7 Hz, 2H, Ar$\underline{H}$).

^{13}C{^{1}H} NMR (101 MHz, CD_3CN): δ = 25.1 (Bpin-$\underline{C}H_3$), 55.9 (O$\underline{C}H_3$), 67.1 ($\underline{C}H_2$-OBpin), 83.7 (BO$\underline{C}(CH_3)_2$), 114.7 (Ar$\underline{C}$), 129.6 (Ar$\underline{C}$), 132.6 (Ar$\underline{C}$), 160.2 (Ar$\underline{C}$).

^{11}B{^{1}H} NMR (128 MHz, CD_3CN): δ = 22.5.

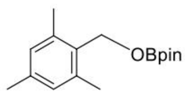

^{1}H NMR (400 MHz, CD_3CN): δ = 1.27 (s, 12H, Bpin-C$\underline{H}_3$), 2.26 (s, 3H, ArC$\underline{H}_3$), 2.37 (s, 6H, ArC$\underline{H}_3$), 4.95 (s, 2H, C$\underline{H}_2$-OBpin), 6.87 (s, 2H, Ar$\underline{H}$).

^{13}C{^{1}H} NMR (101 MHz, CD_3CN): δ = 19.7 (Ar$\underline{C}H_3$), 21.3 (Ar$\underline{C}H_3$), 25.1 (Bpin-$\underline{C}H_3$), 61.9 ($\underline{C}H_2$-OBpin), 83.6 (BO$\underline{C}(CH_3)_2$), 129.8 (Ar$\underline{C}$), 133.3 (Ar$\underline{C}$), 138.5 (Ar$\underline{C}$).

^{11}B{^{1}H} NMR (128 MHz, CD_3CN): δ = 22.4.

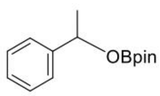

^{1}H NMR (400 MHz, CD_3CN): δ = 1.20 (s, 6H, Bpin-C$\underline{H}_3$), 1.23 (s, 6H, Bpin-C$\underline{H}_3$), 1.47 (d, J = 6.5 Hz, 3H, C$\underline{H}_3$), 5.23 (q, J = 6.5 Hz, 1H, C$\underline{H}$-OBpin), 7.25 – 7.30 (m, 1H, Ar$\underline{H}$), 7.33 – 7.38 (m, 4H, Ar$\underline{H}$).

^{13}C{^{1}H} NMR (101 MHz, CD_3CN): δ = 24.9 ($\underline{C}H_3$), 25.6 ($\underline{C}H_3$), 73.2 ($\underline{C}$H-OBpin), 83.6 (BO$\underline{C}(CH_3)_2$), 126.2 (Ar$\underline{C}$), 128.2 (Ar$\underline{C}$), 129.3 (Ar$\underline{C}$), 145.7 (Ar$\underline{C}$).

^{11}B{^{1}H} NMR (128 MHz, CD_3CN): δ = 22.3.

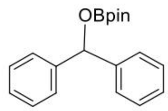

^{1}H NMR (400 MHz, CD_3CN): δ = 1.21 (s, 12H, Bpin-C$\underline{H}_3$), 6.22 (s, 1H, C$\underline{H}$-OBpin), 7.25 – 7.29 (m, 2H, Ar$\underline{H}$), 7.33 – 7.37 (m, 4H, Ar$\underline{H}$), 7.40 – 7.44 (m, 4H, Ar$\underline{H}$).

^{13}C{^{1}H} NMR (101 MHz, CD_3CN): δ = 24.9 (Bpin-$\underline{C}H_3$), 78.7 ($\underline{C}$H-OBpin), 83.9 (BO$\underline{C}(CH_3)_2$), 127.1 (Ar$\underline{C}$), 128.4 (Ar$\underline{C}$), 129.4 (Ar$\underline{C}$), 130.7 (Ar$\underline{C}$), 133.5 (Ar$\underline{C}$), 138.5 (Ar$\underline{C}$), 144.3 (Ar$\underline{C}$).

^{11}B{^{1}H} NMR (128 MHz, CD_3CN): δ = 22.6.

NMR charts of hydroboration products

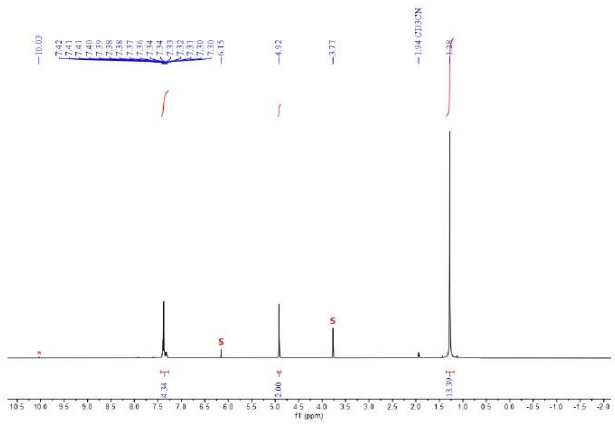

Figure S13. ^{1}H NMR spectrum of benzaldehyde reduction in CD_3CN (0.5 mol % of **2**, 0.5 h). The resonances of internal standard (1,3,5-trimethoxybenzene) are marked with an S and residual benzaldehyde with asterisks *.

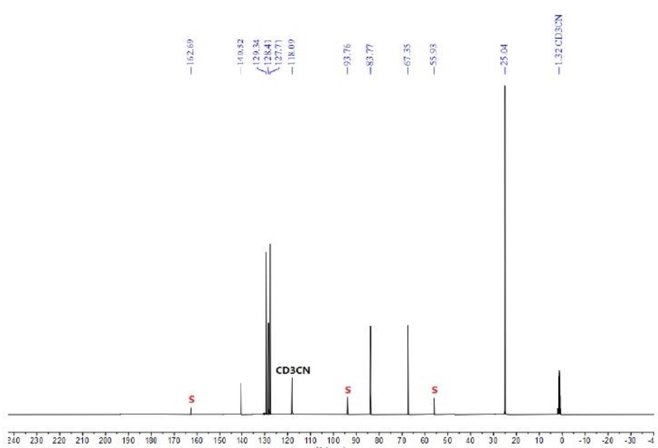

Figure S14. $^{13}C\{^1H\}$ NMR spectrum of benzaldehyde reduction in CD_3CN (0.5 mol % of **2**, 0.5 h). The resonances of internal standard (1,3,5-trimethoxybenzene) are marked with an S.

S16

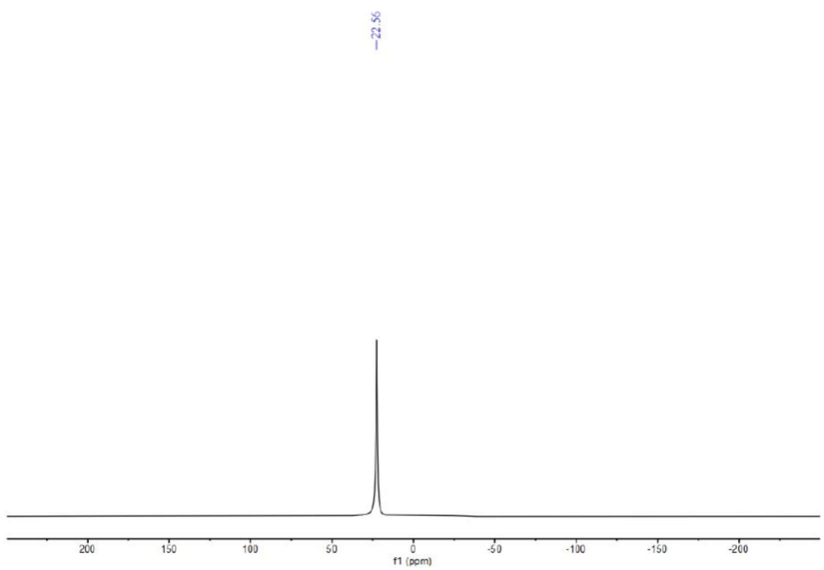

Figure S15. $^{11}B\{^1H\}$ NMR spectrum of benzaldehyde reduction in CD_3CN (0.5 mol % of **2**, 0.5 h).

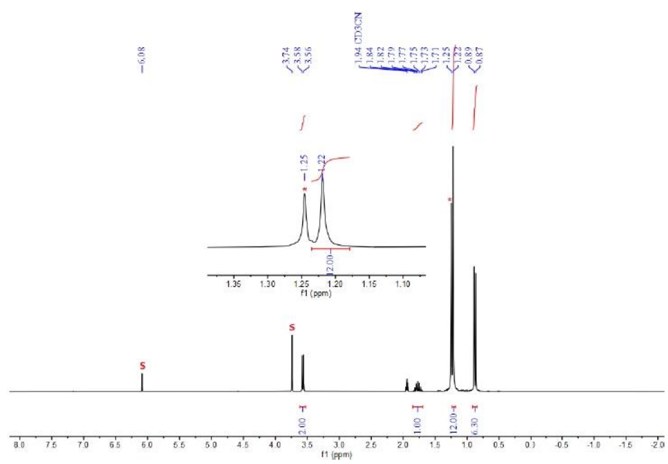

Figure S16. ^1H NMR spectrum of isobutyraldehyde reduction in CD_3CN (0.5 mol % of **2**, 2 h). The resonances of internal standard (1,3,5-trimethoxybenzene) are marked with an S and residual HBpin with asterisks *.

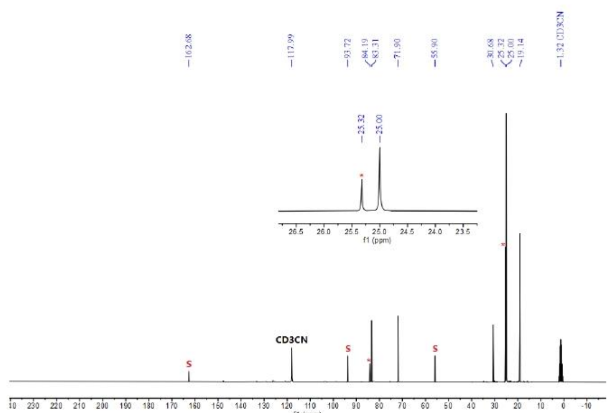

Figure S17. $^{13}C\{^1H\}$ NMR spectrum of isobutyraldehyde reduction in CD_3CN (0.5 mol % of **2**, 2 h). The resonances of internal standard (1,3,5-trimethoxybenzene) are marked with an S and residual HBpin with asterisks *.

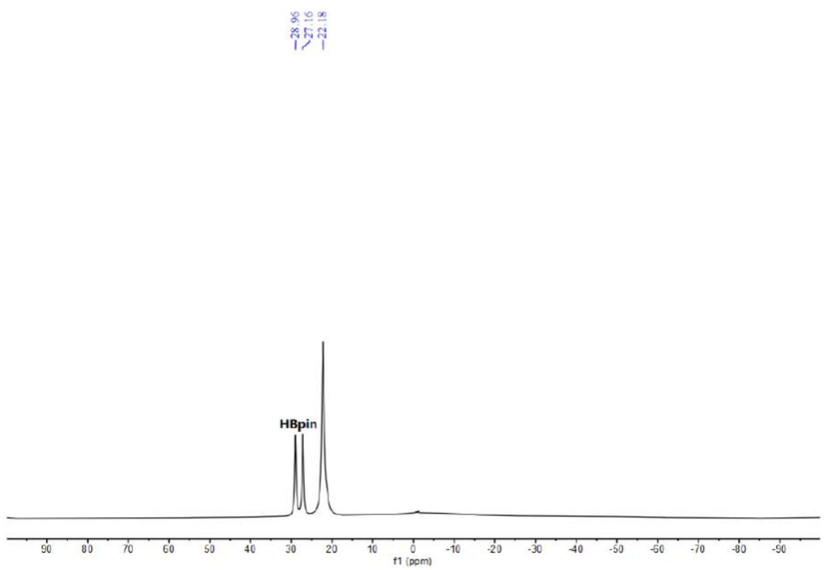

Figure S18. $^{11}B\{^1H\}$ NMR spectrum of isobutyraldehyde reduction in CD_3CN (0.5 mol % of **2**, 2 h).

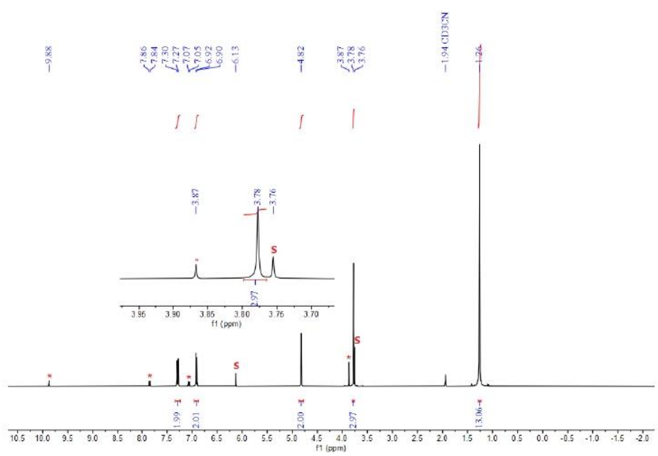

Figure S19. ^{1}H NMR spectrum of 4-methoxybenzaldehyde reduction in CD_3CN (0.5 mol % of **2**, 120 h). The resonances of internal standard (1,3,5-trimethoxybenzene) are marked with an S and residual 4-methoxybenzaldehyde with asterisks *.

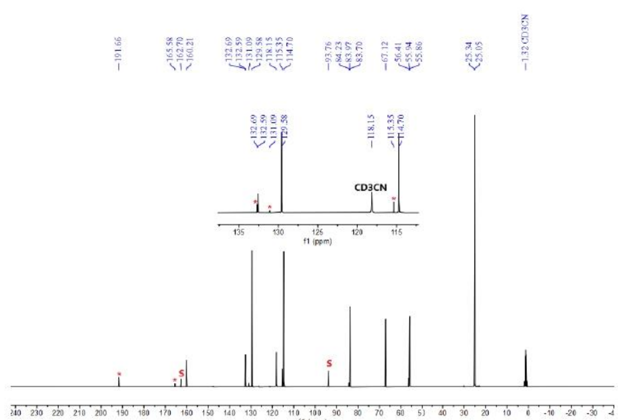

Figure S20. $^{13}C\{^{1}H\}$ NMR spectrum of 4-methoxybenzaldehyde reduction in CD_3CN (0.5 mol % of **2**, 120 h). The resonances of internal standard (1,3,5-trimethoxybenzene) are marked with an S and residual 4-methoxybenzaldehyde with asterisks *.

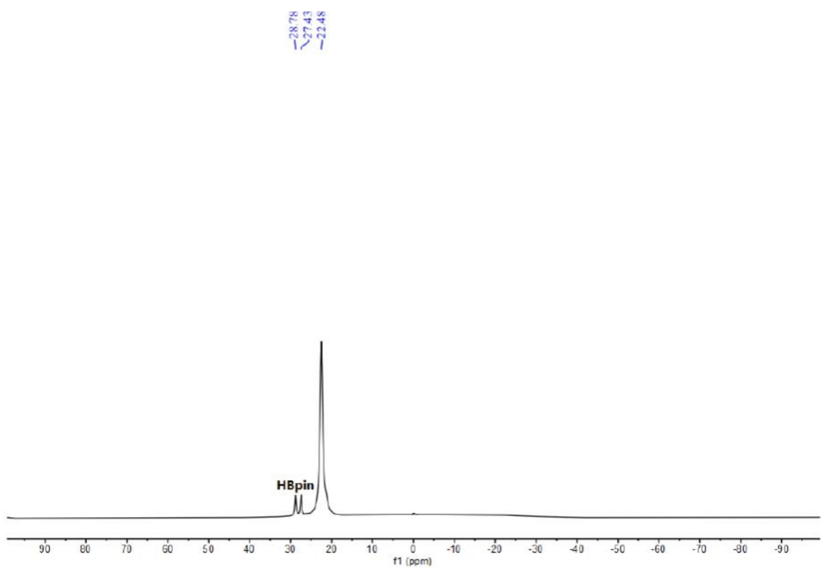

Figure S21. $^{11}B\{^{1}H\}$ NMR spectrum of 4-methoxybenzaldehyde reduction in CD_3CN (0.5 mol % of **2**, 120 h).

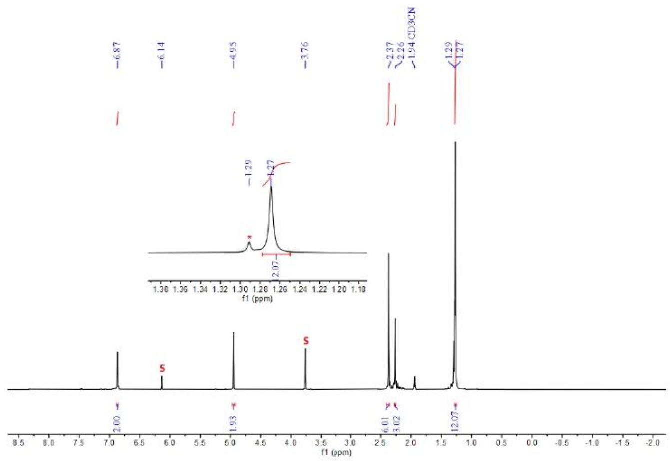

Figure S22. ^1H NMR spectrum of mesitaldehyde reduction in CD_3CN (0.5 mol % of **2**, 36 h). The resonances of internal standard (1,3,5-trimethoxybenzene) are marked with an S and residual HBpin with asterisks *.

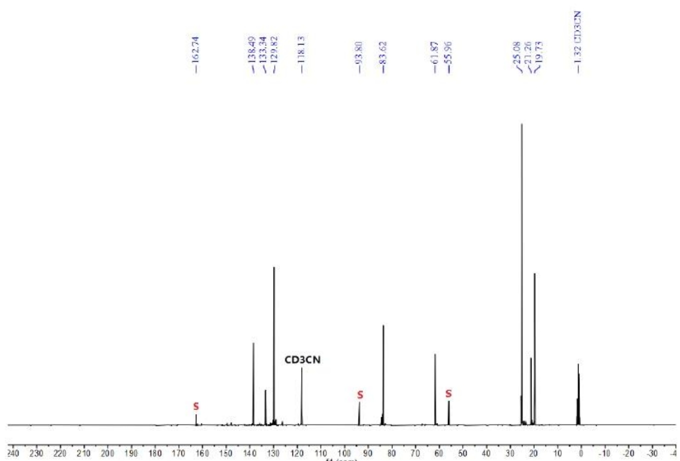

Figure S23. $^{13}C\{^1H\}$ NMR spectrum of mesitaldehyde reduction in CD_3CN (0.5 mol % of **2**, 36 h). The resonances of internal standard (1,3,5-trimethoxybenzene) are marked with an S.

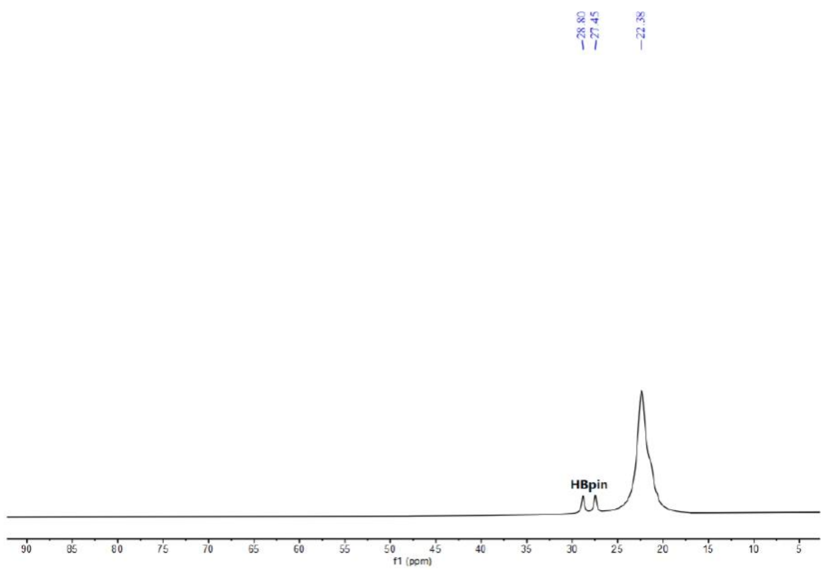

Figure S24. $^{11}B\{^1H\}$ NMR spectrum of mesitaldehyde reduction in CD_3CN (0.5 mol % of **2**, 36 h).

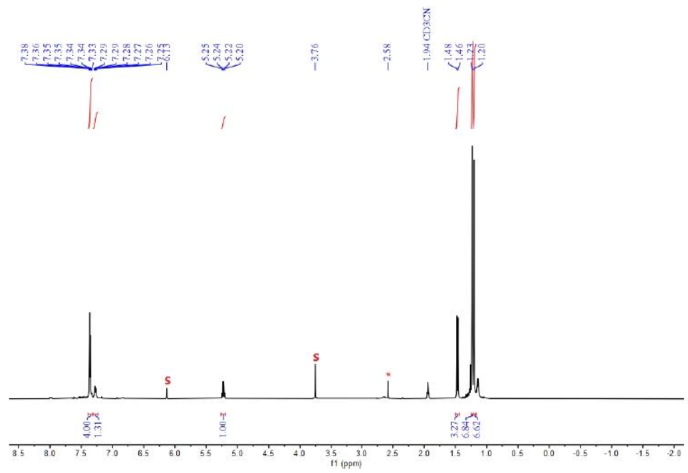

Figure S25. ^{1}H NMR spectrum of acetophenone reduction in CD_3CN (5 mol % of **2**, 19 h). The resonances of internal standard (1,3,5-trimethoxybenzene) are marked with an S and residual acetophenone with asterisks *.

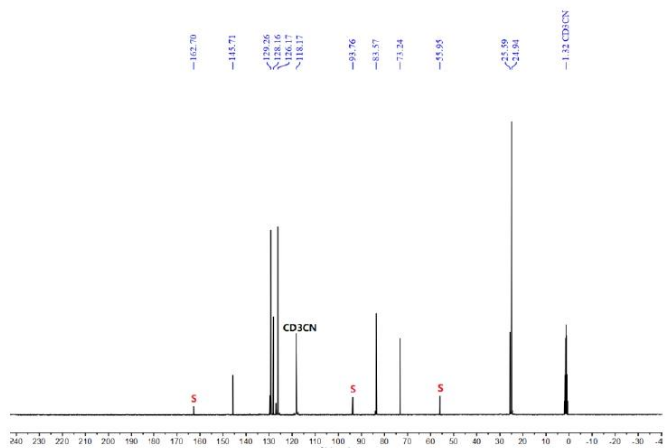

Figure S26. $^{13}C\{^{1}H\}$ NMR spectrum of acetophenone reduction in CD_3CN (5 mol % of **2**, 19 h). The resonances of internal standard (1,3,5-trimethoxybenzene) are marked with an S.

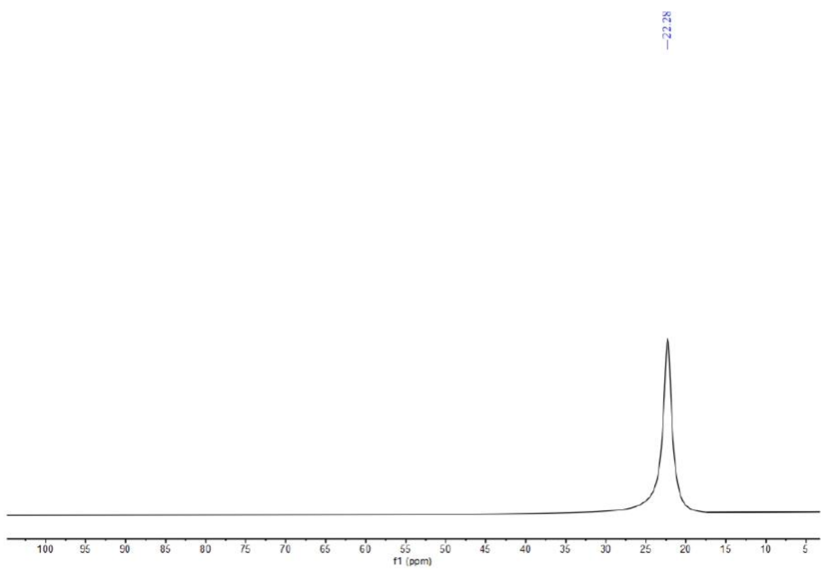

Figure S27. $^{11}B\{^1H\}$ NMR spectrum of acetophenone reduction in CD_3CN (5 mol % of **2**, 19 h).

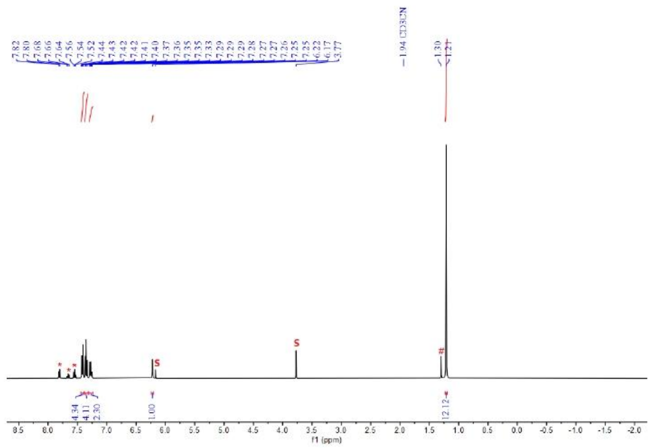

Figure S28. ^{1}H NMR spectrum of benzophenone reduction in CD_3CN (5 mol % of **2**, 156 h). The resonances of internal standard (1,3,5-trimethoxybenzene) are marked with an S, residual benzophenone with asterisks * and residual HBpin with #.

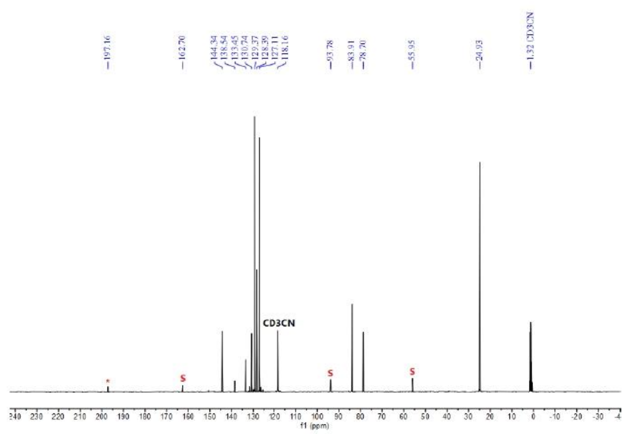

Figure S29. $^{13}C\{^{1}H\}$ NMR spectrum of benzophenone reduction in CD_3CN (5 mol % of **2**, 156 h). The resonances of internal standard (1,3,5-trimethoxybenzene) are marked with an S and residual benzophenone with asterisks *.

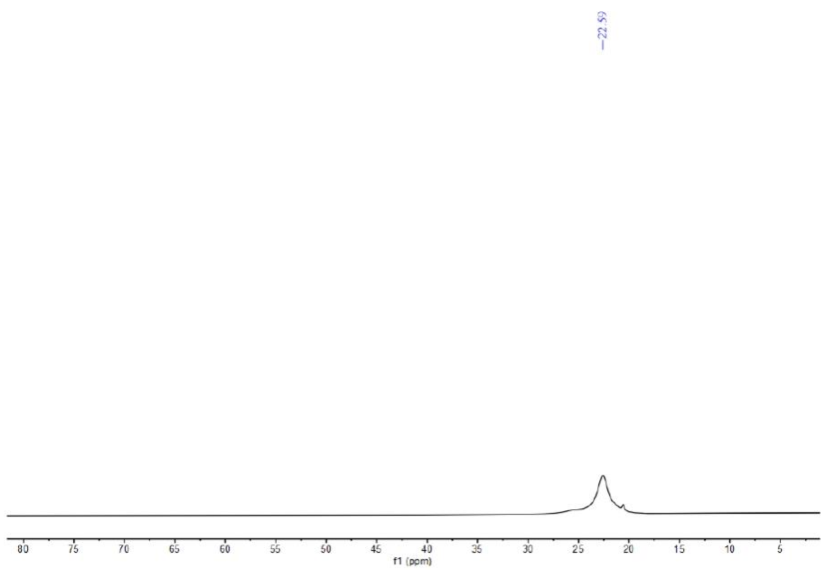

Figure S30. $^{11}B\{^{1}H\}$ NMR spectrum of benzophenone reduction in CD_3CN (5 mol % of **2**, 156 h).

2. X-ray Crystallographic Data

General Information

The X-ray intensity data of compounds **1**, **2** and **3** were collected on an X-ray single crystal diffractometer equipped with a CMOS detector (Bruker Photon-100), an IMS microsource with MoKα radiation (λ = 0.71073 Å) and a Helios mirror optic by using the APEX III software package.[S4] The measurements were performed on single crystals coated with the perfluorinated ether Fomblin® Y. The crystals were fixed on the top of a microsampler, transferred to the diffractometer and frozen under a stream of cold nitrogen. A matrix scan was used to determine the initial lattice parameters. Reflections were merged and corrected for Lorenz and polarization effects, scan speed, and background using SAINT.[S5] Absorption corrections, including odd and even ordered spherical harmonics were performed using SADABS.[S5] Space group assignments were based upon systematic absences, E statistics, and successful refinement of the structures. Structures were solved by direct methods with the aid of successive difference Fourier maps, and were refined against all data using the APEX III software in conjunction with SHELXL-2014[S6] and SHELXLE.[S7] All H atoms were placed in calculated positions and refined using a riding model, with methylene and aromatic C–H distances of 0.99 and 0.95 Å, respectively, and Uiso(H) = 1.2·Ueq(C). Full-matrix least-squares refinements were carried out by minimizing $\Sigma w(Fo^2–Fc^2)^2$ with SHELXL-97[S8] weighting scheme. Neutral atom scattering factors for all atoms and anomalous dispersion corrections for the non-hydrogen atoms were taken from International Tables for Crystallography.[S9] The images of the crystal structure were generated by Mercury.[S10] The CCDC number 2174491 (**2**) and 2174492 (**3**) contain the supplementary crystallographic data for the structures. The data can be obtained free of charge from the Cambridge Crystallographic Data Centre *via* https://www.ccdc.cam.ac.uk/structures/.

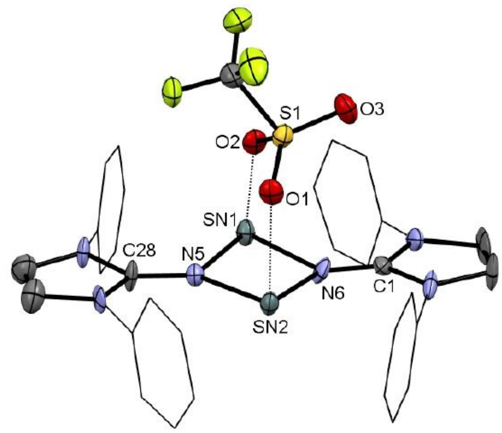

Figure S31. Molecular structure of **1**. Thermal ellipsoids are shown at 50% probability level. Hydrogen atoms, isopropyl groups, and counterion are omitted for clarity. Selected bond lengths [Å] and angles [°]: Sn1–O2 2.3944, Sn2–O1 2.3990, Sn1–N5 2.1531, Sn1–N6 2.1721, Sn2–N5 2.1454, Sn2–N6 2.1729, N5–C28 1.3548, N6–C1 1.2971, N5–Sn1–N6 76.38, N5–Sn2–N6 76.53, Sn1–N5–C28 127.18, Sn1–N6–C1 128.34, Sn2–N5–C28 128.33, Sn2–N6–C1 128.43, Sn1–N5–Sn2 104.01, Sn1–N6–Sn2 102.45.

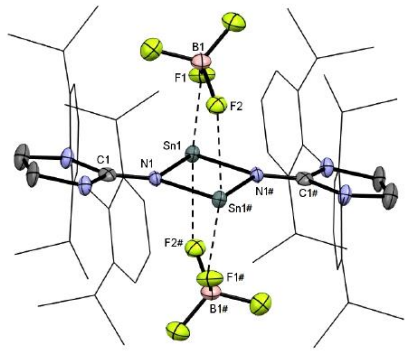

Figure S32. Molecular structure of **2**. Thermal ellipsoids are shown at 50% probability level. Hydrogen atoms are omitted for clarity. Selected bond lengths [Å] and angles [°]: Sn1–N1 2.155(3), Sn1–N1# 2.166(3), Sn1···F1 2.461(2), Sn1···F2# 2.501(2), N1–C1 1.296(4), Sn1–N1–C1 129.1(2), Sn1–N1#–C1# 128.1(2), Sn1–N1–Sn1# 102.1(1), N1–Sn1–N1# 77.9(1).

Table S1. Crystal data and structure refinement for compound **2**.

Chemical formula	$C_{54}H_{72}B_2F_8N_6Sn_2$
Formula weight	1216.22
Radiation source	IMS microsource (Mo)
Temperature (K)	100
Wavelength (Å)	0.71073
Crystal system (Space group)	Monoclinic, $P2_1/n$
Unit cell dimensions	a = 12.6890(8) Å, α = 90° b = 13.5478(8) Å, β = 98.772(3)° c = 16.3399(10) Å, γ = 90°
Volume (Å^3)	2776.1(3)
Z	2
Density Dx (g/cm^3)	1.455
Absorption coefficient μ (mm^{-1})	0.967
Absorption correction	Multi-Scan

F(000)	1240.0
Theta (max) (°)	25.350
Index ranges	–15<=h<=15, –16<=k<=16, –19<=l<=19
Absorption Correction Tmin, Tmax	0.694, 0.745
Coverage of independent reflections (%)	97.8
Refinement method	Full-matrix least-squares on F^2
Data / Parameter / Restraints	4977 / 333 / 0
Goodness-of-fit on F^2	0.887
Final R indices (I>2σ(I))	R1(all) = 0.0622, wR2(all) = 0.0954 R1 = 0.0366, wR2 = 0.0839

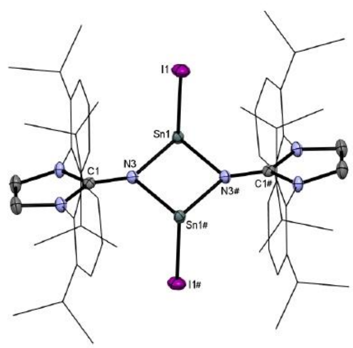

Figure S33. Molecular structure of **3**. Thermal ellipsoids are shown at 50% probability level. Hydrogen atoms are omitted for clarity. Selected bond lengths [Å] and angles [°]: Sn1–I1 2.9176(4), Sn1–N3 2.168(1), Sn1–N3# 2.182(1), N3–C1 1.295(2), I1–Sn1–N3 85.90(4), I1–Sn1–N3# 87.87(4), N3–Sn1–N3# 77.72(5), Sn1–N3–C1 126.4(1), Sn1–N3#–C1# 130.3(1), Sn1–N3–Sn1# 102.28(5).

Table S2. Crystal data and structure refinement for compound **3**.

Chemical formula	$C_{54}H_{72}I_2N_6Sn_2$
Formula weight	1296.40
Radiation source	IMS microsource (Mo)
Temperature (K)	100
Wavelength (Å)	0.71073
Crystal system (Space group)	Monoclinic, $P2_1/n$
Unit cell dimensions	a = 12.5623(14) Å, α = 90° b = 13.6118(15) Å, β = 99.176(4)° c = 16.4082(18) Å, γ = 90°
Volume (Å^3)	2769.8(5)
Z	2
Density Dx (g/cm^3)	1.554
Absorption coefficient μ (mm^{-1})	2.055
Absorption correction	Multi-Scan
F(000)	1288.0
Theta (max) (°)	25.360
Index ranges	–15<=h<=15, –16<=k<=16, –19<=l<=19
Absorption Correction Tmin, Tmax	0.709, 0.745
Coverage of independent reflections (%)	99.9
Refinement method	Full-matrix least-squares on F^2
Data / Parameter / Restraints	5083 / 304 / 9
Goodness-of-fit on F^2	1.081
Final R indices (I>2σ(I))	R1(all) = 0.0160, wR2(all) = 0.0373 R1 = 0.0154, wR2 = 0.0370

3. References

[S1] D. Franz, E. Irran, S. Inoue, *Dalton Trans.* **2014**, *43*, 4451-4461.

[S2] P. Jutzi, F. Kohl, P. Hofmann, C. Krüger, Y.-H. Tsay, *Chem. Ber.* **1980**, *113*, 757-769.

[S3] F. X. Kohl, P. Jutzi, *Chem. Ber.* **1981**, *114*, 488-494.

[S4] *APEX suite of crystallographic software*, APEX 3 version 2015.5-2; Bruker AXS Inc.: Madison, Wisconsin, USA, **2015**.

[S5] *SAINT*, Version 7.56a and SADABS Version 2008/1; Bruker AXS Inc.: Madison, Wisconsin, USA, **2008**.

[S6] G. M. Sheldrick, *SHELXL-2014*, University of Göttingen, Göttingen, Germany, **2014**.

[S7] C. B. Hübschle, G. M. Sheldrick, B. Dittrich, *J. Appl. Cryst.* **2011**, *44*, 1281-1284.

[S8] G. M. Sheldrick, *SHELXL-97*, University of Göttingen, Göttingen, Germany, **1998**.

[S9] A. J. C. Wilson, *International Tables for Crystallography*, Vol. C, Tables 6.1.1.4 (pp. 500-502), 4.2.6.8 (pp. 219-222), and 4.2.4.2 (pp. 193-199); Kluwer Academic Publishers: Dordrecht, The Netherlands, **1992**.

[S10] C. F. Macrae, I. J. Bruno, J. A. Chisholm, P. R. Edgington, P. McCabe, E. Pidcock, L. Rodriguez-Monge, R. Taylor, J. van de Streek, P. A. Wood, *J. Appl. Cryst.* **2008**, *41*, 466-470.

9.4 Supporting Information for Chapter 7

Supporting Information

Isolation and Reactivity of Stannylenoids Stabilized by Amido/Imino Ligands

Xuan-Xuan Zhao,[†] *Shiori Fujimori,*[†] *John A. Kelly,*[†] *and Shigeyoshi Inoue**[,†]

[†]Department of Chemistry, WACKER-Institute of Silicon Chemistry and Catalysis Research Center, Technische Universität München, Lichtenbergstraße 4, 85748 Garching bei München, Germany

Table of Contents

1. Experimental Section

General Considerations

All experiments and manipulations were carried out under dry oxygen-free argon atmosphere using standard Schlenk techniques or in a glovebox. All glass junctions were coated with PTFE-based grease Merkel Triboflon III. All the solvents were dried and freshly distilled under Ar atmosphere prior to use by standard techniques. The ^{1}H, $^{13}C\{^{1}H\}$, $^{119}Sn\{^{1}H\}$, $^{29}Si\{^{1}H\}$ NMR spectra were recorded on Bruker 400 MHz spectrometer. Chemical shifts are referenced to (residual) solvent signals (C_6D_6: $\delta(^{1}H) = 7.16$ ppm and $\delta(^{13}C) = 128.06$ ppm). Abbreviations: s = singlet, br. = broadened, d = doublet, t = triplet, m = multiplet. Elemental analysis (EA) was conducted with a EURO EA (HEKA tech) instrument equipped with a CHNS combustion analyzer. Liquid Injection Field Desorption Ionization Mass Spectrometry (LIFDI-MS) was measured directly from an inert atmosphere glovebox with a Thermo Fisher Scientific Exactive Plus Orbitrap equipped with an ion source from Linden CMS. Unless otherwise stated, all commercially available chemicals were purchased from *abcr GmbH*, *Sigma-Aldrich Chemie GmbH* or *Tokyo Chemical Industry Co., Ltd.*, and used without further purification. The starting materials Dipp($^{i}Pr_3Si$)NLi (Dipp = 2,6-$^{i}Pr_2C_6H_3$)[S1], and IPrNLi (IPrN = bis(2,6-diisopropylphenyl)imidazolin-2-imino)[S2] were prepared according to the literature procedures, respectively.

Synthetic Procedures

Synthesis of compound 1

Dipp(^{i}Pr$_3$Si)NLi (2.0 g, 5.89 mmol) dissolved in THF (40 mL) was added dropwise to a solution of $SnCl_2$ (1.12 g, 5.89 mmol, 1.0 eq.) in THF (20 mL) at room temperature. The reaction mixture was stirred for 2 h. The solvent was removed *in vacuo* and the solid residue was extracted with toluene (10 mL × 3). After filtration, the solvent was removed from the filtrate *in vacuo* to afford **1** as a pale-yellow solid (3.28 g, 83%), and colorless crystals were recrystallized from a saturated solution in *n*-pentane at -30 ºC.

^{1}H NMR (400 MHz, C_6D_6) δ = 7.19 (d, *J* = 7.7 Hz, 2H, Ar$\underline{H}$), 7.06 (t, *J* = 7.7 Hz, 1H, Ar$\underline{H}$), 3.84 (septet, *J* = 6.8 Hz, 2H, C$\underline{H}$(CH$_3$)$_2$), 3.51 (m, 8H, 2,5-C$\underline{H}_2$), 1.48 (septet, *J* = 6.8 Hz, 3H, C$\underline{H}$(CH$_3$)$_2$), 1.39 (d, *J* = 6.8 Hz, 12H, CH(C$\underline{H}_3$)$_2$), 1.33 (m, 8H, 3,4-C$\underline{H}_2$), 1.25 (d, *J* = 7.5 Hz, 18H, CH(C$\underline{H}_3$)$_2$).

^{13}C{^{1}H} NMR (101 MHz, C_6D_6) δ = 146.4 (Ar$\underline{C}$), 143.6 (Ar$\underline{C}$), 124.6 (Ar$\underline{C}$), 124.0 (Ar$\underline{C}$), 28.0 ($\underline{C}$H(CH$_3$)$_2$), 27.5 (CH($\underline{C}$H$_3$)$_2$), 25.5 (CH($\underline{C}$H$_3$)$_2$), 24.4 (CH($\underline{C}$H$_3$)$_2$), 19.5 (CH($\underline{C}$H$_3$)$_2$), 14.5 (CH($\underline{C}$H$_3$)$_2$).

^{119}Sn{^{1}H} NMR (149 MHz, C_6D_6) δ = 197.7.

^{29}Si{^{1}H} NMR (79 MHz, C_6D_6) δ = 7.8.

Anal. Calcd. [%] for $C_{29}H_{54}Cl_2LiNO_2SiSn$: C, 51.73; H, 8.08; N, 2.08. Found [%]: C, 51.70; H, 8.13; N, 2.04.

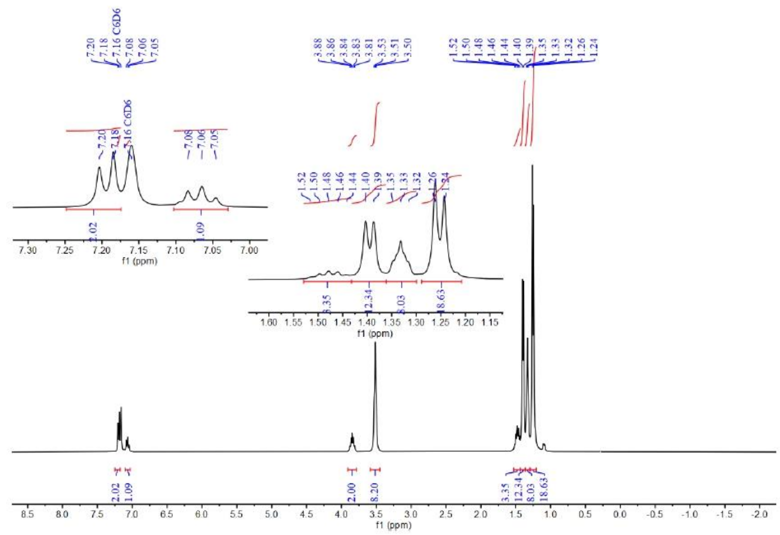

Figure S1. ^{1}H NMR spectrum of compound **1** in C_6D_6.

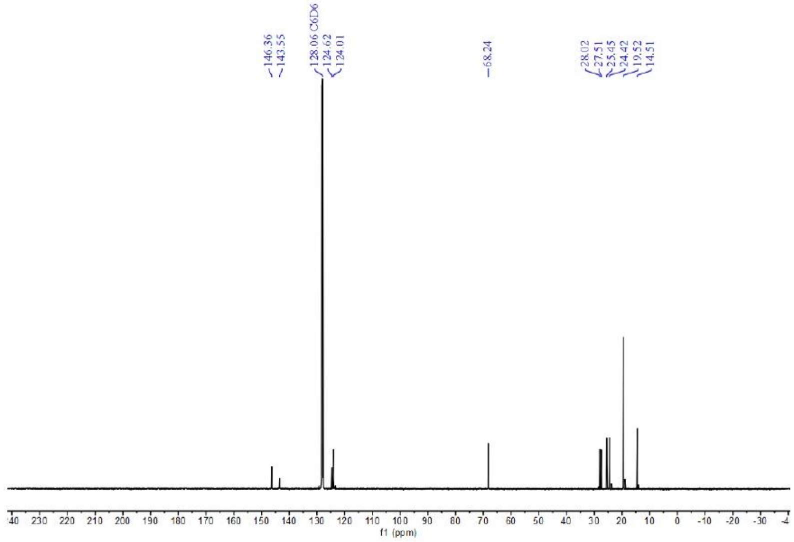

Figure S2. $^{13}C\{^1H\}$ NMR spectrum of compound **1** in C_6D_6.

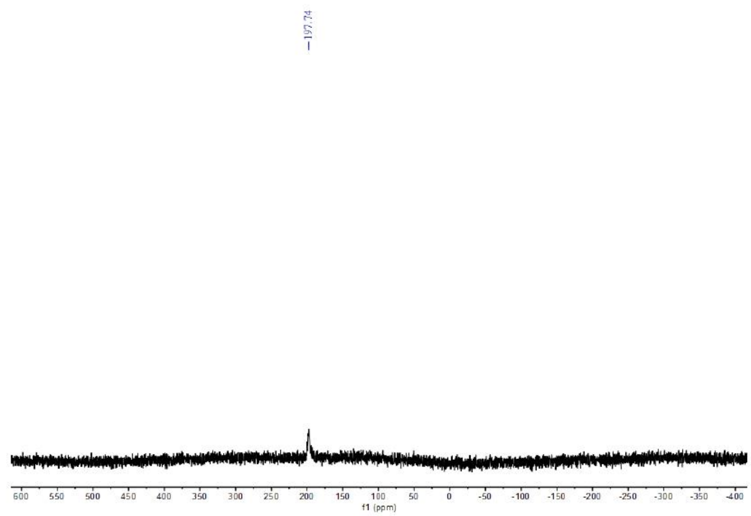

Figure S3. $^{119}Sn\{^1H\}$ NMR spectrum of compound **1** in C_6D_6.

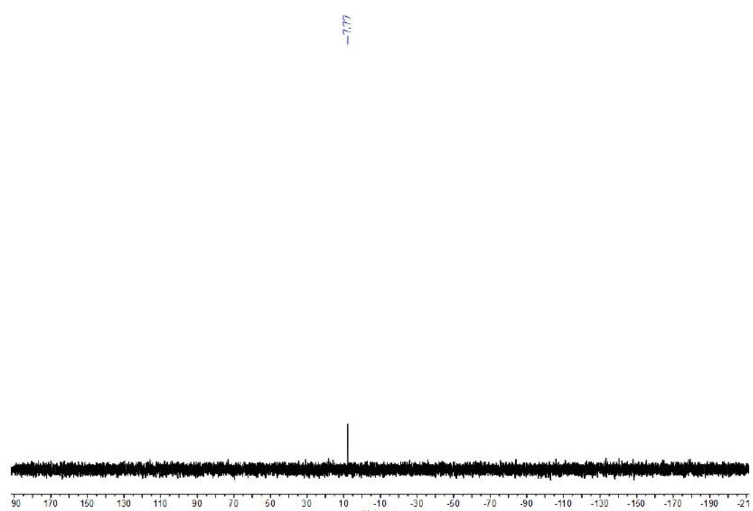

Figure S4. $^{29}Si\{^1H\}$ NMR spectrum of compound **1** in C_6D_6.

S5

Synthesis of compound 2

The solution of **1** (2.0 g, 2.97 mmol) in toluene (20 mL) in a Schlenk tube equipped with a PTFE-coated magnetic stirring bar was stirred at 80 ºC for 2 days. The reaction mixture was allowed to cold to room temperature. After filtration, the solvent was removed from the filtrate *in vacuo* to afford **2** as a pale-yellow solid (1.35 g, 93%), and pale-yellow crystals were recrystallized from a saturated solution in *n*-pentane at -30 ºC.

^{1}H NMR (400 MHz, C_6D_6) δ = 7.13 (d, *J* = 7.7 Hz, 4H, Ar$\underline{H}$), 7.03 (t, *J* = 7.7 Hz, 2H, Ar$\underline{H}$), 3.55 (septet, *J* = 6.8 Hz, 4H, C$\underline{H}$(CH_3)$_2$), 1.35 (septet, *J* = 7.5 Hz, 6H, C$\underline{H}$(CH_3)$_2$), 1.28 (d, *J* = 6.8 Hz, 12H, CH(C$\underline{H}_3$)$_2$), 1.25 (d, *J* = 6.8 Hz, 12H, CH(C$\underline{H}_3$)$_2$), 1.12 (d, *J* = 7.5 Hz, 36H, CH(C$\underline{H}_3$)$_2$).

^{13}C{^{1}H} NMR (101 MHz, C_6D_6) δ = 146.2 (Ar$\underline{C}$), 143.9 (Ar$\underline{C}$), 143.0 (Ar$\underline{C}$), 140.9 (Ar$\underline{C}$), 124.9 (Ar$\underline{C}$), 124.1 (Ar$\underline{C}$), 123.9 (Ar$\underline{C}$), 123.4 (N$\underline{C}$H), 68.3 ($\underline{C}$H(CH_3)$_2$), 28.5 (CH($\underline{C}H_3$)$_2$), 28.0 (CH($\underline{C}H_3$)$_2$), 27.5 (CH($\underline{C}H_3$)$_2$), 25.4 (CH($\underline{C}H_3$)$_2$), 24.3 (CH($\underline{C}H_3$)$_2$), 23.8 (CH($\underline{C}H_3$)$_2$), 19.4 (CH($\underline{C}H_3$)$_2$), 18.9 (CH($\underline{C}H_3$)$_2$), 14.4 (CH($\underline{C}H_3$)$_2$), 14.0 (CH($\underline{C}H_3$)$_2$).

^{119}Sn{^{1}H} NMR (149 MHz, C_6D_6) δ = 187.2.

^{29}Si{^{1}H} NMR (79 MHz, C_6D_6) δ = 7.7.

Anal. Calcd. [%] for $C_{42}H_{76}Cl_2N_2Si_2Sn_2$: C, 51.82; H, 7.87; N, 2.88. Found [%]: C, 51.71; H, 7.97; N, 2.73.

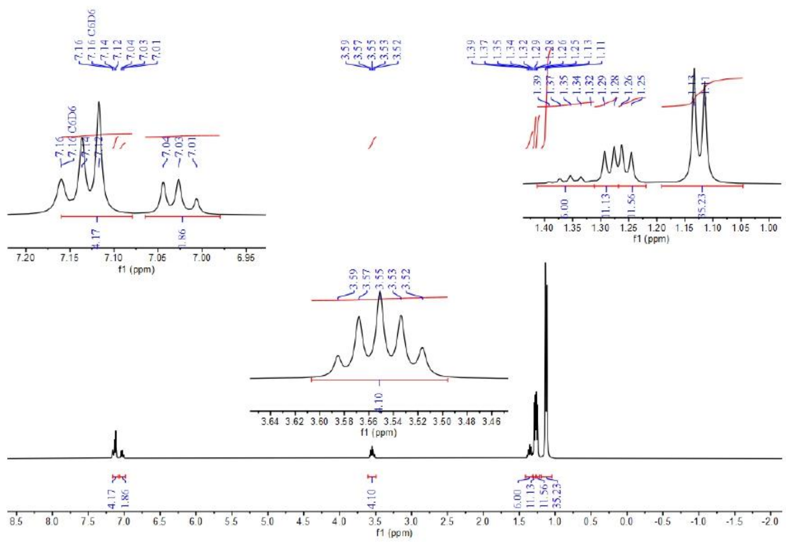

Figure S5. ^{1}H NMR spectrum of compound **2** in C_6D_6.

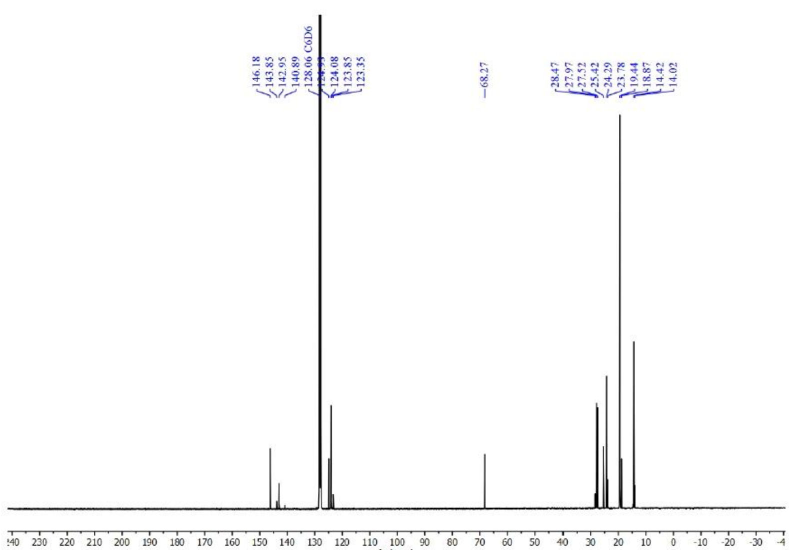

Figure S6. $^{13}C\{^{1}H\}$ NMR spectrum of compound **2** in C_6D_6.

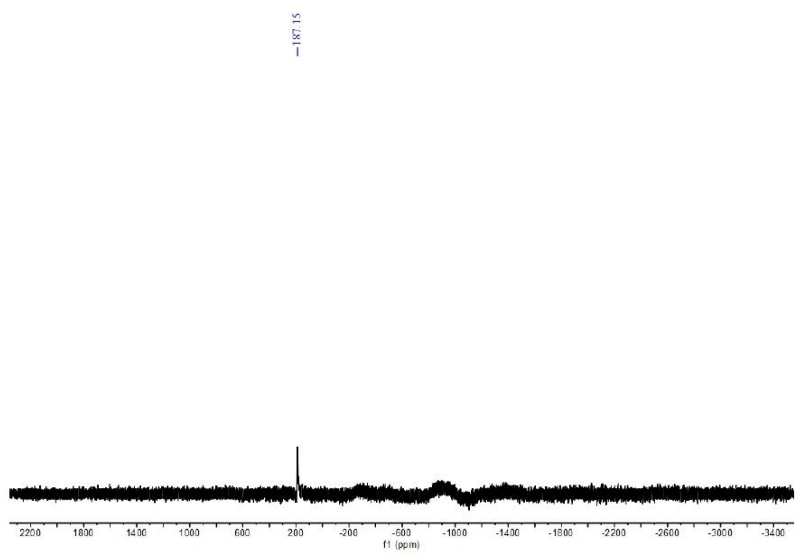

Figure S7. $^{119}Sn\{^1H\}$ NMR spectrum of compound **2** in C_6D_6.

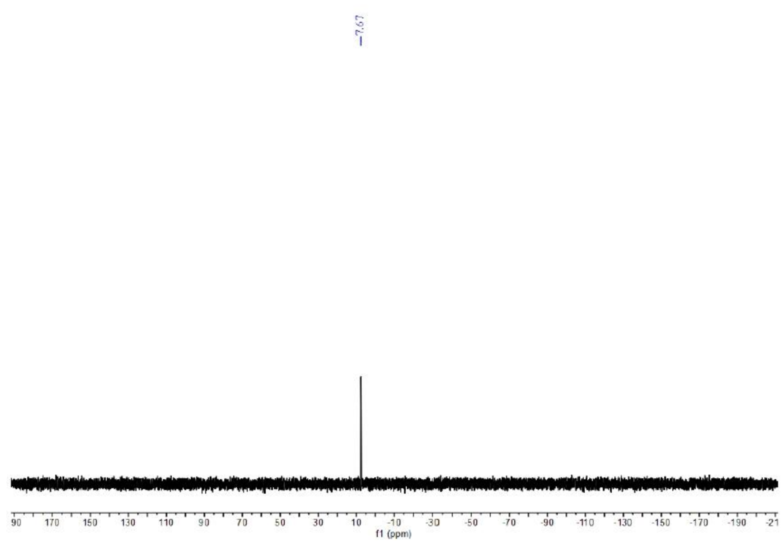

Figure S8. $^{29}Si\{^1H\}$ NMR spectrum of compound **2** in C_6D_6.

S8

Synthesis of compound 3

Method **a**: 5 mL toluene was added to a flask containing **2** (300 mg, 308 μmol) and freshly prepared potassium graphite (KC_8) (125 mg, 924 μmol, 3.0 eq.) at room temperature with vigorous stirring. Gradually the solution turned dark orange and the stirring was continued for 24h at RT. The resulted solution was filtered, and the solid residue was extracted with toluene (2 mL × 3). After filtration, the solvent was removed from the filtrate *in vacuo* to afford **3** as an orange solid (193 mg, 80%), and red crystals were recrystallized from a saturated solution in Et_2O at -30 ºC.

Method **b**: Dipp($^iPr_3Si$)NLi (300 mg, 884 μmol) dissolved in THF (4 mL) was added dropwise to a solution of $SnCl_2$ (84 mg, 442 μmol, 0.5 eq.) in THF (6 mL) at room temperature. The reaction mixture was stirred for 2 h. The solvent was removed *in vacuo* and the solid residue was extracted with toluene (10 mL × 3). After filtration, the solvent was removed from the filtrate *in vacuo* to afford **3** as an orange solid (616 mg, 89%), and red crystals were recrystallized from a saturated solution in Et_2O at -30 ºC.

^{1}H NMR (400 MHz, C_6D_6) δ = 6.98 – 6.96 (m, 4H, Ar*H*), 6.91 – 6.87 (m, 2H, Ar*H*), 3.58 (septet, *J* = 6.8 Hz, 4H, C*H*(CH_3)$_2$), 1.35 (septet, *J* = 6.8 Hz, 6H, C*H*(CH_3)$_2$), 1.26 (d, *J* = 6.8 Hz, 12H, CH(C*H*$_3$)$_2$), 1.14 (d, *J* = 7.5 Hz, 36H, CH(C*H*$_3$)$_2$), 0.78 (d, *J* = 6.8 Hz, 12H, CH(C*H*$_3$)$_2$).

^{13}C{^{1}H} NMR (101 MHz, C_6D_6) δ = 146.1 (Ar*C*), 145.5 (Ar*C*), 124.5 (Ar*C*), 124.3 (Ar*C*), 27.8 (*C*H(CH_3)$_2$), 27.7 (*C*H(CH_3)$_2$), 24.2 (CH(*C*H$_3$)$_2$), 20.0 (CH(*C*H$_3$)$_2$), 14.7 (CH(*C*H$_3$)$_2$).

^{119}Sn{^{1}H} NMR (149 MHz, C_6D_6) δ = 517.5.

^{29}Si{^{1}H} NMR (79 MHz, C_6D_6) δ = 8.7.

Anal. Calcd. [%] for $C_{42}H_{76}N_2Si_2Sn$: C, 64.35; H, 9.77; N, 3.57. Found [%]: C, 63.97; H, 9.95; N, 3.50.

LIFDI-MS: calculated for $C_{42}H_{76}N_2Si_2Sn$: 784.45690. Found: 784.45133.

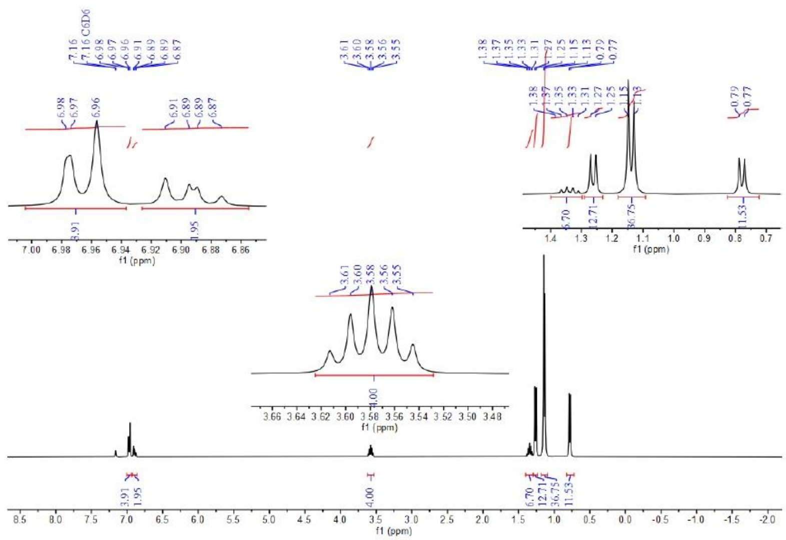

Figure S9. [1]H NMR spectrum of compound **3** in C_6D_6.

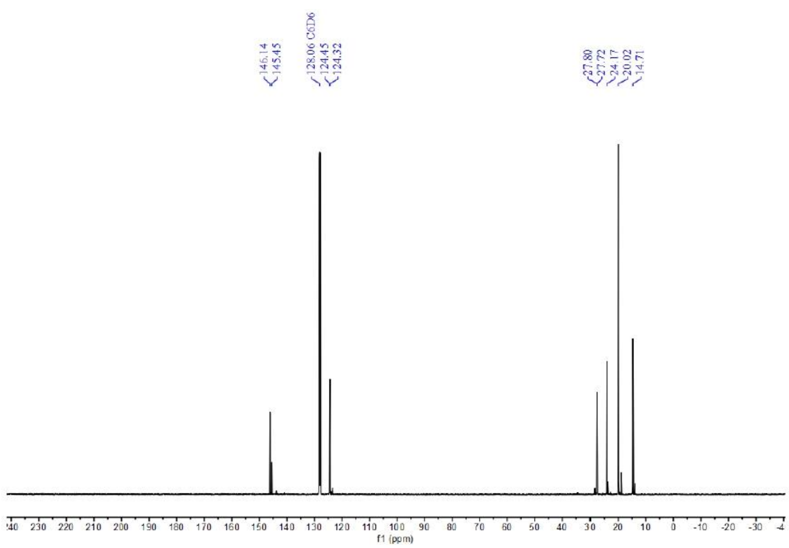

Figure S10. $^{13}C\{^1H\}$ NMR spectrum of compound **3** in C_6D_6.

S10

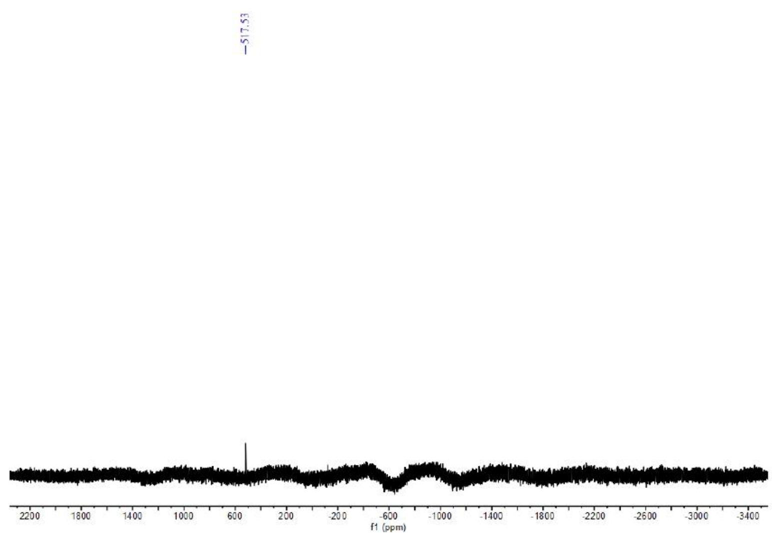

Figure S11. $^{119}Sn\{^1H\}$ NMR spectrum of compound **3** in C_6D_6.

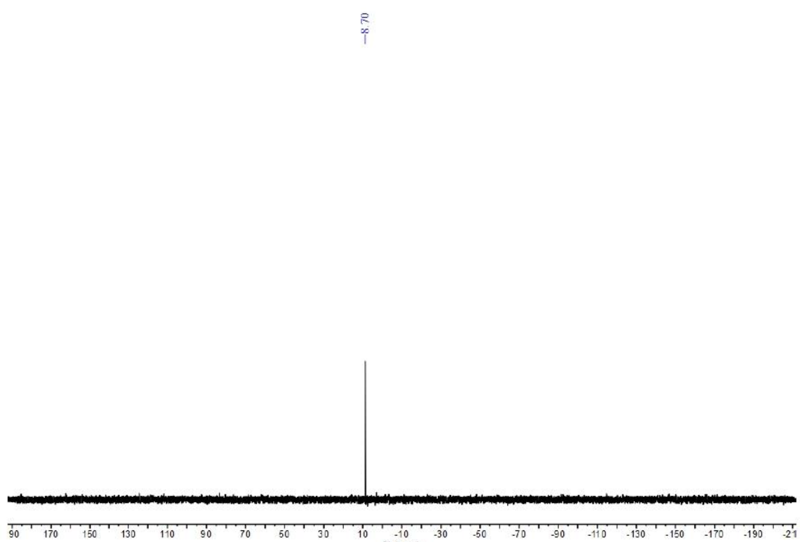

Figure S12. $^{29}Si\{^1H\}$ NMR spectrum of compound **3** in C_6D_6.

S11

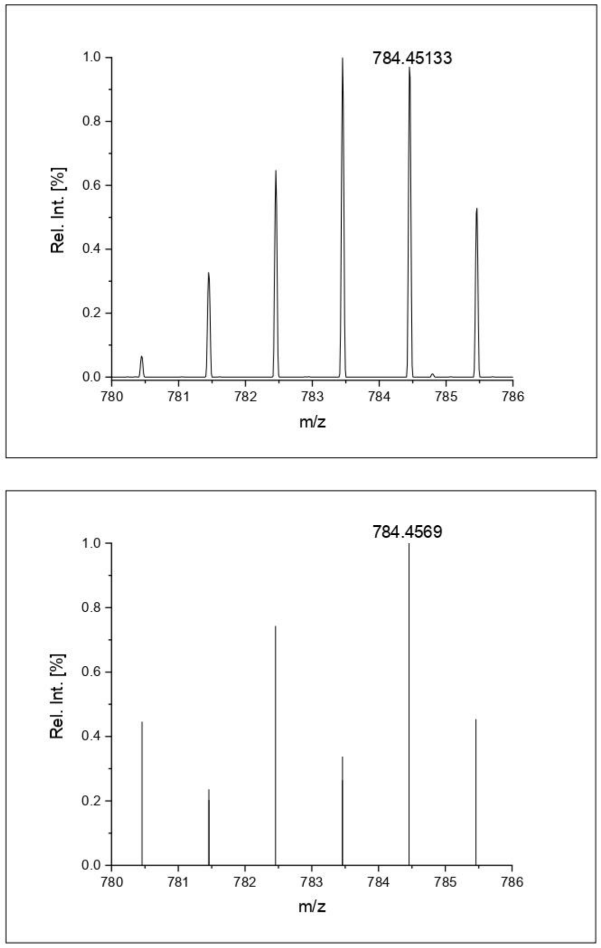

Figure S13. LIFDI-MS spectrum: expanded region of the compound signal showing the isotopic pattern of compound **3**. Measured (top) and calculated (bottom).

S12

Synthesis of compound 4

Method **a**: IPrNLi (500 mg, 1.22 mmol) dissolved in THF (10 mL) was added dropwise to a solution of **2** (595 mg, 610 µmol, 0.5 eq.) in THF (20 mL) at room temperature. The reaction mixture was stirred for 2 h. The solvent was removed *in vacuo* and the solid residue was extracted with toluene (10 mL × 3). After filtration, the solvent was removed from the filtrate *in vacuo* to afford **4** as an orange solid (730 mg, 70%), and red crystals were recrystallized from a saturated solution in Et_2O at -30 ºC.

Method **b**: IPrNLi (500 mg, 1.22 mmol) dissolved in THF (10 mL) was added dropwise to a solution of **1** (822 mg, 1.22 mmol, 1.0 eq.) in THF (20 mL) at room temperature. The reaction mixture was stirred for 2 h. The solvent was removed *in vacuo* and the solid residue was extracted with toluene (10 mL × 3). After filtration, the solvent was removed from the filtrate *in vacuo* to afford **4** as an orange solid (749 mg, 72%), and red crystals were recrystallized from a saturated solution in Et_2O at -30 ºC.

^{1}H NMR (400 MHz, C_6D_6) δ = 7.21 – 7.17 (m, 3H, Ar$\underline{H}$), 7.11 – 7.08 (m, 6H, Ar$\underline{H}$), 6.05 (s, 2H, NC$\underline{H}$), 3.72 (septet, *J* = 6.8 Hz, 2H, C$\underline{H}$(CH$_3$)$_2$), 3.14 (septet, *J* = 6.8 Hz, 4H, C$\underline{H}$(CH$_3$)$_2$), 1.56 (septet, *J* = 6.8 Hz, 3H, C$\underline{H}$(CH$_3$)$_2$), 1.34 (d, *J* = 6.8 Hz, 18H, CH(C$\underline{H}_3$)$_2$), 1.15 (d, *J* = 6.8 Hz, 12H, CH(C$\underline{H}_3$)$_2$), 1.10 (d, *J* = 6.8 Hz, 24H, CH(C$\underline{H}_3$)$_2$).

^{13}C{^{1}H} NMR (101 MHz, C_6D_6) δ = 153.3 (N$\underline{C}$N), 147.8 (N$\underline{C}$Ar), 147.1 (N$\underline{C}$Ar), 145.9 (N$\underline{C}$Ar), 134.8 (Ar$\underline{C}$), 129.8 (Ar$\underline{C}$), 124.6 (Ar$\underline{C}$), 123.6 (Ar$\underline{C}$), 115.2 (N$\underline{C}$H), 29.1 ($\underline{C}$H(CH$_3$)$_2$), 27.9 ($\underline{C}$H(CH$_3$)$_2$), 27.1 (C$\underline{H}$(CH$_3$)$_2$), 24.9 (CH($\underline{C}$H$_3$)$_2$), 23.7 (CH($\underline{C}$H$_3$)$_2$), 23.1 (CH($\underline{C}$H$_3$)$_2$), 20.0 (CH($\underline{C}$H$_3$)$_2$), 18.9 (CH($\underline{C}$H$_3$)$_2$), 14.3 (CH($\underline{C}$H$_3$)$_2$).

^{29}Si{^{1}H} NMR (79 MHz, C_6D_6) δ = 4.7.

Anal. Calcd. [%] for $C_{48}H_{74}N_4SiSn$: C, 67.51; H, 8.74; N, 6.56. Found [%]: C, 67.81; H, 8.77; N, 6.48.

LIFDI-MS: calculated for $C_{48}H_{74}N_4SiSn$: 854.47047. Found: 854.47222.

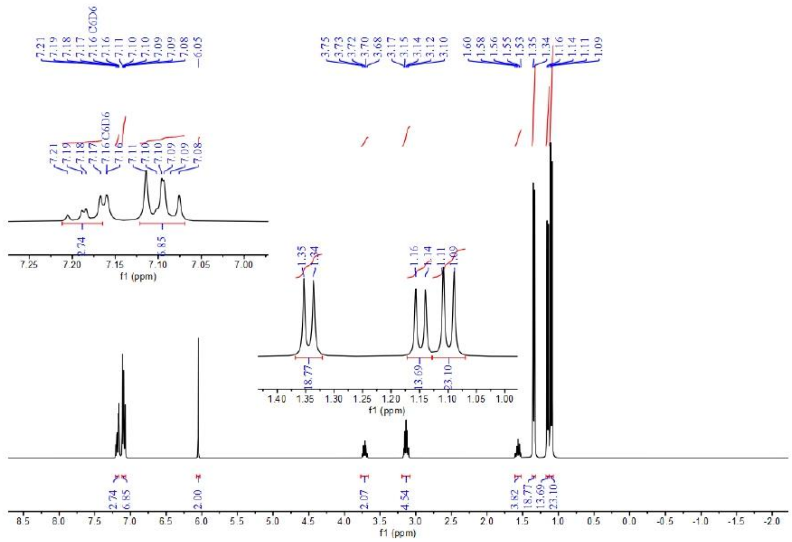

Figure S14. ^{1}H NMR spectrum of compound **4** in C_6D_6.

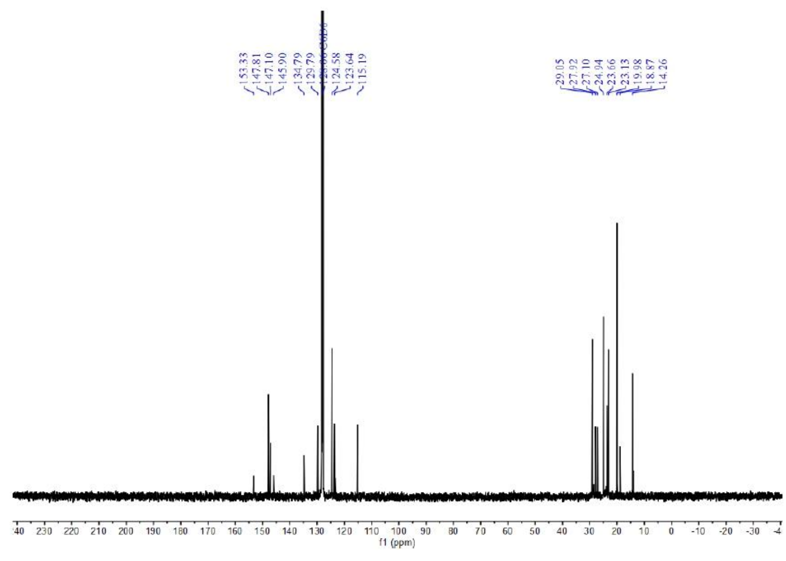

Figure S15. $^{13}C\{^{1}H\}$ NMR spectrum of compound **4** in C_6D_6.

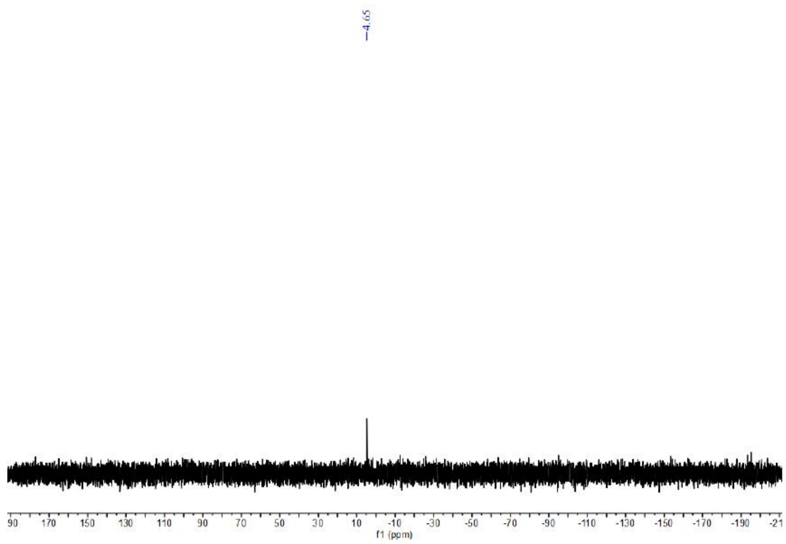

Figure S16. $^{29}Si\{^{1}H\}$ NMR spectrum of compound **4** in C_6D_6.

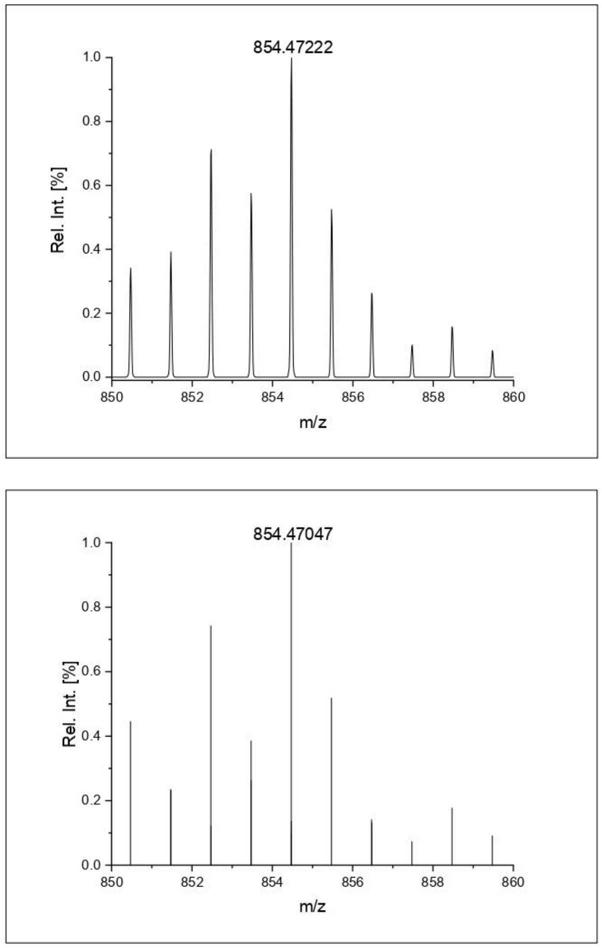

Figure S17. LIFDI-MS spectrum: expanded region of the compound signal showing the isotopic pattern of compound **4**. Measured (top) and calculated (bottom).

Synthesis of compound J

$SnCl_2$•dioxane (339 mg, 1.22 mmol, 1.0 eq.) dissolved in THF (20 mL) was added dropwise to a solution of IPrNLi (1.0 g, 2.44 mmol, 2.0 eq.) in THF (30 mL) at 0 ºC. The reaction mixture was stirred for 2 h at 0 ºC. The volatiles were removed *in vacuo* and the solid residue was extracted with toluene (10 mL × 3). After filtration the solvent was removed from the filtrate *in vacuo* to obtain a yellow solid (1.04 g, 88%).

^{1}H NMR (400 MHz, C_6D_6) δ = 7.18 (t, *J* = 7.7 Hz, 4H, Ar*H*), 7.06 (d, *J* = 7.7 Hz, 8H, Ar*H*), 5.94 (s, 4H, NC*H*), 3.18 (septet, *J* = 6.8 Hz, 8H, C*H*(CH_3)$_2$), 1.30 (d, *J* = 6.8 Hz, 24H, CH(C*H*$_3$)$_2$), 1.14 (d, *J* = 6.8 Hz, 24H, CH(C*H*$_3$)$_2$).

^{13}C{^{1}H} NMR (101 MHz, C_6D_6) δ = 154.6 (N*C*N), 148.4 (N*C*Ar), 137.9 (N*C*Ar), 135.2 (Ar*C*), 129.5 (Ar*C*), 129.3 (Ar*C*), 128.6 (Ar*C*), 125.7 (Ar*C*), 124.6 (Ar*C*), 113.5 (N*C*H), 28.7 (*C*H(CH_3)$_2$), 25.0 (CH(*C*H$_3$)$_2$), 24.0 (CH(*C*H$_3$)$_2$), 23.9 (CH(*C*H$_3$)$_2$), 21.4 (CH(*C*H$_3$)$_2$).

^{119}Sn{^{1}H} NMR (149 MHz, C_6D_6) δ = -52.1.

Anal. Calcd. [%] for $C_{54}H_{72}ClLiN_6Sn$: C, 67.12; H, 7.51; N, 8.70. Found [%]: C, 67.10; H, 7.49; N, 8.75.

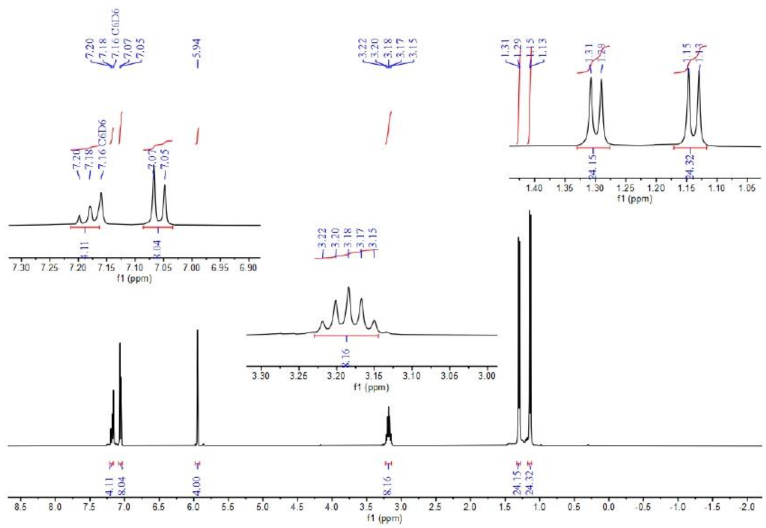

Figure S18. ^{1}H NMR spectrum of compound **J** in C_6D_6.

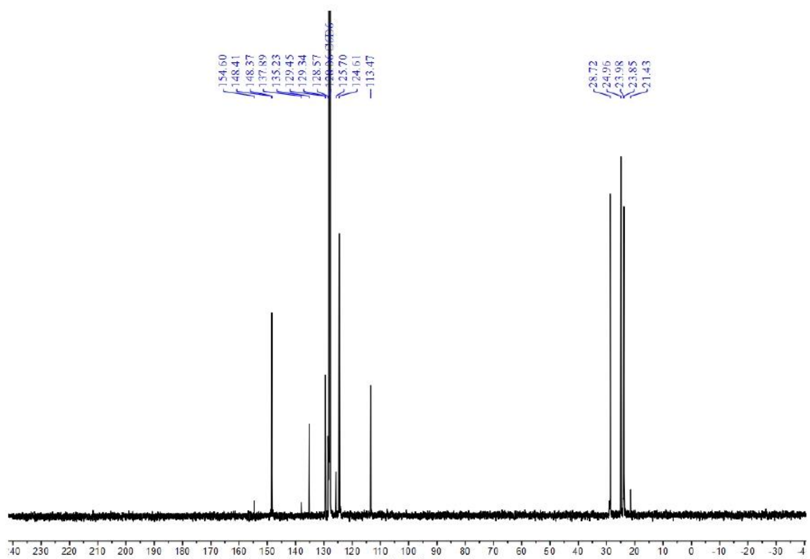

Figure S19. $^{13}C\{^{1}H\}$ NMR spectrum of compound **J** in C_6D_6.

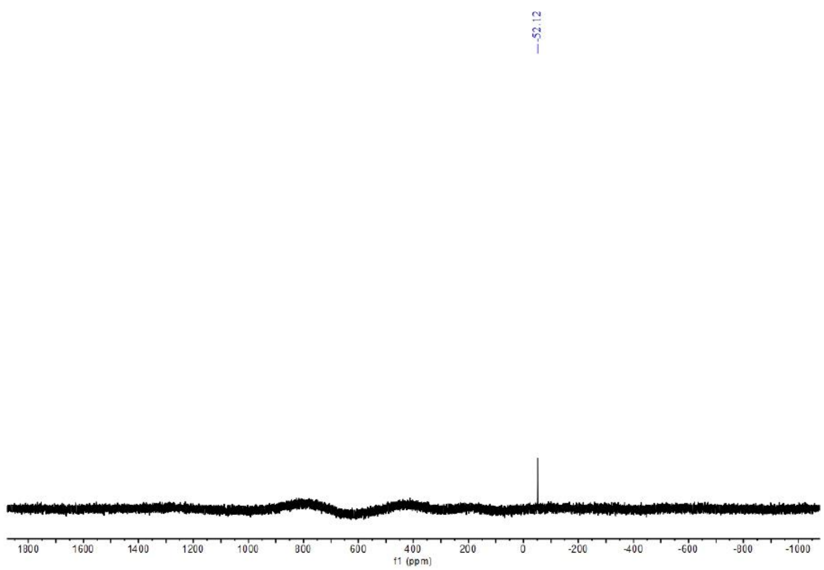

Figure S20. $^{119}Sn\{^1H\}$ NMR spectrum of compound **J** in C_6D_6.

Synthesis of compound 5

The solution of **5** (1.14 g, 1.30 mmol) in toluene (20 mL) in a Schlenk tube equipped with a PTFE-coated magnetic stirring bar was cooled to be solidified. The upper argon atmosphere was replaced with N_2O gas (1.0 bar). The reaction mixture was allowed to warm to room temperature, and then was stirred for 12 h. Removal of the solvent gave an orange crude solid, and **5** was recrystallized from a saturated solution in Et_2O at -30 ºC as pale-yellow crystals (1.03 g, 89%).

^1H NMR (400 MHz, C_6D_6) δ = 7.28 – 7.22 (m, 16H, Ar$\underline{H}$), 7.18 – 7.16 (m, 8H, Ar$\underline{H}$), 5.86 (s, 8H, NC$\underline{H}$), 3.32 (septet, J = 6.8 Hz, 8H, C$\underline{H}(CH_3)_2$), 3.21 (septet, J = 6.8 Hz, 8H, C$\underline{H}(CH_3)_2$), 1.41 (d, J = 6.8 Hz, 24H, CH(C$\underline{H}_3)_2$), 1.31 (d, J = 6.8 Hz, 24H, CH(C$\underline{H}_3)_2$), 1.26 (d, J = 6.8 Hz, 24H, CH(C$\underline{H}_3)_2$), 1.22 (d, J = 6.8 Hz, 24H, CH(C$\underline{H}_3)_2$).

$^{13}C\{^1H\}$ NMR (101 MHz, C_6D_6) δ = 154.6 (N<u>C</u>N), 150.3 (N<u>C</u>Ar), 148.6 (N<u>C</u>Ar), 147.1 (N<u>C</u>Ar), 136.0 (Ar<u>C</u>), 129.1 (Ar<u>C</u>), 124.3 (Ar<u>C</u>), 124.2 (Ar<u>C</u>), 114.5 (N<u>C</u>H), 29.0 (<u>C</u>H(CH$_3$)$_2$), 28.9 (<u>C</u>H(CH$_3$)$_2$), 25.1 (CH(<u>C</u>H$_3$)$_2$), 24.9 (CH(<u>C</u>H$_3$)$_2$), 24.7 (CH(<u>C</u>H$_3$)$_2$), 24.5 (CH(<u>C</u>H$_3$)$_2$), 24.0 (CH(<u>C</u>H$_3$)$_2$), 23.6 (CH(<u>C</u>H$_3$)$_2$).

$^{119}Sn\{^1H\}$ NMR (149 MHz, C_6D_6) δ = -273.2.

Anal. Calcd. [%] for $C_{108}H_{144}Cl_2Li_2N_{12}O_2Sn_2$: C, 66.03; H, 7.39; N, 8.56. Found [%]: C, 66.00; H, 7.45; N, 8.50.

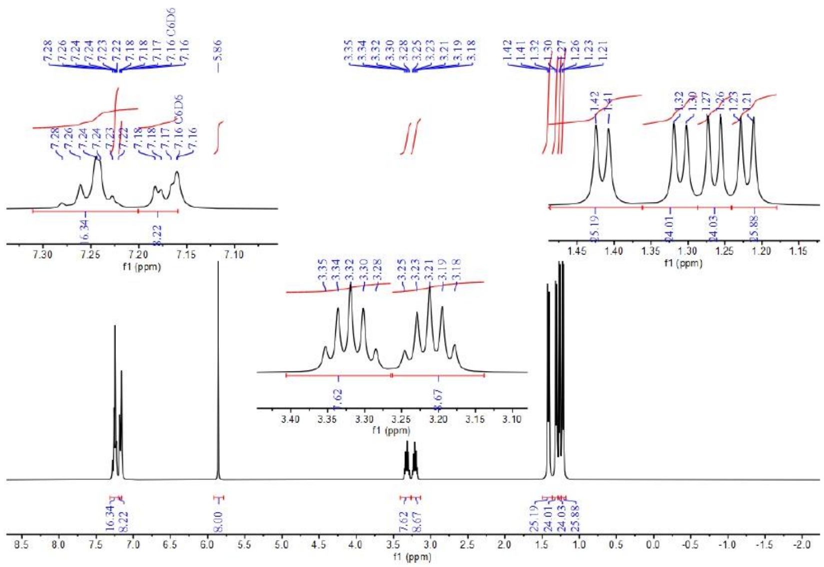

Figure S21. ^1H NMR spectrum of compound **5** in C_6D_6.

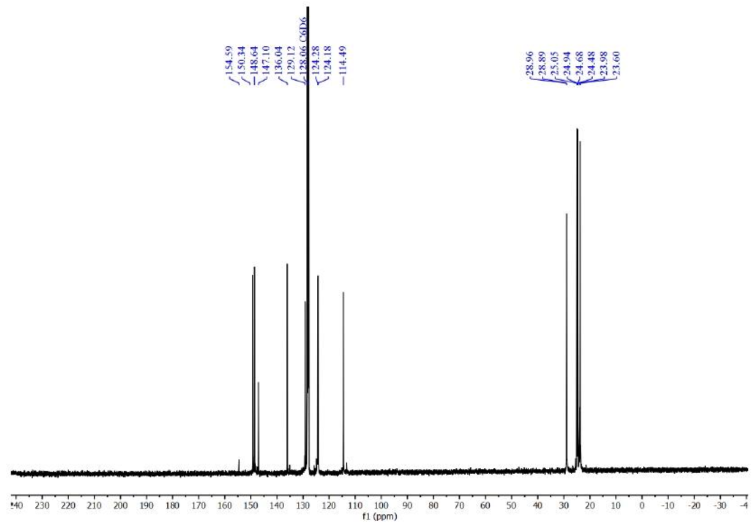

Figure S22. $^{13}C\{^{1}H\}$ NMR spectrum of compound **5** in C_6D_6.

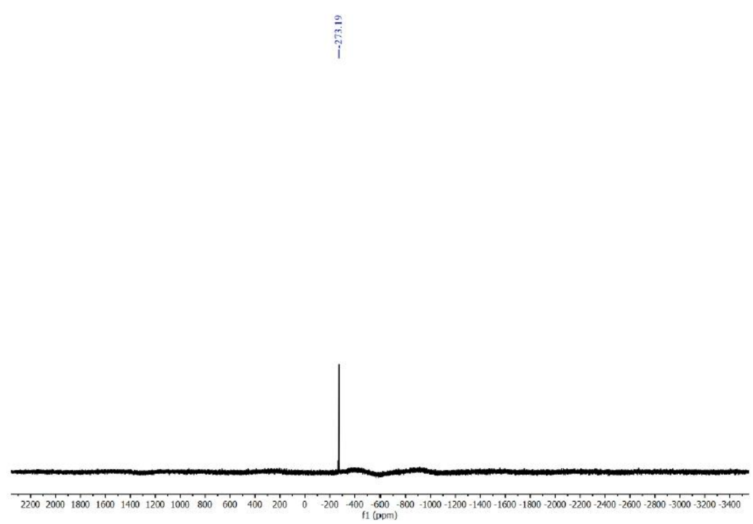

Figure S23. $^{119}Sn\{^{1}H\}$ NMR spectrum of compound **5** in C_6D_6.

S21

Reaction of compound 3 with N_2O

The solution of **3** (40 mg) in C_6D_6 (0.4 mL) in a J. Young PTFE tube was cooled to be solidified. The upper argon atmosphere was replaced with N_2O gas (1.0 bar). The reaction mixture was allowed to warm to room temperature. The reaction was monitored regularly using ^1H NMR spectroscopy.

Reaction of compound 4 with N_2O

The solution of **4** (40 mg) in C_6D_6 (0.4 mL) in a J. Young PTFE tube was cooled to be solidified. The upper argon atmosphere was replaced with N_2O gas (1.0 bar). The reaction mixture was allowed to warm to room temperature. The reaction was monitored regularly using ^1H NMR spectroscopy.

2. X-ray Crystallographic Data

General Information

The X-ray intensity data of compounds **1**, **2**, **3**, **4** and **5** were collected on an X-ray single crystal diffractometer equipped with a CMOS detector (Bruker Photon-100), an IMS microsource with MoKα radiation ($\lambda = 0.71073$ Å) and a Helios mirror optic by using the APEX III software package.[S3] The measurements were performed on single crystals coated with the perfluorinated ether Fomblin® Y. The crystals were fixed on the top of a microsampler, transferred to the diffractometer and frozen under a stream of cold nitrogen. A matrix scan was used to determine the initial lattice parameters. Reflections were merged and corrected for Lorenz and polarization effects, scan speed, and background using SAINT.[S4] Absorption corrections, including odd and even ordered spherical harmonics were performed using SADABS.[S4] Space group assignments were based upon systematic absences, E statistics, and successful refinement of the structures. Structures were solved by direct methods with the aid of successive difference Fourier maps, and were refined against all data using the APEX III software in conjunction with SHELXL-2014[S5] and SHELXLE.[S6] All H atoms were placed in calculated positions and refined using a riding model, with methylene and aromatic C–H distances of 0.99 and 0.95 Å, respectively, and Uiso(H) = $1.2 \cdot U$eq(C). Full-matrix least-squares refinements were carried out by minimizing $\Sigma w(Fo^2–Fc^2)^2$ with SHELXL-97[S7] weighting scheme. Neutral atom scattering factors for all atoms and anomalous dispersion corrections for the non-hydrogen atoms were taken from International Tables for Crystallography.[S8] The images of the crystal structure were generated by Mercury.[S9] The CCDC number 2191800 (**1**), 2191801 (**2**), 2191802 (**3**), 2191803 (**4**), and 2191804 (**5**) contain the supplementary crystallographic data for the structures. The data can be obtained free of charge from the Cambridge Crystallographic Data Centre *via* https://www.ccdc.cam.ac.uk/structures/.

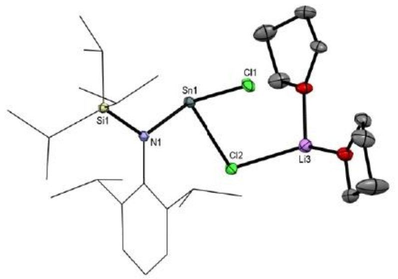

Figure S24. Molecular structure of **1**. Thermal ellipsoids are shown at 50% probability level. Hydrogen atoms are omitted for clarity. Selected bond lengths [Å] and angles [°]: Sn1–Cl1 2.5679(6), Sn1–Cl2 2.5077(5), Sn1–N1 2.115(1), Si1–N1 1.752(1), Cl2–Li3 2.410(3), Cl1–Sn1–Cl2 88.96(2), Cl1–Sn1–N1 100.81(4), Cl2–Sn1–N1 96.09(4), Sn1–N1–Si1 121.20(7), Sn1–Cl2–Li3 107.82(7).

Table S1. Crystal data and structure refinement for compound **1**.

Chemical formula	$C_{29}H_{54}Cl_2LiNO_2SiSn$
Formula weight	673.37
Radiation source	IMS microsource (Mo)
Temperature (K)	100
Wavelength (Å)	0.71073
Crystal system (Space group)	Monoclinic, $P2_1/c$
Unit cell dimensions	a = 10.0453(13) Å, α = 90° b = 11.0558(15) Å, β = 90° c = 30.603(4) Å, γ = 90°
Volume (Å^3)	3398.7(8)
Z	4
Density Dx (g/cm^3)	1.316
Absorption coefficient μ (mm^{-1})	0.969
Absorption correction	Multi-Scan
F(000)	1408.0
Theta (max) (°)	25.350

Index ranges	–12<=h<=12, –13<=k<=13, –36<=l<=36
Tmin, Tmax	0.678, 0.745
Coverage of independent reflections (%)	99.8
Refinement method	Full-matrix least-squares on F^2
Data / Parameter / Restraints	6207 / 344 / 0
Goodness-of-fit on F^2	1.002
Final R indices ($I>2\sigma(I)$)	R1(all) = 0.0198, wR2(all) = 0.0490 R1 = 0.0188, wR2 = 0.0485

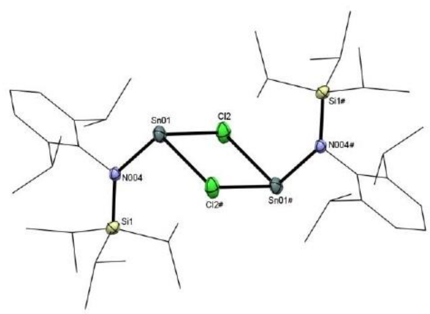

Figure S25. Molecular structure of **2**. Thermal ellipsoids are shown at 50% probability level. Hydrogen atoms are omitted for clarity. Selected bond lengths [Å] and angles [°]: Sn01–Cl2 2.6147(8), Sn01–Cl2# 2.716(1), Sn01–N004 2.076(3), Si1–N004 1.770(3), Cl2–Sn01–Cl2# 80.60(3), Cl2–Sn01–N004 102.92(8), Cl2#–Sn01–N004 102.93(8), Sn01–Cl2–Sn01# 99.40(3), Sn01–N004–Si1 136.6(2).

Table S2. Crystal data and structure refinement for compound **2**.

Chemical formula	$C_{42}H_{76}Cl_2N_2Si_2Sn_2$
Formula weight	973.55
Radiation source	IMS microsource (Mo)
Temperature (K)	100

Wavelength (Å)	0.71073
Crystal system (Space group)	Triclinic, P -1
Unit cell dimensions	a = 9.1127(7) Å, α = 101.791(3)° b = 9.6163(7) Å, β = 96.134(3)° c = 14.9113(11) Å, γ = 109.400(3)°
Volume (Å^3)	1184.69(16)
Z	1
Density Dx (g/cm^3)	1.365
Absorption coefficient μ (mm^{-1})	1.246
Absorption correction	Multi-Scan
F(000)	504.0
Theta (max) (°)	25.790
Index ranges	–11<=h<=11, –11<=k<=11, –18<=l<=18
Absorption Correction Tmin, Tmax	0.624, 0.745
Coverage of independent reflections (%)	99.7
Refinement method	Full-matrix least-squares on F^2
Data / Parameter / Restraints	4542 / 236 / 0
Goodness-of-fit on F^2	0.953
Final R indices (I>2σ(I))	R1(all) = 0.0587, wR2(all) = 0.0728 R1 = 0.0348, wR2 = 0.0700

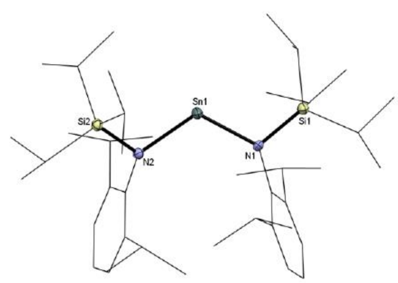

S26

Figure S26. Molecular structure of **3**. Thermal ellipsoids are shown at 50% probability level. Hydrogen atoms are omitted for clarity. Selected bond lengths [Å] and angles [°]: Sn1–N1 2.091(7), Sn1–N2 2.124(8), N1–Si1 1.784(9), N2–Si2 1.780(8), N1–Sn1–N2 118.3(3), Sn1–N1–Si1 114.0(4), Sn1–N2–Si2 111.3(4).

Table S3. Crystal data and structure refinement for compound **3**.

Chemical formula	$C_{42}H_{76}N_2Si_2Sn$
Formula weight	783.94
Radiation source	IMS microsource (Mo)
Temperature (K)	100
Wavelength (Å)	0.71073
Crystal system (Space group)	Triclinic, P -1
Unit cell dimensions	a = 16.0599(13) Å, α = 90° b = 15.3996(12) Å, β = 103.174(2)° c = 17.8338(16) Å, γ = 90°
Volume (Å^3)	4294.5(6)
Z	2
Density Dx (g/cm^3)	1.212
Absorption coefficient μ (mm^{-1})	0.680
Absorption correction	Multi-Scan
F(000)	1680.0
Theta (max) (°)	25.717
Index ranges	–19<=h<=19, –18<=k<=18, –21<=l<=21
Absorption Correction Tmin, Tmax	0.701, 0.745
Coverage of independent reflections (%)	99.9
Refinement method	Full-matrix least-squares on F^2
Data / Parameter / Restraints	16369 / 888 / 0
Goodness-of-fit on F^2	1.275
Final R indices (I>2σ(I))	R1(all) = 0.0912, wR2(all) = 0.2516 R1 = 0.0833, wR2 = 0.2482

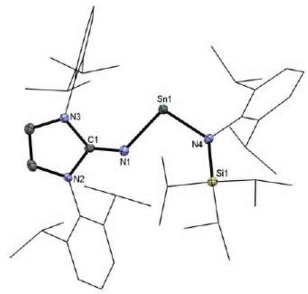

Figure S27. Molecular structure of **4**. Thermal ellipsoids are shown at 50% probability level. Hydrogen atoms are omitted for clarity. Selected bond lengths [Å] and angles [°]: Sn1–N1 2.023(2), Sn1–N4 2.112(2), N1–C1 1.281(3), N4–Si1 1.758(2), N1–Sn1–N4 100.42(7), Sn1–N4–Si1 133.5(1), Sn1–N1–C1 128.1(2).

Table S4. Crystal data and structure refinement for compound **4**.

Chemical formula	$C_{48}H_{74}N_4SiSn$
Formula weight	853.91
Radiation source	IMS microsource (Mo)
Temperature (K)	100
Wavelength (Å)	0.71073
Crystal system (Space group)	Triclinic, P -1
Unit cell dimensions	a = 10.5600(16) Å, α = 74.424(5)° b = 12.2106(19) Å, β = 84.900(5)° c = 19.593(3) Å, γ = 77.143(6)°
Volume (Å^3)	2371.5(6)
Z	2
Density Dx (g/cm^3)	1.196
Absorption coefficient μ (mm^{-1})	0.598
Absorption correction	Multi-Scan
F(000)	908.0
Theta (max) (°)	25.760
Index ranges	–12<=h<=12, –14<=k<=14, –23<=l<=23

Tmin, Tmax	0.701, 0.739
Coverage of independent reflections (%)	99.6
Refinement method	Full-matrix least-squares on F^2
Data / Parameter / Restraints	9027 / 505 / 0
Goodness-of-fit on F^2	0.982
Final R indices ($I>2\sigma(I)$)	R1(all) = 0.0801, wR2(all) = 0.0697 R1 = 0.0351, wR2 = 0.0663

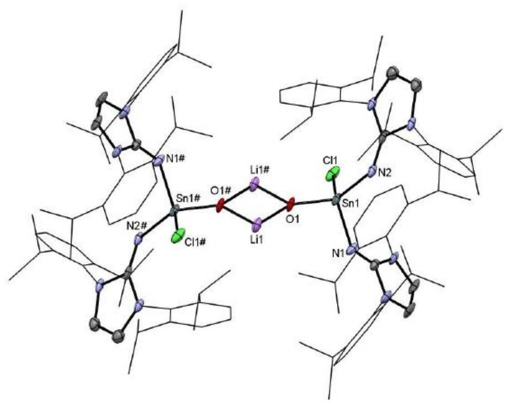

Figure S28. Molecular structure of **5**. Thermal ellipsoids are shown at 50% probability level. Hydrogen atoms and solvent molecules are omitted for clarity. Selected bond lengths [Å] and angles [°]: Sn1–N1 1.991(6), Sn1–N2 2.010(5), Sn1–O1 1.886(4), Sn1–Cl1 2.384(2), O1–Li1 1.71(1), O1–Li1# 1.96(1), N1–Sn1–N2 110.4(2), N1–Sn1–Cl1 109.5(2), N1–Sn1–O1 101.6(2), N2–Sn1–O1 119.7(2), N2–Sn1–Cl1 106.4(2), Cl1–Sn1–O1 109.1(1), Sn1–O1–Li1 124.3(5), Sn1–O1–Li1# 152.2(4).

Table S5. Crystal data and structure refinement for compound **5•5(C_4H_8O)**.

Chemical formula	$C_{108}H_{144}Cl_2Li_2N_{12}O_2Sn_2$•5($C_4H_8O$)
Formula weight	2325.16

Radiation source	IMS microsource (Mo)
Temperature (K)	100
Wavelength (Å)	0.71073
Crystal system (Space group)	Monoclinic, C2/c
Unit cell dimensions	a = 32.90300 Å, α = 90° b = 13.61000 Å, β = 113.4300° c = 34.59900 Å, γ = 90°
Volume (Å^3)	14216
Z	1
Density Dx (g/cm^3)	1.186
Absorption coefficient μ (mm^{-1})	0.441
Absorption correction	Multi-Scan
F(000)	5400.0
Theta (max) (°)	28.119
Index ranges	–40<=h<=40, –16<=k<=16, –45<=l<=45
Tmin, Tmax	0.656, 0.745
Coverage of independent reflections (%)	78.4
Refinement method	Full-matrix least-squares on F^2
Data / Parameter / Restraints	13609 / 772 / 132
Goodness-of-fit on F^2	1.287
Final R indices ($I>2\sigma(I)$)	R1(all) = 0.1057, wR2(all) = 0.2167 R1 = 0.0759, wR2 = 0.2045

3. References

[S1] B. Shen, L. Ying, J. Chen, Y. J. Luo, *Inorg. Chim. Acta* **2008**, *361*, 1255-1260.

[S2] D. Franz, E. Irran, S. Inoue, *Dalton Trans.* **2014**, *43*, 4451-4461.

[S3] *APEX suite of crystallographic software*, APEX 3 version 2015.5-2; Bruker AXS Inc.: Madison, Wisconsin, USA, **2015**.

[S4] *SAINT*, Version 7.56a and SADABS Version 2008/1; Bruker AXS Inc.: Madison, Wisconsin, USA, **2008**.

[S5] G. M. Sheldrick, *SHELXL-2014*, University of Göttingen, Göttingen, Germany, **2014**.

[S6] C. B. Hübschle, G. M. Sheldrick, B. Dittrich, *J. Appl. Cryst.* **2011**, *44*, 1281-1284.

[S7] G. M. Sheldrick, *SHELXL-97*, University of Göttingen, Göttingen, Germany, **1998**.

[S8] A. J. C. Wilson, *International Tables for Crystallography*, Vol. C, Tables 6.1.1.4 (pp. 500-502), 4.2.6.8 (pp. 219-222), and 4.2.4.2 (pp. 193-199); Kluwer Academic Publishers: Dordrecht, The Netherlands, **1992**.

[S9] C. F. Macrae, I. J. Bruno, J. A. Chisholm, P. R. Edgington, P. McCabe, E. Pidcock, L. Rodriguez-Monge, R. Taylor, J. van de Streek, P. A. Wood, *J. Appl. Cryst.* **2008**, *41*, 466-470.

9.5 Licenses for Copyrighted Content

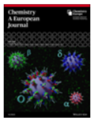

An Isolable Three-Coordinate Germanone and Its Reactivity

Author: Xuan-Xuan Zhao, Tibor Szilvási, Franziska Hanusch, et al

Publication: Chemistry - A European Journal

Publisher: John Wiley and Sons

Date: Oct 5, 2021

Open Access Article

This is an open access article distributed under the terms of the Creative Commons CC BY license, which permits unrestricted use, distribution, and reproduction in any medium, provided the original work is properly cited.

You are not required to obtain permission to reuse this article.

For an understanding of what is meant by the terms of the Creative Commons License, please refer to Wiley's Open Access Terms and Conditions.

Permission is not required for this type of reuse.

Wiley offers a professional reprint service for high quality reproduction of articles from over 1400 scientific and medical journals. Wiley's reprint service offers:

- Peer reviewed research or reviews
- Tailored collections of articles
- A professional high quality finish
- Glossy journal style color covers
- Company or brand customisation
- Language translations
- Prompt turnaround times and delivery directly to your office, warehouse or congress.

Please contact our Reprints department for a quotation. Email corporatesaleseurope@wiley.com or corporatesalesusa@wiley.com or corporatesalesDE@wiley.com.

Dear Xuan-Xuan Zhao,

Item 1:

The requested material is from an Open Access article, please see copyright holder below. You may re-use the material provided re-use is accordance with the conditions of the license (we have included the link to the CC-license below):

Item 2:

The requested material is from an Open Access article, please see copyright holder below. You may re-use the material provided re-use is accordance with the conditions of the license (we have included the link to the CC-license below):

Item 3:

Kind regards

Bettina Loycke
Senior Rights Manager
Rights & Licenses

Wiley-VCH GmbH
Boschstraße 12
69469 Weinheim
Germany
www.wiley-vch.de

T +(49) 6201 606-280
F +(49) 6201 606-332
rightsDE@wiley.com

WILEY

Celebrate ***100 Years of Growing Knowledge*** with us:
2021 marks our anniversary year: VCH was founded in 1921, Wiley-VCH in 1996. Please join us in celebrating this success and have a look at our anniversary website.

10. References

[1] J. C. Slater, *J. Chem. Phys.* **1964**, *41*, 3199-3204.

[2] D. H. Harris, M. F. Lappert, *J. Chem. Soc. Chem. Commun.* **1974**, 895-896.

[3] R. West, M. J. Fink, J. Michl, *Science* **1981**, *214*, 1343-1344.

[4] M. Yoshifuji, I. Shima, N. Inamoto, K. Hirotsu, T. Higuchi, *J. Am. Chem. Soc.* **1981**, *103*, 4587-4589.

[5] A. G. Brook, F. Abdesaken, B. Gutekunst, G. Gutekunst, R. K. Kallury, *J. Chem. Soc. Chem. Commun.* **1981**, 191-192.

[6] P. Jutzi, *Angew. Chem. Int. Ed.* **1975**, *14*, 232-245.

[7] P. P. Power, *Chem. Rev.* **1999**, *99*, 3463-3503.

[8] C. Weetman, *Chem. Eur. J.* **2021**, *27*, 1941-1954.

[9] C. Weetman, S. Inoue, *ChemCatChem* **2018**, *10*, 4213-4228.

[10] P. P. Power, *Nature* **2010**, *463*, 171-177.

[11] G. H. Spikes, J. C. Fettinger, P. P. Power, *J. Am. Chem. Soc.* **2005**, *127*, 12232-12233.

[12] L. Zhao, F. Huang, G. Lu, Z. X. Wang, P. Schleyer, *J. Am. Chem. Soc.* **2012**, *134*, 8856-8868.

[13] R. L. Melen, *Science* **2019**, *363*, 479-484.

[14] G. C. Welch, R. R. San Juan, J. D. Masuda, D. W. Stephan, *Science* **2006**, *314*, 1124-1126.

[15] S. Yadav, S. Saha, S. S. Sen, *ChemCatChem* **2016**, *8*, 486-501.

[16] Y. Peng, B. D. Ellis, X. Wang, J. C. Fettinger, P. P. Power, *Science* **2009**, *325*, 1668-1670.

[17] E. Fritz-Langhals, *Org. Process Res. Dev.* **2019**, *23*, 2369-2377.

[18] D. Bourissou, O. Guerret, F. P. Gabbai, G. Bertrand, *Chem. Rev.* **2000**, *100*, 39-92.

[19] D. J. Cardin, B. Cetinkaya, M. F. Lappert, *Chem. Rev.* **1972**, *72*, 545-574.

[20] V. Nair, S. Bindu, V. Sreekumar, *Angew. Chem. Int. Ed.* **2004**, *43*, 5130-5135.

[21] K. Öfele, *J. Organomet. Chem.* **1968**, *12*, P42-P43.

[22] H. W. Wanzlick, H. J. Schönherr, *Angew. Chem. Int. Ed.* **1968**, *7*, 141-142.

[23] A. Igau, H. Grutzmacher, A. Baceiredo, G. Bertrand, *J. Am. Chem. Soc.* **1988**, *110*, 6463-6466.

[24] A. J. Arduengo, R. L. Harlow, M. Kline, *J. Am. Chem. Soc.* **1991**, *113*, 361-363.

[25] N. Marion, S. Diez-Gonzalez, S. P. Nolan, *Angew. Chem. Int. Ed.* **2007**, *46*, 2988-3000.

[26] V. Nesterov, D. Reiter, P. Bag, P. Frisch, R. Holzner, A. Porzelt, S. Inoue, *Chem. Rev.* **2018**, *118*, 9678-9842.

[27] A. Doddi, M. Peters, M. Tamm, *Chem. Rev.* **2019**, *119*, 6994-7112.

[28] a) D. Enders, O. Niemeier, A. Henseler, *Chem. Rev.* **2007**, *107*, 5606-5655; b) M. N. Hopkinson, C. Richter, M. Schedler, F. Glorius, *Nature* **2014**, *510*, 485-496.

[29] a) B. Rao, H. Tang, X. Zeng, L. Liu, M. Melaimi, G. Bertrand, *Angew. Chem. Int. Ed.* **2015**, *54*, 14915-14919; b) M. Melaimi, R. Jazzar, M. Soleilhavoup, G. Bertrand, *Angew. Chem. Int. Ed.* **2017**, *56*, 10046-10068.

[30] a) P. Schwab, M. B. France, J. W. Ziller, R. H. Grubbs, *Angew. Chem. Int. Ed.* **1995**, *34*, 2039-2041; b) P. Schwab, R. H. Grubbs, J. W. Ziller, *J. Am. Chem. Soc.* **1996**, *118*, 100-110.

[31] T. Weskamp, W. C. Schattenmann, M. Spiegler, W. A. Herrmann, *Angew. Chem. Int. Ed.* **1998**, *37*, 2490-2493.

[32] M. Scholl, S. Ding, C. W. Lee, R. H. Grubbs, *Org. Lett.* **1999**, *1*, 953-956.

[33] T. Ochiai, D. Franz, S. Inoue, *Chem. Soc. Rev.* **2016**, *45*, 6327-6344.

[34] M. M. D. Roy, E. Rivard, *Acc. Chem. Res.* **2017**, *50*, 2017-2025.

[35] N. Kuhn, R. Fawzi, M. Steinmann, J. Wiethoff, D. Bläser, R. Boese, *Z. Naturforsch.* **1995**, 1779-1784.

[36] F. Dielmann, O. Back, M. Henry-Ellinger, P. Jerabek, G. Frenking, G. Bertrand, *Science* **2012**, *337*, 1526-1528.
[37] Y. K. Loh, M. Angeles Fuentes, P. Vasko, S. Aldridge, *Angew. Chem. Int. Ed.* **2018**, *57*, 16559-16563.
[38] N. Tokitoh, R. Okazaki, *Coord. Chem. Rev.* **2000**, *210*, 251-277.
[39] Y. Mizuhata, T. Sasamori, N. Tokitoh, *Chem. Rev.* **2009**, *109*, 3479-3511.
[40] a) P. J. Davidson, M. F. Lappert, *J. Chem. Soc. Chem. Commun.* **1973**, 317; b) D. E. Goldberg, D. H. Harris, M. F. Lappert, K. M. Thomas, *J. Chem. Soc. Chem. Commun.* **1976**, 261.
[41] a) P. Jutzi, F. Kohl, P. Hofmann, C. Krüger, Y.-H. Tsay, *Chem. Ber.* **1980**, *113*, 757-769; b) P. Jutzi, D. Kanne, C. Kruger, *Angew. Chem. Int. Ed.* **1986**, *25*, 164-164; c) P. Jutzi, R. Dickbreder, H. Nöth, *Chem. Ber.* **1989**, *122*, 865-870.
[42] G. H. Lee, R. West, T. Muller, *J. Am. Chem. Soc.* **2003**, *125*, 8114-8115.
[43] a) M. Kira, R. Yauchibara, R. Hirano, C. Kabuto, H. Sakurai, *J. Am. Chem. Soc.* **1991**, *113*, 7785-7787; b) M. Kira, S. Ishida, T. Iwamoto, M. Ichinohe, C. Kabuto, L. Ignatovich, H. Sakurai, *Chem. Lett.* **1999**, *28*, 263-264; c) M. Kira, S. Ishida, T. Iwamoto, C. Kabuto, *J. Am. Chem. Soc.* **1999**, *121*, 9722-9723.
[44] M. Veith, M. Grosser, *Z. Naturforsch.* **1982**, *37*, 1375-1381.
[45] B. Gehrhus, P. B. Hitchcock, M. F. Lappert, J. Heinicke, R. Boese, D. Bläser, *J. Organomet. Chem.* **1996**, *521*, 211-220.
[46] R. Dasgupta, S. Das, S. Hiwase, S. K. Pati, S. Khan, *Organometallics* **2019**, *38*, 1429-1435.
[47] a) S. Fujimori, S. Inoue, *Eur. J. Inorg. Chem.* **2020**, *2020*, 3131-3142; b) C. Shan, S. Yao, M. Driess, *Chem. Soc. Rev.* **2020**, *49*, 6733-6754.
[48] B. D. Rekken, T. M. Brown, J. C. Fettinger, H. M. Tuononen, P. P. Power, *J. Am. Chem. Soc.* **2012**, *134*, 6504-6507.
[49] A. V. Protchenko, K. H. Birjkumar, D. Dange, A. D. Schwarz, D. Vidovic, C. Jones, N. Kaltsoyannis, P. Mountford, S. Aldridge, *J. Am. Chem. Soc.* **2012**, *134*, 6500-6503.
[50] A. V. Protchenko, A. D. Schwarz, M. P. Blake, C. Jones, N. Kaltsoyannis, P. Mountford, S. Aldridge, *Angew. Chem. Int. Ed.* **2013**, *52*, 568-571.
[51] T. J. Hadlington, J. A. Abdalla, R. Tirfoin, S. Aldridge, C. Jones, *Chem. Commun.* **2016**, *52*, 1717-1720.
[52] Y. K. Loh, L. Ying, M. Angeles Fuentes, D. C. H. Do, S. Aldridge, *Angew. Chem. Int. Ed.* **2019**, *58*, 4847-4851.
[53] M. M. D. Roy, M. J. Ferguson, R. McDonald, Y. Zhou, E. Rivard, *Chem. Sci.* **2019**, *10*, 6476-6481.
[54] M. M. D. Roy, S. R. Baird, E. Dornsiepen, L. A. Paul, L. Miao, M. J. Ferguson, Y. Zhou, I. Siewert, E. Rivard, *Chem. Eur. J.* **2021**, *27*, 8572-8579.
[55] M. W. Lui, C. Merten, M. J. Ferguson, R. McDonald, Y. Xu, E. Rivard, *Inorg. Chem.* **2015**, *54*, 2040-2049.
[56] E. Hupf, F. Kaiser, P. A. Lummis, M. M. D. Roy, R. McDonald, M. J. Ferguson, F. E. Kuhn, E. Rivard, *Inorg. Chem.* **2020**, *59*, 1592-1601.
[57] S. Inoue, K. Leszczynska, *Angew. Chem. Int. Ed.* **2012**, *51*, 8589-8593.
[58] D. Wendel, A. Porzelt, F. A. D. Herz, D. Sarkar, C. Jandl, S. Inoue, B. Rieger, *J. Am. Chem. Soc.* **2017**, *139*, 8134-8137.
[59] D. Reiter, P. Frisch, D. Wendel, F. M. Hormann, S. Inoue, *Dalton Trans.* **2020**, *49*, 7060-7068.
[60] D. Reiter, R. Holzner, A. Porzelt, P. J. Altmann, P. Frisch, S. Inoue, *J. Am. Chem. Soc.* **2019**, *141*, 13536-13546.

[61] V. Nesterov, R. Baierl, F. Hanusch, A. E. Ferao, S. Inoue, *J. Am. Chem. Soc.* **2019**, *141*, 14576-14580.
[62] D. Sarkar, C. Weetman, D. Munz, S. Inoue, *Angew. Chem. Int. Ed.* **2021**, *60*, 3519-3523.
[63] F. T. Edelmann, D. M. Freckmann, H. Schumann, *Chem. Rev.* **2002**, *102*, 1851-1896.
[64] B. Shen, L. Ying, J. Chen, Y. J. Luo, *Inorg. Chim. Acta* **2008**, *361*, 1255-1260.
[65] Y. Luo, X. Wang, J. Chen, C. Luo, Y. Zhang, Y. Yao, *J. Organomet. Chem.* **2009**, *694*, 1289-1296.
[66] Y. Luo, S. Fan, J. Yang, J. Fang, P. Xu, *Dalton Trans.* **2011**, *40*, 3053-3059.
[67] G. Boche, J. C. Lohrenz, *Chem. Rev.* **2001**, *101*, 697-756.
[68] G. Boche, M. Marsch, A. Müller, K. Harms, *Angew. Chem. Int. Ed.* **1993**, *32*, 1032-1033.
[69] E. Niecke, P. Becker, M. Nieger, D. Stalke, W. W. Schoeller, *Angew. Chem. Int. Ed.* **1995**, *34*, 1849-1852.
[70] E. Niecke, M. Nieger, O. Schmidt, D. Gudat, W. W. Schoeller, *J. Am. Chem. Soc.* **1999**, *121*, 519-522.
[71] T. Cantat, X. Jacques, L. Ricard, X. F. Le Goff, N. Mezailles, P. Le Floch, *Angew. Chem. Int. Ed.* **2007**, *46*, 5947-5950.
[72] K. Tamao, A. Kawachi, M. Asahara, A. Toshimitsu, *Pure Appl. Chem.* **1999**, *71*, 393-400.
[73] a) A. Kawachi, K. Tamao, *Bull. Chem. Soc. Jpn.* **1997**, *70*, 945-955; b) Y. Tanaka, M. Hada, A. Kawachi, K. Tamao, H. Nakatsuji, *Organometallics* **1998**, *17*, 4573-4577.
[74] a) N. Tokitoh, K. Hatano, T. Sadahiro, R. Okazaki, *Chem. Lett.* **1999**, *28*, 931-932; b) K. Hatano, N. Tokitoh, N. Takagi, S. Nagase, *J. Am. Chem. Soc.* **2000**, *122*, 4829-4830.
[75] a) M. E. Lee, H. M. Cho, Y. M. Lim, J. K. Choi, C. H. Park, S. E. Jeong, U. Lee, *Chem. Eur. J.* **2004**, *10*, 377-381; b) Y. M. Lim, H. M. Cho, M. E. Lee, K. K. Baeck, *Organometallics* **2006**, *25*, 4960-4964; c) H. M. Cho, Y. M. Lim, M. E. Lee, *Dalton Trans.* **2010**, *39*, 9232-9234; d) H. M. Cho, Y. M. Lim, B. W. Lee, S. J. Park, M. E. Lee, *J. Organomet. Chem.* **2011**, *696*, 2665-2668.
[76] T. Ohtaki, W. Ando, *Organometallics* **1996**, *15*, 3103-3105.
[77] Y. Suzuki, T. Sasamori, J. D. Guo, S. Nagase, N. Tokitoh, *Chem. Eur. J.* **2016**, *22*, 13784-13788.
[78] A. M. Arif, A. H. Cowley, T. M. Elkins, *J. Organomet. Chem.* **1987**, *325*, C11-C13.
[79] H. Arp, J. Baumgartner, C. Marschner, T. Muller, *J. Am. Chem. Soc.* **2011**, *133*, 5632-5635.
[80] C. Yan, Z. Li, X. Q. Xiao, N. Wei, Q. Lu, M. Kira, *Angew. Chem. Int. Ed.* **2016**, *55*, 14784-14787.
[81] T. Ochiai, D. Franz, X. N. Wu, E. Irran, S. Inoue, *Angew. Chem. Int. Ed.* **2016**, *55*, 6983-6987.
[82] V. S. Swamy, S. Pal, S. Khan, S. S. Sen, *Dalton Trans.* **2015**, *44*, 12903-12923.
[83] P. Jutzi, F. Kohl, C. Krüger, *Angew. Chem. Int. Ed.* **1979**, *18*, 59-60.
[84] T. Probst, O. Steigelmann, J. Riede, H. Schmiclbaur, *Angew. Chem. Int. Ed.* **1990**, *29*, 1397-1398.
[85] H. V. R. Dias, W. Jin, *J. Am. Chem. Soc.* **1996**, *118*, 9123-9126.
[86] M. J. Taylor, A. J. Saunders, M. P. Coles, J. R. Fulton, *Organometallics* **2011**, *30*, 1334-1339.
[87] J. Li, C. Schenk, F. Winter, H. Scherer, N. Trapp, A. Higelin, S. Keller, R. Pottgen, I. Krossing, C. Jones, *Angew. Chem. Int. Ed.* **2012**, *51*, 9557-9561.
[88] C. L. Macdonald, R. Bandyopadhyay, B. F. Cooper, W. W. Friedl, A. J. Rossini, R. W. Schurko, S. H. Eichhorn, R. H. Herber, *J. Am. Chem. Soc.* **2012**, *134*, 4332-4345.
[89] J. C. Avery, M. A. Hanson, R. H. Herber, K. J. Bladek, P. A. Rupar, I. Nowik, Y. Huang, K. M. Baines, *Inorg. Chem.* **2012**, *51*, 7306-7316.
[90] J. Flock, A. Suljanovic, A. Torvisco, W. Schoefberger, B. Gerke, R. Pottgen, R. C. Fischer, M. Flock, *Chem. Eur. J.* **2013**, *19*, 15504-15517.

[91] M. Bouška, L. Dostál, A. Růžička, R. Jambor, *Organometallics* **2013**, *32*, 1995-1999.
[92] S. Khan, G. Gopakumar, W. Thiel, M. Alcarazo, *Angew. Chem. Int. Ed.* **2013**, *52*, 5644-5647.
[93] A. Hinz, *Chem. Eur. J.* **2019**, *25*, 3267-3271.
[94] a) S. L. Powley, S. Inoue, *Chem. Rec.* **2019**; b) P. Frisch, S. Inoue, *Dalton Trans.* **2020**, *49*, 6176-6182.
[95] D. Sarkar, S. Dutta, C. Weetman, E. Schubert, D. Koley, S. Inoue, *Chem. Eur. J.* **2021**, *27*, 13072-13078.
[96] a) F. S. Tschernuth, F. Hanusch, T. Szilvasi, S. Inoue, *Organometallics* **2020**, *39*, 4265-4272; b) S. V. Hirmer, F. S. Tschernuth, F. Hanusch, R. Baierl, M. Muhr, S. Inoue, *Mendeleev Commun.* **2022**, *32*, 16-18.
[97] T. Ochiai, D. Franz, X. N. Wu, S. Inoue, *Dalton Trans.* **2015**, *44*, 10952-10956.
[98] T. Ochiai, D. Franz, E. Irran, S. Inoue, *Chem. Eur. J.* **2015**, *21*, 6704-6707.
[99] T. Ochiai, T. Szilvasi, D. Franz, E. Irran, S. Inoue, *Angew. Chem. Int. Ed.* **2016**, *55*, 11619-11624.
[100] S. U. Ahmad, T. Szilvasi, S. Inoue, *Chem. Commun.* **2014**, *50*, 12619-12622.
[101] D. Sarkar, C. Weetman, S. Dutta, E. Schubert, C. Jandl, D. Koley, S. Inoue, *J. Am. Chem. Soc.* **2020**, *142*, 15403-15411.
[102] S. U. Ahmad, T. Szilvasi, E. Irran, S. Inoue, *J. Am. Chem. Soc.* **2015**, *137*, 5828-5836.
[103] D. Sarkar, V. Nesterov, T. Szilvasi, P. J. Altmann, S. Inoue, *Chem. Eur. J.* **2019**, *25*, 1198-1202.
[104] F. Hanusch, D. Munz, J. Sutter, K. Meyer, S. Inoue, *Angew. Chem. Int. Ed.* **2021**, *60*, 23274-23280.
[105] N. Takagi, T. Shimizu, G. Frenking, *Chem. Eur. J.* **2009**, *15*, 8593-8604.
[106] P. K. Majhi, T. Sasamori, *Chem. Eur. J.* **2018**, *24*, 9441-9455.
[107] S. Yao, Y. Xiong, M. Driess, *Acc. Chem. Res.* **2017**, *50*, 2026-2037.
[108] N. Wiberg, H.-W. Lerner, S.-K. Vasisht, S. Wagner, K. Karaghiosoff, H. Nöth, W. Ponikwar, *Eur. J. Inorg. Chem.* **1999**, *1999*, 1211-1218.
[109] T. Iwamoto, T. Abe, C. Kabuto, M. Kira, *Chem. Commun.* **2005**, 5190-5192.
[110] T. Iwamoto, H. Masuda, C. Kabuto, M. Kira, *Organometallics* **2005**, *24*, 197-199.
[111] Y. Wang, Y. Xie, P. Wei, R. B. King, H. F. Schaefer, 3rd, R. S. P. von, G. H. Robinson, *Science* **2008**, *321*, 1069-1071.
[112] A. Sidiropoulos, C. Jones, A. Stasch, S. Klein, G. Frenking, *Angew. Chem. Int. Ed.* **2009**, *48*, 9701-9704.
[113] C. Jones, A. Sidiropoulos, N. Holzmann, G. Frenking, A. Stasch, *Chem. Commun.* **2012**, *48*, 9855-9857.
[114] K. C. Mondal, H. W. Roesky, M. C. Schwarzer, G. Frenking, B. Niepotter, H. Wolf, R. Herbst-Irmer, D. Stalke, *Angew. Chem. Int. Ed.* **2013**, *52*, 2963-2967.
[115] Y. Li, K. C. Mondal, H. W. Roesky, H. Zhu, P. Stollberg, R. Herbst-Irmer, D. Stalke, D. M. Andrada, *J. Am. Chem. Soc.* **2013**, *135*, 12422-12428.
[116] K. C. Mondal, P. P. Samuel, H. W. Roesky, R. R. Aysin, L. A. Leites, S. Neudeck, J. Lubben, B. Dittrich, N. Holzmann, M. Hermann, G. Frenking, *J. Am. Chem. Soc.* **2014**, *136*, 8919-8922.
[117] Y. L. Shan, W. L. Yim, C. W. So, *Angew. Chem. Int. Ed.* **2014**, *53*, 13155-13158.
[118] K. C. Mondal, S. Roy, B. Dittrich, D. M. Andrada, G. Frenking, H. W. Roesky, *Angew. Chem. Int. Ed.* **2016**, *55*, 3158-3161.
[119] A. Rit, J. Campos, H. Niu, S. Aldridge, *Nat. Chem.* **2016**, *8*, 1022-1026.
[120] Y. Xiong, S. Yao, S. Inoue, J. D. Epping, M. Driess, *Angew. Chem. Int. Ed.* **2013**, *52*, 7147-7150.

[121] Y. Xiong, S. Yao, G. Tan, S. Inoue, M. Driess, *J. Am. Chem. Soc.* **2013**, *135*, 5004-5007.
[122] T. Chu, L. Belding, A. van der Est, T. Dudding, I. Korobkov, G. I. Nikonov, *Angew. Chem. Int. Ed.* **2014**, *53*, 2711-2715.
[123] B. Su, R. Ganguly, Y. Li, R. Kinjo, *Chem. Commun.* **2016**, *52*, 613-616.
[124] T. Kuwabara, M. Nakada, J. Hamada, J. D. Guo, S. Nagase, M. Saito, *J. Am. Chem. Soc.* **2016**, *138*, 11378-11382.
[125] T. Sugahara, T. Sasamori, N. Tokitoh, *Angew. Chem. Int. Ed.* **2017**, *56*, 9920-9923.
[126] J. Keuter, A. Hepp, C. Muck-Lichtenfeld, F. Lips, *Angew. Chem. Int. Ed.* **2019**, *58*, 4395-4399.
[127] M. T. Nguyen, D. Gusev, A. Dmitrienko, B. M. Gabidullin, D. Spasyuk, M. Pilkington, G. I. Nikonov, *J. Am. Chem. Soc.* **2020**, *142*, 5852-5861.
[128] S. Yao, Y. Xiong, A. Saddington, M. Driess, *Chem. Commun.* **2021**, *57*, 10139-10153.
[129] Y. P. Zhou, M. Karni, S. Yao, Y. Apeloig, M. Driess, *Angew. Chem. Int. Ed.* **2016**, *55*, 15096-15099.
[130] Y. Wang, M. Karni, S. Yao, A. Kaushansky, Y. Apeloig, M. Driess, *J. Am. Chem. Soc.* **2019**, *141*, 12916-12927.
[131] Y. Wang, M. Karni, S. Yao, Y. Apeloig, M. Driess, *J. Am. Chem. Soc.* **2019**, *141*, 1655-1664.
[132] J. Xu, C. Dai, S. Yao, J. Zhu, M. Driess, *Angew. Chem. Int. Ed.* **2021**.
[133] S. Yao, A. Kostenko, Y. Xiong, A. Ruzicka, M. Driess, *J. Am. Chem. Soc.* **2020**, *142*, 12608-12612.
[134] S. Yao, A. Kostenko, Y. Xiong, C. Lorent, A. Ruzicka, M. Driess, *Angew. Chem. Int. Ed.* **2021**, *60*, 14864-14868.
[135] R. Okazaki, N. Tokitoh, *Acc. Chem. Res.* **2000**, *33*, 625-630.
[136] Y. Xiong, S. Yao, M. Driess, *Angew. Chem. Int. Ed.* **2013**, *52*, 4302-4311.
[137] Y. K. Loh, S. Aldridge, *Angew. Chem. Int. Ed.* **2021**, *60*, 8626-8648.
[138] F. S. Kipping, L. L. Lloyd, *J. Chem. Soc., Trans.* **1901**, *79*, 449-459.
[139] R. S. Ghadwal, R. Azhakar, H. W. Roesky, K. Propper, B. Dittrich, S. Klein, G. Frenking, *J. Am. Chem. Soc.* **2011**, *133*, 17552-17555.
[140] Y. Xiong, S. Yao, M. Driess, *J. Am. Chem. Soc.* **2009**, *131*, 7562-7563.
[141] S. Yao, M. Brym, C. van Wullen, M. Driess, *Angew. Chem. Int. Ed.* **2007**, *46*, 4159-4162.
[142] J. D. Epping, S. Yao, M. Karni, Y. Apeloig, M. Driess, *J. Am. Chem. Soc.* **2010**, *132*, 5443-5455.
[143] A. C. Filippou, B. Baars, O. Chernov, Y. N. Lebedev, G. Schnakenburg, *Angew. Chem. Int. Ed.* **2014**, *53*, 565-570.
[144] S. Ishida, T. Abe, F. Hirakawa, T. Kosai, K. Sato, M. Kira, T. Iwamoto, *Chem. Eur. J.* **2015**, *21*, 15100-15103.
[145] I. Alvarado-Beltran, A. Rosas-Sanchez, A. Baceiredo, N. Saffon-Merceron, V. Branchadell, T. Kato, *Angew. Chem. Int. Ed.* **2017**, *56*, 10481-10485.
[146] A. Rosas-Sanchez, I. Alvarado-Beltran, A. Baceiredo, N. Saffon-Merceron, S. Massou, D. Hashizume, V. Branchadell, T. Kato, *Angew. Chem. Int. Ed.* **2017**, *56*, 15916-15920.
[147] R. Kobayashi, S. Ishida, T. Iwamoto, *Angew. Chem. Int. Ed.* **2019**, *58*, 9425-9428.
[148] N. Tokitoh, R. Okazaki, *Adv. Organometal. Chem.* **2001**, *47*, 121-166.
[149] J. Barrau, M. Massol, D. Mesnard, J. Satgé, *J. Organomet. Chem.* **1971**, *30*, C67-C69.
[150] J. Barrau, J. Escudie, J. Satge, *Chem. Rev.* **1990**, *90*, 283-319.
[151] N. Tokitoh, T. Matsumoto, R. Okazaki, *Chem. Lett.* **1995**, *24*, 1087-1088.
[152] G. L. Wegner, R. J. F. Berger, A. Schier, H. Schmidbaur, *Organometallics* **2001**, *20*, 418-423.
[153] J. Kapp, M. Remko, P. v. R. Schleyer, *J. Am. Chem. Soc.* **1996**, *118*, 5745-5751.
[154] R. C. Fischer, P. P. Power, *Chem. Rev.* **2010**, *110*, 3877-3923.

[155] S. Yao, Y. Xiong, M. Driess, *Chem. Commun.* **2009**, 6466-6468.
[156] S. Yao, Y. Xiong, W. Wang, M. Driess, *Chem. Eur. J.* **2011**, *17*, 4890-4895.
[157] a) L. Li, T. Fukawa, T. Matsuo, D. Hashizume, H. Fueno, K. Tanaka, K. Tamao, *Nat. Chem.* **2012**, *4*, 361-365; b) P. P. Power, *Nat. Chem.* **2012**, *4*, 343-344.
[158] L. Kristinsdottir, N. L. Oldroyd, R. Grabiner, A. W. Knights, A. Heilmann, A. V. Protchenko, H. Niu, E. L. Kolychev, J. Campos, J. Hicks, K. E. Christensen, S. Aldridge, *Dalton Trans.* **2019**, *48*, 11951-11960.
[159] A. V. Zabula, T. Pape, A. Hepp, F. M. Schappacher, U. Rodewald, R. Pottgen, F. E. Hahn, *J. Am. Chem. Soc.* **2008**, *130*, 5648-5649.